THE FISH BRANCHIAL EPITHELIUM:
AN IMMUNOLOGICAL APPROACH TO ION TRANSPORT PROTEIN LOCALIZATION

By

Jonathan Mark Wilson

B.Sc., University of British Columbia, 1993
M.Sc., University of British Columbia, 1995

A THESIS SUBMITED IN PARTIAL FULFILMENT
OF THE REQUREMENTS FOR THE
DEGREE OF DOCTOR OF PHILOSOPHY
in
THE FACULTY OF GRADUATE STUDIES
DEPARTMENT OF ZOOLOGY

We accept this thesis as conforming
to the required standard

THE UNIVERSITY OF BRITISH COLUMBIA
1999

Department of ____Zoology____

The University of British Columbia
Vancouver, Canada

Date ___17th DEC 1999___

DE-6 (2/88)

ABSTRACT

In my thesis the cellular and subcellular distributions of various ion transport proteins were determined in the fish branchial epithelium using an immunological approach employing non-homologous antibodies. The viabilities of current models of transepithelial ion transport in the gills of freshwater, and seawater fishes and an unusual amphibious air-breathing fish were tested. My thesis work primarily addresses the mechanisms involved in the translocation of Na^+ and Cl^- and their counterions, H^+ and HCO_3^-, respectively and of NH_4^+.

In freshwater fishes (tilapia: *Oreochromis mossambicus*; trout: *Oncorhynchus mykiss*) the vH^+-ATPase colocalizes apically with an epithelial Na^+ channel (ENaC)-like protein, however, the distribution of these proteins is restricted to pavement cells (PVCs) in tilapia while being found in both PVCs and mitochondria-rich (MR) cells in trout. An Na^+/H^+ exchanger-like (NHE) protein is also identified in the gill of the freshwater tilapia. In tilapia and coho salmon (*Oncorhynchus kisutch*), an apical band 3-like Cl^-/HCO_3^- anion exchanger (AE) is localized to MR cells demonstating the presence of a freshwater-type chloride cell (involved in Cl^- uptake).

In seawater fishes, the chloride cell has been well characterized as the site of active Cl^- elimination. In my observations of seawater fishes (*O.kisutch*; turbot: *Scophthamus maximus*) and the brackishwater, air-breathing mudskipper fish (*Periophthalmodon schlosseri*), ion transport proteins involved in active Cl^- elimination are localized to chloride cells (Na^+,K^+-ATPase, $Na^+:K^+:2Cl^-$ cotransporter (NKCC) and apical cystic fibrosis transmembrane receptor (CFTR)-like anion channel). The AE and NHE proteins that are potentially involved in acid-base regulation are localized to the chloride cell apical crypt and accessory cell, respectively, in the stenohaline turbot. However, in the euryhaline coho the apical AE of the freshwater MR cell is not observed in the seawater acclimated fish.

In the mudskipper fish, I have shown that NHE, Na^+,K^+-ATPase, and carbonic anhydrase in gill MR cells contribute to active ammonia (NH_4^+) excretion in pharmacological studies. The branchial epithelium contains an unusual abundance of MR cells and immunolocalization studies show the presence of NHE-2 and 3-like isoforms, CFTR, and CA associated with the apical crypt and Na^+,K^+-ATPase and NKCC with the tubular system of these cells. And so it goes….

TABLE OF CONTENTS

LIST of TABLES

LIST of FIGURES

LIST OF ABBREVIATIONS

AC	Accessory cell
AE	Anion exchanger
AE1t	Anion exchanger 1 (band-3 protein) trout
AP	Alkaline phosphatase
BCIP	5-bromo-4-chloro-3-indolyl phosphate
BSA	Bovine serum albumin
BSC	Bumetanide sensitive cotransporter (a.k.a NKCC)
CC	Chloride cell
CD	Collecting duct
CFTR	Cystic fibrosis transmembrane regulator
ddH_2O	Double distilled water
DIDS	4,4'-diisothiocyanostilbene-2,2'-disulfonic acid
DMSO	Dimethylsulfoxide
DPC	Diphenylamine-2-carboxylate
ECL	Enhanced chemiluminescence
ENaC	Epithelial Sodium Channel
FITC	Fluorescein isothiocyanate
FR cell	Filament-rich cell
Glut	Glutaraldehyde
H	Hypothesis
HEPES	N-[2-hydroxethyl] piperazine-N'-[2-ethane sulfonic acid]
HRP	Horse radish peroxidase
J_{ACID}	Net acid flux
J_{AMM}	Net ammonia excretion
MR cell	Mitochondria-rich cell
MTAL	medulla thick ascending limb
MW	Molecular weight
NBT	Nitroblue tetrazolium
NEM	N-ethylmaleimide

NGS	Normal goat serum
NH_3	Gaseous or unionized ammonia
NH_4^+	Ionized ammonia or ammonium
NHE	Na^+/H^+ exchanger
NKA	Na^+/K^+-ATPase
NKCC	$Na^+:K^+:2Cl^-$ contransporter
NMS	Normal mouse serum
NPPB	5-nitro-2-(3-phenylpropylamino) benzoic acid
NRS	Normal rabbit serum
PAGE	Polyacrylamide gel electrophoresis
PBS	Phosphate buffered saline
PFA	Paraformaldehyde
PLP	Paraformaldehyde-lysine-periodate
PVC	Pavement cell
rt	Room temperature
RT-PCR	Reverse Transcriptase-Polymerase Chain Reaction
SDS	Sodium dodecyl sulfate
SEI	Sucrose, EDTA, Imidazole buffer
SITS	4-acetomido-4'-isothiocyanatostilbene-2,2'-disulfonic acid
TA	Titratable acidity
TEM	Transmission electron microscopy
TEP	Transepithelial potential difference
TPBS	Tween-20 in Phosphate buffered saline
vH^+-ATPase	vacuolar (V-type) proton ATPase

ACKNOWLEDGMENTS

I am indebted to my supervisor, Dave Randall, who I have had the pleasure of knowing for the past seven or so years. He has provided me with opportunities and shown me that there is much to appreciate in life. This Ph.D. has not been so much about studying ion regulation in fishes but getting out and seeing the world, to see how other people from diverse backgrounds study ion regulation in fishes. I have had the opportunity to return to the womb, so to speak, to the land of my birth, Hong Kong, to work on the mudskipper, an air-breathing amphibious fish (if you believe such things exist). I was there to see the Pearl in the Crown returned to the Motherland. I also had the pleasure to collaborate with Alex K-Y. Ip of the National University of Singapore on project *"mudskipper"*. I have lived in the picturesque capital of the New Europe, Strasbourg, to work in a place where they work on penguins and I worked on fish. I was there to see the French win the World Cup (Allez les Blues!). To my French host, Pierre Laurent, my palate will forever remember the country potatoes. And here at home (Vancouver), I owe a debt of gratitude to Wayne Vogl of the Department of Anatomy who has always left the door open for me to return from my expeditions.

When I started, my son, Matthew was far from making his first cell division and now (many cell divisions later) he will be 3 years old. How can any of this make sense to him? My wife, Cristina, has been very understanding during this unsettled period but I did spend many an afternoon with her in MongKok. My parents, sisters, and brother have also been supportive in my pursuit occasionally providing floor space for me to rest my head.

Chapter 1. GENERAL INTRODUCTION

In this general introduction I will describe the gill and its role in active ion regulation as well as provide some background information on the ion transport proteins involved. In the following chapters on freshwater, and seawater fishes and the mudskipper I will introduce in more detail the different models for Na^+, and Cl^- uptake and elimination and ammonia excretion, respectively.

1.1. Basic description of the fish gill

The fish gill is designed to accommodate gas exchange, ion regulation and the elimination of nitrogenous waste (ammonia) (see reviews by Piiper and Scheid 1984; Karnaky 1998; Walsh 1998; Evans et al. 1999). To optimize the exchange between the internal (blood) and external (water) environments, the gill has a large surface area with a short diffusion distance between blood and water, which is well perfused (receiving the full cardiac output), and well ventilated. The high perfusion and ventilation ensure diffusion gradients are maximized. The typical teleost fish gill is composed of gill arches with paired rows of filaments extending in a laterocaudal direction (Figure 1). Regularly spaced rows of lamellae on both upper and lower sides of the filament are arranged perpendicular to the long axis of the filaments. These thin lamellae account for the greatest surface area of the gill and provide an interface ideal for gas exchange. Blood, delivered to the lamellae from the afferent arteries, flows through the lamellar blood spaces and is collected by the efferent arteries to enter the systemic circulation (arterio-arterial circulation). The water flow between lamellae is counter current to the blood flow within the lamellae. The water flow is forced over the filaments by having them in a sieve-like arrangement whereby the tips of filaments from adjacent gill arches come into close contact. The thicker filament epithelium is generally associated with ion regulation due to the presence of a
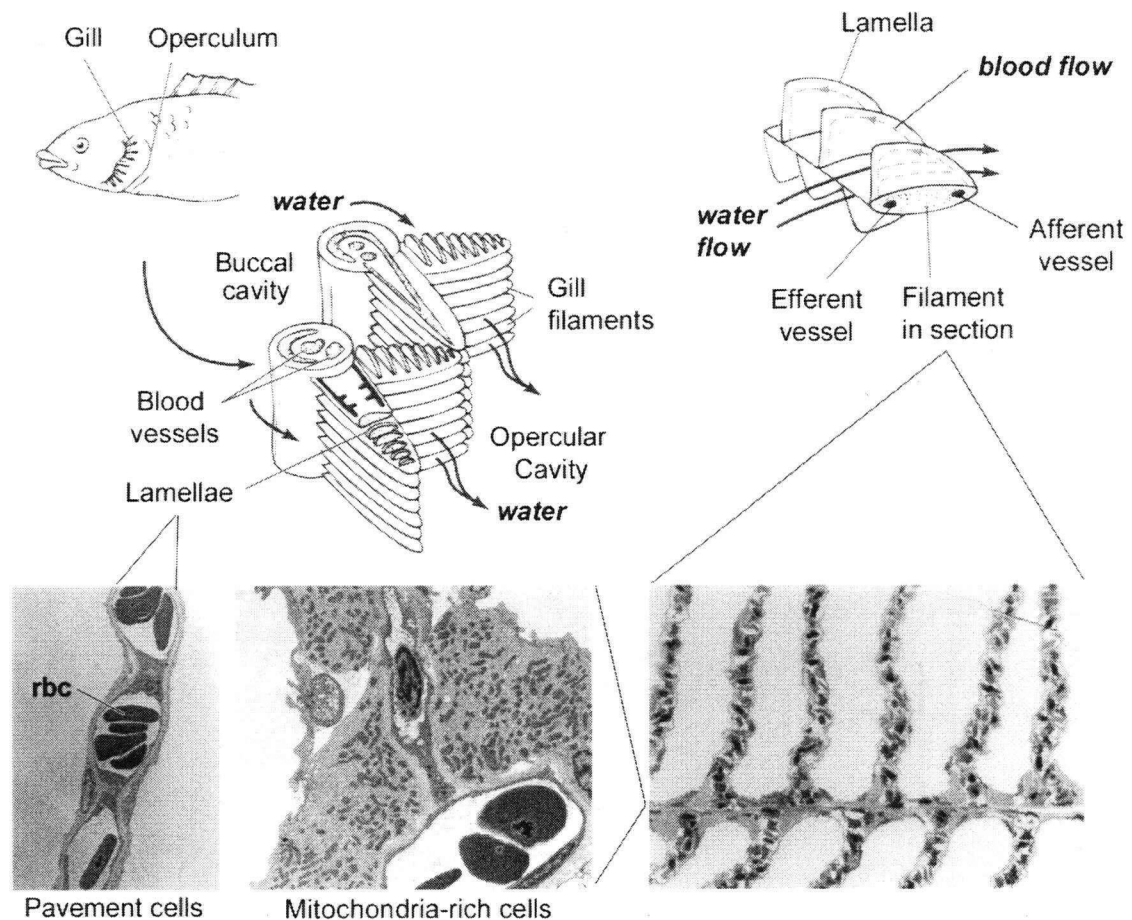
FIGURE 1.1 Basic description of the teleost fish gill. The gills are found in the mouth between the buccal and opercular cavities. The four pairs of gill arches have paired rows of filaments extending in a laterocaudal direction. Regularly spaced rows of lamellae on both upper and lower sides of the filament are arranged perpendicular to the long axis of the filaments. Blood, delivered to the lamellae from the afferent arteries flows through blood spaces within the lamellae and is collected by the efferent arteries to enter the systemic circulation (arterio-arterial circulation). The water flow between lamellae is counter current to the blood flow within the lamellae. The water flow is forced over the filaments by having them in a sieve-like arrangement whereby the tips of filaments from adjacent gill arches come into close contact. (Modified from Eckert *et al*. 1997). The micrographs show the dominant cell types of lamellar and filament epithelia, the pavement cell and MR cell, respectively. They also illustrate the short distance from the blood (**rbc**; red blood cell) to water present in lamellae.

population of ionocytes (MR cells) and has an arterio-venous circulation. The arterio-venous or secondary circulation is served by a central venous sinus (CVS) that runs the length of the filament and drains into the branchial vein. Blood is delivered to the CVS via anastomoses on the efferent and/or afferent vessels. (see reviews by Hughes 1984; Laurent 1984).

1.1.1 Branchial epithelium

The branchial epithelium can be sub-divided into the lamellar and filament epithelia on the basis of location and appearance. The lamellar epithelium that covers the lamellae is pseudo-stratified and composed mainly of squamous epithelial cells commonly referred to as pavement (PVC) or respiratory cells. Mucocytes or goblet cells are not commonly found within the lamellar epithelium. Modified endothelial cells called pillar cells define the lamellar blood spaces. As their name would imply, pillar cells have a pillar-like shape and have thin flanges that extend to contact neighbouring pillar cell flanges (Newstead 1967). Separating the endothelium and epithelium is the basal lamina. The filament epithelium covers the filament leading and trailing edges and the spaces between lamellae (interlamellar spaces). This epithelium is much thicker than the lamellar epithelium and is composed of cells similar to the pavement cell (PVC) as well as columnar cell, mucocytes and MR cells. The MR cells tend to be more numerous toward the trailing edge of the filament within the interlamellar space and on the trailing edge (van der Heijden *et al.* 1997). However, fish living in extremely ion poor water also have MR cells on their lamellae (Laurent *et al.* 1985; Avella *et al.* 1987).

Two cell types that are likely directly involved in ion regulation are the MR cell and PVC (Laurent 1984). Mucocytes indirectly contribute to ion regulation through the mucus they secrete, which modifies boundary layer properties of the epithelium (Handy 1989; Randall *et al.* 1991; Shephard 1992). Much work has been done describing the morphology of the MR cells

and PVC's and identifying morphological correlates to changes in environmental or physiological conditions (reviews by Laurent 1984; Laurent and Perry 1991; Pisam and Rambourg 1991; Goss *et al.* 1995).

1.1.2 Mitochondria-rich (MR) cells

The MR cells generally make up less than 10% of the epithelium yet are generally considered to be the dominant site of branchial ion regulation (Karnaky 1986; Jürss and Bastrop 1994; Zadunaisky 1996). In addition to having two unique intracellular membrane systems (the subapical tubulovesicular system and an extensive tubular system) these cells are rich in mitochondria, as their name implies (Phillpot 1980; Pisam and Rambourg 1991). The tubulovesicular system is a collection of irregular tubules and vesicles found in the subapical region of the cell. They are likely involved in the transport of glycoproteins from the Golgi apparatus to the apical membrane (Pisam *et al.* 1980). The tubular system is found throughout the cytoplasm of the cell closely associated with the mitochondria except in the Golgi region and in close proximity to the apical membrane. The tubular system is composed of anastomosing tubules of constant diameter that are in continuity with the basolateral membrane. The tubular system can be differentiated from the tubulovesicular system and the endoplasmic reticulum through the use of extracellular markers (lanthanum, ruthenium red, and horseradish peroxidase; Phillipot 1980) and the ferrocyanide-reduced osmium staining technique (Pisam 1981). The tubular system is also associated with high concentrations of Na^+,K^+-ATPase (Karnaky *et al.* 1976; Hootman and Phillpot 1979; Witters *et al.* 1996).

Pisam and co-wokers (1987, 1990) have been able to elegantly demonstrate that there are at least two sub-types of MR cells (α and β cells) in freshwater fishes (*Lebistes reticulatus, Gobio gobia, Cobitus taenia*). The α-MR cell is found at the base of the secondary lamellae

closely associated with the arterio-arterial circulation and is elongate and pale (less electron dense). The apical membrane is flat and not elaborated. The tubulovesicular system is poorly developed while the tubular system forms a regular meshwork throughout the cytoplasm. The β-MR cell is found closer to the centre of the interlamellar space and is associated with the arterio-venous circulation (central venous sinus). The β-cell is darker (more electron dense) and ovoid or cuboidal in shape with a slightly concave and wavy apical membrane. The tubular system forms an irregular meshwork and the tubulovesicular system has additional electron-dense bodies (using a magnesium-lead stain; Pisam *et al.* 1987). In other species the appearance of the apical membrane can be highly variable ranging from flat and unornamented to sponge-like (Perry *et al.* 1992). Morphological variation is also introduced by cells undergoing the processes of apoptosis and necrosis (Wendelaar Bonga and van der Meij 1989).

In the MR cell of seawater fishes, the tubular system is more developed and the apical membrane tends to be invaginated forming a crypt. Higher Na^+,K^+-ATPase activities are associated with the seawater type MR cell. The seawater type MR cell is typically referred to as the *chloride* cell (see chapter 4). In fish transferred from freshwater to seawater, it is the β-MR cell that develops into the chloride cell (Pisam *et al.* 1987). Closely associated with the apical region of the chloride cell is a small *accessory* MR cell with a poorly developed tubular system and fewer mitochondria. This *accessory* cell sends cytoplasmic projections into its larger neighbour that emerge at the apical crypt. The tight junctions between chloride and accessory cells have fewer strands and are considered leaky (Sardet *et al.* 1979) and the accessory cell projections increase the length of leaky junction. This leaky paracellular pathway is important in the Na^+ efflux pathway (see chapter 4 for more details). Interestingly, these accessory cells are

found in euryhaline fishes living in freshwater although the number of projections is much-reduced (Pisam *et al.*1988, 1989).

1.1.3 Pavement cells (PVC)

The pavement cells are generally characterized by a flattened appearance, the presence of concentric microridges on their apical surface (however, not in all species), lack of a tubular system, and relatively few mitochondria (Laurent 1984). However, there have been reports of mitochondria-rich PVCs in the brown bullhead (*Ictalurus nebulosus*; Goss *et al.*1992; 1994).

1.2. The importance of environment on ion transport protein expression

In the preceding section I have mentioned that there are some morphological and biochemical differences between MR cells of freshwater and seawater fishes. Teleost fishes are osmoregulators maintaining their internal milieu relatively constant (NaCl ~150mM) despite the large extremes in the salinity of their environment. Seawater (NaCl ~450mM) represents a hyperosmotic environment and confronts the animal with large inward ion gradients resulting in salt gain and dehydration (osmotic water loss) while freshwater (NaCl ~0.5mM) represents the opposite extreme: salt loss and water gain. To achieve an ionic homeostasis animals must be able to excrete and take up ions against large gradients in marine and freshwater environments, respectively. Also marine fishes drink seawater to replace osmotically lost water while freshwater fishes get rid of their excess water by producing copious amounts of urine (see review by Karnaky 1998).

Since the demands for ion homeostasis are diametrically opposed in marine and freshwater fishes so too must be the expression and arrangement of ion transport proteins which mediate the transepithelial ion movements. So the freshwater fish gill will be organized for salt uptake while the seawater fish gill will be organized for salt elimination. The mechanisms for

NaCl elimination by the seawater type MR cell are well characterized while the exact mechanism of NaCl uptake in freshwater is still being contested (Karnaky 1998; Perry 1997).

Movement of fishes between these salinity extremes represents a dramatic yet natural event encountered by many species. Some euryhaline estuarine and tidepool fishes face such changes on a daily basis (tidal cycles; e.g. killifish) while others may do so only a few times in their lives (for spawning; e.g. salmonids and anguillids) while some never venture out of their salinity regime (stenohaline marine and freshwater fishes).

1.2.1 Freshwater NaCl uptake models

Measurements of transepithelial potentials (TEP) in freshwater fishes predict active uptake of both Na^+ and Cl^- (Potts 1984). The uptake of Na^+ and Cl^- is not directly coupled but involves Na^+/H^+ and Cl^-/HCO_3^- exchange processes. Krogh originally proposed these mechanisms in 1937 yet the exact nature of the exchanges has still yet to be fully elucidated. The Na^+/H^+ exchange is thought to be the result of an apical vaculolar-type proton-ATPase (vH^+-ATPase) driving Na^+ uptake via a Na^+ channel (ENaC) rather than by direct coupling via a Na^+/H^+ exchanger (NHE) (Avella and Bornancin 1989; Lin and Randall 1995). It has largely been accepted that Cl^- uptake is facilitated by an apical Cl^-/HCO_3^- anion exchanger (AE; Goss *et al.* 1995). The exit step of Cl^- uptake into the blood is not known, although a basolateral Cl^- channel and a $K:Cl^-$ cotransporter have been suggested (Wright 1991). The use of H^+ and HCO_3^- as counterions implies a role for these exchange processes in acid-base balance (Heisler 1993). The freshwater mechanism of NaCl uptake will be explored in more depth in chapter 3 and additional information on the individual ion transport proteins can be found in the section *1.4* (below) on ion transport protein properties.

1.2.2 Seawater NaCl elimination model

The model for NaCl elimination in sea water centres on the chloride cell-accessory cell complex and is the same as that applied to the dogfish rectal gland and avian salt gland (Silva *et al.* 1977; e.g. Marshall *et al.* 1998). In euryhaline marine fishes, the TEP predicts active Cl^- elimination (Potts 1984). The basolateral Na^+,K^+-ATPase creates a Na^+ gradient to drive Cl^- entry via a Na^+:K^+:Cl^- cotransporter into the chloride cell (Eriksson *et al.* 1985). Potassium cycles through a K^+ channel (Suzuki *et al.* 1999). The accumulated Cl^- exits the cell apically via a CFTR (Cystic fibrosis transmembrane regulator)-like anion channel down its electrochemical gradient (Singer *et al.* 1998). Na^+ on the other hand, accumulates in the extracellular spaces and leaks out paracellularly down its electrochemical gradient (Sardet *et al.* 1979). The Na^+ equilibrium potential is generally near the measured transepithelial potential (+20mV TEP) (Evans 1979; Potts 1984).

Acid-base balance in marine fishes is achieved by Na^+/H^+ and Cl^-/HCO_3^- exchange processes but in this case driven by the inward NaCl gradients (Heisler 1993; Claiborne 1998). The cell type distribution of these exchanges is unknown. The vH^+-ATPase, which may be involved in acid-base regulation in freshwater fishes, is down regulated in fish transferred to seawater (Lin and Randall 1995). Chapter 4 will focus on the seawater fish gill ion transport processes in more detail while section *1.4* (below) provides more details on the ion transporters.

1.2.3 Models of gill NH_4^+ elimination

The majority of teleost fishes use ammonia as a nitrogenous waste product for excretion that takes place across the gill (see review by Walsh 1998). Generally, with the high ventilatory water flows across the gill and low ambient ammonia concentration, NH_3 partial pressure (P_{NH3}) gradients can account for the total ammonia efflux (Cameron and Heisler 1983). When fish are in

high environmental ammonia and the gradients for both NH_4^+ and P_{NH3} are directed inwards then the efflux component may be active. However, the analysis is complicated by boundary layer pH effects that may involve the vH^+-ATPase–ENaC and NH_3 movement rather than Na^+/NH_4^+ exchange (Wilson and Taylor 1994). Yet, there are some fish species that clearly must be using active NH_4^+ elimination because they can tolerate extremely high environmental ammonia levels and can still maintain an ammonia efflux (30mM NH_4Cl, *Periophthalmodon schlosseri*; Randall *et al.* 1999). There have been a number of ion transport proteins that have been shown to be able to substitute NH_4^+ ions for H^+ or K^+ ions and potentially could facilitate transbranchial NH_4^+ movements. Notably the Na^+/H^+ exchanger (NHE), Na^+,K^+-ATPase and Na^+: K^+: Cl^- cotransporter (NKCC) (Evans and Cameron 1986). This model will be examined in greater detail in chapter 5.

1.3 Other model iono acid-base regulatory epithelia

The models of transepithelial ion transport and cell type composition of 'tight' epithelia like turtle/toad bladder, frog skin, cortical collecting duct have been applied to fresh water fish gill and common mechanisms assumed to be present. For example, the vH^+-ATPase –epithelial sodium channel model for Na^+ uptake was proposed by Avella *et al.* (1989). Higher vertebrate distal renal epithelia and amphibian skin and bladder show some structural and functional similarities to the freshwater fish gill (turtle bladder, Stetson and Steinmetz, 1985; amphibian skin, Ehrenfeld *et al.* 1990; Larson 1991; collecting duct, Brown *et al.* 1988). These tight or high resistance epithelia have tight junctions (zonulae occludens) which minimize paracellular movements (leaks) of ions and water and allow for the generation or maintenance of steep ion gradients across the epithelia. Ion transport proteins within the apical and basolateral membrane domains of the epithelial cells constitute the principal pathways of transepithelial ion fluxes.

These epithelia also have in common, populations of MR cells that are involved in active Na^+ and Cl^- uptake in addition to acid-base regulation. Three functional types (α (A), β (B), and γ) of MR cells have been described in these epithelia (Larsen 1991). MR cells in these epithelia are also characterized by high levels of intracellular carbonic anhydrase activity (Brown *et al.* 1983; Stetson and Steinmetz 1985; Lönnerholm and Wistrand 1984). CA catalyzes the hydration of CO_2 to provide H^+ and HCO_3^- for ion transport proteins (vH^+-ATPase and AE).

The α type or acid excreting MR cell has been described in collecting duct (CD) and urinary bladder as well as amphibian skin. An apical vH^+-ATPase (Brown *et al.* 1988; Gluck and Nelson 1992) and basolateral Cl^-/HCO_3^- exchanger (AE1; Verlander *et al.* 1988; Alper *et al.* 1989) characterize these cells. Morphologically these cells have numerous apical membrane microplicae and subapical vesicles associated with rod shaped intramembranous particles and immunoreactivity to various subunits of the vH^+-ATPase complex. The intramembranous rod shaped particles are interpreted as being the transmembrane domain of the vH^+-ATPase complex (Brown *et al.* 1987a,b; Stetson and Steinmetz, 1985).

The β type MR cell, found in CD and urinary bladder epithelia, is involved in HCO_3^- elimination and electroneutral Cl^- uptake. An apical Cl^-/HCO_3^- antiporter is responsible for this exchange (AE2, Alper *et al.* 1997). HCO_3^- generated from catalyzed CO_2 hydration provides the driving gradient for Cl^- uptake while the generated H^+s are pumped across the basolateral membrane by a vH^+-ATPase (Brown *et al.* 1988). Morphologically, these cells have simple apical microvilli, a darker cytoplasm, and an amplified basolateral membrane domain associated with intramembranous rod shaped particles (Madsen and Tisher 1985).

The γ type MR cell has been described in toad skin (Larsen *et al.* 1992) and chinese crab gill (Onken and Putzenlechner 1995). Cl^- uptake by these cells is mediated by an apical AE

driven by an apical vH^+-ATPase at low mucosal Cl^- concentrations. However, in toad skin at high mucosal Cl^- concentrations an apical Cl^- channel, activated by apical membrane depolarization, mediates Cl^- uptake. Cl^- leaves through basolateral Cl^- channels. These cells have also been shown to have a significant apical Na^+ conductance (see Larsen 1991).

The principal or granular cell is another cell type that can be differentiated from the MR cells. These cells are involved in active Na^+ uptake via apical amiloride-sensitive Na^+ channels (Brown *et al.* 1989) and a basolateral Na^+,K^+-ATPase (Madsen and Tisher 1985; Sabolic *et al.* 1999). The frog skin MR cell apical vH^+-ATPase hyperpolarizes the apical membrane creating a favourable electrochemical potential for Na^+ uptake while in CD, the epithelium does not function as a syncitium and Na^+ uptake is driven by the basolateral Na^+,K^+-ATPase. These cells also have a basolateral $Na^+:K^+:Cl^-$ cotransporter which is involved in cell volume regulation.

The seawater fish gill is a leaky epithelium and involved in NaCl elimination. Other functionally similar epithelia include the avian salt gland and the shark rectal gland (Riordan *et al.* 1994). A common model is used to describe NaCl elimination in these epithelia (see *Section 2.2* above).

The mammalian kidney medulla thick ascending limb (MTAL) is involved in carrier mediated movement of ammonia (Palliard 1998).

1.4 Ion transport protein properties and evidence for their presence in the fish gill.

The translocation of ions across the plasma membrane against electrochemical gradients can be achieved through the input of energy in the form of ATP. In animal cells, the most important plasma membrane ATPase is Na^+,K^+-ATPase which is ubiquitously expressed, while a vacuolar type proton ATPase (vH^+-ATPase) is emerging as an important contributor in some epithelia. These primary active ion transporters are not only important in direct translocation of

ions but also in creating standing gradients for coupled secondary transport of other ions against otherwise unfavourable conditions. Coupling can be in the same direction, (symport or cotransport) or in the opposite direction, (antiport or exchange).

In the following section, I will give a brief description of some of the transporters involved in active ion transport which I have immunolocalized and follow with the evidence for these transporters in the fish gill.

1.4.1 Na^+,K^+-ATPase

The sodium pump or Na^+,K^+-ATPase is a ubiquitous basolateral plasma membrane protein in epithelial cells, however, in cells involved in transcellular ion transport, levels of Na^+,K^+-ATPase expression are higher (see reviews by Skou and Esmann 1992; Blanco and Mercer 1998). This ATPase is important in maintaining low intracellular Na^+ and high intracellular K^+ and the negative intracellular membrane potential. The potential difference is created by the movement of 3 Na^+ out and 2 K^+ in for each ATP consumed by the pump. The Na^+ gradient is also used to drive secondary Na^+ coupled transporters (eg Na^+/H^+ exchanger (NHE) for H^+ excretion out of the cell, or $Na^+:K^+:2Cl^-$ cotransporter (NKCC) for Cl^- uptake into the cell; see below). Na^+,K^+-ATPase belongs to the P-type class of ATPases having a phosphorylated intermediate state which makes it sensitive to inhibition by vanadate. However, Na^+,K^+-ATPase activity can be specifically inhibited by ouabain. The sodium pump is composed of an α and β subunit and possibly a third γ-subunit. The α subunit (~112kDa) is responsible for catalytic and transport properties of the pump and is the site of cation, ATP and ouabain binding. The glycosylated β subunit (40-60kDa) is essential for pump activity and is involved in modulation of Na^+ and K^+ affinities as well as having a chaperone role in α-subunit folding and insertion in to the plasma membrane. In mammals there are four α ($\alpha1$, $\alpha2$, $\alpha3$ and $\alpha4$) and three

β-subunit (β1, β2 and β3) isoforms that have been identified (Blanco and Mercer 1998). These isoforms exhibit tissue specific patterns of expression and the different αβ-heterodimer combinations contribute to the variation in Na^+ pump enzymatic properties. The γ-subunit (8-14 kDa) is not required for normal Na^+,K^+-ATPase activity, although there is accruing evidence that it can modify Na^+,K^+-ATPase activity.

In the fish gill, Na^+,K^+-ATPase has probably been the most studied ion transport protein from enzyme kinetics, to mechanism of regulation, to subunit expression (McCormick 1995). Na^+,K^+-ATPase has been localized to the MR cells using [^{3}H] ouabain autoradiography (Karnaky et al. 1976) and anthroylouabain fluorescent staining (McCormick 1990), enzyme histochemistry (Hootman and Philpott 1979; Conley and Mallatt 1987) and immunohistochemistry (eg Witters et al. 1996; Ura et al. 1996). The use of in vito assays of ouabain sensitive ATPase activity are commonplace in determining gill Na^+,K^+-ATPase activities in fishes (see McCormick 1995). Levels of Na^+,K^+-ATPase activity are closely correlated with numbers of seawater-type MR cells. The association of Na^+,K^+-ATPase with the tubular system of MR cells makes it a good cell type specific marker. It has been assumed that Na^+,K^+-ATPase in PVCs is below the level of detection by [^{3}H] ouabain binding and immunohistochemistry rather than being completely absent (Hootman and Phillpot 1979; Witters et al. 1996; Ura et al. 1996).

The α-subunit (Kawakami et al. 1985; Schorock et al 1991; Kisen et al. 1994; Cutler et al. 1995a) and the β-subunit (Noguchi et al. 1986; Appel et al. 1996; Culter et al. 1995b; Cutler et al. 1997) have been sequenced in a number of fish species. There is generally high sequence similarity amongst vertebrates (Pressley 1992). In the gill, α1 and β1 isoforms are expressed while the β2 and β3 have been shown to be absent (Cutler et al. 1995a,b, 1997). Lee et al. (1998)

13

have also shown immunoreactivity of $\alpha1$ and $\alpha3$-like subunits in the gill of fresh and sea water acclimated tilapia.

1.4.2 vH⁺-ATPase

Another plasma membrane protein involved in energizing active ion transport is the electrogenic vacuolar proton ATPase (vH⁺-ATPase or V-type ATPase; named after the H⁺-ATPase originally found in plant and fungi vacuolar membranes) (reviewed by Harvey and Wieczorek 1997; Nelson and Harvey 1999). In animals, the vH⁺-ATPase is found in lysosomes, coated vesicles, and chromaffin granules, in addition to the plasma membrane of specialized H⁺ excreting cells (eg Harvey 1992). The vH⁺-ATPase creates an electric potential difference ($\Delta\psi$) across the cell membrane in which it resides by coupling the hydrolysis of ATP to the translocation of H⁺ out of the cytoplasm (across the plasma membrane or into cellular compartments). The proton-translocation can be used for direct acidification or the $\Delta\psi$ used for secondary ion movements by channels or by sym or anti-porters. The vH⁺-ATPase is specifically inhibited by bafilomycin A_1 and concanamycin A in nanomolar concentrations (Bowman *et al.* 1988; Dröse and Altendorf 1997), N-ethylmaleimide (NEM) in micromolar concentrations and nitrate (NO_3^-) and other oxidizing agents in millimolar concentrations (Moriyama and Nelson 1987; Dschida and Bowman 1997).

The vH⁺-ATPase is a complex heteromultimeric protein composed of a cytoplasmic, peripheral catalytic (V_1) domain and a membrane spanning (V_o) domain (reviews by Finbow and Harrison 1997; Nelson and Harvey 1999). For example the kidney brush boarder vH⁺-ATPase (~580kDa) is composed of subunits 70, 56, 45, 42, 33, 31, 15, 14, and 12 kDa in size (Wang and Gluck 1990). Multiple 56 kDa B-subunit isoforms with differential expression patterns have been found (Puopolo *et al.* 1992; van Hille *et al.* 1994) as well as microheterogeneitity within the

31 kDa E-subunit (Wang and Gluck 1990; Hemken et $al.$ 1992). These differences may explain

the enzymatic differences between brush boarder and microsomal vH^+-ATPase found by Wang

and Gluck (1990) in kidney and differences found between and within other tissues and species.

The 70 kDa A-subunit is the most highly conserved of the vH^+-ATPase subunits (Finbow and

Harrison 1997) and has two characteristic cysteine residues (254 and 532) which also are

involved in NEM binding and redox modulation of vH^+-ATPase activity (Feng and Forgac 1994;

Oluwatosin and Kane 1997). There are however, also A-subunit isoforms (van Hille et $al.$ 1993).

Less is known about the other subunits (Finbow and Harrison 1997).

The vH^+-ATPase complex has been visualized by freeze fracture and high-resolution

electron microscopy as studding of vH^+-ATPase membranes (Brown et $al.$ 1992). The stud is the

V_1 domain or portasome of the complex. Immunological techniques have been used in a number

of studies to determine the cellular and subcellar distributions of the vH^+-ATPase in a number of

epithelia (in a variety of species) involved in acid-base regulation and/or ion regulation (e.g.

mammalian kidney: Brown et $al.$1988; male reproductive tract: Breton et $al.$ 1996; frog skin:

Klein et $al.$1997).

In the fish gill, vH^+-ATPase has been localized to the epithelium using immunohisto-

chemistry (70kDa A subunit: Lin et $al.$ 1994; Wilson et $al.$ 1997; 31 kDa E-subunit, Sullivan et

$al.$ 1995; Perry and Fryer 1997). Bafilomycin A_1 sensitive ATPase activity has been measured in

$vitro$ in gill homogenates (Lin et $al.$ 1993) and has been used in $vivo$ to look at the role of the

vH^+-ATPase (Morgan and Iwama 1999; Fenwick et $al.$ 1999). The use of other inhibitors also

indicates the presence of a proton pump in fish gills (Klungsøyr 1987; Lin et $al.$ 1993; Justensen

et $al.$ 1993). In addition, studding of subapical vesicles has been observed in gill epithelial PVCs

(Laurent et $al.$ 1994). Recently, the B subunit has been cloned independently by Perry et $al.$

(1999), Pelster and Niederstätter (1999) and M. Sundin (University of Odensa, DK personal communication). They all report a high degree of sequence identity with the mammalian forms.

1.4.3 Na$^+$/H$^+$ exchanger (NHE)

The sodium proton exchanger (NHE) or antiporter catalyzes the electroneutral exchange of Na$^+$ for H$^+$ in a 1:1 ratio (Bianchini and Pouysségur 1994). In vertebrates, there are at least 6 different NHE isoforms (NHE1, 2, 3, 4, 5, β; Tse *et al*. 1993). The NHE-1 is a ubiquitous basolateral isoform with the important housekeeping functions of cell pHi and volume regulation. The NHE-2, NHE-3, and NHE-4 isoforms participate in transcellular Na$^+$ movements and are expressed in epithelia and have cellular and tissue specific distributions (Hoogerwerf *et al*. 1996; Bookstein *et al*. 1997; Chambrey *et al*. 1997). The NHE-2 and NHE-3 isoforms reside in the apical plasma membrane while the NHE-4 has a basolateral location. The NHE-5 isoform is specifically expressed in the brain (Klanke *et al*. 1995). Amiloride and its analogues are very potent and specific inhibitors of sodium transport including both Na$^+$/H$^+$ exchanger and Na$^+$ channel (Benos 1982; Kleyman and Cragoe 1988). The amiloride analogues 5-(N,N-dimethyl) amiloride (HMA) and 5-(N,N-hexamethene) amiloride (DMA) are commonly used specific inhibitors of the NHE. The NHE isoforms vary in their amiloride sensitivities.

There also is evidence that NH$_4^+$ can substitute for H$^+$ in exchange for Na$^+$ by the NHE in kidney tubule (Kinsella and Aronson 1980; Nagami 1988; Blanchard *et al*. 1998). Although both NHE-2 and NHE-3 isoforms are expressed in this kidney tubule segment, the NHE-3 is present in greater amounts and believed to mediate the apical NH$_4^+$ movement (Palliard 1998).

In the trout erythrocyte a βNHE isoform has been characterized (Borgese *et al*. 1994). The βNHE is catacholamine stimulated and is important in erythrocyte pHi regulation during periods of acidosis (i.e. during exercise) that would otherwise decrease hemoglobin-oxygen

16

affinity. In the sculpin (*Myoxocephalus octodecimspinosus*), the βNHE and NHE2-like isoforms have been identified using molecular techniques (Reverse Transcriptase-Polyerase Chain Reaction (RT-PCR); Claiborne *et al.* 1999). NHE1-like immunoreactivity has also been demonstrated in gill homogenates of sculpin and killifish (*F. heteroclitus*) adapted to freshwater and seawater. Externally applied amiloride has been shown to reduce Na^+ uptake by 84-94% (Perry and Randall 1981; Wright and Wood 1985), however with no effect on net acid or ammonia fluxes (Avella and Bornancin 1989; Lin and Randall 1991). NHE has also been proposed to be involved in facilitating NH_4^+ elimination (Na^+/NH_4^+ exchange) but unequivocal evidence is lacking (Wright and Wood, 1985; Wilson *et al.* 1994). The cellular distribution (MR cells vs PVC) of these NHE isoforms in the gill is still unknown although the NHE1-like and βNHE isoforms are probably ubiquitously distributed to the basolateral membrane of both epithelial cell types.

1.4.4 Apical epithelial Na^+ channel (ENaC)

The epithelial sodium channel (ENaC) facilitates the uptake of Na^+ across the plasma membrane following its electrochemical gradient. The ENaC is a hetero-oligomer composed of three subunits (α,β,γ; 85-95 kDa) that have been identified in a number of different tissues and species (Canessa *et al.* 1994; Garty and Palmer 1997). There is also an amiloride blockable Na^+ channel that has been purified from bovine renal papillae and A6 cells (Benos *et al.* 1995). It is not entirely clear if this purified Na^+ channel represents an entirely different ENaC or a complex incorporating subunits of the αβγENaC (Garty and Palmer 1997). As mentioned earlier, Na^+ uptake via the channel is sensitive to amiloride and its analogues, notably benzamil (Benos 1982; Kleyman and Cragoe 1988).

In the fish gill, the only evidence for the presence of an apical Na^+ channel comes from the equivocal experiments using water borne amiloride (Perry and Randall 1981; Wright and Wood 1985). In these experiments it is not possible to distinguish between the inhibition of NHE or ENaC-vH^+-ATPase. Since there are conditions where the NHE mechanism cannot explain Na^+ uptake the alternative model has been used. Recently, Fenwick *et al.* (1999) have reported that Na^+ uptake in larval tilapia is sensitive to bafilomycin A1.

1.4.5 Cl^-/HCO_3^- anion exchanger (AE)

The chloride-bicarbonate antiporter mediates the 1:1 electroneutral exchange of chloride and bicarbonate across the plasma membrane (reviewed by Alper 1991). The AE is involved in intracellular pH and volume regulation as well as transepithelial acid-base transport. There are three AE that have been identified to date (AE1, AE2, and AE3; Alper 1991; Brosius *et al.* 1997). The erythrocyte Cl^-/HCO_3^- exchanger (AE1) or band 3 protein (the most abundant transmembrane protein and is recognized as the third band on SDS-PAGE) was the first AE to be characterized (Kopito and Lodish 1985). Band-3 related proteins have also been found in non-erythroid tissues in the basolateral membrane domain, notably in a subpopulation of kidney cortical collecting duct intercalated cells which are involved in acid excretion (A-type cells; Wagner *et al.* 1987; Verlander *et al.* 1988; Kudrycki and Shull 1989). The AE1 is sensitive to the disulfonic stilbene inhibitors of Cl^- transport DIDS (4,4'-diisothiocyanatostilbene-2,2'-disulfonic acid) and SITS (4-acetamido-4'-isothiocynato-stilbene-2,2'-disulfonic acid; Cabantchik and Rothstein 1972; Schuster *et al.* 1986). AE-2 has been identified in a number of non-erythroid tissues in either an apical or basolateral location and is thought to be primarily involved in bicarbonate secretion (Martínez-Ansó *et al.* 1994; Stuart-Tilley *et al.* 1994; Alper *et al.* 1997). In the kidney cortical collecting duct, AE2 is found apically in a subpopulation of intercalated cells

involved in base excretion (B-type cells; Alper *et al.* 1997). AE2 is relatively insensitive to stilbene inhibition (Schuster *et al.* 1986; Tago *et al.* 1986). The AE-3 has only been found expressed in excitable tissues (brain and cardiac muscle; Brosius *et al.* 1997).

In the fish gill, evidence for a Cl^- / HCO_3^- exchanger comes from studies using the stilbene inhibitors SITS and DIDS. In a number of studies, this inhibitor has been shown to reduce Cl^- influx and cause an alkalosis; results consistent with Cl^-/HCO_3^- exchanges (Perry *et al.* 1981). Goss and Wood (1990) using a two substrate model were able to demonstrate a 1:1 Cl^-/HCO_3^- exchange ratio. Recently, Claiborne *et al.* (1997) have demonstrated that a DIDS sensitive mechanism exists that contributes to acid-base regulation in a seawater fish. Sullivan *et al.* (1997) were able to demonstrate in situ hybridization of an oligonucleotide probe for mammalian kidney AE1 (Kudrycki and Shull 1989), however, Northern analysis was not done.

There is also the possibility that anion exchange is driven by Cl^-/HCO_3^- -ATPase (Bornancin *et al.* 1980). This mechanism is however not widely accepted as mitochondrial contamination is a likely source of membrane associated activity (Claiborne 1998).

1.4.6 Na^+ :K^+ :$2Cl^-$ cotransporter (NKCC)

The Na^+: K^+: $2Cl^-$ cotransporter (NKCC) or bumetanide sensitive cotransporter (BSC) makes use of the inward sodium gradient to drive the electroneutral cotransport of K^+ and 2 Cl^-. There are two NKCC isoforms, NKCC1 (BSC2) and NKCC2 (BSC1), which are found expressed in the apical and basolateral membrane domains, respectively, of sections of the kidney tubule. In specialized salt secreting organs, like the dogfish rectal gland and the bird nasal salt gland, the NKCC2 plays an important role in the movement of Cl^- into the cell against its electrochemical gradient. The NKCC also contributes to cell volume regulation. The NKCC is

sensitive to the loop diuretics furosamide and bumetanide (see reviews by O'Grady *et al.* 1987; Payne and Forbush 1995).

In the fish gill, the NKCC plays a similar role in the seawater chloride cell as in the special elasmobrach and avian salt glands. In marine teleosts, Cl^- excretion has been shown to be sensitive to basolaterally applied furosemide and bumetanide (Erikkson *et al.* 1985). In the elasombranch, NKCC mRNA has been shown to be expressed (Xu *et al.* 1994). Recently, C. Cutler (personal communication) has cloned a NKCC in a teleost fish.

1.4.7 CFTR anion channel

In mammalian tracheal epithelia, colonic cells and pancreatic duct cells, the movement of Cl^- out across the apical membrane is facilitated by a small conductance, voltage insensitive, cAMP activated Cl^- channel (Cohen 1994). This anion channel has been identified as a cystic fibrosis transmembrane regulator(CFTR; Anderson *et al.* 1991; Bear *et al.* 1992). Bicarbonate is another anion which makes use of this channel and may represent an important mechanism for HCO_3^- secretion and acid-base regulation (Smith and Welsh 1992; Poulsen *et al.* 1994; Hogan *et al.* 1997; Lee *et al.* 1998; Clarke and Harline 1998). In addition the CFTR is involved in the regulation of other apical membrane channels (e.g. ENaC; Schwiebert *et al.* 1999). The CFTR channel is inhibited by diphenylamine-2-carboxylate (DPC) and 5-nitro-2-(3-phenylpropylamino) benzoic acid (NPPB) but insensitive to 4,4'-diisothiocyanostilbene-2,2'-disulfonic acid (DIDS).

In fishes, a CFTR-like Cl^- channel has been found to be expressed in the gills and is involved in the same pathway for Cl^- elimination as found in the elasmobranch and bird salt glands (Riordan *et al.* 1994). The fish CFTR has been cloned in the killifish *Fundulus heteroclitus* and shows low homology with human and shark forms (59 and 60% identity,

respectively; Singer *et al.* 1998). Patch-clamp recordings have identified a Cl⁻ channel with similar properties to the CFTR in seabass (*Dicentrarchus labrax*) primary culture respiratory-like cells (Duranton *et al.* 1997) and overnight primary cultures of killifish opercular epithelial cells (Marshall *et al.* 1995).

1.4.8 Others

There are also numerous other ion channels, co-transporters and antiporters and ATPases present in the branchial epithelium that are involved in the transepithelial movements of ions however, since I have not immunolocalized them I have not described them in detail (above). I will however, now mention some of them and review recent publications. An inwardly rectifying K^+ channel had been cloned and immunolocalized to branchial MR cells in the eel (Suzuki *et al.* 1999). There is postulated to be a basolateral K^+:Cl⁻ cotransporter in fish MR cells but there is no work on this subject (Wright 1991; Mount *et al.* 1998; see Chapter 3 disscusion). The group of Flik and Wendelaar-Bonga has extensively studied the ion transport proteins involved in Ca^{++} uptake. They have characterized a basolateral plasma membrane (PM) Ca^{++} ATPase, and Na^+ /Ca^{++} exchanger (Flik *et al.* 1995). There is an apical Ca^{++} channel that is not well characterized.

1.5 Study of fish ion regulation using in vitro models

The complex anatomical organization of the gill has made it a difficult organ to study using traditional electrophysiological techniques. To date there is but one *in situ* measurement of potential differences across apical or basolateral membranes of the branchial epithelium (filament PVC; Clarke and Potts 1998b) and intracellular concentrations of ions have only been measured using x-ray microanalysis (Morgan *et al.*1994; Morgan and Potts 1995). However, intracellular ion concentrations have been measured using fluorescent dyes in isolated branchial cells (Li *et al.* 1997). Complicating matters is the thinness of the lamellar PVCs (1-15μm), the

presence of the MR cell tubular system that infiltrates the cell that is easily damaged by electrode insertion, and the presence of a mucus coat covering the epithelium (Shepard 1992; Sandbacka *et al.* 1998).

The use of surrogate model epithelia, which can be mounted in Ussing chambers, to study transport properties of the branchial epithelium under rigorous conditions has allowed the elucidation of the mechanism of NaCl transport in the seawater fish (see chapter 4; Karnaky *et al.* 1977; Foskett and Scheffey1982; Marshall 1985). Such models also are yielding some interesting results that might lead us to reevaluate our current thinking. The seawater model for NaCl elimination is based largely on work using the opercular epithelium MR cell surrogate model, yet studies using a primary culture of seabass (*Dicentrarchus labrax*) branchial PVCs show similar transport properties (active Cl^- efflux; Avella and Ehrenfeld 1997; Duranton *et al.* 1997; Avella *et al.* 1999). In primary cultures of freshwater fish branchial PVCs active Cl^- uptake can be demonstrated, yet there is no active Na^+ uptake (Wood *et al.* 1998). The finding of active Cl^- uptake by PVCs is unusual because *in vivo* studies have indicated that MR cells are the sites of Cl^- uptake and that active Na^+ uptake should be performed by PVCs (see review by Goss *et al.* 1995). It seems that the PVC primary culture is only useful for studying permeability properties of the branchial epithelium (Gilmour *et al.* 1999). Perhaps showing greater promise is the opercular epithelia preparation of freshwater acclimated tilapia (*O.niloticus*) which is capable of unidirectional Na^+ and Cl^- (and Ca^{++}) uptake (Burgess *et al.* 1998). Unfortunately, however, like in the freshwater primary cultures, these influx rates are dwarfed by large efflux rates.

1.6 Thesis problem

In the gill we have an organ that is very plastic, adapting to changing environmental conditions to meet the needs of whole animal ion regulation. From the many decades of work on

this organ we have become fully aware of its importance (to the fish) but many of the details still remain unknown. Surrogate models have helped address some of our questions but also have created others. Ion transport proteins facilitate the transepithelial transport of ions and their patterns of expression determine the ion regulatory function of the epithelium. The following hypotheses, formed from current models of ion regulation, are posed and tested in this thesis using immunological techniques to localize ion transport proteins, which form the basis of the different models.

In freshwater teleost fishes, the following hypotheses are tested, 1.) Hypothesis (*H*): Branchial PVCs are involved in vH$^+$-ATPase driven Na$^+$ uptake via an ENaC and 2.) *H*: Branchial MR cells are involved in Cl$^-$ uptake via an apical AE protein. In marine teleost fishes, the following hypotheses are tested, 1.) *H*: Branchial PVCs are involved in active Cl$^-$ excretion and 2.) *H*: Branchial PVCs are involved in acid-base regulation via apical NHE and AE proteins. Finally, in the terrestrial mudskipper fish, the following hypothesis is tested, *H*: The branchial epithelium is the site of active NH$_4^+$ elimination.

Immunolocalization techniques enable the determination of the cellular and subcellular distributions of proteins. Since many of the ion transport proteins are common to many vertebrates ranging from human to fishes and even invertebrates and unicellular forms of life, the use of non-homologous antibodies may be useful in the study of the fish gill epithelium. Antibodies make very specific, high affinity probes for the detection of proteins of interest. In the next chapter on General Materials and Methods a list of the antibodies used and some background information will be provided. In the following chapters, the different models of ion regulation in freshwater, seawater fishes and the mudskipper will be addressed.

Chapter 2. GENERAL MATERIALS AND METHODS

2.1 Tissue fixation for immunolabeling

Gill tissue was immersion fixed using fixatives designed for post embedding immunolabeling at either light or electron microscopic levels.

A. For light level investigations excised gill arches were fixed in 3% paraformaldehyde (PFA) / phosphate buffered saline (PBS) pH 7.4 or Bouin's solution (24% formalin, 5% acetic acid, 71% saturated aqueous picric acid, pH 2.2) for 2h at rt or overnight at 4°C. Following fixation tissues were rinsed in PBS and 10% sucrose/ PBS and either frozen in liquid nitrogen or processed for paraffin embedding (Paraplast, Fisher Scientific).

B. For immuno-electronmicroscopy smaller pieces of tissue (pairs of filaments) were fixed in either 2% paraformaldehyde, 75mM L-lysine, 10mM sodium m-periodate (PLP) fixative (McLean and Nakane 1974) or by a two step 3% PFA, 20mM ethylacetimidate, PBS and 3% PFA, 0.1% Glut, PBS fixation procedure (Tokuyasu and Singer 1976). Following fixation either overnight at 4°C or 1-2 h at rt, tissue was rinsed in PBS and free aldehyde groups were quenched in a 50mM NH_4Cl solution for 20min. The tissue was then dehydrated through a decreasing temperature (rt to -20°C) ethanol series (1 h at 30%, 50%, 70%, 95% and 3x 100% EtOH), gradually infiltrated with resin (EtOH:Unicryl; 2:1,1:1,1:2 for 30 min at -20°C and 100% Unicryl 2x1h and overnight at –20°C) and transferred to Beem caps for embedding (BioCell Intl. UK; Scala et al. 1992). The resin was polymerized by UV light at -10°C over 3 days.

Note: In Chapter 5 Material and Methods there is a section on tissue fixation and processing for routine electron microscopy.

2.2 Immunocytochemistry

2.2.1 Immunofluorescence microscopy

Cryosections (5-10 μm) were cut on a cryostat at -20°C, collected onto either 0.01% poly-lysine (Sigma) coated slides or electrostatically charged slides (SuperFrost Plus, Fisher Scientific) and fixed in acetone at -20°C for 5 minutes. Sections were then air dried.

Paraffin sections (5 μm) were collected onto charged slides, air dried at 37°C overnight, and dewaxed though a series of xylene baths and rehydrated through an ethanol series finishing in PBS. Sections were circled with a hydrophobic barrier (DakoPen, Dako DK) and sections were blocked with 5% NGS/0.1% BSA /TPBS, pH7.4 for 20 min. Incubation with primary antibody diluted 1:50-1:200 in 1%NGS/ 0.1% BSA/ TPBS, pH 7.3 for 1-2 hour at 37°C. Sections were then rinsed in 0.1% BSA/ TPBS or PBS followed by incubation with secondary antibody conjugated to fluorescein isothiocyanate (1:50 FITC, Chemicon Intl. Inc), Texas Red (1:100, Molecular Probes or Jackson Lab), or Cy3 (1:200, Sigma) for 1 h at 37°C. Following rinsing with 0.1% BSA/ TPBS, sections were mounted with glycerol:PBS or VectaShield mounting media and viewed on a Ziess AxioPhot photomicroscope with the appropriate filter sets.

2.2.2 Immunoelectron microscopy

Ultrathin sections were made on a Reichart ultramicrotome and collected onto either formvar or formvar-carbon coated nickel grids. Following air-drying, sections were rehydrated by floating grids on drops of PBS. Grids were then transfered to drops of diluted 1° antisera (1:100) and incubated at rt for 1h. Grids were then rinsed and transferred to drops of diluted 2° antisera (1:100) conjugated to colloidal gold (10 or 20nm, Sigma, Chemicon) and incubated for 1h at room temperature. Grids were rinsed with PBS and fixed for 10 min in 1% glut/PBS and rinsed again in ddH$_2$O before counter staining with lead citrate (Reynolds 1963) and saturated

uranyl acetate. Sections were viewed on a Phillips 300 TEM and photographed with Kodak EM

plate film 4489.

2.3 Antigen Retrieval

A number of antigen retrieval techniques were employed to enhance immunoreactivity of

tissue sections with various antisera used (see Antibodies below). These techniques expose

epitopes masked during tissue fixation or cause the refolding of proteins in such a way that they

now possess epitopes not normally present. Two unmasking techniques that were most useful

included the preincubation of sections with 1%SDS (sodium dodecyl sulphate) in PBS pH 7.3

(Brown, *et al.* 1996) and heating sections in ddH$_2$O (100°C) (reviews by Werner *et al.* 1996;

Taylor *et al.* 1996). Enzymatic treatment using trypsin was also attempted (Curran and Gregory

1977; Wilson *et al.* 1997) but abandoned in favour of the other techniques.

The SDS pre-treatment was conducted on sections mounted on charged slides only

(Brown *et al.* 1996). Following dewaxing of paraffin sections or air drying of cryosection, the

sections were circled with a hydrophobic marker and flooded with 1% SDS in PBS, pH 7.3 for 5

min at rt. The sections were then rinsed in a stream of PBS and put through a series of PBS baths

(Coplin jars; 5,10,15min) with gentle agitation. The sections tended to be very hydrophobic so

care had to be taken when applying the blocking buffer so as to make sure the sections did not

dry. The standard immunolabeling protocol was then followed (see section 2.2.1 on

Immunofluorescence microscopy).

The heat denaturation technique was conducted on paraffin and cryo-sections mounted on

either charged or poly-l-lysine coated slides. After, their respective dewaxing or air drying, slides

were placed in boiling water for 10 to 30 min. The slides were placed within a coplin jar

submerged within a beaker of boiling water on a hot plate to avoid bubbles disturbing the

sections. Sections were then air-dried and circled with a hydrophobic pen, the sections blocked and the standard immunolabeling protocol followed through (see section 2.2.1 on *Immunofluorescence microscopy*).

2.4 SDS-PAGE and Western Analysis

Tissue was thawed in ice-cold SEI buffer (300 mM sucrose, 20mM EDTA, 100mM imidazole, pH 7.3) and filaments were scraped from the arch with a blunt razor blade. Filaments were then homogenized with a Potter-Elvehjem tissue grinder on ice (1000 rpm, 10 strokes). The homogenate was centrifuged at 2000 g and the supernatant discarded. The pellet was resuspended in 2.4 mM deoxycholate in SEI buffer and re-homogenized. Following a second centrifugation at 2000 g the supernatant was saved.

Total protein was measured by either the Bradford (Bradford 1976) or Lowry (Lowry *et al.* 1951) methods using a BSA standard and the homogenate diluted to $1\mu g \cdot \mu l^{-1}$ in Laemmli's buffer (Laemmli 1970). Proteins were separated by polyacrylamide gel electrophoresis (PAGE) under denaturing conditions described by Laemmli (1970) using a vertical mini-slab apparatus (Bio-Rad, Richmond CA). Proteins were transferred to either Immobilon P membranes (PVDF polyvinylidene difluoride; Millipore) or nitrocellulose membranes using a semidry transfer apparatus (Bio-Rad; Blattler *et al.* 1972; Towbin *et al.* 1979). Blots were then blocked in 3% skim milk/ TTBS (0.05% Tween 20 in Tris Buffered Saline: Tris-HCl; 500 mM NaCl 5 mM KCl, pH 7.5).

Blots were incubated with primary antisera for 1 h at rt or overnight at 4°C. Following a series of washes with TTBS, blots were incubated with either goat anti-rabbit or anti-mouse HRP (horse radish peroxidase) or AP (alkaline phosphatase) conjugated antibody (Sigma). Bands were

visualized by enhanced chemiluminescence with HRP (ECL; Amersham) or BCIP/NBT (5-bromo-4-chloro-3-indolyl phosphate/ nitroblue tetrazolium) reaction with AP.

2.5 *Antibodies*

The antibodies used in this thesis are described in detail below and are also found listed in Appendix 1. A list of species' crossreactive is found in Appendix 2.

2.5.1 vH$^+$-ATPase

The V-ATPase was immunolocalized using a rabbit polyclonal antibody raised against a synthetic peptide corresponding to a sequence from the catalytic 70 kDa A-subunit of the bovine V-type H$^+$-ATPase complex (*C*SHITGGDIYGIVNEN; Südhof *et al.* 1989) (Protein Service Laboratory, University of British Columbia). This sequence is well conserved from plants, and fungi. The peptide was conjugated to keyhole limpet haemocyanin (KLH) using a maleimide linker (Pierce) and (300µg) mixed with Freund's complete adjuvant (Sigma). New Zealand White rabbits were immunized by subcutaneous injection and boost injections (300µg) with incomplete Freund's adjuvant followed at biweekly intervals with test bleed. The rabbits were terminally bled and the sera collected. A pre-immunization serum was collected for use as a control. Sera were tested by peptide ELISA and Western blot analysis of gill homogenates.

A polyclonal antibody raised against the same peptide (Südhof *et al.* 1989) has been used to identify the vH$^+$-ATPase A-subunit distribution in mammalian kidney (Madsen et at. 1991; Kim *et al.* 1992). Using rat kidney as a positive control tissue I found identical results as those published above.

A rabbit polyclonal antibody raised against a peptide sequence from the E-subunit of the vH$^+$-ATPase was kindly donated by S.F Perry and J.N. Fryer (University of Ottawa). This is the same antibody used by Sullivan *et al.* (1995). I was, however, unable to reproduce the results of

Sullivan *et al.* (1995) or Perry and Fryer (1997) on rainbow trout with the aliquot of antisera provided.

2.5.2 ENaC (Epithelial Na$^+$ channel)

The following epithelial Na$^+$ channel antibodies were kindly provided by Dale Benos (Department of Biophysics and Physiology, University of Alabama at Birmingham).

The amiloride sensitive sodium channel was immunolocalized using a rabbit polyclonal antibody raised against a synthetic peptide corresponding to amino acids 411 to 420 of the β subunit of the human epithelial Na$^+$ channel clone (βhENaC; CGEKYCNNRDF; D.J. Benos, unpublished, McDonald *et al.* 1995). The IgG used was purified on a protein A column (0.8 mg · ml^{-1} in glycine/tris buffer pH 7.5).

The α subunit bovine ENaC (α-bENaC) rabbit polyclonal antibody was raised against a full length fusion protein (Ismailov *et al.* 1996) generated from the cDNA α bENaC clone (Fuller *et al.* 1995). The IgG was purified from whole serum on a protein A column (1.4 mg · ml^{-1} glycine/tris buffer pH7.8).

A rabbit polyclonal antibody raised against biochemically purified bovine renal papilla amiloride-sensitive epithelial Na$^+$ channel complex (αENaC; Sorscher *et al.* 1988). The IgG fraction was purified from whole serum on a protein A column (1.48 mg · ml^{-1} glycine/tris buffer pH 7.4). This antibody has been used in a number of different studies to localize both low and high amiloride sensitive Na$^+$ channels in a number of different tissues (eg. Smith *et al.* 1993; Brown *et al.* 1989)

2.5.3 Na$^+$,K$^+$-ATPase

Gill Na$^+$,K$^+$-ATPase was immunolocalized using a monoclonal antibody specific for the α subunit of chicken Na$^+$,K$^+$-ATPase (Takeyasu *et al.* 1988). The antibody (α5) developed by

D.M. Fambrough (Johns Hopkins University, MD) was obtained from the Developmental Studies Hybridoma Bank maintained by the University of Iowa Department of Biological Sciences, Iowa City, IA 52242, under contract NO1-HD-7-3263 from the NICHD. The antibody was purchased as culture supernatant (0.9 mg · ml^{-1}). This antibody is now in routine use for identifying gill MR cells (Witters *et al.* 1996; Lee *et al.* 1998; Dang *et al.* 1999; Piermarini and Evans 1999).

2.5.4 AE (Cl$^-$ / HCO$_3^-$ Anion exchanger)

Polyclonal antibodies were generated against rainbow trout erythroid band 3 protein (AE1) purified by SDS polyacrylamide electrophoresis (under reducing conditions) (Cameron *et al.* 1996). This antibody has been shown to crossreact with trout and lamprey erythrocyte preparations by Western analysis (Cameron *et al.* 1996). Unpurified rabbit serum was kindly provided by Bruce Tufts (Queens University, Kingston ON).

I attempted to use a rabbit polyclonal antibody generated against the native 43-kDa fragment cytoplasmic domain of human erythroid band 3 (Appell and Low 1981; Verlander *et al.* 1988) (Philip Low Department of Chemistry, Purdue University, West Lafayette, Indiana). This antibody has been used to immunolocalize AE in the basolateral membrane of collecting duct α-type intercalated cells (Wagner *et al.* 1987; Verlander *et al.* 1988; Drenckhahn *et al.* 1987; Madsen, *et al.* 1991; Kim *et al.* 1992). However, it was not found to be crossreactive with fish tissues (gill tissue or erythrocytes).

I also tested a monoclonal antibody generated against a synthetic peptide (NRSLAGQSGQGKPR) corresponding to amino acids 871 to 884 in the deduced primary structure for human kidney AE2 (Martínez-Ansó *et al.* 1994; Eduardo Martínez-Ansó Department of Medicine and Liver Unit, University Clinic and Medical School, University of

Navara, Pamplona, Spain). This amino acid sequence corresponds to the Z-loop, characteristic of non-erythroid AE. This antibody has been shown to cross react with the luminal membrane of shark rectal gland tissue (George *et al.* 1998). I was unable to obtain cross reactivity with teleost fish gill tissue either by Western analysis or immunohistochemistry with either the human AE1 or AE2 antibodies. Rat kidney tissue was used as a positive control.

2.5.5 NHE (Na$^+$ / H$^+$ exchanger)

Rabbit polyclonal antibodies generated against glutathione S-transferase fusion proteins incorporating the last 87 amino acids of NHE2 (Tse *et al.* 1994) and 85 amino acids of NHE3 (Hoogerwerf *et al.* 1996). The NHE2 antibody (597) and two polyclonal antibodies (1380 and 1381) against NHE3 were the kind gift of Mark Donowitz (Departments of Medicine and Physiology, Gastrointestinal Division, The Johns Hopkins University School of Medicine, Baltimore MD). Antibody specificity has been determined in NHE expressing PS120 cell lines. These antibody have been used in a number of different studies for immunolocalization and Western analysis of NHE2 and 3 (He *et al.* 1997; Lee *et al.* 1998; Levine *et al.* 1993; Sun *et al.* 1997).

Three monoclonal antibodies generated against a maltose binding protein fusion protein that contained the carboxyl terminal 131 amino acids of NHE3 were also tested. (Biemesderfer *et al.* 1997). I was unable to demonstrate crossreactivity of gill tissue by either Western analysis or immunohistochemistry with these three commercially available monoclonal antibodies (Chemicon Intl. CA).

2.5.6 CFTR (Cystic Fibrosis Transmembrane Regulator)

A commercial monoclonal antibody specific to human CFTR (165-170 kDa) was purchased from NeoMarkers Inc. (CA). The antibody was raised against a full length human

CFTR recombinant protein and the IgM purified from ascites fluid by ammonium sulphate precipitation (0.2 mg · ml^{-1} 10mM PBS pH 7.4, with 0.2% BSA and 15 mM sodium azide). This antibody did not cross react with dogfish rectal gland DFTR cryosections and has only been reported to cross react with human tissue.

2.5.7 NKCC (Na$^+$: K$^+$:2Cl$^-$ cotransporter)

Gill Na$^+$: K$^+$:2Cl$^-$ cotransporter (145- 205 kDa) was immunolocalized using monoclonal antibodies against shark rectal gland NKCC (J3) (Lytle *et al.* 1992) and human colonic NKCC1 (T4) (Lytle *et al.* 1995). The antibodies (T4, J3) developed by Christian Lytle (Division of Biomedical Sciences, University of California, Riverside, CA) were obtained from the Developmental Studies Hybridoma Bank maintained by the University of Iowa Department of Biological Sciences, Iowa City, IA 52242, under contract NO1-HD-7-3263 from the NICHD. The antibodies were both purchased as cell culture supernatant (0.8 mg · ml^{-1}). Fixed-frozen dogfish (*Squalus acanthias*) rectal gland tissue was used as a positive control. The T4 monoclonal antibody has greater species crossreactivity than J3 whose immunoreactivity is limited to the shark tissues (Lytle *et al.* 1995).

2.6 In vitro ATPase assay

Na$^+$,K$^+$-ATPase and vH$^+$-ATPase activities (μmol Pi · mg^{-1} protein · h^{-1}) in gill homogenates were determined at 22.5°C in a plate reader (Thermomax, Molecular Devices Corp., CA) using a protocol modified from McCormick (1993). In short, ATPase activities were measured using the coupled-enzyme method of Scharschmidt *et al.* (1979). ATPase activity was measured under three conditions for each sample in triplicate 1.) 200μl reaction mixture + 50μl salt solution + 5 μl homogenate, 2.) 200μl reaction mixture containing 1.0 mM ouabain (Sigma) + 50μl salt solution + 5μl homogenate 3.) 200μl reaction mixture containing 100mM KNO$_3$ +

50μl salt solution + 5μl homogenate. The reaction solution contained 50mM Imidazole, 2.8 mM PEP (phosphoenolpyruvate), 0.22 mM NADH (nicotinamide adenine dinucleotide, reduced), 0.7mM ATP (adenosine triphosphate), 4U/ml LDH (lactic dehydrogenase) and 5 U/ml PK (pyruvate kinase) and the salt solution contained 50 mM Imidazole, 189 mM NaCl, 10.5 mM MgCl and 42 mM KCl. Na^+-K^+ ATPase and vH^+-ATPase activities were defined as specific inhibition by 1.0 mM ouabain and 100 mM KNO_3, respectively. However, in chapter 4, vH^+-ATPase activity in gill crude membrane preparation was measured as NEM (N-ethylmaleimide) sensitive activity according to Lin and Randall (1993). Additional KNO_3 and bafilomycin A1 dose response curves were constructed. Since DMSO was used to dissolve the bafilomycin A1 and it interferes with the assay, an equivalent amount of DMSO was added to paired wells for use as a control. The bafilomycin A1 stock concentration was determined photometrically at 280nm using its extinction coefficient of 12100 M/cm and subtracted from a DMSO blank (Werner and Hagenmaier 1984).

Chapter 3. THE FRESHWATER FISH GILL.

3 SUMMARY

Teleost fishes, living in fresh water, engage in active ion uptake for ion homeostasis. Current models of NaCl uptake involve Na^+ uptake via an apical amiloride-sensitive epithelial Na^+ channel (ENaC) energized by an apical vH^+-ATPase or alternatively by an amiloride-sensitive Na^+/H^+ exchange (NHE) protein and apical Cl^- uptake mediated by an electroneutral, SITS-sensitive Cl^-/HCO_3^- anion exchange (AE) protein. Using non-homologous antibodies, I have determined the cellular distributions of these ion transport proteins to test the predicted models. Na^+,K^+-ATPase was used as a cellular marker for differentiating branchial epithelium mitochondria-rich (MR) cells from pavement cells (PVCs). In both the freshwater tilapia (*Oreochromis mossambicus*) and trout (*Oncorhynchus mykiss*) the vH^+-ATPase and ENaC co-localized to PVCs, although in the trout apical membrane labeling is also found in MR cells. In the freshwater tilapia, apical AE immunoreactivity is found in the MR cells. Thus, a freshwater-type MR chloride cell exists in teleost fishes. The NHE-like immunoreactivity is associated with the accessory cell type in freshwater fishes in addition to a small population of PVCs in tilapia.

3.1 INTRODUCTION

In freshwater fish, the active uptake of sodium and chloride is necessary for ionic homeostasis. The consequence of living in a hypoosmotic medium and having a large surface area (the gill) subject to large outward ion gradients is the continual loss of salts by passive diffusion and gain of water by osmosis. The fish manages the water gain by producing copious amounts of urine however this also adds to ion loss problems, as the kidney is not capable of reabsorbing all the salts. Active branchial ion uptake is crucial in ion homeostasis. The uptake of Na^+ and Cl^- is achieved by electroneutral Na^+/H^+ and Cl^-/HCO_3^- exchange mechanisms (Krogh 1939).

3.1.1 Sodium uptake models

Sodium uptake is mediated by an amiloride-sensitive Na^+/H^+ exchange which is either directly or indirectly coupled and shows saturation kinetics (Wright 1991; Potts 1994). It is difficult to explain Na^+ uptake using the directly coupled carrier mediated Na^+/H^+ exchange (NHE) mechanism because of the absence of physiologically relevant gradients to drive the exchange process under many natural conditions (reviewed by Lin and Randall 1995). The Na^+ levels in the epithelium (6.4-16.5 mM in isolated PVCs and MR cells; Li *et al.* 1997) are typically greater than in the freshwater environment (<1mM) where the sodium chemical gradient is insufficient to drive Na^+/H^+ exchange (Avella and Bornancin 1989). Wright (1991) calculated that a pH gradient of 0.3 units would be required to drive Na^+ uptake via a NHE but acid excretion and Na^+ uptake have been measured at water pHs well below that of the epithelium (pHi 7.4 Wood 1991). However, a Na^+/H^+ exchanger could explain Na^+ uptake by a fish in water of 0.5 mM [Na^+], pH 8.0 (Wright 1991). The amiloride concentration typically used (10^{-4} M) does not distinguish between the NHE and ENaC routes of Na^+ uptake (e.g. Wright and

Wood 1985; Clarke and Potts 1998a). The NHE specific inhibitor, amiloride analogue DMA, had no effect on Na^+ uptake rates in isolated gill filament preparations (Clarke and Potts 1998b).

The alterative model employs an apical electrogenic vacuolar-type proton ATPase and an amiloride sensitive Na^+ channel. This indirectly coupled exchange has been proposed for frog skin and several other iono acid-base regulating epithelia (Harvey 1992; Stetson and Steinmetz 1985). The frog skin model (Ehrenfeld *et al.*1985) for sodium uptake has also been proposed by Avella and Bornancin (1989) to operate in freshwater fish. This model has been further substantiated by the work of Lin and Randall (1991,1993) and co-workers (1994).

The basis for the mechanism is an apical (V-type) proton-ATPase which pumps protons across the apical membrane creating a membrane potential capable of driving passive sodium influx via an amiloride sensitive channel against its concentration gradient. The protons are provided from CO_2 hydration catalyzed by intracellular carbonic anhydrase (e.g. Rahim *et al* 1988; Lin and Randall 1991; Clarke and Potts 1998a,b). The accumulated HCO_3^- is thought to exit the cell via a basolateral Cl^- / HCO_3^- exchanger with an associated Cl^- channel, however, experimental evidence is lacking. Na^+ movement across the basolateral membrane is facilitated by Na^+,K^+-ATPase (Richards and Fromm 1970; Payan *et al.* 1975).

Lin and Randall (1993) initially predicted the plasma membrane H^+-ATPase was a P-type rather than the V-type H^+-ATPase based on the pharmacological properties of the enzyme. The relatively low sensitivity of the ATPase to the vH^+-ATPase specific inhibitor bafilomycin A1 and oxyanion NO_3^- can be explained by the level of purification of their membranes (Dröse and Altendorf 1997; Dschida and Bowman 1997).

The immunolocalization of V-type H^+-ATPase to the apical membrane of pavement cells (Lin *et al.* 1994; Sulivan *et al.* 1995) and correlative data from x-ray microanalysis (Morgan, *et*

al. 1994, Morgan and Potts 1995) and morphometric-ion flux studies (reviewed by Goss *et al.* 1995) suggest that sodium uptake is performed by pavement cells. However, Lin *et al.* (1994) also reported apical vH^+-ATPase labeling in MR cells. In addition, high levels of Na^+,K^+-ATPase activity were associated with the MR cell and the levels in PVCs were below detection (Witters *et al.* 1996). Apart from the information that an amiloride-sensitive Na^+ channel exists on the apical surface, the localization of Na^+ channels to the PVC or MR cell apical membrane has yet to be demonstrated.

3.1.2 Chloride uptake model

Evidence for an epithelial Cl^- / HCO_3^- exchanger in fish gills comes from kinetic, pharmacological, and correlative morphological studies (reviewed by Goss *et al.* 1995). Cl^- influx has been shown to be stimulated by infusion of HCO_3^- (Kerstetter and Kirschner 1972) and there is a good correlation between the rate of Cl^- uptake and base secretion (de Renzis and Maetz 1973). More recently, analysis using two substrate enzyme kinetics has further suported a 1:1 Cl^- / HCO_3^- exchange mechanism (Wood and Goss 1990). The use of the anion transport inhibitor SITS (4-acetamido-4'-isothiocynato-stilbene-2,2'-disulfonic acid; Cabantchik and Rothstein 1972) in the external bathing medium resulted in a reduction of Cl^- influx after both short and longer term treatments (66% Perry *et al.* 1981, 71% Perry and Randall 1981, repectively). Interestingly, no effect of short term SITS exposure was seen on net proton efflux (Lin and Randall 1991). No studies on a basolateral SITS sensitive anion exchanger have been conducted. However, apically applied thiocyanate (SCN$^-$; non-specific anion transport inhibitor) has been shown to inhibit Cl^- uptake while SCN$^-$ injection resulted in no change in Cl^- influx (de Renzis 1975). Inhibition of carbonic anhydrase activity by acetazolamide also reduced Cl^- influx (Maetz and Garcia-Romea 1964).

It is, however, somewhat unclear how thermodynamically feasible Cl^-/HCO_3^- exchange would be as a mechanism for Cl^- uptake in the freshwater fish gill (Wright 1991; Perry 1997). X-ray microanalysis would indicate total intracellular Cl^- levels of 40mM (Morgan *et al.* 1994) however intracellular Cl^- activities would likely be much lower. Wright (1991) calculated that HCO_3^- driven Cl^- uptake is possible assuming similar $[Cl^-]_i$ as the frog skin (5-20mM) and $[HCO_3^-]_i$ similar to plasma levels (5mM) and water $[Cl^-]$ of 0.5 mM and $[HCO_3^-]$ of 1 mM. It should be noted that $[HCO_3^-]_i$ has not been measured in the fish gill and intracellular carbonic anhydrase and cellular acid excreting mechanisms (NHE and vH^+-ATPase) may be important in elevating intracellular HCO_3^- levels to make Cl^-/HCO_3^- exchange a more thermodynamically feasible mechanism for Cl^- uptake.

In the freshwater fish gill, Cl^- uptake is thought to occur through the MR cells. Evidence for this location is based on correlative studies of MR cell fractional surface area and Cl^- fluxes (review by Goss *et al.* 1995). In addition, various disturbances resulting in changes in intracellular ion concentrations as measured using x-ray microanalysis tend to support this idea of a freshwater chloride cell (Morgan *et al.* 1994; Morgan and Potts 1995).

It is possible that the mechanism for Cl^- uptake by the MR cell is similar to that proposed for the toad skin (Larsen 1991) and chinese crab (Onken *et al.* 1991, 1995). In the freshwater adapted crab (*Eriocheir sinensis*) transcellular SITS sensitive chloride influx has been shown to be driven by a V-type ATPase (Riestenpatt *et al.* 1995). In this animal, chloride influx was sensitive to externally applied bafilomycin A_1 but insensitive to serosally applied ouabain. Larsen (1991) has given these cells the name γ-cells.

In this chapter I will demonstrate the presence and branchial distribution of the amiloride sensitive sodium channel, Na^+/H^+ exchanger, and SITS sensitive anion exchanger

immunologically through the use of non-homologous antibodies. If the vH^+-ATPase –ENaC model is to be valid then co-localization must be demonstrated. Further clarity of the cell types involved will be provided by the specific labeling of MR cell by a Na^+,K^+-ATPase antibody (Witters *et al.* 1996). The specificities of the antibody probes used will be verified by Western analysis. In addition, the sensitivity of the gill vH^+-ATPase activity to bafilomycin A1 and KNO_3 as measured by Lin and Randall (1993) will be readdressed using purified gill membrane preparations. Data will be presented on two freshwater species of fish: the rainbow trout (*Oncorhynchus mykiss*) and the tilapia (*Oreochromis mossambicus*) although data on the freshwater coho salmon (*Oncorhynchus kisutch*) is also presented in chapter 4.

3.2 MATERIALS AND METHODS

3.2.1 Animals

Four adult tilapia, *Oreochromis mossambicus*, were obtained from the SkekKipMei fish market, Kowloon, Hong Kong. The fish were kept in glass aquaria within a recirculation system and fed commercial fish food. The fish were approximately 500 g and were kept less than one week. The water temperature was 26°C and lighting conditions were not controlled. Water composition (mM): Na^+ 0.435; Cl^- 0.457; Ca^{++} 0.395; pH 8.1.

Adult tilapia were also obtained from the Cambie Seafood Market in Richmond. These animals were approximately 1kg and were kept less than 2 days in the lab and not fed. These animals were only used for ATPase activity measurements.

Rainbow trout, *Oncorhynchus mykiss*, were obtained from local suppliers in the Vancouver and Ottawa areas (Canada) and maintained under local conditions (Table 3.1). Fish were fed commercial trout chow and kept under a natural photoperiod.

3.2.2 Tissue Sampling and Fixation

Fish were quickly netted and killed by a blow to the head. The second gill arch from both left and right sides was excised and immersion fixed in 3% PFA/PBS at ambient temperature (26°C) for 2h. Tissue was then rinsed in PBS and then either frozen (liquid nitrogen) or processed for conventional paraffin embedding (HistoPrep, Fisher Scientific). Fixed-frozen tissue was stored at -70°C until required for sectioning.

Additional gill tissue was also freeze-clamped (liquid nitrogen) and stored frozen for later Western analysis and measurement of ATPase activities. Some fish had their gills perfused for 5 min with ice-cold heparinized saline via the cannulated bulbus arteriosis to remove blood.

The use of paraffin embedded tissue allowed large areas to be sectioned. Basically, sections incorporated leading and trailing edges as well as lamellar and interlamellar filament epithelia.

3.2.3 Tissue preparation for Western analysis and ATPase assay

Most tissue for Western analysis was prepared using the crude membrane method of Zaugg (1982). Briefly, gill tissue was scraped with a microscope slide into ice-cold SEI buffer (0.3 M sucrose, 0.02 M EDTA, 0.1 M imidazole pH 7.3). Tissue was then homogenized using a Potter-Elvehjem tissue grinder. The homogenate was centrifuged at 2000g for 10 min, the supernatant was discarded and the pellet resuspended in SEID (2.4 mM deoxycholate in SEI buffer) with the homogenizer. The homogenate was again centrifuged at 2000g for 10 min and the supernatant saved. Total protein was measured using either the Bradford (1976) or Lowry (1951) method and a BSA standard.

A more refined method was used for preparing membranes for the ATPase assay and some Western analysis. Saline perfused gill tissue was prepared by differential centrifugation using a protocol adapted from Flik and Verbost (1994), and Dubinsky and Monti (1986). The

Table 3.1 Profiles of Ottawa and Vancouver tap waters in which rainbow trout were reared.

mM	Ottawa	Vancouver
$[Na^+]$	0.15	0.02
$[Cl^-]$	0.15	0.01
$[Ca^{++}]$	0.45	0.03
pH	7.5	5.8-6.4
	Bindon *et al.* 1994	GVRDwaterworks

gills were perfused with cold heparinized modified Cortland's saline (Mommsen and Hochachka 1994) for 5 min and the gill arches excised. The tissue was scraped with a glass microscope slide onto an ice-cold piece of glass (~2.5 g material from 150 g fish). The scrapings were then suspended in erythrocyte lysis buffer (9 parts 0.17 M NH_4Cl: 1 part 0.17 M Tris-HCl, pH7.4, 10μg/ml aprotinin; 40 ml for approximately 2.5 g scraped tissue) for 20 minutes at room temperature. Intact branchial cells and pieces of tissue were collected by low-speed spin (200 g for 10 min at 4°C), and the supernatant discarded. The pellet was resuspended in 20-40 ml hypotonic buffer (25mM NaCl, 1mM HEPES-Tris pH 8.0, 1.0 mM DTT, 10μg/ml aprotinin) and homogenized using a loose fitting dounce homogenizer (20-40 strokes). A low-speed spin followed to remove nuclei and cellular debris (550 g for 10 min at 4°C). The supernatant was decanted and centrifuged at 13 000 g for 10 min at 4°C. The mitochondrial pellet was discarded. The supernatant was decanted and centrifuged at 33 000 g for 45 min at 4°C and the membrane pellet saved. The resulting pellet was resuspended with a 23 gauge needle in 0.5-1.0 ml of suspension buffer (100mM mannitol, 5mM HEPES pH 7.6, 10 μg/ml aprotinin) and either frozen or layered on a sucrose step gradient (5-25% sucrose, 1 M KBr 10 mM HEPES, pH 7.4).

An attempt was made to isolate apical membranes from basolateral membrane fractions using a sucrose gradient. The membrane suspension was layered on top of the sucrose step gradient (25, 20, 15, 10 and 5% sucrose) and centrifuged at 100 000 g for 120 min at 4°C. The layers were removed by puncturing the side of the tube with a 23 g needle and 10 ml syringe. Membrane fractions were resuspended in +5 ml suspension buffer and centrifuged at 150 000 g for 15 min. Pellets were resuspended in 200μl suspension buffer and 50 μl aliquots taken for total protein measurement and remainder frozen (-70°C). Total protein was measured using a modified Bradford (1976) method using a BSA standard (Simpson and Sonne 1982).

3.2.4 ATPase Activity

vH^+-ATPase activities (μmol Pi $\cdot$ mg^{-1} protein $\cdot$ h^{-1}) in trout gill membrane prepared by differential centrifugation were determined at 22.5°C in a plate reader (Thermomax, Molecular Devices Corp., CA) modified from McCormick (1993). Dose response curves were also constructed for KNO_3 (0 to 100 mM) and bafilomycin A1 (0.01 μM to 1μM). See General Materials and Methods for additional details of the assay.

3.2.5 Immunocytochemistry, Western analysis, and Antibodies Employed

The distribution of band 3-like anion exchanger (AE), epithelial Na^+ channel (ENaC), Na^+/H^+ exchanger (NHE2,3), vH^+-ATPase A and E subunits, Na^+,K^+-ATPase, and Na^+:K^+:2Cl$^-$ cotransporter (NKCC) were determined by indirect immunofluorescence and immunoperoxidase methods in paraffin and fixed frozen gill tissue as well as unfixed frozen tissue. Antibodies against CFTR, and AE2 were not crossreactive with epithelia. See General Materials and Methods for additional information.

3.3 RESULTS

3.3.1 Tilapia

vH^+-ATPase

The rabbit polyclonal anti-peptide antibody to the A subunit of the V-type proton ATPase cross reacts with a population of squamous epithelial cells covering the lamellae and filament on the up stream or efferent (leading) side (Figure 3.1A). There is an absence of immunoreactive epithelial cells towards the downstream or afferent (trailing) side of the filament (Figure 3.1B). Neither pillar cells, erythrocytes, nor mucocytes show any labeling. In Western blots bands in the high 70 kDa MW range are recognized (Figure 3.1E).

Na^+,K^+-ATPase

The distribution of Na^+,K^+-ATPase as determined using the mouse monoclonal antibody to the α subunit of the Na^+,K^+-ATPase is mainly restricted to a population of cells concentrated on the afferent side of the filament (Figure 3.1D, 3.2C, 3.6A). These cells are frequently found on the trailing edge and in the interlamellar spaces of the filament epithelium. They also are found on the lamellae although generally towards the base. There are clearly fewer immunoreactive cells toward the efferent side of the filament (Figure 3.1C). Immunopositive cells are strongly labeled and ovoid or cuboidal in appearance and sometimes associated with an apical crypt. Nuclei also can be made out as a negative image against the cytoplasmic labeling. Mucocytes that have a similar shape as MR cells and which also appear in the trailing edge of the filament epithelium show no labeling (Figure 3.6A). Control labeling with normal mouse serum and buffer also produces negligible levels of fluorescence (Figure 3.2D). In Western blots a 116 kDa and a weaker 78 kDa band are recognized (Figure 3.1F).

Cl^- / HCO_3^- anion exchanger (AE)

The polyclonal antibody generated against trout erythrocyte AE1 (AE1t) crossreacts strongly with tilapia erythrocytes regardless of the fixation conditions used (Figure 3.2A). However, in order to achieve crossreactivity with epitopes in the epithelium a SDS pre-treatment of sections is required. In SDS treated sections, the antibody cross reacts with the apical region of cells that are also strongly immunoreactive for Na^+,K^+-ATPase (Figure 3.2C). There are, however, Na^+,K^+-ATPase immunoreactive cells not associated with apical AE1t. The number of double-labeled cells is greatest in the afferent region of the filament epithelium. Control incubations of sections with normal rabbit serum result in negligible levels of fluorescence (Figure 3.2B). In Western blots, the antibody crossreacts with a 110 kDa band from saline perfused gill tissue as well as erythrocytes (Figure 3.3). An additional band in the 70 kDa MW

range is the result of antibody crossreactivity with a contaminate in the electrophoresis set-up which is likely of microbial origin (see Marshall and Williams 1984).

Epithelial Na$^+$ channel

In the tilapia, the rabbit polyclonal antibody raised against the β subunit of the human epithelial Na$^+$ channel specifically labels a population of squamous cells in the epithelium on the efferent side of the filament (Figure 3.4A). Both lamellar and filament epithelial cells stain in this region. The labeled cells are in the same location as those that were positive for the vH$^+$-ATPase but do not extend as far toward the afferent side of the filament (Figure 3.4A). Pillar cells and erythrocytes show no immunoreactivity. Normal rabbit serum IgG (Figure 3.4B,C) and buffer control sections were also negative. Western blots of tissue homogenates recognize bands in the 98kDa MW range (Figure 3.4D).

I was unable to successfully use either the αbENaC or biochemically purified amiloride sensitive Na$^+$ channel antibodies for immunohistochemical localization of ENaC. This was despite trying a number of antigen retrieval techniques and fixation protocols. However, in Western blots crossreactivity can be demonstrated (Figure 3.5A,B). The αbENaC and ENaC antibodies both recognize bands in the 74 kDa size range.

Na$^+$ / H$^+$ Exchanger (NHE)

In the freshwater tilapia gill, the rabbit polyclonal antibody against NHE-2 crossreacts with cells in both the lamellar and filament epithelia (Figure 3.6B,D). In the afferent region, immunoreactive cells are found predominantly in the interlamellar space of the filament epithelium. These cells are round in appearance and frequently associated with Na$^+$,K$^+$-ATPase immunoreactive cells (Figure 3.6A). In contrast, immunoreactive cells in the efferent region are

squamous and not associated with Na^+,K^+-ATPase immunoreactive cells (Figure 3.6D). Pillar cells, mucocytes, and erythrocytes show negligible levels of immunoreactivity.

In Western blots the NHE-2 antibody crossreacts with a doublet in the 87 kDa MW range reported for this protein (Figure 3.7). However, there are also immunoreactive bands in the 56, 60 and 100kDa MW ranges. A comparison of separated purified membrane homogenates on a 5-25% sucrose gradient probed for NHE-2 and Na^+,K^+-ATPase (as a basolateral membrane marker) indicates that the 87 kDa bands are not in the basolateral fraction of the sucrose gradient fraction.

The antibody against the NHE-3 isoform (Ab 1380) crossreacts with unidentified material in the basal portion of the epithelium that is also recognized by the normal rabbit serum control. This unidentified material has the appearance of a grape-like cluster.

3.3.2 Trout

In the rainbow trout, the distribution of the vH^+-ATPase and Na^+,K^+-ATPase have been previously described using the same antibodies (Lin *et al.* 1994; Witters *et al.* 1996, respectively). Western analysis data has also been presented by Lin *et al.* (1994) for the vH^+-ATPase A subunit.

The trout reared in Vancouver tap water (ion-poor) have (A-subunit) vH^+-ATPase widely distributed through out the branchial epithelium (Figure 3.8 A,B). This pattern of labeling is similar to that reported by Lin *et al.* (1994). However, immunoreactivity is also observed with branchial mucocyte mucin granules. There are many Na^+,K^+-ATPase immunoreactive cells throughout both the lamellar and filament epithelia. The epithelial Na^+ channel β subunit has an identical staining pattern as the vH^+-ATPase in trout (Figure 3.8C). Western analysis reveals immunoreactivity of the α5 Na^+,K^+-ATPase antibody with a band of approximately 116kDa, the

vH^+-ATPase A-subunit anti-peptide antibody around 70kDa and the β and α subunits of the ENaC with bands at approximately 98 and 74 kDa, respectively (Figure 3.10).

The gill tissue of three of the four Ottawa trout examined have a discontinuous apical distribution of vH^+-ATPase. This pattern of labeling is similar to that reported by Sullivan *et al.* (1995). The number of Na^+,K^+-ATPase immunoreactive cells is also not as prolific as observed in the Vancouver trout. The fourth Ottawa trout has a vH^+-ATPase labeling pattern similar to that observed in Vancouver trout.

Immunogold labeling of the vH^+-ATPase is associated with the apical plasma membrane of both MR cells and PVC (Figure 3.9). There is also clustered subapical labeling of electron-dense areas suggestive of vesicle labeling. The density of labeling decreases toward the basal portion of the epithelial cells.

I was unable to get the vH^+-ATPase E-subunit anti-peptide antibody used by Sullivan *et al.* (1995) to crossreact with tissue sections or Western blots. Also the NHE-2 and NHE-3 antibodies 597 and 1380, respectively, did not crossreact. The antibody against trout erythroid band-3 protein crossreacts only with erythrocytes and never with the branchial epithelium. A number of antigen retrieval techniques were used but all yielded negative results (1% SDS/PBS, trypsin, and heat).

FIGURE 3.1 Double labeled sections on the tilapia gill epithelium from efferent leading (**A,C**) and afferent trailing ends (**B,D**) of the filament using a rabbit polyclonal antibody against the A-subunit of vH^+-ATPase (**A,B**) and mouse monoclonal antibody against the α subunit of Na^+,K^+-ATPase (**C,D**). The arrow indicates a lone MR cell in the efferent filament epithelium. Western blots of crude gill tissue homogenate probed with the vH^+-ATPase (**E**) and Na^+,K^+-ATPase (**F**) antibodies. MW stds: 205, 112, 87, 69, 56, 39, and 33 kDa. Arrows indicate immunoreactive bands. Scale Bar= 50 μm
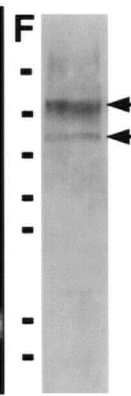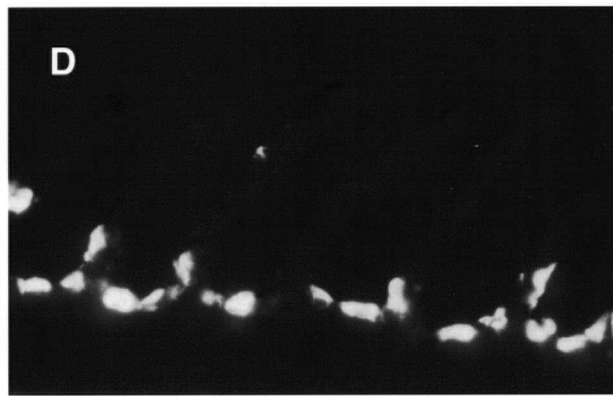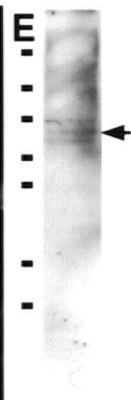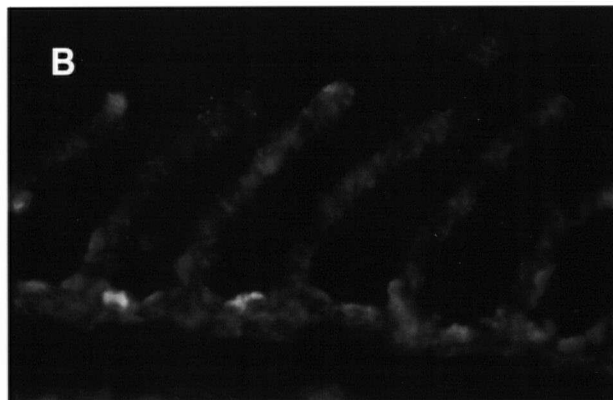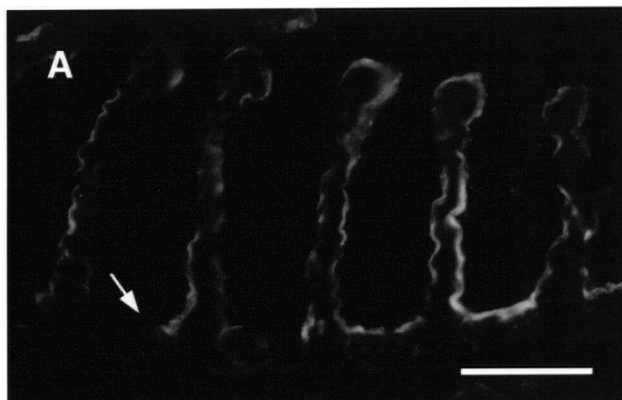
FIGURE 3.2 An SDS treated section of the tilapia gill filament trailing edge duel labeled for AE1t (**A**) and Na^+,K^+-ATPase (**C**) using a rabbit polyclonal antibody generated against trout erythrocyte band 3 (AE1t) and a mouse monoclonal antibody specific of the α subunit of Na^+,K^+-ATPase, respectively. The corresponding phase-contrast image is in panel (**E**). Arrows indicate cells immunopositive for both AE1t and Na^+,K^+-ATPase. Arrowheads indicate erythrocytes (immunopositive for AE1t only). A similarly treated section (**F**; phase-contrast) was incubated with normal rabbit serum (**B**) and normal mouse serum (**D**) for use as controls for (**A**) and (**C**), respectively. Scale bar = 50 μm
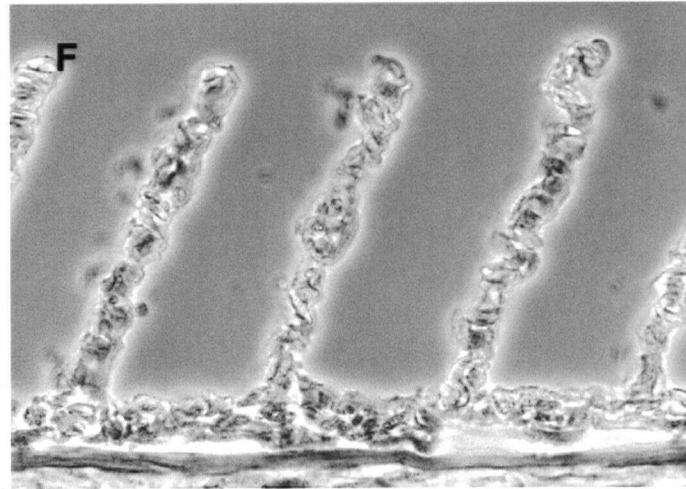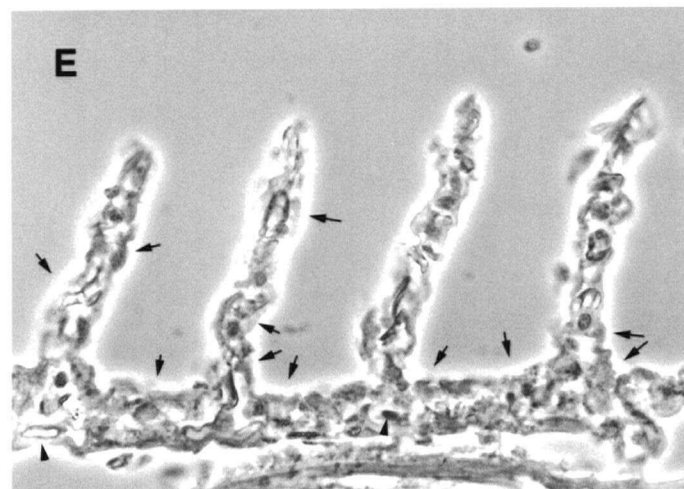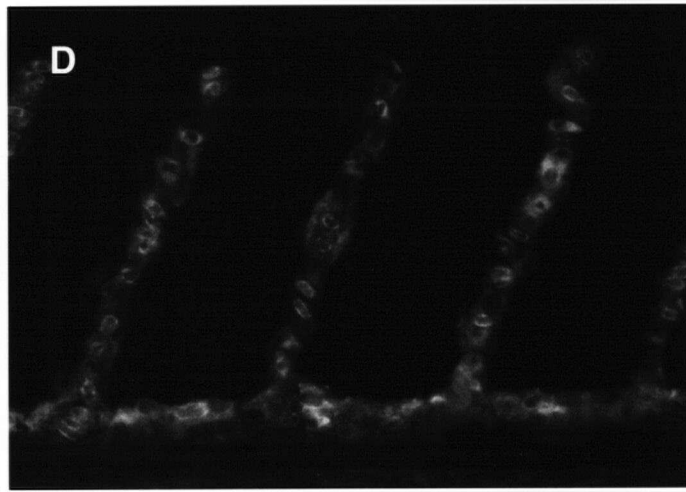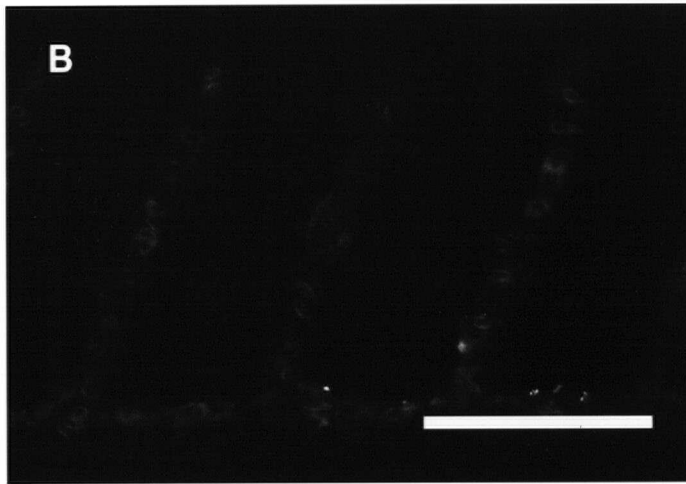
FIGURE 3.3 Western blot of lanes loaded with tilapia red blood cell homogenate (rbc), saline perfused crude gill tissue homogenate (gill), and loading buffer (blk) probed with the AE1t antibody. The arrow indicates an immunoreactive band with an apparent MW of 116 kDa. The arrowhead indicates a non-specific reaction with a contaminant of the system.
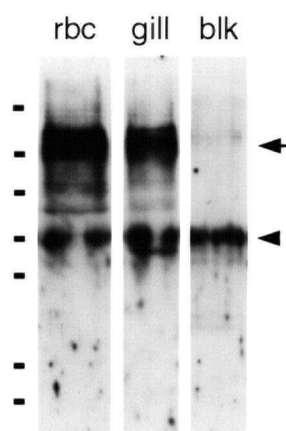
FIGURE 3.4 Indirect immunofluorescence labeling of βENaC in the tilapia afferent lamellar and filament epithelium (**A**). This is the same region as in Figure 3.1A,C. Paired immunofluorescence (**B**) and phase contrast (**C**) images of a control section incubated with normal rabbit serum at an equivalent dilution indicate low non-specific labeling. A western blot of crude gill homogenate probed with the βENaC antibody (**D**). MW stds: 205, 112, 87, 69, 56, 39, and 33 kDa. Scale Bar = 50 μm
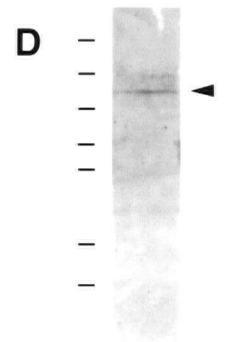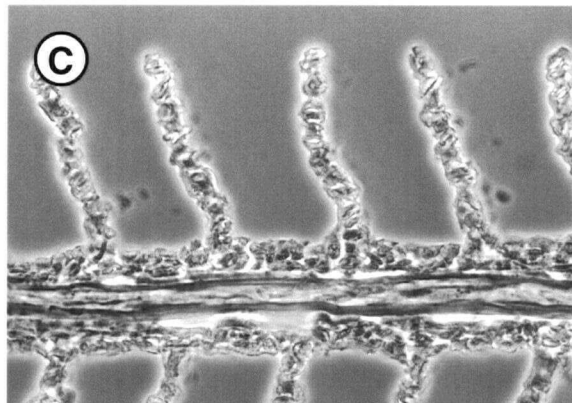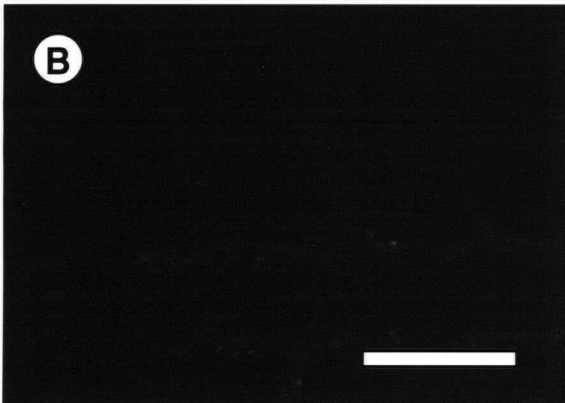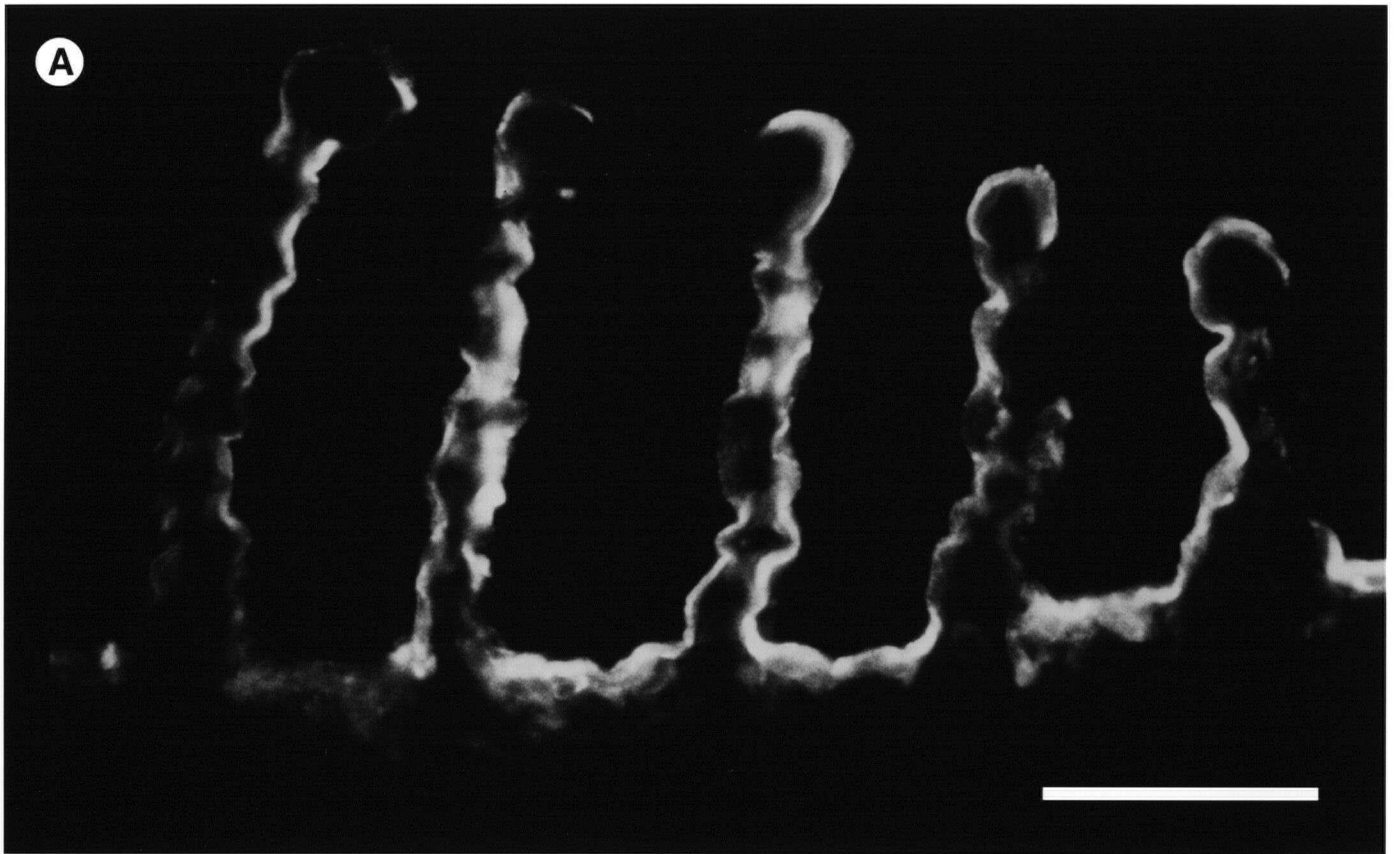
FIGURE 3.5 Western blot of tilapia gill tissue homogenate separated on a 10% polyacrylamide gel and probed with antibodies generated against the α subunit of bovine ENaC (**A**) and biochemically purified bovine amiloride-sensitive Na^+ channel complex (**B**). Both antisera recognize a 74 kDa band.
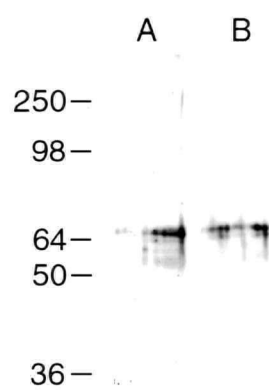
FIGURE 3.6 Immunolocalization of NHE-2 (**b,d**) in the tilapia gill using a rabbit polyclonal antibody. The section from the afferent area of the filament has been duel label with antibody 597 specific for NHE-2 (**b**) and α5 for Na^+,K^+-ATPase (**a**). The corresponding phase-contrast image is shown in (**c**). Arrows indicate Na^+,K^+-ATPase positive cells with apical crypts and arrowheads indicate labeled cells without apical crypts. The crossed arrows indicate cell immunoreactive for NHE-2. The inset (**d**) shows NHE-2 labeling of squamous epithelial cells in the efferent region. Scale bar = 50 μm.

59
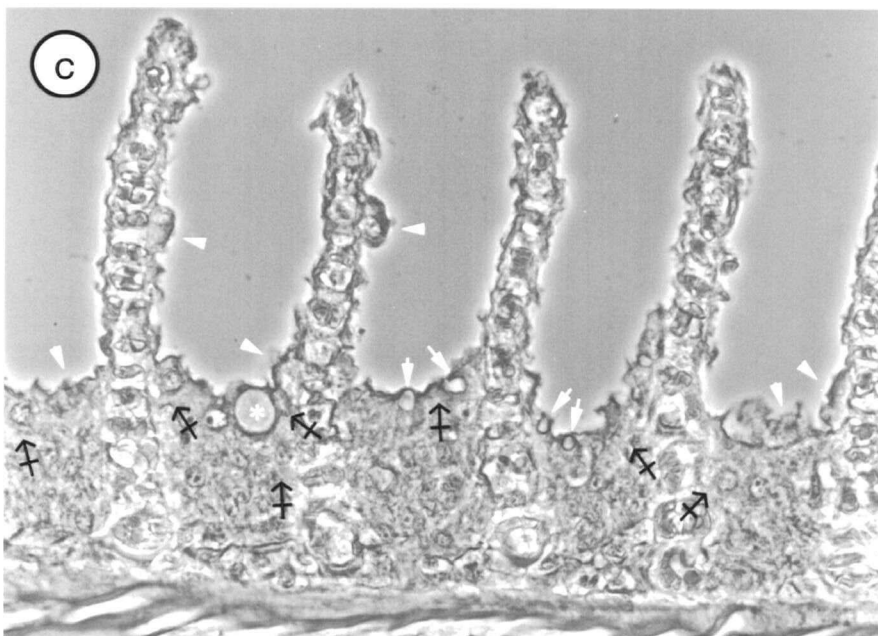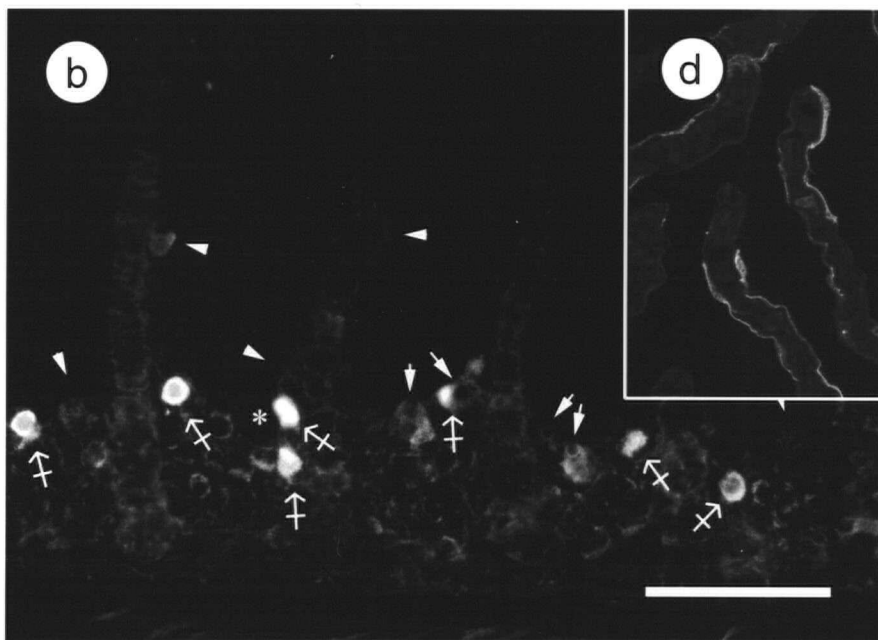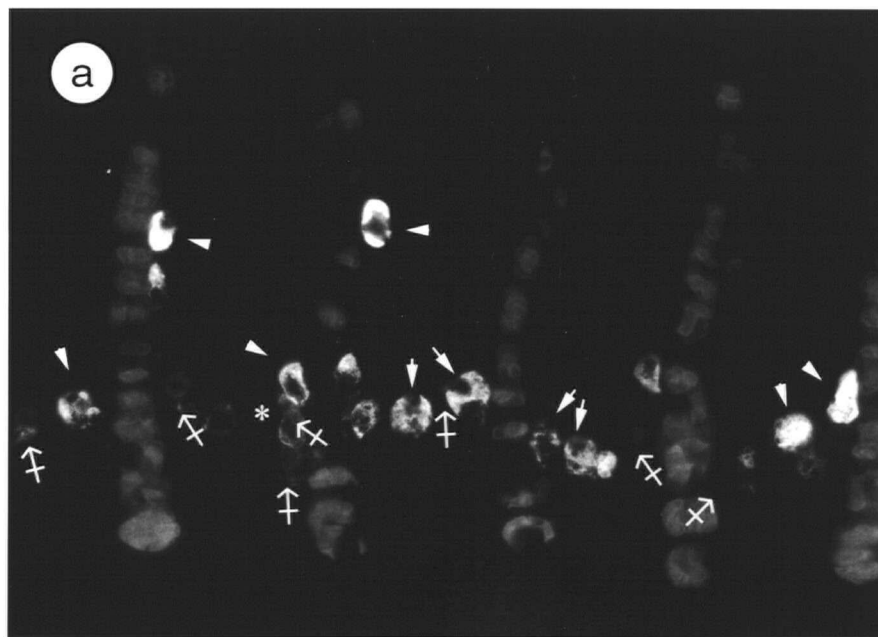
FIGURE 3.7 Western blots of a tilapia gill membrane preparation separated on a sucrose step gradient (**c**). Lanes were loaded with 10μg and separated on a 10% polyacrylamide gel and transferred to PVDF membranes and probed with antibodies against the NHE2 isoform using the polyclonal antibody 597 (**a**) and Na^+,K^+-ATPase using antibody α5 (**b**). Lane 1 was loaded with membrane preparation loaded onto the sucrose gradient. The lane numbers (2-8) refer to the layers collected from the sucrose gradient. Molecular weight standards: 205, 112, 87, 69, 56, 38.5 and 33.5 kDa. Large arrowheads indicate bands of interest, while smaller arrowheads indicate other bands.

a

| | 1 | 2 | 3 | 4 | 5 | 6 | 7 | 8 |

b

| | 1 | 2 | 3 | 4 | 5 | 6 | 7 | 8 |

c

sample (1)
5% Sucrose
10%
15%
20%
25%
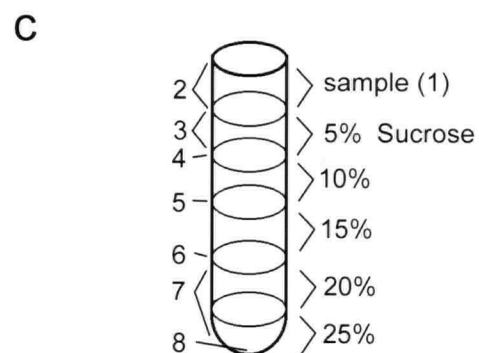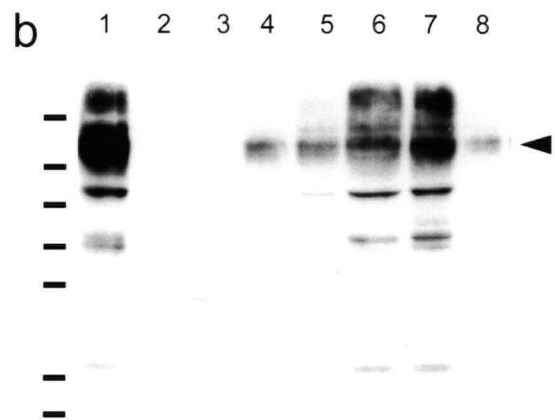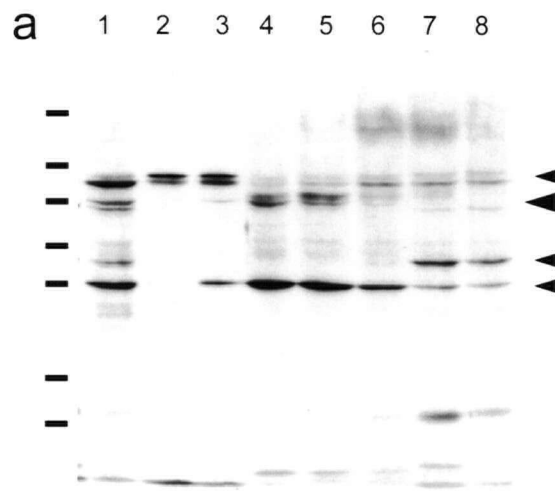
FIGURE 3.8 Immunolocalization of vH^+-ATPase, Na^+,K^+-ATPase and ENaC in trout gill tissue. Indirect double immunofluorescence labeling of vH^+-ATPase (green, FITC) and Na^+,K^+-ATPase (orange, Cy3) in unfixed-frozen (**A**) and fixed-paraffin embedded sections (**B**). In (**A**), the asterisks indicate mucus labeling, the arrows double labeled cells and the arrowheads cells immunoreactive for only Na^+,K^+-ATPase. In (**B**), the arrows indicate double-labeled cells and the arrowheads indicate cells immunoreactive for only vH^+-ATPase or Na^+,K^+-ATPase. In micrograph (**C**) apical immunoreactivity for βhENaC is indicated by arrows in unfixed-frozen sections of trout gill. Scale bars (A) 100, and (B, C) 25 μm
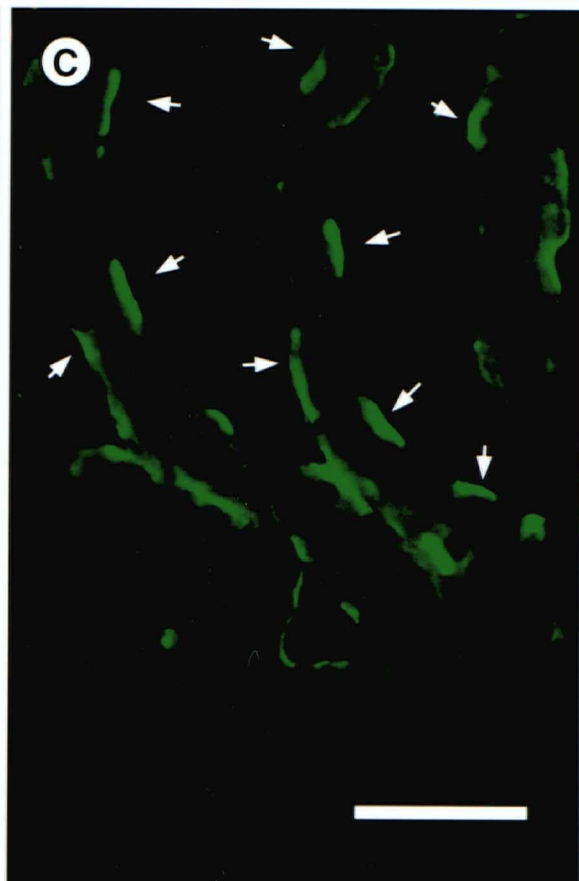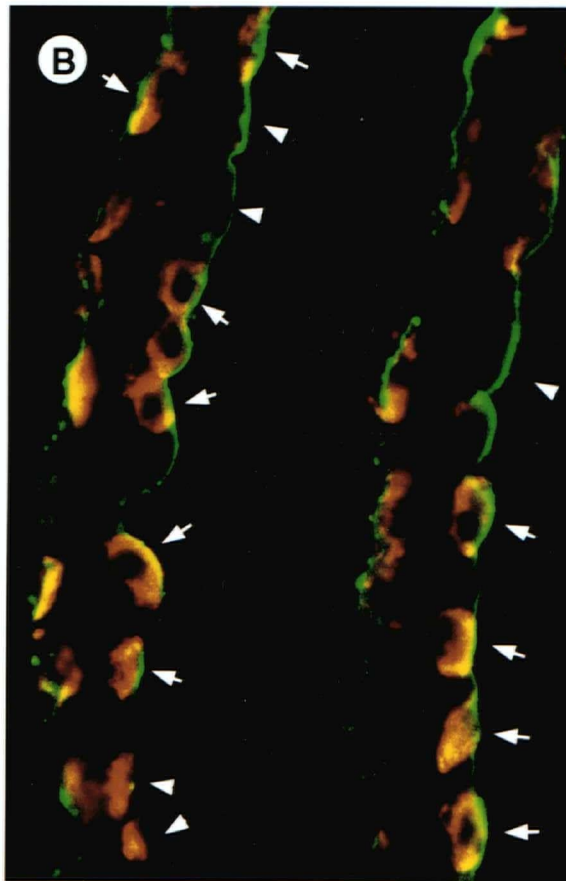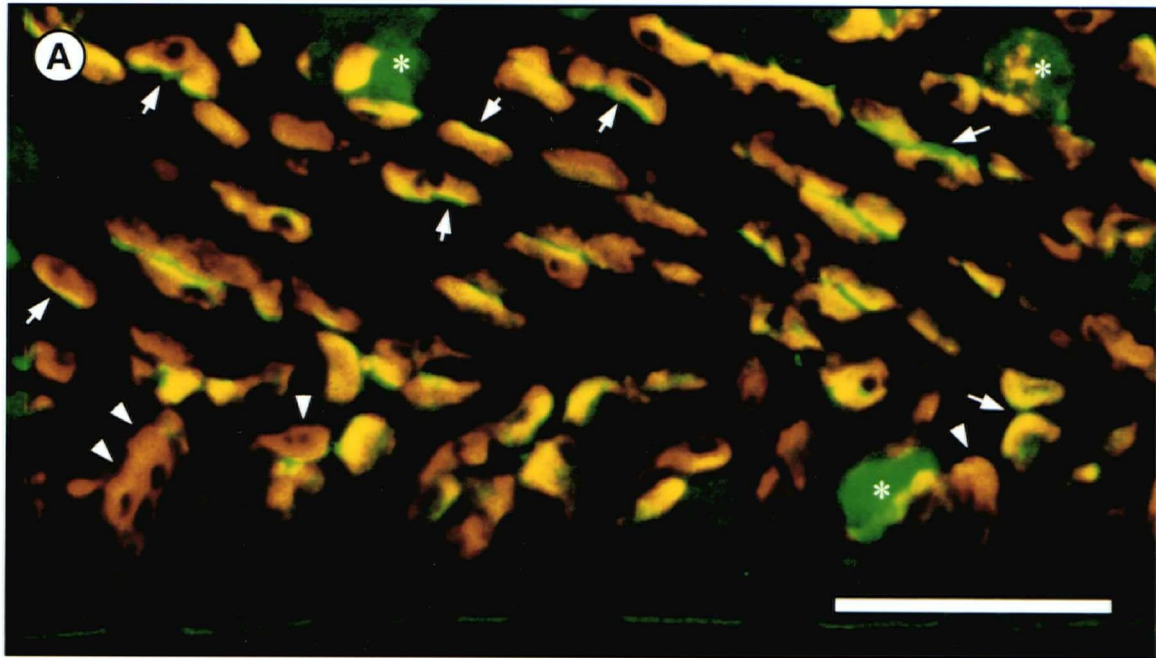
FIGURE 3.9 Immunolocalization of vH$^+$-ATPase in freshwater trout gill using the immunogold technique. There is apical labeling in branchial pavement cells (**a**) as well as MR cells (**b,c**). Subapical labeling is also observed clustering in electron dense areas suggestive of vesicular location. The intensity of immunogold labeling decreases towards the basolateral membrane as seen in the MR cell (**c**). Scale bar s (**a,b**) 0.5 µm and (**c**) 2µm.
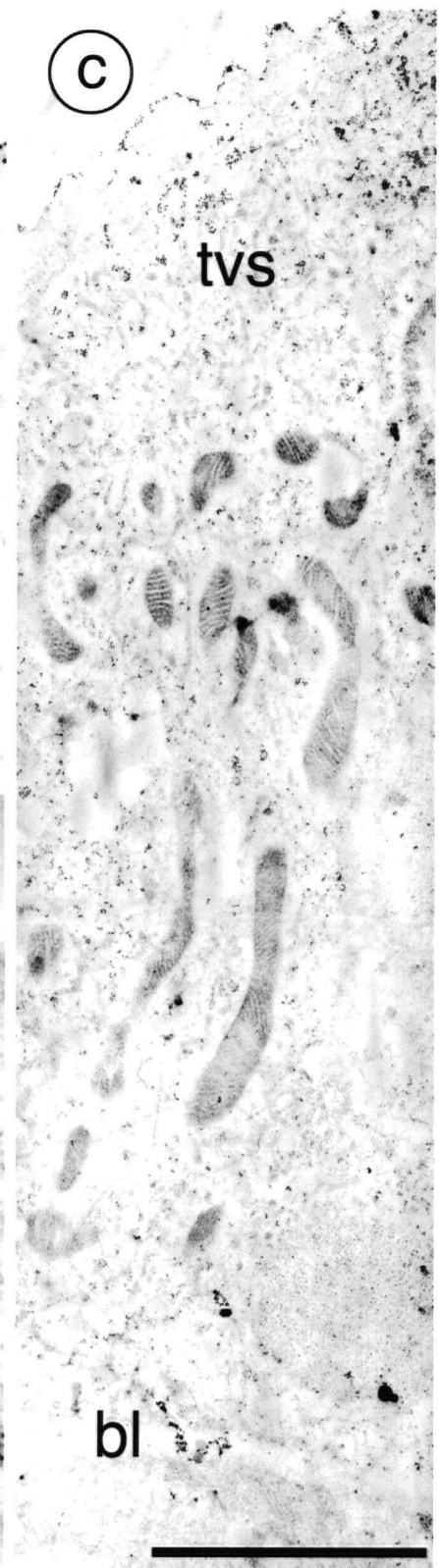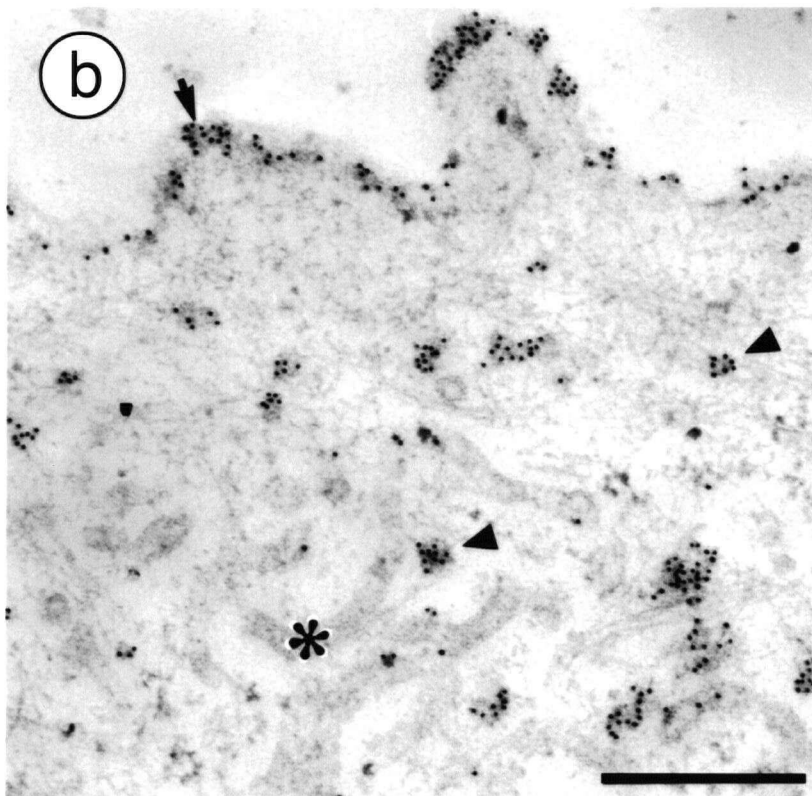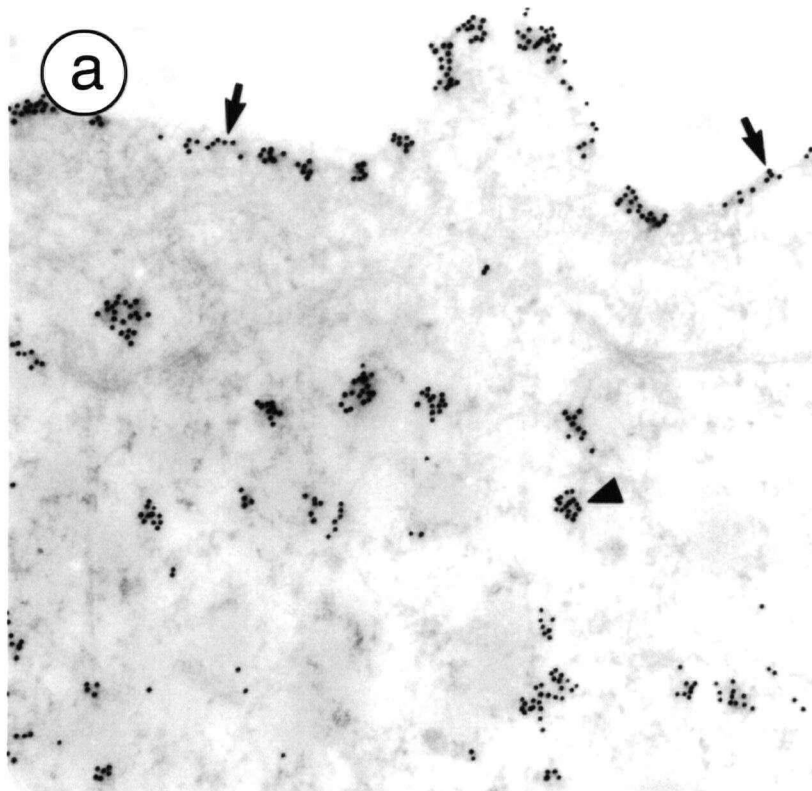
FIGURE 3.10 Western blots of rainbow trout crude gill homogenate loaded onto 10% (**a,c,d**) or 12% (**b**) polyacrylamide gels, transferred to PVD membrane and probed with antibodies against (**a**) α subunit of the Na$^+$,K$^+$-ATPase, (**b**) A-subunit of the vH$^+$-ATPase, (**c**) β-subunit of the ENaC, and (**d**) α subunit of the ENaC. MW markers (**a**) 205, 112, 87, 69, 56, 38.5 and 33.5 kDa; (**b,c,d**) 250, 98, 64, 50, 36, and 30 kDa. Arrowheads indicate bands of interest.
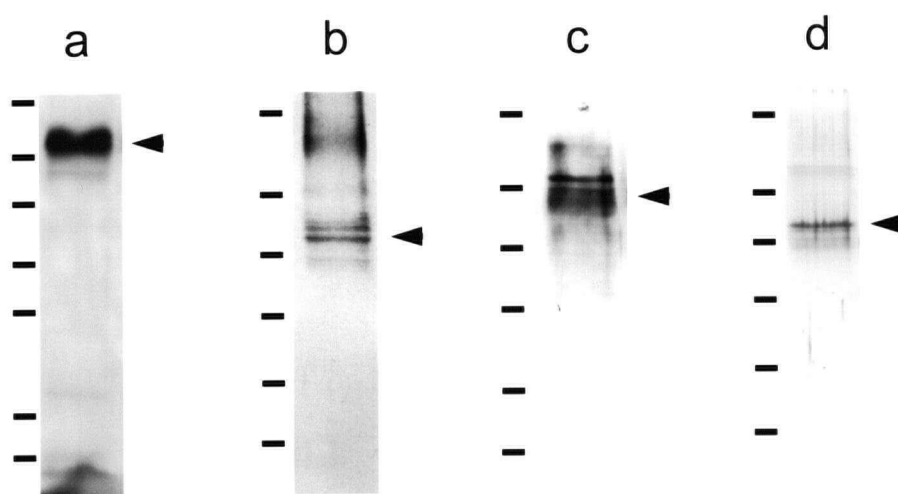
FIGURE 3.11 Dose response curve of rainbow trout ATPase activity (mU/h) to bafilomycin A1 and KNO_3. Membranes prepared from crude gill homogenates using differential centrifugation were used for the measurements of ATPase activity. Bafilomycin A1 (solid circles) and DMSO (hollow circles) used as a control. n = 3.
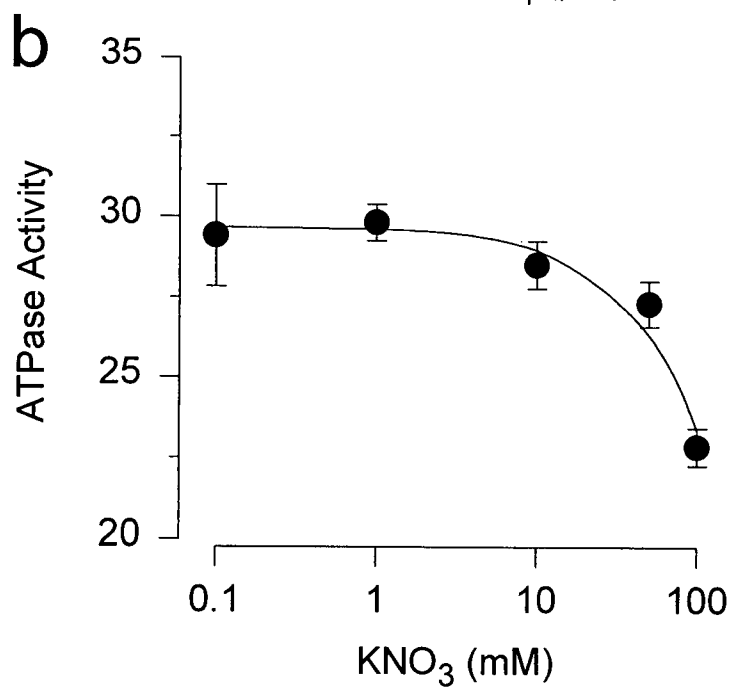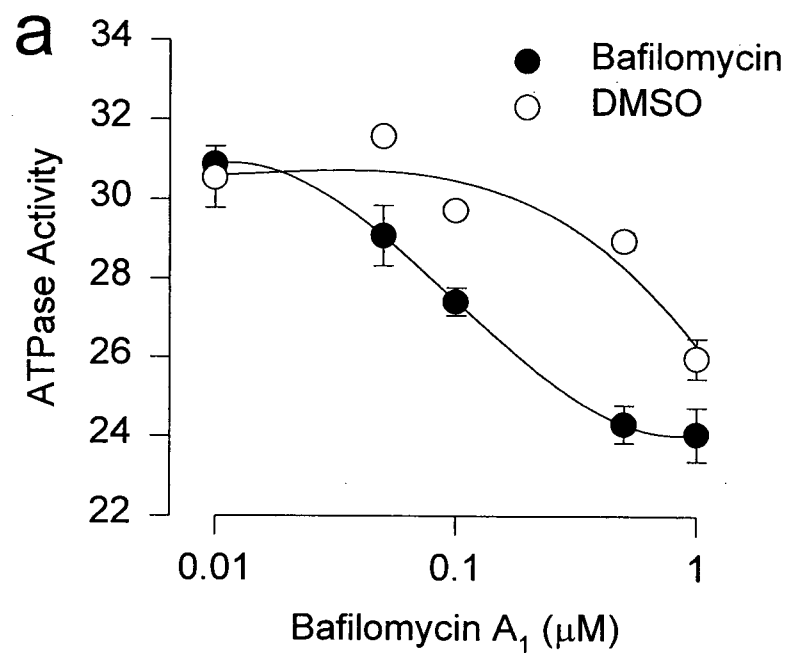
3.4 DISCUSSION

This is the first study to identify the distributions of the apical Cl^-/HCO_3^- and Na^+ / H^+ exchangers and epithelial sodium channels (ENaC) in the branchial epithelium of a fish. In the two freshwater species examined, the patterns of immunolabeling do show some similarities, but also have some major differences.

Na^+,K^+-ATPase antibody as a MR cell marker

The use of antibodies to the Na^+,K^+-ATPase can be used as a reliable tool for identifying MR cells (Witters *et al.* 1996; Ura *et al.* 1996). The α5 monoclonal antibody recognizes a highly conserved epitope within the α-subunit of the Na^+,K^+-ATPase. It has been used to immunolocalize Na^+,K^+-ATPase in animals from invertebrates to mammals (eg Takeyasu *et al.*, 1988; Witters *et al.* 1995; Zeigler 1997; Barradas *et al.* 1999; Lignon *et al.* 1999; Sabolic *et al.* 1999). In fishes, the α5 antibody makes a good tool to identify MR cells because the unique tubular system of these cells is rich in Na^+,K^+-ATPase in both fresh and seawater fishes although to varying degrees (McCormick 1995). Labeling is generally absent from the PVC but considered to be present at levels below detection sensitivity by immunohistochemistry (or autoradiography) since Na^+,K^+-ATPase is generally considered to be a ubiquitous basolateral membrane protein.

The freshwater Chloride cell and the apical anion exchanger

The apical localization of the AE in the tilapia MR cell provides convincing evidence that these presumed freshwater *chloride* cells are aptly named. In seawater fishes, the evidence that branchial MR cells are involved in the active Cl^- efflux has been until now far more convincing than the evidence that Cl^- uptake occurs via the freshwater MR cell (Perry 1997). The tilapia MR cell apical AE is immunogenically related to the erythrocyte band-3 of trout (Figure 3.). This is

70

unlike the pattern seen in higher vertebrates where non-erythroid band-3 like proteins are restricted to the basolateral membrane domain of acid excreting cells (A or α-type cells of bladder and CCT; Drenckhahn *et al.* 1987; Alper *et al.*1989). In these higher vertebrates the apical Cl^-/HCO_3^- exchanger is an AE2 isoform (Alper *et al.* 1997) which is not immunogenically related to band-3 (AE1) and shows less sensitivity to disulfonic stilbenes (SITS; Cohen *et al.* 1978). In the trout, apically applied SITS has been shown to inhibit Cl^- uptake and cause an alkalosis; results consistent with an apical Cl^-/HCO_3^- exchanger (Perry *et al.* 1981; Perry and Randall 1981). Sullivan *et al.* (1996) were also able to localize band-3 mRNA by *in situ* hybridization using a 28-mer oligonucleotide probe (Kudrycki and Shull 1989) to the filament interlamellar epithelium which is typically populated by MR cells. Thus unlike higher vertebrates, it appears that fishes make use of a band-3 like AE for apical Cl^- / HCO_3^- exchange.

There was no crossreactivity of fish tissue with an antibody against mammalian AE2 (Martinez-Anso *et al.* 1994) raised against a peptide derived from the Z-loop (highly conserved region among non-erythroid AE and also found in the AE1 of fish). A comparison of the amino acid sequences of the synthetic peptide and that of trout AE1 Z-loop region show very little similarity. It would thus appear that if the gill-type band-3 and the erythroid band-3 are indeed closely related then no cross reactivity would be expected.

I would like to note that immunolabeling of gill tissue with the trout AE1t antibody was only possible after pre-treating the sections with detergent (SDS). In retrospect, such a treatment makes sense as the polyclonal antibody was generated against band-3 protein purified under denaturing conditions (SDS-PAGE). Thus the conformational changes that occur in the native protein with denaturation and subsequent refolding (upon removal of SDS) result in different epitopes. The polyclonal antibody, which is composed of a battery of different antibodies that

recognize different epitopes on the band-3 protein, is capable of recognizing the erythrocyte band-3 protein in a number of different species. These epitopes may not be present in the native protein of either the gill epithelium or erythrocyte and thus account for the negative results observed without pretreatment. Erythrocytes of both species showed strong crossreactivity regardless of pre-treatment. It also is possible that SDS pretreatment exposes epitopes masked by tissue fixation (protein crosslinking), however, heat denaturation did not enhance reactivity.

So why is it that the antibody raised against trout band-3 does not crossreact with the branchial epithelium band-3 like protein in trout when it does in tilapia? One possible explanation is that the AE expressed in the trout gill is an isoform(s) that does not have the epitopes recognized in both fish erythrocytes and tilapia gill. Interestingly, salmonids belong to a tetraploid lineage and thus have more gene copies (Wittbrodt 1998).

Na$^+$ uptake mechanisms

The co-localization of the vH$^+$-ATPase and ENaC in both tilapia and trout greatly increases the viability of this Na$^+$ uptake model in freshwater fishes. This is also the first study to even identify the distribution of the ENaC in a vertebrate lower than an amphibian (Harvey 1992). However, it is interesting that the co-localized vH$^+$-ATPase and ENaC are found exclusively in PVCs in a particular area of the branchial epithelium in one species (tilapia) and found in a mixed population of PVCs and MR cells throughout the branchial epithelium in the other (trout). It seems that the tilapia exclusive PVC distribution follows the predicted distribution (Goss et al. 1995; Perry 1997) while the trout does not. It is not clear in the trout if Na$^+$ uptake differs in PVCs and MR cells. It maybe that the higher Na$^+$,K$^+$-ATPase activities associated with the MR cell are required to aid Na$^+$ uptake. There is nothing to preclude the possibility that both Na$^+$ and Cl$^-$ uptake mechanisms can be found in a subpopulation of branchial

MR cells. In the trout, Na$^+$ influx has been shown to be sensitive to SITS and Cl$^-$ uptake to amiloride (Perry and Randall 1981). A case in point is the amphibian skin MR cells, which have both apical ENaC and AE proteins along with the vH$^+$-ATPase (γ-cell; Larsen 1991).

I was only able to identify the distribution of the ENaC using the polyclonal antibody against the β-subunit while the α-subunit antibody was negative. Perhaps it is not surprizing that the β-subunit of the ENaC was recognized in fish while the α-subunit was not since there is greater amino acid identity within the β than the α-subunit isoform groups within higher vertebrates (human vs frog; β 79%: α 59%; Garty and Palmer 1997).

The finding of NHE-2 crossreactivity in the branchial epithelium of the freshwater tilapia was not expected. However, Wright (1991) calculated that it is possible to operate a NHE for Na$^+$ uptake in water with greater than 0.5 mM [Na$^+$] and a pH greater than 8. Also since the tilapia is euryhaline, the NHE may be expressed in fresh water in expectation of movement into a more saline environment where it could potentially operate for acid excretion or Na$^+$ uptake. Claiborne *et al.* (1999) have identified a NHE 2-like sequence in the marine sculpin while they appeared to be unable to confirm the presence of a NHE-3 homolog (Blackston *et al.* 1997). I was also unable to detect any NHE-3 crossreactivity.

The localization of NHE-2 to subapical cells adjacent to MR cells is interesting and again may be due to the tilapia being a euryhaline fish. Based on the location of these cells it appears they may be a freshwater-type accessory cell. These cells have been found in a number of freshwater euryhaline fishes (Pisam *et al.* 1988, 1989). The function of the accessory cell is poorly understood and the function of the NHE-2 in such an arrangement is not known. This finding will be discussed in more detail in chapter 4 which focuses on seawater fishes.

vH$^+$-ATPase E subunit and A subunit distributions

Within the literature there are two conflicting reports regarding the distribution of the vH^+-ATPase in the freshwater rainbow trout (*O. mykiss*) by Lin and co-workers (1994) and Sullivan and co-workers (1995). Lin and co-workers (1994) using an anti-peptide antibody directed against the A-subunit (Südhof *et al.* 1989) found extensive apical staining of the branchial epithelium and concluded that both epithelial pavement cells and MR cells expressed the vH^+-ATPase. Sullivan and co-workers (1995) using an anti-peptide antibody directed against the E-subunit (Hemken *et al.* 1992) found a small population of lamellar cells with apical immunoreactivity. On the basis of immunogold studies they concluded that labeling was restricted to pavement cells.

Recently Evans *et al.* (1999) have suggested that the differences may be due to the rearing conditions of the fish (see Table 3.1). Vancouver tap water has a much lower pH and ionic strength (pH 6.4-6.8; $[Na^+]$ 0.01mM) compared to Ottawa tap water (pH 8; $[Na^+]$ 0.5mM). Laurent *et al.* (1985) have shown that such ion poor conditions result in the proliferation of branchial MR cells implying a greater need for ion uptake. With a central role in driving Na^+ uptake, increased vH^+-ATPase would be predicted under such conditions as seen in the Vancouver trout. This does explain the more extensive distribution seen in Vancouver trout but does not explain why the vH^+-ATPase should be found in MR cells in addition to PVC's in Vancouver trout.

I have been using the same anti-A subunit antibody as Lin *et al.* (1994) and can confirm their observation but unfortunately my attempts at getting the anti-E subunit antibody used by Sullivan *et al.* (1995) to work were unsuccessful. However, I have been able to look at gill tissue collected from Ottawa trout and can report a similar labeling pattern as observed by Sullivan *et al.* (1995) using the A-subunit antibody. Additionally, I have also done double labeling

experiments and can clearly show that some of the apical vH^+-ATPase labeling is associated with Na^+,K^+-ATPase immunoreactive cells (MR cells). This observation would contradict the immunogold studies of Sullivan *et al.* (1995), but in their paper they admit their observations were not exhaustive and did not entirely exclude the possibility that a subpopulation of MR cells may also apically express the vH^+-ATPase. It may also be that different isoforms of the E-subunit are expressed in PVCs and MR cells. Studies of the mammalian kidney have shown that there are heterogenous forms of the E subunit which have different tissue and membrane distributions (Hemken *et al.* 1992). The antibody that Sullivan *et al.* (1995) employed was generated against the same synthetic peptide used by Hemken *et al.* (1992) in the development of a battery of monoclonal antibodies. The immunologically determined distribution of the E subunit was not the same for all of the antibodies suggesting that different variants of the E subunit may exist and possibly impart functional variation on the vH^+-ATPase. Immunolocalization of the 56 (B) and 70kDa (A) subunits was found not to differ in the rat kidney (Brown *et al.* 1987a). Comparing results obtained on trout obtained from Ottawa but using the A-subunit probe suggests that the immunoreactivity observed by Sullivan *et al.* (1995) is localized to gill MR cells and not only PVC as had been suggested.

There is also an interesting hypothesis put forward by Feng and Forgac (1994) that reducing conditions favour vH^+-ATPase activity or conversely that oxidizing conditions inhibit activity. When the A subunit cystein (Cys) 254 is oxidize it forms a disulphide bond with Cys 532 inactivating the ATPase. It has been argued that the 'redox modulation' allows the vH^+-ATPase to be active in vesicle acidification under the reducing condition of the cytoplasm but when the vH^+-ATPase cycles through the plasma membrane it is inactive. It may also explain why the plasma membrane vH^+-ATPase is frequently found in MR cells where reducing

conditions can be maintained by mitochondrial cytochrome c oxidase (Harvey and Weiczorek 1997). However, how does the vH^+-ATPase manage to operate in the gill, which of course is the central gas exchange organ in fishes and subjected to high P_{O2}? The mitochondria may act as reducing agents within close proximity but it is unclear what may be going on in PVC's. In the brown bullhead, Goss *et al.* (1992, 1994) have found PVC's which have many mitochondria and which show an increase in microvillar density with hypercapnia. Hypercapnia has been shown to increase vH^+-ATPase activity (Lin and Randall 1993) and protein level expression (Sullivan *et al.* 1995). These cells were distinguished from 'MR cells' by the absence of a tubular system in the brown bullhead (Goss *et al.* 1992, 1994). In tilapia which have only upstream pavement cells expressing the vH^+-ATPase, mitochondria may be numerous, however, in the trout immunogold analysis of PVC's by Sullivan *et al.* (1995), PVC's were characterized by their absence of mitochondria. I also have used mitochondria density as a characteristic for distinguishing MR cells from PVC's and have observed apical immunogold labeling in cells with few mitochondria. Immunocytochemistry places limitations on tissue fixation or morphological preservation in favour of preservation of antigenicity making the identifcation of the tubular system within the cell uncertain. Alternatively, the trout vH^+-ATPase might possess an A-subunit isoform that has a reduced sensitivity to oxidizing conditions. Nitrate (NO_3^-) acts as an oxidizing agent inhibiting the vH^+-ATPase by promoting the formation of disulfide bonds (Dschida and Bowman 1995). The degree of NO_3^- inhibition of total ATPase activity in purified membranes is similar to bafilomycin A1. The question of redox modulation of the teleost gill vH^+-ATPase will probably be resolved once the A-subunit is cloned.

Upstream acidification in tilapia

In the tilapia there is an interesting upstream distribution of the H^+ excreting mechanisms (vH^+-ATPase and NHE-2). One possible explanation of this arrangement may be to aid ammonia unloading by boundary layer acidification (Randall *et al.* 1991). This seems a more plausible explanation rather than some specific condition necessary for sodium uptake. Acidification of the boundary layer by both H^+ excretion and hydration of respiratory CO_2 ($\rightarrow H^+ + HCO_3^-$) aids ammonia excretion by maintaining the transbranchial ammonia partial pressure (P_{NH3}) gradient by removing NH_3 by protonation to form NH_4^+. The transbranchial P_{NH3} gradient can account for the majority of the total ammonia efflux (Cameron and Heisler 1983) and the disruption of the boundary layer pH effect by addition of buffer to the water inhibits ammonia excretion (Wright *et al.* 1989; Wilson *et al.* 1994). The contribution of CO_2 hydration to boundary layer acidification would be greatest downstream, decreasing upstream as P_{CO2} levels of transiting blood decrease. Presumably, upstream acidification of the boundary layer by the vH^+-ATPase and NHE would aid ammonia elimination whilst downstream alkalinization by Cl^- / HCO_3^- exchange would not interfere. The absence of such a relationship in trout maybe related to a greater need for Na^+ uptake, H^+ efflux and/or boundary layer acidification in these animals.

Summary

Figure 3.12 a and b summarize the immunolocalization data collected from the tilapia and trout, respectively. In the freshwater adapted tilapia and trout there is a clear co-localization of the ENaC with the vH^+-ATPase. However, in the trout the vH^+-ATPase-ENaC colocalize to Na^+,K^+-ATPase rich MR cells as well as pavement cells whereas in the tilapia the vH^+-ATPase-ENaC colocalize exclusively to pavement cells. In the tilapia it is possible to demonstrate the presence of an apical AE with Na^+,K^+-ATPase rich MR cells. The NHE-2 immunolocalized to

subapical ovoid cells in the interlammelar space of the filament epithelium as well as to pavement cells in the same region as the vH^+-ATPase-ENaC.

In the tilapia we have a near complete picture of the organization of NaCl uptake and acid-base regulatory mechanisms, whereas in the trout the picture is far from complete. The absence of crossreactivity should not be taken to mean that that particular transporter is not present in the gill. There are numerous technical reasons for the absence of cross reactivity. However, the partial picture of the trout gill is important in highlighting the point that the organization of the gill for iono and acid-base regulation need not be uniform among fishes and that generalizations need to be taken with some caution. There are of course at least 25,000 different species of teleost fishes and our understanding of the few we have studied is still far from complete.

FIGURE 3.12 Illustrations of the freshwater tilapia and coho salmon (**a**) and rainbow trout (**b**) branchial epithelium cell types (MR cells and PVCs) to summarize the immunolocalization data. In the tilapia (and coho) there is immunological evidence for an apical Cl^-/HCO_3^- exchanger in some MR cells (as defined by high Na^+,K^+-ATPase immunoreactivity) or freshwater-type chloride cells (fwCC) and the vH^+-ATPase-ENaC in PVCs. In the trout there is evidence of a mixed population of PVCs and MR cells with the vH^+-ATPase and ENaC. The NHE was found apically in branchial PVCs in tilapia but was absent from trout. The data on the freshwater coho salmon is presented in chapter 4.

(a) Tilapia and Coho salmon

Water

PVC

HCO$_3^-$

Cl$^-$

fwCC

Blood

AE   NKA   v-ATPase   NHE   NKCC
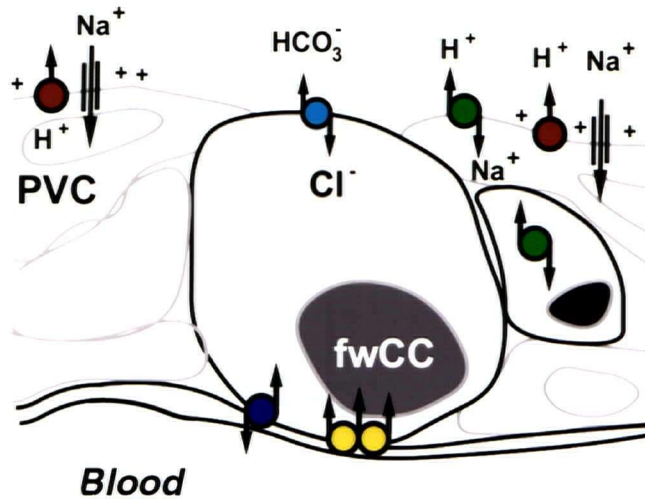
(b) Rainbow trout

Water

PVC

MRcell

Blood
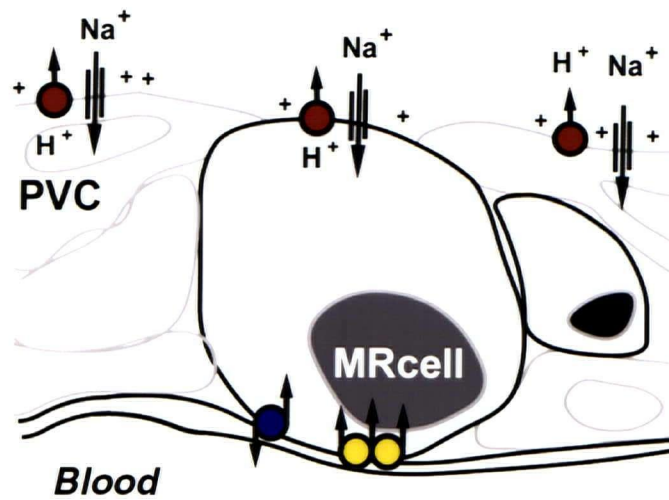
Chapter 4. THE SEAWATER FISH GILL

4. SUMMARY

Teleost fishes living in seawater engage in active ion elimination for ion homeostasis. The accepted model of NaCl elimination involved branchial MR chloride cells that have been shown to be involved in active Cl^- excretion via a basolateral NKCC ($Na^+:K^+:2Cl^-$ cotransporter) and apical CFTR (Cystic Fibrosis Transmembrane Regulator)-like anion channel, energized by a basolateral Na^+,K^+-ATPase while Na^+ moves paracellularly. Acid-base regulation is believed to be mediated by an electroneutral Cl^-/HCO_3^- anion exchanger (AE) and an Na^+/H^+ exchanger (NHE). Using non-homologous antibodies, I have determined the cellular distributions of these ion transport proteins to test the predicted models in the stenohaline turbot (*Scophthalmus maximus*) and euryhaline coho salmon (*Oncorhynchus kisutch*; which was also acclimated to freshwater for comparison). Na^+,K^+-ATPase was used as a cellular marker for differentiating branchial epithelium mitochondria-rich (MR) cells from pavement cell s (PVCs). Branchial MR cells have an apical CFTR-like anion channel and basolateral NKCC and Na^+,K^+-ATPase. The NHE-like immunoreactivity is associated with the accessory cell type in both seawater fishes and the AE-like protein with the MR cell apical crypt in turbot. However, the apical AE-like protein is not found in the seawater-type chloride cell of the coho salmon even though it is found in the freshwater counterpart. In the coho salmon it is possible to demonstrate the loss of the freshwater ion uptake mechanisms (vH^+-ATPase and AE) in sea water adapted fishes. The specificity of the NHE-2 antibody (597) for NHE-like proteins in the gill may be questionable (based on Western blot results of multiple band immunoreactivity) but it may still make a useful marker for the accessory cell type.

4.1 INTRODUCTION
4.1.1 Mechanisms of NaCl elimination

Fish living in seawater achieve ionic homeostasis through the active elimination of NaCl by the gills (Keys 1931a,b). The model of NaCl elimination in teleost fishes (Silva *et al.* 1977; Sardet *et al.* 1979) emerged at about the same time as the avian and shark salt gland models (recent reviews by Evans 1993; Karnaky 1998; Marshall and Bryson 1998; Riordan *et al.* 1994). Briefly, NaCl elimination by the seawater fish takes place via the mitochondria-rich 'chloride' and 'accessory' cell complex. These MR cell types are found in intimate contact sharing an apical crypt (reviewed by Pisam and Rambourg 1991). The smaller, peripheral accessory cell has less developed membrane systems than the larger chloride cell. Leaky tight junctions are found only between chloride cells and accessory cells (Sardet *et al.* 1979). The chloride cell is associated with high levels of basolateral Na^+,K^+-ATPase (Karnaky *et al.* 1976; Hootman and Phillpot 1979) which maintains an inward Na^+ gradient that is used to drive Cl^- uptake by a $Na^+:K^+:2Cl^-$ cotransporter (Eriksson *et al.* 1985). The accumulated intracellular Cl^- moves across the apical plasma membrane via a CFTR-like channel down its electrochemical gradient (Foskett and Scheffey 1982; Singer *et al.* 1997). Na^+ on the other hand, which is accumulated in high concentrations in the interstitial space between chloride and accessory cells by the Na^+,K^+-ATPase, leaks out paracellularly via leaky tight junctions down its electrochemical gradient. (Sardet *et al.* 1979; Potts 1984).

Much of the mechanistic understanding of transepithelial ion transport has come from work using *in vitro* skin preparations (Degnan *et al.* 1977; see recent review by Marshall and Bryson 1998; Marshall 1995). Notably, it was the vibrating probe experiment on a tilapia opercular epithelium preparation by Foskett and Scheffey (1982) that provided definitive evidence that the MR chloride cell was the source of the outward Cl^- current. On the basis of

similarities in morphology and expression of key enzymes (e.g. Na^+,K^+-ATPase) the branchial MR or chloride cells have been ascribed the same function as their opercular epithelium counterparts.

Although the opercular membrane preparations have provided convincing evidence that the MR chloride cells are the site of Cl^- elimination, Avella and Ehrenfeld (1997; Avella *et al.*1999) have found that primary cultures of sea bass (*Dicentrarchus labrax*) respiratory or pavement-like cells are capable of active Cl^- secretion as well. They were unable to find morphological evidence of MR cells in their cultures. Interestingly, on the basis of inhibitor sensitivity of short circuit current, they concluded that the cultured respiratory-like cells use the same cellular transporters used in the MR cell model of Cl^- elimination. Basolateral entry of Cl^- was via a DIDS sensitive Cl^-/HCO_3^- exchanger and a bumetanide sensitive NKCC cotransporter energized by ouabain sensitive Na^+,K^+-ATPase. The apical exit was via a DPC and NPPB sensitive, cAMP stimulated Cl^- channel (Avella and Ehrenfeld 1997). They were also able to provide evidence of an apical Cl^- channel using patch-clamping techniques (Duranton *et al.* 1997) and evidence that Cl^- secretion in these cultured cells is under the hormonal control of arginine vasotocin (AVT)(+), prostaglandin (+) and α (-) and β (+) adrenergic receptors (Avella *et al.* 1999). Evans *et al.* (1999) recently estimated from the measured Cl^- current of the two surrogate model epithelia and relative areas of the two cell types that PVC and CC could contribute roughly equally to total Cl^- efflux *in vivo*. Therefore, it appears that some direct observations of the branchial epithelium chloride cell (CC), accessory cells (AC) and PVC are warranted to address this blurring picture.

4.1.2 Mechanisms of acid-base regulation in fishes (Cl^-/HCO_3^- and Na^+/H^+ exchange)

Although the Na^+ / H^+ exchanger is not thought to operate in the freshwater fish gill because of the lack of physiological gradients for driving exchange (Na^+ uptake), the Na^+ gradients in marine fish are capable of driving Na^+ / H^+ exchange for acid-base regulation (H^+ efflux). As well the favourable inward Cl^- gradient would be capable of driving HCO_3^- efflux. The accumulated Na^+ and Cl^- could be eliminated by the excretory mechanism described above and has been estimated to be relatively small (~10% of the total unidirectional NaCl efflux; see Claiborne 1998).

In support of this model, H^+ efflux has been shown to be dependent on external Na^+ concentration and Claiborne and co-workers (1997) have shown in a marine fish (*Myoxocephalus octodecimspinosus*) that proton efflux is sensitive to the NHE specific inhibitor 5-N,N-hexamethylene-amiloride. In addition, preliminary findings by Blackston, Claiborne and co-workers (1997) using Northern blot analysis indicate the presence of mRNA transcripts in *M. octodecimspinosus* homologous to a human cDNA probe for the NHE-1 and NHE-3 isoforms. Claiborne *et al.* (1999) have more recently confirmed the presence of a βNHE-like (NHE1) and NHE2-like isoforms but not the NHE3-like isoform in this species. The NHE-1 is a basolateral isoform and functions in the housekeeping roles of cell volume and pHi regulation. It is the apical NHE isoforms that are of interest in transbranchial acid-base balance.

Claiborne and co-workers (1997) were also able to show that acid excretion is increased by DIDS and low [Cl^-] in the water. These findings indicate that an apical DIDS sensitive Cl^- /HCO_3^- exchange is occurring. There is virtually nothing known about the distribution of the apical transporters, although basolateral NHE and AE have been found to operate in MR cell pHi regulation (Zadunaisky *et al.* 1995).

1.1.3 Seawater versus freshwater

Movement of fishes between marine and freshwater environments implies a switch in ionoregulatory strategy. Lin and Randall (1993) have shown that the vH^+-ATPase, which is thought to be involved in Na^+ uptake in freshwater fishes, is lower in fish acclimated to seawater or solutions with high NaCl. Both vH^+-ATPase activity and the cellular distribution are reduced (Lin and Randall 1993; Lin *et al.* 1994). Concurrent with a downregulation of freshwater ion uptake mechanisms is an up-regulation of ion excretory mechanisms. Gill Na^+,K^+-ATPase activities and MR chloride cell numbers greatly increase during sea water acclimation (e.g. Sargent and Thomson 1974; Pisam *et al.* 19; Marshall *et al.* 1999; McCormick 1995).

In this chapter the ion transport proteins involved in NaCl elimination (Na^+,K^+-ATPase, NKCC and CFTR) are immunolocalized to address the question of whether branchial PVCs could contribute to the efflux. In addition, the ion transport proteins that have been suggested to be involved in acid-base regulation will be immunolocalized. These are the apical NHE 2 and NHE 3-like, Na^+/H^+ exchangers and band 3-like AE (anion exchanger). Finally, changes in ion transport protein expression in fresh water and sea water adapted representatives of species are addressed, specifically looking at changes in the vH^+-ATPase, Na^+,K^+-ATPase, NHE and AE expression patterns. I will present data on the stenohaline marine turbot (*Scophthalmus maximus*), the euryhaline seawater and freshwater adapted coho salmon (*Oncorhynchus kisutch*) and finally a limited part of the data on the brackish water mudskipper fish (*Periophthalmodon schlosseri*). A more extensive data set on the mudskipper will appear in chapter 5 in the study of active NH_4^+ elimination by this species.

4.2 MATERIALS AND METHODS

4.2.1 Animals

Coho salmon (*Oncorhynchus kisutch*) of both sexes were obtained from the Department of Fisheries and Oceans West Vancouver facility which have been reared in either freshwater or seawater. Three to four fishes ranging from 35-50g were sampled on-site from each group for gill tissue and intestinal tissue (for an unrelated study). An additional group of juvenile coho were transported to the Bamfield Marine Station and used in a salinity acclimation experiment. These fish were 157.5 ± 14.5 g (n = 39) and maintained in an outdoor tank in freshwater.

Juvenile turbot (*Scophthalmus maximus*) obtained from a French hatchery were maintained at the Augusto Nobre Labratorio da Foz of the Universade do Porto, Portugal. Fish were fed twice daily, and were control fish used as part of a growth study (Pereira *et al.* 1999).

Adult mudskippers (*Periophthalmodon schlosseri*) of both sexes were collected from the Pasir Ris, a small estuary on the eastern coast of Singapore and transported to City University of Hong Kong. In the laboratory, fish in individual plastic aquaria were kept partially submerged in 50% seawater (15 ‰). Every other day the water was changed and the animals were fed goldfish *ad libitum*. The fish mass ranged from 55 to 120 g. The room air and water temperatures remained constant around 26°C. No attempts were made to control lighting conditions and a natural photoperiod was followed.

4.2.2 Salinity acclimation experiment

In this experiment, coho salmon were gradually acclimated to full strength (32‰) sea water at a rate of 1‰ h^{-1}. Fish (5-9) were randomly netted in freshwater (0h) and 12h, 24h, 2, 4, and 8 days after the start of the salinity increase. Fish were killed by an overdose of anaesthetic (1:5000 MS-222) and sampled for blood and gill tissue. Blood was collected by caudal puncture

using a heparinized needle and syringe and plasma was separated and saved. The gill arches were excised and divided to be either fixed (3%PFA/PBS) or freeze-clamped and stored in liquid nitrogen. The frozen gill tissue was prepared for measurements of ATPase activity (see General Material and Methods section 2.for details). Unfortunately, the fixed tissue was rendered useless by improper storage.

Plasma Na^+ and Cl^- ion concentrations were measured using an atomic absorption spectrophotometer (Perkin-Elmer 2380) and by coulometric titration (Haake Buchler Instruments digital chloridometer), respectively. Gill Na^+,K^+-ATPase and vH^+-ATPase activities were determined using the microplate method (See General Materials and Methods for details).

4.2.3 Fixation and Immunolabeling

Turbot and coho gill tissues were fixed by immersion in Bouin's solution and paraffin embedded. Coho gill tissue was additionally fixed in 3%PFA/PBS and either embedded in paraffin or frozen.

The standard immunolabeling protocol was followed in addition to the various pre-treatment epitope-unmasking techniques. See General Material and Methods for details.

4.2.5 Antibodies employed in this study

Sections of turbot and coho gill tissue were probed with antibodies against Na^+,K^+-ATPase, NKCC, CFTR, NHE-2 and 3, AE1t and vH^+-ATPase. See General Material and Methods for additional details.

4.2.6 Statistical Analysis

Data are presented as mean $\pm$ SEM. Statistical differences between the means of the dependent variables were determined by one-way ANOVA and *post hoc* Student-Neuman-Keuls test. Differences were accepted as significant at the 95% level of confidence ($P<0.05$).

4.3 RESULTS

Na⁺/H⁺ exchanger

In the branchial epithelium of the stenohaline marine turbot, the polyclonal antibody (597) raised against the NHE-2 fusion protein immunoreacts with small cells juxtaposed to larger cells showing strong Na^+,K^+-ATPase immunoreactivity (presumed MR cells) in a pair-like fashion (Figure 4.1). Labeling is restricted to the filament epithelium and double labeling of single cells is seldom observed. In addition to being smaller than Na^+,K^+-ATPase immunolabeled cells, NHE-2 immunoreactive cells display a cytoplasmic labeling pattern with nuclei having negligible immunoreactivity. Lamellar PVCs do not show detectable immunoreactivity, nor do erythrocytes or pillar cells.

In both the seawater and fresh water adapted coho salmons' branchial epithelium, a similar labeling pattern as in the turbot is observed (seawater coho; Figure 4.2). Na^+,K^+-ATPase and NHE-2 immunoreactive cells show alternating labeling and are seldom double labeled. Within the filament epithelium both types of immunoreactive cell tend to be more elongate, however, the Na^+,K^+-ATPase cells remains larger. Na^+,K^+-ATPase cells are also found in the lamellar epithelium while NHE-2 cells are not.

The polyclonal antibody (1380) raised against a NHE3 fusion protein does not show a specific labeling pattern in either the turbot or coho. A non-specific staining pattern is observed as in the freshwater tilapia. Antigen retrieval techniques do not alter the pattern of labeling relative to normal rabbit serum controls with either of these antibodies.

Band 3-like AE

The rabbit polyclonal antibody raised against trout erythrocyte band-3 protein immunolabels the apical crypt region of the turbot (Na^+,K^+-ATPase immunoreactive) MR cells

following SDS pretreatment (Figure 4.3). Staining is clearly seen following the edge of the apical membrane of the MR cell. There is also some faint sub-apical labeling of MR cells. Since, SDS pretreatment tends to increase the background signal it is difficult to determine if other epithelial cells have significant labeling. A comparison of labeling intensity with normal rabbit serum controls does not appear significantly greater in lamellar PVCs while MR cell apical crypt labeling clearly is.

In the seawater adapted coho salmon and mudskipper gills, tissue does not immunoreact although erythrocytes show specific labeling (Figure 4.6D). However, in the freshwater adapted coho, MR cells have apical AE immunoreactivity (Figure 4.6A) similar to the freshwater tilapia (see Figure 3.2). Control incubations with normal rabbit serum substituted for AE1t antisera result in weak labeling of erythocytes (Figure 4.6G).

Na^+,K^+-ATPase and NKCC

In seawater adapted coho and marine turbot, Na^+,K^+-ATPase is used as a marker for MR cells (Figure 4.1, 4.2B, 4.6E). Immunoreactive cells display an intense signal throughout the cell body, indicative of labeling associated with the invasive tubular system. These ovoid cells tend to be quite large and the basally located nucleus can be visualized as a negative image against the cell body fluorescence. A characteristic population of these immunoreactive cells is found in the filament epithelium and is concentrated towards the efferent side of the filament. A deep apical crypt is commonly associated with these cells. Strong NKCC immunoreactivity is observed using the T4 monoclonal antibody in an identical pattern as the Na^+,K^+-ATPase (Figure 4.3B). Control incubations with normal mouse serum substituted for α5 antiserum result in weak labeling of erythrocytes (Figure 4.6H).

CFTR anion channel

CFTR immunoreactivity could not be demonstrated in either of these species. However, in mudskippers, the CFTR-like protein is immunolocalized to the apical crypt of branchial MR cells. Mudskipper MR cells also have high Na^+,K^+-ATPase and NKCC immunoreactivity associated with their tubular system (basolateral membrane). The CFTR antibody was not immunoreactive with paraffin embedded tissues indicating that the epitope may be heat denatured. Fixed-frozen tissue was used to obtain immunohistochemical labeling.

Seawater acclimation

During seawater acclimation, plasma Na^+ ions show a marked temporal elevation and a recovery by day 8 (Figure 4.4). Plasma Cl^- levels show a less substantial increase. After some initial variability gill Na^+,K^+-ATPase activity shows a significant increase while vH^+-ATPase activity shows a decreasing trend albeit statistically insignificant (Figure 4.5). vH^+-ATPase immunoreactivity of branchial epithelial cells is greater in lamellae of fresh water adapted fishes than in fish transferred to seawater (Figure 4.7). Immunoreactivity of mucocytes is observed in both fresh water and seawater adapted animals although the intensity of labeling is higher in seawater fishes.

FIGURE 4.1 Double labeled sections on the turbot gill epithelium using a rabbit polyclonal antibody (597) against the NHE-2 fusion protein (FITC, green) and mouse monoclonal antibody against the α subunit of Na^+,K^+-ATPase (Texas Red). The Na^+,K^+-ATPase identifies chloride-type MR cells while the NHE-2 is localized to smaller closely juxtaposed cells. The nuclei of some of these cells can be made out as negative image against the cytoplasmic fluorescence. Scale Bar= 50 μm
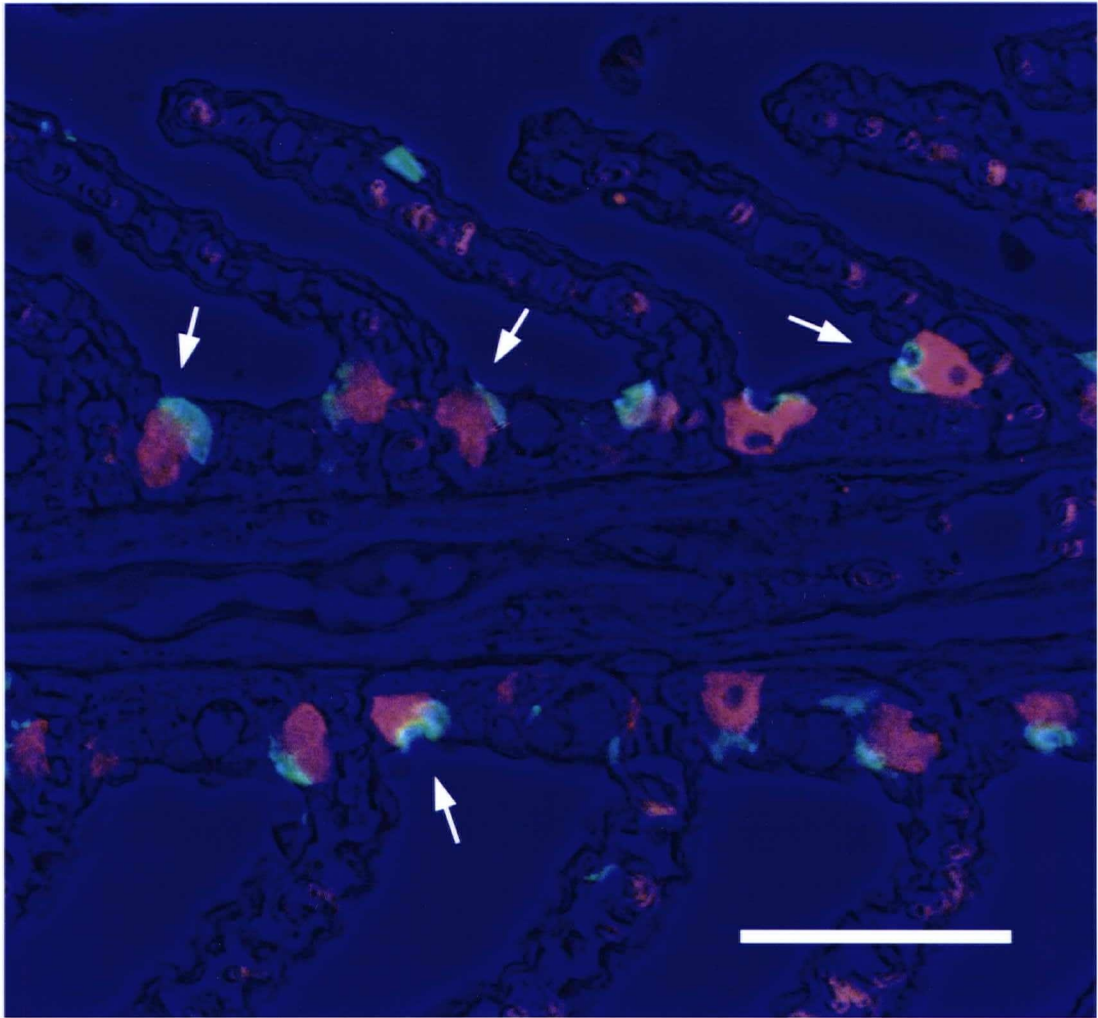
FIGURE 4.2 Double labeled section of the seawater adapted coho gill epithelium using a rabbit polyclonal antibody (597) against the NHE-2 fusion protein (**A**) and mouse monoclonal antibody against the α subunit of Na$^+$,K$^+$-ATPase (**B**). The corresponding phase contrast image is shown in (**C**). The labeling pattern is similar to the turbot with alternating cells in the interlamellar filament immunoreacting with each antibody (Figure 4.1). Nuclei of immunoreactive cells can clearly be made out in negative image. The NHE-2 immunoreactive cells in coho tend be more elongate extending from the surface to the basement membrane and are indicated by *arrows*. Scale Bar= 50 μm
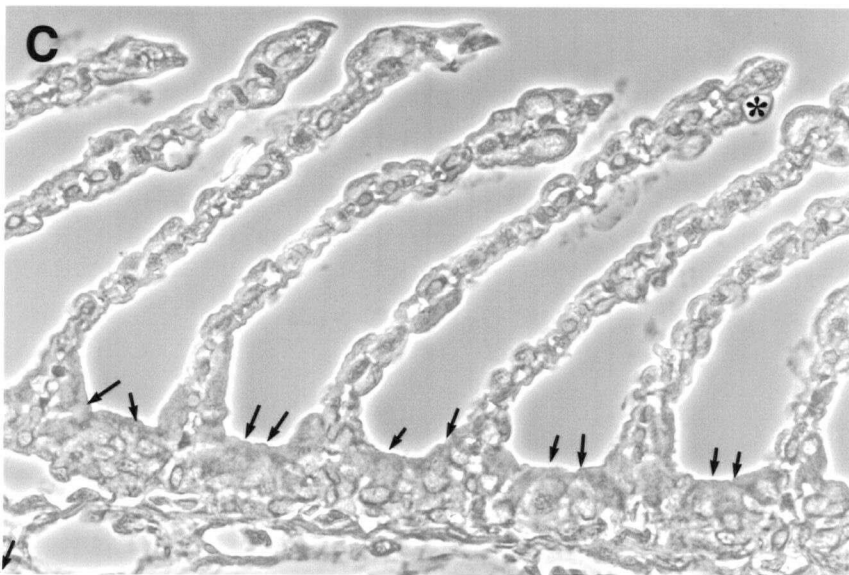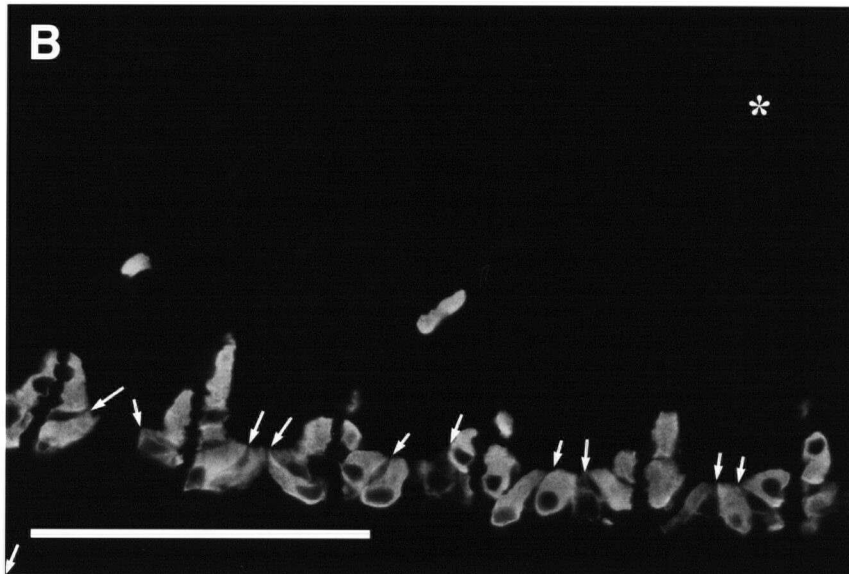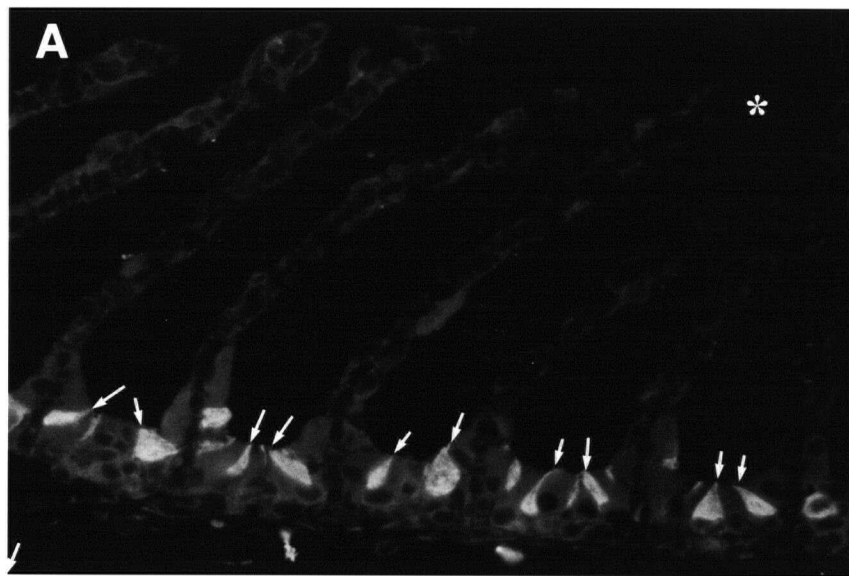
FIGURE 4.3 An SDS treated section of the turbot gill epithelium duel labeled for AE1t and NKCC using a rabbit polyclonal antibody generated against trout erythrocyte band 3 (AE1t) (**A**) and a mouse monoclonal antibody (T4) specific for NKCC (**B**), respectively. The corresponding phase contrast image is shown in the bottom panel (**C**). Note the high background staining with the AE1t antibody. The arrows indicate strong labeling associated with the apical crypt of NKCC immunoreactive cells. Scale bar = 50 μm
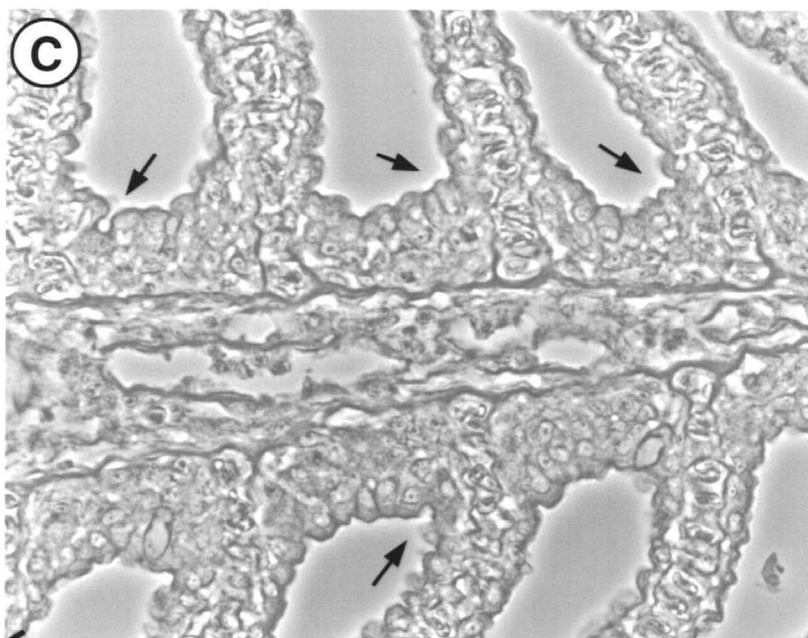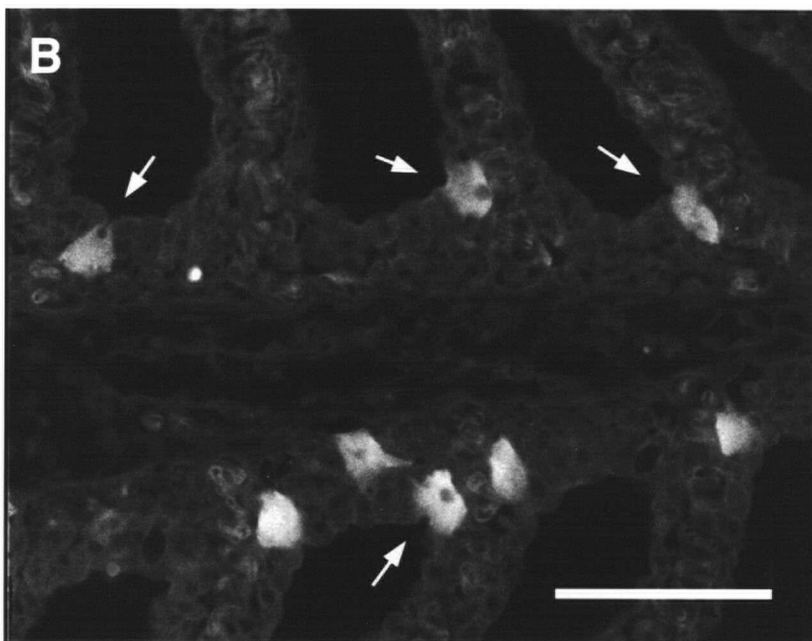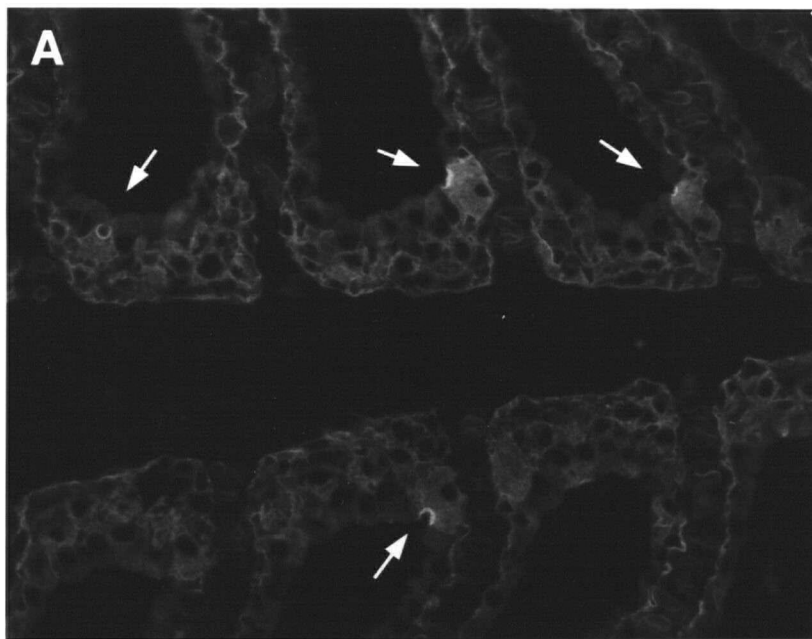
FIGURE 4.4 Mean changes in sodium and chloride ion concentrations in the plasma of coho salmon in freshwater (time 0) and after a gradual increase in external salinity for 8 days. Changes in salinity of the holding water are plotted on the lower graph. The askerisks indicate mean values significantly different from those measured in freshwater fishes at time zero. n= 5-9
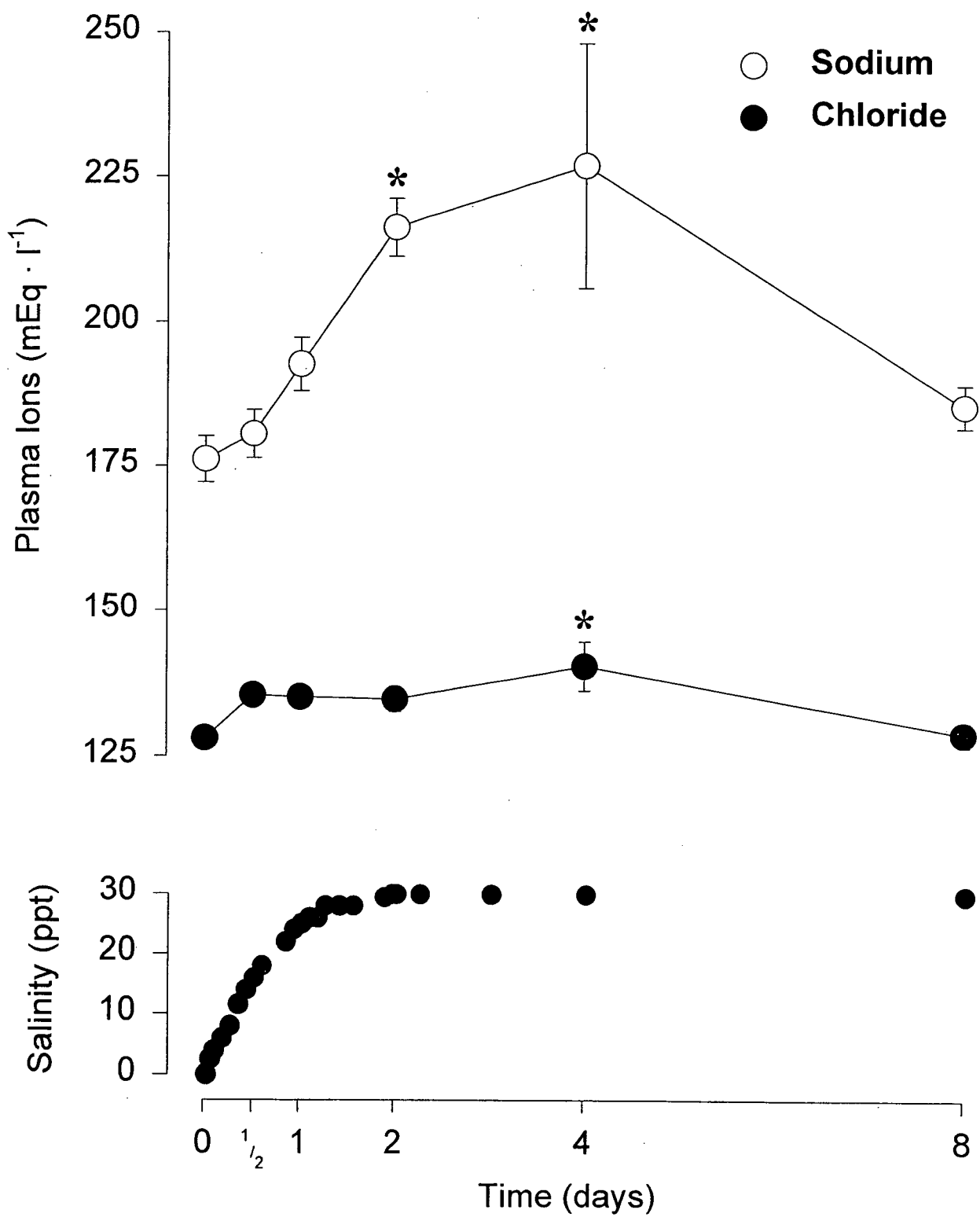
FIGURE 4.5 Changes in the vH^+-ATPase and Na^+,K^+-ATPase activities in the gill homogenates of coho salmon during sea water acclimation as determined by NEM and ouabain sensitive activity. Fish were sampled at 0, 12h, 24h, 2, 4, and 8 days. The asterisks indicate a significant difference from the zero hour freshwater control. n = 5
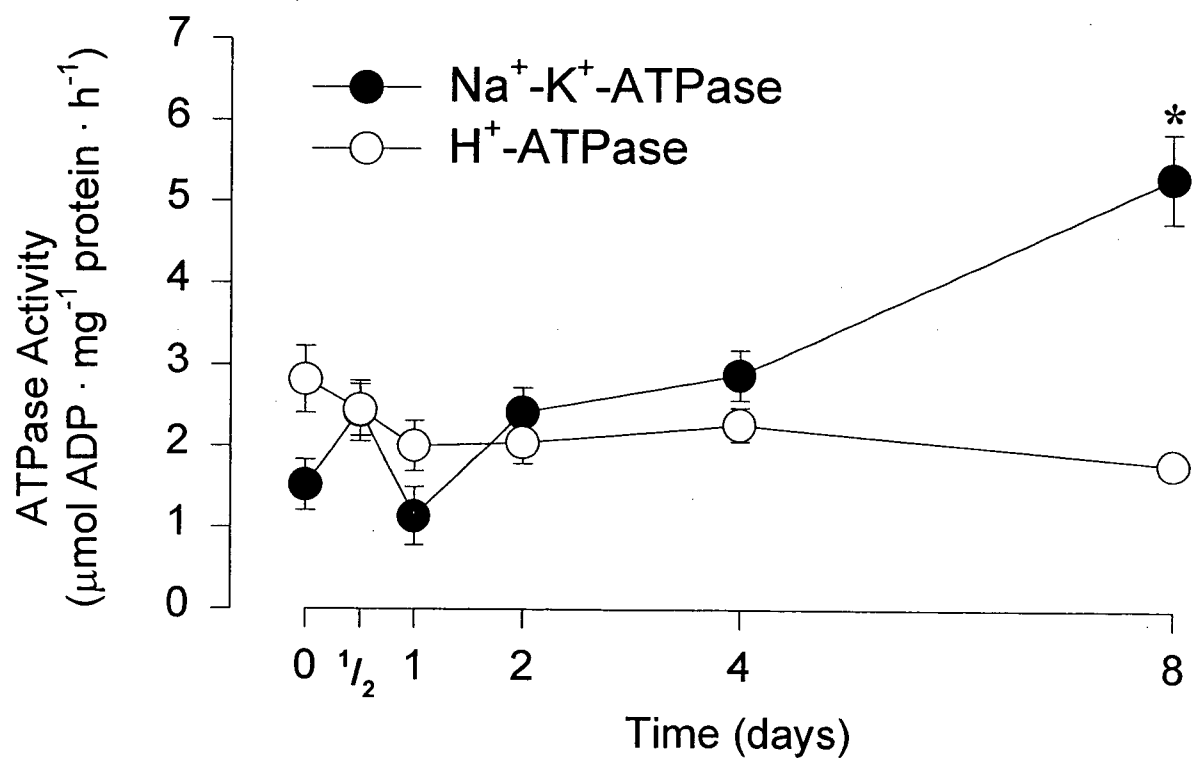
FIGURE 4.6 Immunohistochemistry of gill from coho salmon (*O. kitsutch*) adapted to either freshwater (upper and lower panels **ABC, GHI**) or seawater (middle panel **DEF**) showing the distributions of the band 3-like anion exchanger (AE1t;**A,D**) and Na^+,K^+-ATPase (**B,E**).The corresponding phase contrast images are shown (**C** and **F**, respectively). The lower panel shows control labeling using normal rabbit serum (**G**) or normal mouse serum (**H**) of a section from freshwater coho gill. There is some non-specific labeling of erythrocytes. Scale bar = 50μm.

102
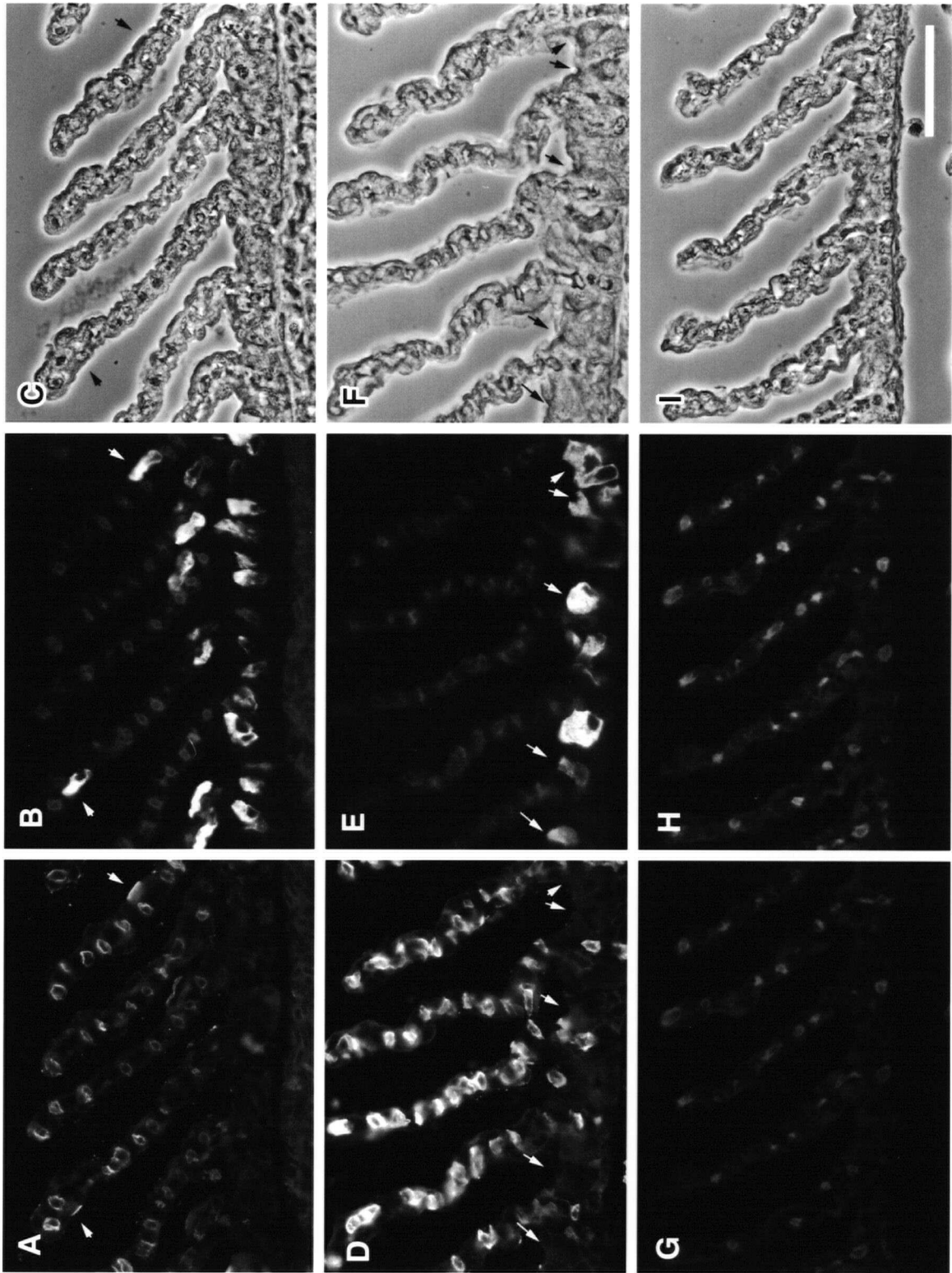
FIGURE 4.7 Paired fluorescent (**A,C**) and phase contrast (**B,D**) micrographs of fixed-frozen sections of gills from *O. kisutch* held in freshwater (**A,B**) and after 2 days (**C,D**) exposure to a progressive increase in external salinity. The sections were immunolabeled for vH^+-ATPase using a peptide antibody derived from the A-subunit of bovine brain vH^+-ATPase. In the freshwater fish gill (**A,B**), asterisks indicate weakly labeled mucocyte and the arrowheads noticeably immunoreactive cells for vH^+-ATPase. In the seawater fish gill (**C,D**), the arrowheads indicate strongly immunoreactive mucocytes. Scale bar = 50 μm.
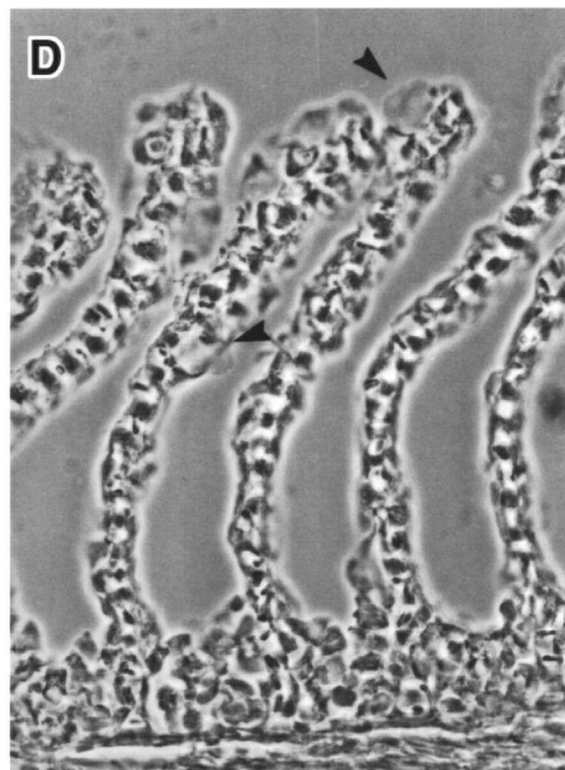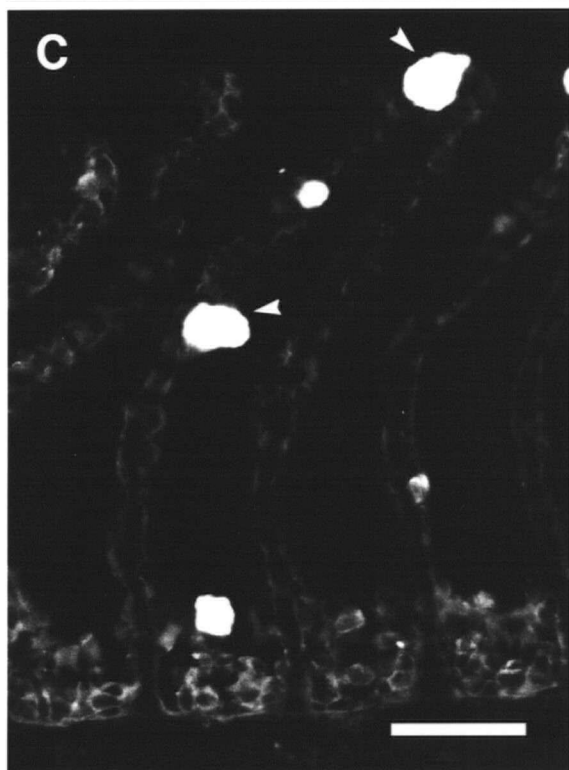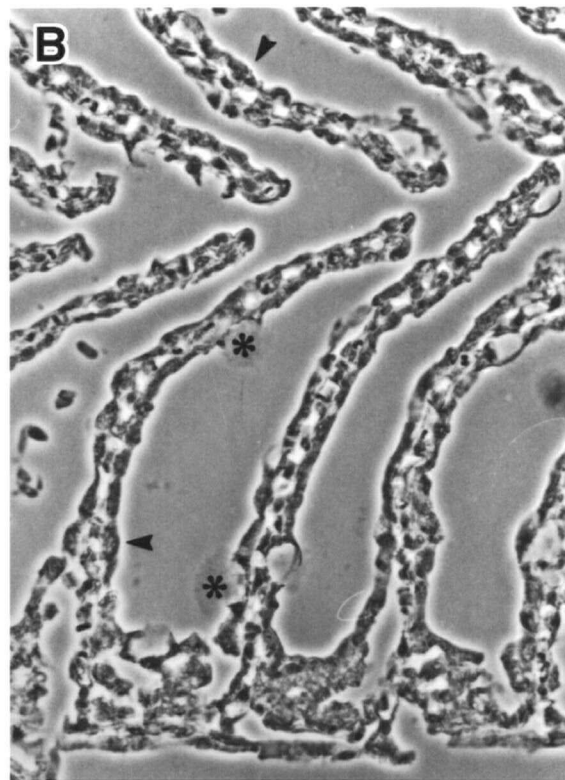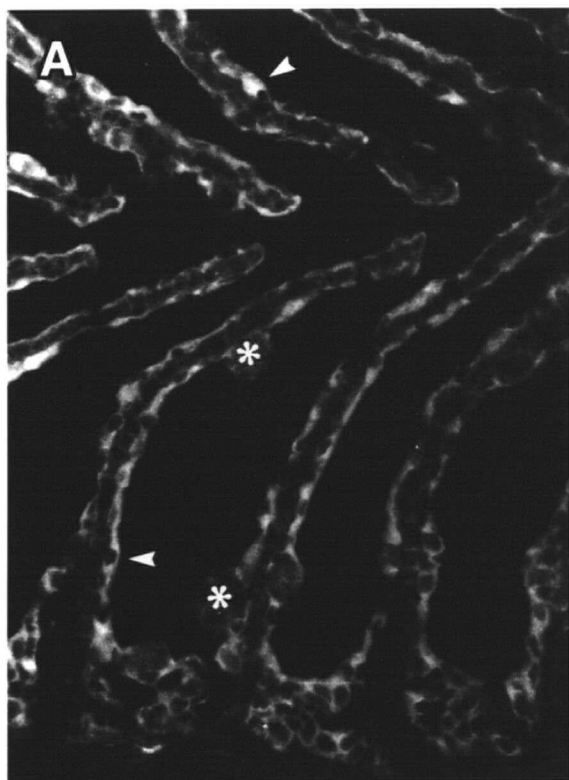
4.4 DISCUSSION

In the marine species of teleost fishes investigated, Na$^+$,K$^+$-ATPase and NKCC immunoreactivity was greatest in chloride cells (CC). The levels of immunoreactivity in other cell types were not significant. Unfortunately, CFTR immunoreactivity was only observed in the mudskipper. This can be explained by the fact that fish CFTR generally has low amino acid identity compared to mammalian CFTR homologues (59% killifish: human; Singer *et al*. 1998). In the mudskipper I could only find immunoreactivity associated with the apical crypt of MR cells and not lamellar PVC. So in these data I do not find any evidence to support the proposed role of the branchial PVC in the active Cl$^-$ efflux (Avella *et al*. 1997). It should be noted that this absence of immunoreactivity is not proof of the absence of these ion transport proteins in the branchial PVCs. It only indicates that levels in the MR cell are higher than in PVCs and that levels in PVCs may be just below the level of detection of the technique. It is also possible that different isoforms of these proteins are involved in transepithelial ion movements in PVCs.

Interestingly, apical band 3-like AE immunoreactivity is associated with the turbot MR cell apical crypt as is also seen in the freshwater tilapia and coho salmon. Since apical labeling was not seen in all Na$^+$,K$^+$-ATPase labeled MR cells and the CFTR antibody was not crossreactive in this species, it is not possible to say whether these two anion transport proteins would be co-localized to the same MR cells. The finding of Degnan *et al*. (1980) of an absence of Cl$^-$/Cl$^-$ self-exchange in opercular membrane preparations would argue against the presence of both apical transporters. However, it has been shown in the frog skin that both homologous CFTR anion channel and Cl$^-$/HCO$_3^-$ exchanger are situated apically in MR cells (Larsen *et al.* 1999). The finding of Claiborne and co-workers (1997) of apical DIDS sensitivity and low [Cl$^-$] effect on acid excretion indicates presence of a Cl$^-$/HCO$_3^-$ exchanger in the sculpin and it may

follow that perhaps branchial MR cells differ from the opercular type observed by Degan et al. (1980). However, in support of Degan et al. (1980) is the finding that the apical AE is absent from the seawater adapted coho MR cell. It appears that the apical exchanger is present only in the freshwater type MR cell of this species.

The comparison of the freshwater and seawater adapted coho, nicely illustrates how the mechanisms for Na^+ and Cl^- uptake can be lost upon change in the salinity regime. The vH^+-ATPase activity and epithelial distributions both decrease in seawater and the freshwater-type chloride cell is lost in favour of the seawater-type chloride cell (Cl^- uptake versus Cl^- elimination, respectively). The down regulation of the vH^+-ATPase in seawater is similar to that reported by Lin and Randall (1993; Lin et al. 1994) in rainbow trout although not as dramatic. The immunoreactive material they observed appears to be mucocyte mucin granules.

The morphology and location of the NHE immunoreactive cells suggests that they are the accessory-type MR cell (AC; Hootman and Phillipot 1980; Laurent 1984; Pisam and Rambourg 1991). Both the NHE immunoreactive cells and AC have an intimate relationship with larger MR *chloride* cells (shared apical crypt, and peripheral, slightly superficial juxtaposition), a similar shape (semi-lunar or elongate) and low levels of Na^+,K^+-ATPase activity (Hootman and Phillpot 1980). The finding of similar cells in the eurhyaline freshwater tilapia (chapter 3) and coho salmon is also consistent with the idea of AC immunoreactivity because Pisam and co-workers have been able to identify AC in euryhaline freshwater fish (*Salmo salar* smolts: Pisam et al. 1988; juvenile *O. mykiss*: Pisam et al. 1989).

The accessory cell has basically been a cell without a function. It is generally inferior to the chloride cell having a less developed tubular system, fewer mitochondria and low levels of Na^+,K^+-ATPase. The contribution of the AC to NaCl efflux is a leaky tight junction shared with

the CC, which facilitates the paracellular Na^+ movement (Sardet *et al.* 1979). It is possible that this AC-NHE2 is involved in the amiloride-sensitive acid excretion reported by Claiborne *et al.* (1997). However, what is uncertain is why the NHE should have a cytoplasmic distribution. In mammalian renal epithelia the NHE-3 isoform has been detected in the endomembrane compartment where it is thought to have a role in maintenance of endosomal pH (Biemesderfer *et al.* 1995; D'Souza *et al.* 1998). It may also be non-specific crossreactivity, but the finding of an apparently specific marker for ACs may have an application of its own even if we can not explain its function. Generally, electron microscopy is required to identify this cell type but with this antibody light level microscopic identification is simple.

Summary

Figure 4.8 summarizes the immunolocalization data collected on seawater fishes. The immunodetection results generally corroborate the classical model of active NaCl elimination (Silva *et al.* 1977). Basolateral Na^+,K^+-ATPase and NKCC are associated with the MR chloride cell and a CFTR anion channel with the apical crypt (see Marshall and Bryson 1998; Singer *et al.* 1998). The presence of NHE 2-like protein within the accessory cell and AE-like protein within the apical crypt complicate the model. However, the apical AE-like protein is not found in the seawater-type chloride cell of the coho salmon even though it is found in the freshwater counterpart. Also the NHE immunoreactivity may not be specific although it may make a useful marker for the accessory cell type. In the coho salmon it is possible to demonstrate the loss of the freshwater ion uptake mechanisms (vH^+-ATPase and AE) in sea water adapted fishes.

FIGURE 4.8 Illustration of cell types of the branchial epithelium of a seawater fish summarizing the immunolocalization data. The seawater MR chloride cell has a basolateral Na^+,K^+-ATPase and NKCC and an apical CFTR anion channel. The band 3-like Cl^-/HCO_3^- exchanger is found in the stenohaline turbot but not in the euryhaline seawater adapted coho salmon or mudskipper. NHE-like immunoreactivity is found in MR accessory cells of both seawater and freshwater fishes.

Seawater fish

water

H⁺

HCO₃⁻

Cl⁻

Na⁺

AC

CC

blood

NKA AE CFTR NHE NKCC
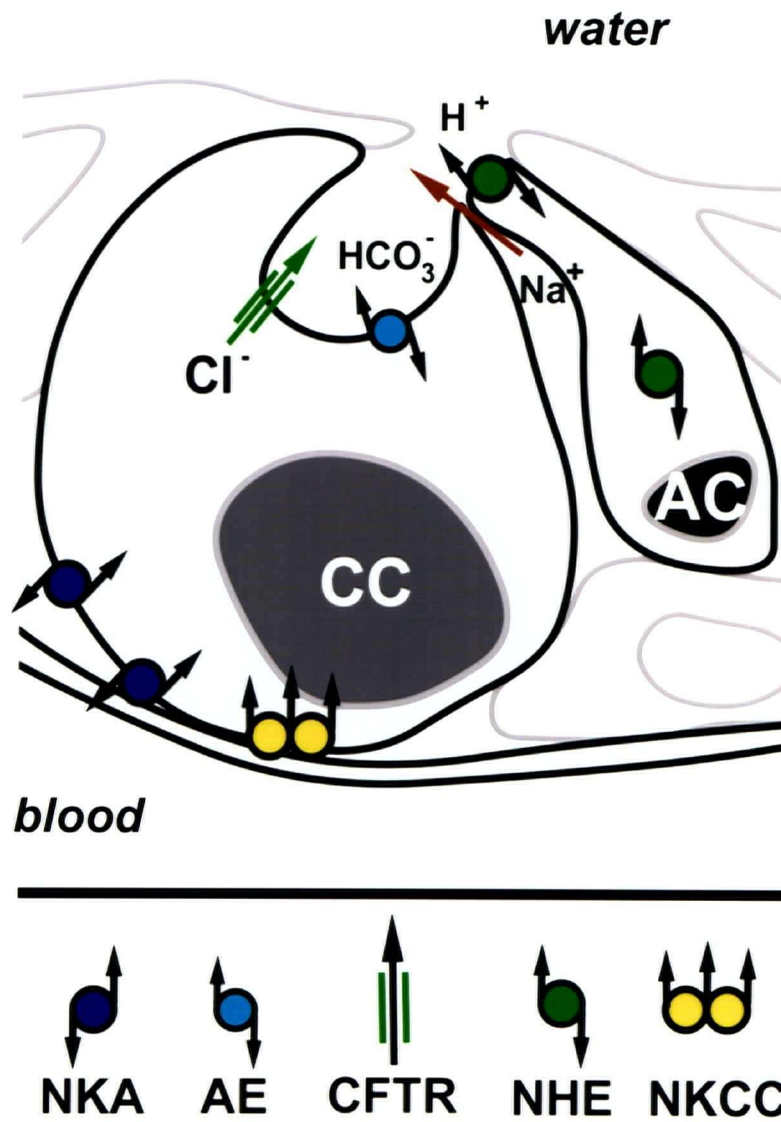
Chapter 5. THE MUDSKIPPER GILL

5 SUMMARY

The mudskipper, *Periophthalmodon schlosseri*, is able to tolerate extremely high environmental ammonia concentrations that would necessitate the active elimination of NH_4^+ ions to explain the absence of internal elevations of ammonia. In this chapter, the contribution of various ion transport proteins to net ammonia excretion were determined pharmacologically and their presence in the gill MR cells determined using immunolocalization techniques. A component of the ammonia eliminated by *P. schlosseri* involves an amiloride-sensitive Na^+/H^+ exchanger (NHE) and carbonic anhydrase (CA) and is not dependent on boundary layer pH effects. An apical CFTR-like (Cystic fibrosis transmembrane regulator) anion channel may be serving as a HCO_3^- channel accounting for the acid-base neutral effects observed with NH_4^+ inhibition. Na^+,K^+-ATPase plays a role in ammonia elimination only against a gradient. Although a vH^+-ATPase is present its role in ammonia elimination is not certain. These animals are able to eliminate significant quantities of ammonia when out of water. The findings that branchial epithelium of *P. schlosseri* has an unusual high density of mitochondria-rich cells that express all of the above proteins link the animal's ability to actively eliminate ammonia to the gill. It also is clear that gas exchange across the gill lamellae would be severely handicapped by the long diffusion distances present. The observation of intra-epithelial capillaries in the inner operculum and to a lesser extent in the gill filament would present more practical sites for gas exchange.

5.1 INTRODUCTION

In 1929 Homer Smith originally demonstrated that ammonia was the dominant nitrogenous waste product eliminated by fishes and that the major site of elimination was the gills (rather than the kidneys). Studies since then have further corroborated this view but the mechanism(s) of transbranchial ammonia elimination is still debated (reviews by Evans and Cameron 1986; Walsh 1998). Theoretically, ammonia can move across the epithelium by diffusion (NH_3 and NH_4^+) either transcellularly or paracellularly with ion transport proteins facilitating the transcellular movement of NH_4^+, as lipid solubility is low. The difficulty is in determining the importance of the various pathways when ammonia exists in both gaseous (NH_3) and ionized (NH_4^+) forms in an equilibrium dependent on a number of factors (pH, temperature, and ionic strength) and when NH_4^+ versus $NH_3 + H^+$ movement cannot be experimentally distinguished.

Cameron and Heisler (1983) were able to demonstrate that P_{NH3} gradients across the branchial epithelium could account for the majority of total ammonia elimination under normal conditions of pH and low ambient ammonia in the freshwater rainbow trout. However, when fish are subjected to inward NH_3 and NH_4^+ gradients they are still able to maintain plasma levels below that of the ambient water. Under these conditions the active exchange of NH_4^+ for either external H^+ or Na^+ has been suggested (Cameron and Heisler 1983; Cameron 1986; Claiborne and Evans, 1988; Wilson and Taylor 1992). However, it is possible that the contribution of gill boundary layer acidification by CO_2 and H^+ transport is an important factor in maintaining outward P_{NH3} gradients even under these conditions (*in vitro* Wright *et al.* 1989; *in vivo* Wilson *et al.* 1994). In these studies, the addition of buffers to the water has been used to eliminate the contribution of boundary layer acidification. Boundary layer acidification, facilitates NH_3

diffusion by trapping NH_3 by protonation maintaining the P_{NH3} gradient ($NH_3 + H^+ \rightarrow NH_4^+$). The low ionic conductance of the freshwater fish gill indicates that paracellular NH_4^+ diffusion is likely a minor component of the total ammonia efflux.

The ionic permeability of the gill of seawater fishes is orders of magnitude larger than freshwater fishes (Evans 1979) as a result of leaky paracellular junctions found between chloride and accessory cells (see Chapter 4 Introduction; Sardet *et al.* 1979). Thus in seawater fishes paracellular NH_4^+ diffusion is an important component to J_{AMM}. The large inward Na^+ gradient is also thought to contribute to J_{AMM} by driving Na^+/NH_4^+ exchange. NH_4^+ has also been shown to substitute for H^+ on the Na^+/H^+ exchanger (NHE) protein (Kinsella and Aronson 1981). In addition, Evans *et al.* (1989) were able to find that 22% of total ammonia elimination in a perfused head preparation of toadfish was sensitive to Na^+,K^+-ATPase inhibition by ouabain in the perfusate. K^+ and NH_4^+ share a similar hydration radius and in *in vitro* studies NH_4^+ has been shown to compete with K^+ for binding sites on Na^+,K^+-ATPase (Mallery 1983; Kurtz and Balaban 1986; Garvin *et al.* 1985; Towle and Hølleland 1987; Wall and Koger 1994) and also the $Na^+:K^+:2Cl^-$ cotransporter (Kinne *et al.* 1986).

In order to examine the mechanism of active NH_4^+ elimination and the role of ion transport proteins I focused my attention on a marine fish that is able to tolerate high environmental ammonia levels (Peng *et al.* 1998) and that also happens to be an amphibious obligate air-breather (Ishimatsu *et al.* 1999). This fish is the mudskipper *Periophthamodon schlosseri*. The tolerance of the mudskipper to environmental ammonia is much higher than that of other fishes. The 96h LC_{50} for *P. schlosseri* is 514 μM NH_3 (Peng *et al.* 1998) compared to literature values ranging from 8.2 to 247 μM for other fishes (Thurston *et al.* 1983). *P. schlosseri* has an ammonia tolerance similar to the Lake Magadi tilapia (*Oreochromis alcalicus* grahami;

Randall *et al.* 1989) and the air breathing catfish *Heteropneustes fossilis* (Saha and Ratha 1990). However, these species make use of the ornithine-urea cycle to produce urea as a means of detoxifying ammonia while the mudskipper does not (Peng *et al.* 1998). Mudskippers make use of free amino acids and have a powerful glutamate dehydrogenase-glutamine synthetase system for ammonia detoxification in the brain (Peng *et al.* 1998). Interestingly, the mudskipper *P. schlosseri* shows no response to $36\mu M$ NH_3 in its bath water. It is able to maintain plasma and muscle ammonia, urea, and TFAA constant in spite of steep inward ammonia gradients of 8 mM NH_4^+ ($36\mu M$ NH_3). Although ammonia fluxes were not measured during these experiments it seems likely that active elimination of ammonia was occurring since endogenous production was continuing and internal levels were not changing.

These animals also have a high terrestrial affinity. A significant problem encountered during terrestrial excursions is the lost capacity for the elimination of ammonia (into water) (Morii *et al.* 1978; Iwata *et al.* 1981). During terrestrial exposure *P.schlosseri* remain ammonotelic and increase ammonia, urea and free amino acid stores (Ip *et al.* 1993), but not enough to account for the >90% inhibition of the excretory pathway for ammonia reported in other species of mudskippers (Morii *et al.* 1978; Iwata *et al.* 1981). *P. schlosseri* is more active out of water (Kok *et al.* 1998) and must, therefore, be producing significant amounts of ammonia. Interestingly, some ammonotelic terrestrial isopods and crustaceans overcome this problem by alkalinizing their gills and eliminating ammonia by volatilization (eg Wieser 1972; Greenaway and Nakamura 1991; Speeg and Campbell 1968).

Studies by Schöttle (1931), Low and co-workers (1988, 1990), and Yadav and co-workers (1990) all recognize the uniqueness of the gills of *P. schlosseri*. The gill filaments are short and branched and lamellae are thickened and have interlamellar fusions. The total gill

surface area is less than other mudskippers (Schöttle 1931; Low *et al.* 1988,1990). These characteristics have been interpreted as adaptations for air exposure to prevent collapse of the lamellae. A mucus coat and microridges also reduce desiccation (Low *et al.* 1990; Yadav *et al.* 1990). None of these studies, however, describe the fine structure of the branchial epithelium that would help in understanding gill function in this amphibious fish.

In this chapter, the mechanism of active ammonia elimination will be investigated by first determining which ion transport proteins are involved in ammonia excretion using a pharmacological approach, and then determining a morphological or cellular basis for ammonia excretion by examining the fine structure of the branchial epithelium. Finally, a pathway for NH_4^+ elimination will be constructed by localization of ion transport proteins using immunological techniques. In addition, terrestrial ammonia excretion rates as well as body and gill surface pH are presented to address the contribution of ammonia volatilization to terrestrial nitrogen elimination.

5.2 MATERIALS AND METHODS

5.2.1 Animals

Adult *Periophthalmodon schlosseri* of both sexes were collected from the Pasir Ris, a small estuary on the east coast of Singapore and transported to City University of Hong Kong. In the laboratory, fish in individual plastic aquaria were kept partially submerged in 50% seawater (15 ‰). Every other day the water was changed and the animals were fed goldfish *ad libitum*. The fish mass ranged from 55 to 120 g. The room air and water temperatures remained constant around 26°C. No attempts were made to control lighting conditions and a natural photoperiod was followed.

5.2.2 Measurements of ammonia fluxes in water and air

Animals were fasted 3 days prior to the start of experiments. A pair of flux measurements was performed on groups of fish kept individually in horizontal 1000 ml polypropylene bottles while half full of 50% SW and then with no SW. The containers were capped and provided with humidified air and the exiting air was passed through a series of acid traps (0.1N HCl). The animals were subjected to a three-hour partially submerged flux period followed by a twenty-four hour air exposed period. At the end of the 3h flux, the water was removed and a sample was acidified and stored at 4°C. At the end of the 24h air exposure, the containers with animals still inside were rinsed with 50%SW. A sample of this wash water was saved and stored as above. Blank runs were also made to account for naturally occurring ammonia in the system. Water and acid-trap samples were assayed for total ammonia (Verdouw *et al.* 1978) from which ammonia flux rates (J_{AMM}) were calculated (μmol ammonia $\cdot$ kg^{-1} fish $\cdot$ h^{-1}). Appropriate standards were prepared with either 50% SW or 0.1 N HCl. A total of 8 animals had paired flux measurements made.

5.2.3 Inhibitor Studies

Animals were fasted 3 days prior to the start of experimentation. A series of three flux periods was performed on fishes kept in 500 or 1000 ml of 50% SW. An initial three hour control flux period was followed by a three hour experimental flux period and finally a three hour recovery flux period. The experimental exposures consisted of exposing fish to either inhibit carbonic anhydrase with 0.1 mM acetazolamide, Na^+/H^+ exchange with 0.1 mM amiloride-HCl, boundary layer acidification with 5.0 mM HEPES at either pH 7 or pH 8, or vH^+-ATPase with 100mM KNO_3 (and 100mM KCl as a K^+ control) in 50%SW. Control and recovery

fluxes were conducted in 50% SW. For the first two flux periods water samples were taken at 0, 1, 2, and 3 hours but only at 0 and 3 hours for the recovery period.

In initial experiments the Na^+,K^+-ATPase inhibitor ouabain was shown to have no effect on J_{AMM} in 50%SW (T. Kok and K-Y Ip, personal communication). Therefore, an additional series of ammonia flux measurements were made on fish in 2 mM NH_4Cl in 50% SW followed by 2 mM NH_4Cl in 50% SW with either 0.1 or 0.01 mM ouabain. Water samples were taken at 0, 1, 2, and 3h during each exposure period.

Water samples were assayed for total ammonia concentration (Verdouw *et al.* 1978) from which ammonia flux rates (J_{AMM}) were calculated (μmol ammonia $\cdot$ kg^{-1} fish $\cdot$ h^{-1}). Appropriate standards were prepared with the inhibitors in 50% SW . Titratable acidity (TA) flux was measured according to the method of McDonald and Wood (1981) from the difference between 0 and 3h water samples from control and experimental periods. In short, 100 ml water samples were aerated overnight to remove respiratory CO_2 and a 25 ml sub-sample (weighed to 0.01g) was titrated to pH 4.00 with 0.01 N HCl using a Radiometer autotitrator and Orion Ross type combination electrode. Aeration continued during titration to remove liberated CO_2. The net acid flux (J_{ACID}; μEq $H^+ \cdot kg^{-1} \cdot h^{-1}$) was calculated as the sum of the TA and J_{AMM}, signs considered.

5.2.4 Surface pH measurements

Measurements of the surface pH of the skin and gills were made during air exposure using a solid state micro pH electrode (PHR-146; Lazar Research Laboratories, CA) coupled to a Radiometer PHM 84 meter (Radiometer-Copenhagan, DK). The dorsal surface behind the eyes, and below the dorsal fin, laterally between the base of the pectoral fin and the body wall as well as the gills were measured repeatedly and values averaged for 4 animals.

5.2.5 Acclimation to different ambient salinities

Groups of 6 animals were acclimated over two weeks to either 5‰ SW, 15‰ SW or 25‰ SW. Every other day the water was changed and the animals were fed goldfish ad libitum. At the end of the second week, ammonia and urea flux measurements were made over a 3h period (as described above) and the animals were sacrificed by an overdose of MS-222 and cervical transsection. A 1 ml blood sample was taken by caudal puncture using a heparinized syringe. Whole blood pH was measured using an Orion micro-tip Ross type combination electrode coupled to a Radiometer-Copenhagen PHM 84 meter. Blood P_{O2}, P_{CO2}, and pH were also measured on a Corning blood-gas analyzer. The remainder of the sample was centrifuged and the plasma collected and frozen for later analysis of ammonia, urea, and Cl^-.

5.2.6 Plasma analytical procedures

Plasma total ammonia concentrations (Tamm) were determined using a commercial diagnostic kit (GLDH/NADH: Sigma, St. Louis, MO) and the P_{NH3} and $[NH_4^+]$ calculated from the pH and Tamm values using a rearrangement of the Henderson-Hasselbalch equation and pK' and NH_3 solubility values determined by Cameron and Heisler (1983). Plasma chloride concentrations $[Cl^-]$ were determined by coulometric titration (Haake Buchler Instruments digital chloridometer) and plasma urea concentrations were measured by the diacetyl monoxime method (Sigma).

5.2.7 ATPase Activity

Na^+,K^+-ATPase and vH^+-ATPase activities (μmol Pi · mg^{-1} protein · h^{-1}) in crude gill homogenates were determined at 22.5°C in a plate reader (Thermomax, Molecular Devices Corp., CA) modified from McCormick (1993). Na^+-K^+ ATPase and vH^+-ATPase activities were

defined as specific inhibition by 1.0 mM ouabain and 100mM KNO₃, respectively. See General

materials and methods for additional details of the assay.

5.2.8 Tissue fixation for Standard TEM (Transmission electron microscopy)

Animals were anaesthetized with MS-222 (3-aminobenzoic acid ethylester; 1:5000) and

killed by cervical transection. The gill arches were excised as well as pieces of the inner

opercular membrane. Pieces of tissue were immersed in fixative containing 1.5% glutaraldehyde,

1.5% paraformaldehyde, buffered with 0.1M sodium cacodylate (pH 7.4) over night at 4°C.

Following primary fixation the tissue was rinsed with 0.1 M cacodylate buffer and post fixed on

ice in 1% osmium tetroxide in 0.1 M sodium cacodylate. The tissue was then rinsed with dH₂O,

and stained *en bloc* with 1% aqueous uranyl acetate. Tissue was embedded in Epon 812

(PolyScience) following serial dehydration with ethanol followed by propylene oxide.

Thin sections (70-90 nm) were made on an Ultracut microtome and mounted on copper

grids and counter stained with lead citrate and uranyl acetate. Sections were viewed on a Phillips

300 TEM at 60kV. Semithin sections (1μm) were also made and stained with toludine blue.

5.2.9 Tissue fixation for immunocytochemistry

Whole gill arches were fixed for immunolocalization studies at both light and em levels

using 3%PFA/PBS and PLP fixatives, respectively, overnight at 4°C. Tissue for

immunofluorscence was frozen as well as paraffin embedded. Tissue for immuno-em was

embedded in Unicryl. See General Materials and Methods for additional information.

5.2.10 Immunocytochemistry and Antibodies Employed

The distribution of Na^+,K^+-ATPase, $Na^+:K^+:2Cl^-$ cotransporter (NKCC), Na^+/H^+

exchanger (NHE2,3), CFTR, carbonic anhydrase (CA) and vH^+-ATPase was determined by

indirect immunofluorescence and immunoperoxidase methods in paraffin and fixed frozen gill

tissue. Antibodies against AE were not crossreactive with epithelial. See General Materials and Methods for additional information.

5.2.11 Statistical Analysis

Data are presented as mean ± SEM (n). Ammonia excretion rates from the different treatments were compared using a one way repeated measures ANOVA and post hoc SNK. Net ammonia, titratable acidity and acid fluxes under control and experimental conditions were compared using paired t-tests. The fudicial limit was set at 0.05.

5.3 RESULTS

5.3.1 Ammonia fluxes and effects of inhibitors

Flux rates for ammonia of fish kept partially submerged are 486.2 ± 35.0 μmol ammonia · kg^{-1} fish · h^{-1}. During emergence the total ammonia excretion rate is significantly reduced to 288.74 ± 29.57. The volatilized component is minor, usually contributing less than 3% to the total (7.75 ± 1.07).

Addition of the NHE inhibitor (0.1 mM) amiloride to the water reduces J_{AMM} by 42% but has no effect on J_{ACID} which remains around zero (Figure 5.1.1). During the subsequent hours of exposure, J_{AMM} increases slightly and begins to recover after changing the bath to fresh 50% SW without amiloride.

The carbonic anhydrase inhibitor (0.1 mM) acetazolamide reduces J_{AMM} by 48% yet does not have a significant effect on J_{ACID} (Figure 5.1.2). J_{AMM} starts to recover during exposure to acetazolamide and after its removal.

The addition of 5 mM HEPES to 50% SW is sufficient to fix the water pH at either 7 or 8 during the 3h experimental period (Figure 5.1.3e). Buffering the water at pH 7.0 does not

119

significantly affect either J_{AMM} or J_{ACID} (Figure 5.1.3a,b). However, addition of 5mM HEPES pH 8 significantly increases J_{ACID} while having no effect on J_{AMM} (Figure 5.1.3c,d).

In vivo the vH^+-ATPase inhibitor KNO_3 only significantly affects J_{AMM} after the second hour of exposure (Figure 5.1.4a). However, the averaged J_{AMM} value over the 3h period is not significantly different from the initial control (Figure 5.1.4b). Although, J_{ACID} is significantly reduced from the initial control, so too is the parallel KCl control exposure (Figure 5.1.4d). Animals fail to recover J_{AMM} after their experimental treatments.

Animals exposed to 2mM NH_4Cl in 50% SW at pH 7.8 are still able to eliminate ammonia (Figure 5.1.5) at rates comparable to control animals from other experiments (Figure 5.1.3a,c). Addition of 0.1 mM ouabain significantly reduces J_{AMM} while 0.01 mM ouabain is without effect. There is also a significant increase in plasma total ammonia in animals exposed to 0.1 mM ouabain (Table 5.1).

Animals acclimated to salinities of 5, 15 and 25 ‰ SW for two weeks show no differences in net ammonia or urea fluxes (Table 5.2a). However, plasma $[NH_4^+]$ and P_{NH3} are significantly higher in fish acclimated to higher salinity (25‰) (Table 5.2a).

In vitro ATPase activities

Na^+,K^+-ATPase and vH^+-ATPase enzyme activities measured in crude gill homogenates as specific inhibition with 1 mM ouabain and 100 mM KNO_3, respectively, are shown in Table 5.2. Significant levels of activity are present in gill homogenates but there are no differences in Na^+,K^+-ATPase or vH^+-ATPase activities in groups of fish acclimated to the high and low salinities.

Surface pH

The measurements of the skin surface pH in air-exposed animals taken from several sites around the body are consistent within and between animals and not significantly different from seawater (Table 5.3). However, the surface pH of the gills is significantly lower than seawater and the other body surfaces measured.

5.3.2 Ultrastructural level examination of the gill epithelium

Basic organization of the gill

The gills of *P. schlosseri* are composed of four pairs of gill arches. The first gill arch supports a fold of opercular tissue. In addition, *P. schlosseri* has a pair of pseudobranches. The gill filaments are short and occasionally have complicated branching patterns. They are not organized in a sieve-like arrangement of orderly rows seen in most gills. Instead, the filaments dangle in the opercular cavity, which is more often than not filled with air.

Filament

Along the length of the filament are parallel rows of semi-circular shaped lamellae on both the top and bottom filament edges. A cross section through the filament reveals the afferent (AV) and efferent (EV) vessels seen at opposing ends and embedded in loose connective tissue (Figure 5.2.1a). The central venous sinus, nutritive vessels and nerve bundles are found below the lamellar bases (Figure 5.2.1e). Blood spaces are also sometimes seen in the spaces between the filament epithelium and AV and EV (Figure 5.2.1a,b,c). The filament (in cross section) tends to be consistent in appearance along its length except during branching when bundles of skeletal muscle are observed between the AV and trailing edge epithelium (Figure 5.2.1c). A cartilaginous support rod runs closely parallel to the afferent vessel (Figure 5.2.1a). Following branching of a filament, the cartilaginous rod disappears.

The stratified filament epithelium along afferent and efferent edges consists mainly of squamous and columnar pavement cells with a few large mucocytes. MR cells are not very common along this part of the epithelium but intraepithelial capillaries are sometimes observed along the efferent edge notably during filament branching (Figure 5.2.1b). Associated with the appearance of these intraepithelial capillaries is a system of larger sub-epithelial vessels that deliver and return blood to the venous circulation.

Lamellae

The lamellae of *P. schlosseri* follow the basic piscine plan of blood spaces defined by modified endothelial cell (pillar cell) supporting a pseudo-stratified epithelium of pavement cells (PVC) and mitochondria-rich (MR) cells (Figure 5.2.2a). However, the lamellae of *P. schlosseri* have some unique features not found in any other type of fish gill so far described. The blood to water diffusion distance is large (~ 15 μm) because the epithelium consists of a thick layer of mitochondria-rich and filament-rich (FR) cells covered by a layer of pavement cells. In addition, adjacent lamellae are frequently seen fused together and this restricts the water space to a narrow channel (Figure 5.2.2b). Typically the cross-sectional area of the blood space is greater than that for the external milieu. Within the fused areas it is not possible to distinguish from which lamellae the cells arose. The bases of neighbouring lamellae are often not separated by (interlamellar) filament epithelium.

Mitochondria-rich (MR) cells and accessory cells

The lamellar epithelium is composed almost entirely of large mitochondria-rich cells (Figure 5.2.2a). These cells sit on a thick basal lamina and are either ovoid or cuboidal. The cells are characterized by their abundant mitochondria, by an extensive system of regularly branching and anastomosing tubules that is continuous with the basolateral plasmalemma (tubular system),

and by a subapical collection of irregular tubules and vesicles (vesiculotubular system). The subapical area is rich in microfilaments. The apical plasmalemma forms a deep crypt with a variable number of microvilli. The MR cell sends cytoplasmic projections into the PVCs lining the rim of its apical crypt.

Apical crypts appear to be formed as invaginations in the apical surface of single MR cells; that is, apical crypts seldom have more than one MR cell forming their boundaries. In cases where crypts are bordered by more than one cell, thin or shallow tight junctions are observed between the neighbouring MR cells (Figure 5.2.3a,b). Moreover, one of the MR cells is smaller in size, has a more granular cytoplasm and is in a peripheral position relative to the other (Figure 5.2 3a). Multiple cytoplasmic processes from the smaller MR cell make their way through the apical cytoplasmic region of the larger MR cell to the apical membrane to increase the total shallow junction length, in sections, this region appears as a 'mosaic'. This smaller MR cell has been termed the 'accessory cell' and the intimate relationship seen with the larger MR (chloride) cells is typical of marine teleost gills (see review by Laurent 1984). Generally, direct contact between neighbouring MR cells was rarely observed because a special type of cell, the filament rich cell, physically separates neighbouring MR cells.

Filament Rich (FR) Cells

These cells, that are flattened in appearance and are found between neighbouring MR cells, attach to the basal lamina and have cytoplasmic processes extending between, and sometimes into, neighbouring MR cells (Figure 5.2.4a-d). They extend up to the mucosal pavement cells and have not been observed to contact the external medium. These cells have a denser cytoplasm than MR cells, and have thick bundles of intermediate filaments associated with desmosomes (Figure 5.2.4d), in addition to some vesicles and a few mitochondria. Within

123

the narrow space between MR cells, these filament rich (FR) cells often have an interstitial space created from an invagination of the plasmalemma (Figure 5.2.4a-c). The space is quite irregular with branching and anastomosing cytoplasmic processes within. This extracellular space may form isolated pockets or possibly channels (canaliculi).

Pavement cells (PVC)

The pavement or squamous epithelial cells cover the majority of the lamellar surface with MR cell apical areas restricted to apical crypts. Thick tight junctions join neighbouring PVCs. The surface of these cells displays a system of microridges. These flattened cells have a dense, granular cytoplasm, Golgi system, numerous mitochondria with sparse, loosely arranged crista, and vesicles of various sizes and densities (Figure 5.2.2b). PVCs and FR cells together encapsulate MR cells, isolating them from one another.

Pillar cells

The lamellar blood spaces are defined by pillar type cells characteristic of fish lamellar endothelium (Figure 5.2.2b, 3a; Newstead 1967; Hughes and Weibel 1972). Generally, the lamellae have 4-6 roughly parallel blood spaces including the marginal and basal channels. The irregular distribution of pillar cells accounts for the changing position of the channels. Weibel-Palade bodies (osmiophillic) are seen within the cytoplasm of flattened endothelial cells of the basal and marginal channels. The marginal channel at the top of the lamellae is larger than other blood spaces and the basal channel is not deeply embedded within the filament.

Opercular membrane

Schöttle (1931) has identified the opercular membrane as an accessory respiratory organ (ARO) in *P. schlosseri* and a number of other species of mudskipper. The inner operculum is well vascularized, and numerous papillae and furrows increase the surface area. Lining these

papillae are capillaries found within the stratified epithelium (Figure 5.2.5). The capillaries pass through the epithelium basal lamina and retain their own sheath of basal lamina separating them from the true epithelial cells. The blood spaces are separated from the opercular cavity by an endothelial cell, basal lamina, a capillary associated epithelial cell and pavement cell layer (Figure 5.2. 5c). The surface of the pavement cell is covered by pronounced microridges. The pavement cells of this epithelium are very similar to those found in the gill. These PVCs are electron-dense, having mitochondria with sparse crista, and have a range of vesicles. Mucocytes are quite common in this epithelium and can often be found along side a capillary. MR cells are generally rare. This epithelium is very similar to that found along some sections of the filament leading edge (see Figure 5.2.1b). Nerve bundles often are seen in the papillae in association with blood vessels. The blood vessels appear to contain a system of valves for controlling blood flow.

5.3.3 Immunohistochemistry

Na^+,K^+-ATPase

Figure 5.3.1 shows the abundance of Na^+,K^+-ATPase immunoreactivity associated with the lamellar epithelium. Immunopositive cells are also found in the epithelium of the gill arch. Immunoreactivity for Na^+,K^+-ATPase is restricted to the large epithelial MR cells (Figures 5.3.2a). The labeling is throughout the cell body with the exception of the nucleus and apical crypt area. Immunogold labeling for Na^+,K^+-ATPase reveals that the intracellular staining observed by immunofluorescence is restricted to elements of the tubular system and there is no labeling associated with the apical crypt (Figure 5.3.3a,b). In Western blots, the $\alpha5$ antibody cross reacts strongly with a band with an apparent MW of 116kDa (Figure 5.3.7a).

NKCC

The NKCC essentially has an identical distribution as Na^+,K^+-ATPase (Figure 5.3.3e,f). NKCC immunofluorescence labeling shows a diffuse cytoplasmic distribution while the higher resolution immunogold technique indicates that labeling is associated with the MR cell tubular system. No labeling is associated with the apical crypt. However, I was unable to demonstrate immunoreactivity with Western blots using the J3 and T4 NKCC antibodies.

CFTR

The mouse monoclonal antibody against the human cystic fibrosis transmembrane regulator (CFTR) crossreacts specifically with the MR cell apical crypt (Figure 5.3.3c,d). In sections, labeled crypts appear as either a ring or "U" shape indicative of cross or longitudinal sections through the crypt, respectively. This antibody was only useful with fixed-frozen tissue and not fixed-paraffin embedded tissue. No immunolabeling is associated with the basal portion of the MR cell, pavement cells, pillar cells, mucocytes or erythrocytes. Western blots indicate an immunoreactive band with an apparent MW of 150 kDa (Figure 5.3.7b).

Carbonic anhydrase

Immunoperoxidase staining for carbonic anhydrase in fixed-frozen sections is restricted to the apical crypt region of the MR cells (Figure 5.3.4a,b). Staining is not associated with the rest of the cell. Erythrocytes also show immunoreactivity while no immunoreactivity is associated with pavement cells, or pillar cells. Incubation of control sections with normal rabbit serum at an equivalent dilution results in insignificant levels of labeling.

vH^+-ATPase

The vH^+-ATPase was immunolocalized using a polyclonal antibody directed against the A-subunit of the vacuolar proton pump complex. Immunoperoxidase staining shows that the

vH$^+$-ATPase is restricted to the apical crypt region of MR cells (Figure 5.3.4c). It should be noted that some difficulty was encountered in consistently reproducing these results. Western blots show an immunoreactive band with an apparent MW of 78 kDa (Figure 5.3.7c).

Na$^+$/H$^+$ Exchanger

The distribution of apical isoforms of the Na$^+$/ H$^+$ exchanger (NHE-2, and 3) were determined in the mudskipper gill using antibodies Ab597 and Ab1380 specific for NHE-2 and NHE-3, respectively. Both NHE isoforms are immunolocalized to the apical crypts of MR cells (Figure5.3.5 and 5.3.6). From low power photomicrographs, most crypts can be seen to be labeled (Figure 5.3.5a). The NHE-3 antibody Ab1381 was not useful for tissue localization. In Western blots of crude membrane preparations, immunoreactivity is seen with bands in the predicted MW ranges (~85 kDa), however, additional major bands are also recognized at lower MWs (Figure 5.3.7 d,e).

Table 5.1 Plasma total ammonia concentrations (mM $\pm$ SEM) in *P.schlosseri* exposed to 50%SW (n=6) or 2mM NH$_4$Cl in 50% seawater in the presence of either 0.1 of 0.01 mM ouabain (n=5 and 6, respectively). The asterisk indicates a significant difference from the control value (P<0.05).

0 mM NH$_4$Cl in 50% SW	2mM NH$_4$Cl in 50% SW	
NO Ouabain	0.1 mM Ouabain	0.01 mM Ouabain
114.6 $\pm$ 9.6	245.3 $\pm$ 52.9*	97.1 $\pm$ 12.6

Table 5.2 Net ammonia and urea flux rates (μmol N $\cdot$ kg^{-1} fish $\cdot$ h^{-1}), and plasma [NH$_4^+$] (mM), P_{NH3} (torr), and urea (mM) of *P. schlosseri* acclimated to salinities of 5, 15 and 25‰ for 2 weeks (n = 6). Blood gas (P_{O2}, P_{CO2}) and acid-base (pH, [HCO$_3^-$]) and total CO$_2$ (tCO$_2$) variables are shown in the lower half of the table. Total *in vitro* ATPase activity (μmol ADP $\cdot$ mg^{-1} protein $\cdot$ h^{-1}) in crude mudskipper gill homogenates from fish acclimated to 5 and 25‰ SW (n = 5 and 6, respectively). Na$^+$,K$^+$-ATPase (1 mM ouabain) and vH$^+$-ATPase activities (100mM KNO$_3$) were determined from inhibitor sensitivities. Like characters indicate no statistically significant difference. (P<0.05)

Seawater Salinity	J_{AMM}	J_{Urea}	[NH$_4^+$] (mM)	P_{NH3} (torr)	[Urea] (mM)	Total ATPase	Na$^+$,K$^+$-ATPase	vH$^+$-ATPase
5 ‰	439.6[a] ±29.2	129.6[a] ±12.5	0.091[a] ±0.010	68.4[a] ±8.0	2.83[a] ±0.26	16.24[a] ±1.44	12.85[a] ±1.50	4.18[a] ±0.46
15 ‰	447.3[a] ±48.6	106.9[a] ±9.6	0.115[b] ±0.010	71.0[a] ±3.6	2.80[a] ±0.11	---	---	---
25 ‰	569.4[a] ±67.2	96.0[a] ±10.8	0.150[c] ±0.027	111.1[b] ±23.1	3.78[a] ±0.42	15.41[a] ±2.81	11.66[a] ±2.18	3.83[a] ±0.79

Blood/Salinity	P_{O2} (torr)	pH	P_{CO2} (torr)	[HCO$_3^-$] (mM)	tCO$_2$ (mM)
5‰	18.3 ± 0.6	7.535 ± 0.021	13:7 ± 1.2	10.7 ± 0.9	11.4 ± 0.9
15‰	20.2 ± 1.2	7.453 ± 0.023	14.0 ± 0.7	9.4 ± 0.4	10.1 ± 0.4
25‰	16.7 ± 2.1	7.509 ± 0.025	14.2 ± 1.8	10.7 ± 0.8	11.4 ± 0.9

Table 5.3 Surface pH measurements of the skin and gills of *Periophthalmodon schlosseri* during emersion. Asterisk (*) indicates significant difference from all other groups. n = 4, $P \leq 0.05$.

Location	Surface pH
Lateral (base of pectoral fin)	7.73 ± 0.19
Dorsal body	7.78 ± 0.18
Dorsal head region	7.98 ± 0.15
Gill	$7.14 \pm 0.03^{*}$
50% SW	7.78 ± 0.08

FIGURE 5.1.1 The effects of the Na^+/H^+ exchange inhibitor amiloride (0.1 mM) on (**a**) net ammonia (J_{AMM}; $\mu mol \cdot kg^{-1} \cdot h^{-1}$) and (**b**) net acid fluxes ($J_{ACID} = J_{TA} + J_{AMM}$; $\mu Eq \cdot kg^{-1} \cdot h^{-1}$) in mudskippers in 50% SW. The flux series (**a**) consists of an initial 3h-control flux (C1-3) followed by 3h exposure (E1-3) and recovery flux (R3) periods. The J_{AMM} is calculated for each hour during the control and exposure periods and only over the 3h period during the recovery. In (**b**) J_{ACID} is calculated from the 3h TA and J_{AMM} values. Values marked with like characters in (**a**) are not significantly different and the asterisks in (**b**) indicate a significant difference from the corresponding initial 3h-control value. Note the significant reduction in J_{AMM} following addition of amiloride and the recovery of J_{AMM} with its removal and the absence of changes in J_{ACID}. n = 6. $P \leq 0.05$

a

b

Titratable acidity (TA)

Net Ammonia Flux (J_{Amm})

Net Acid Flux (=TA + J_{Amm})
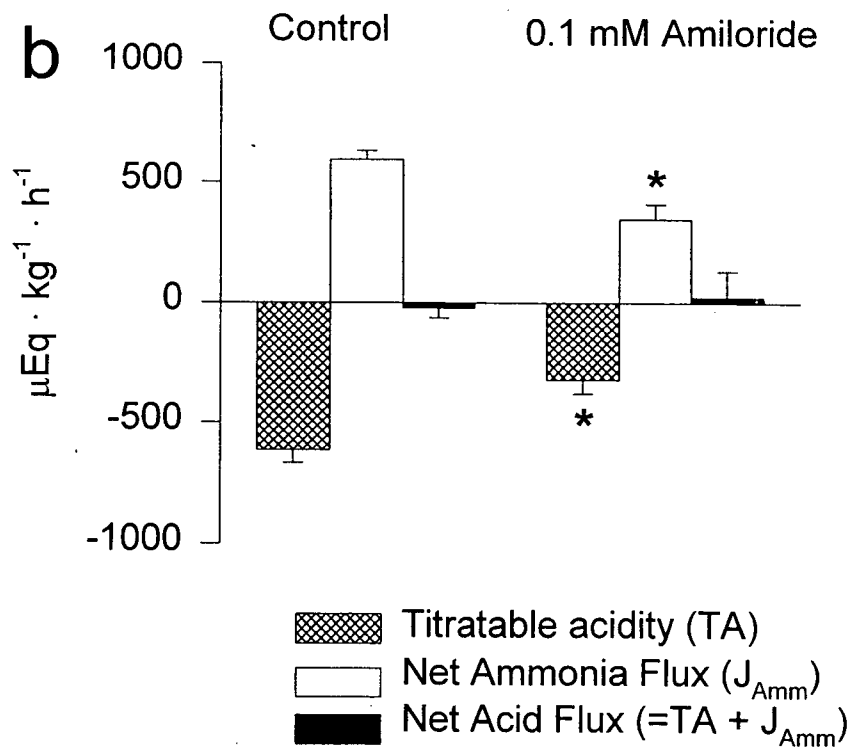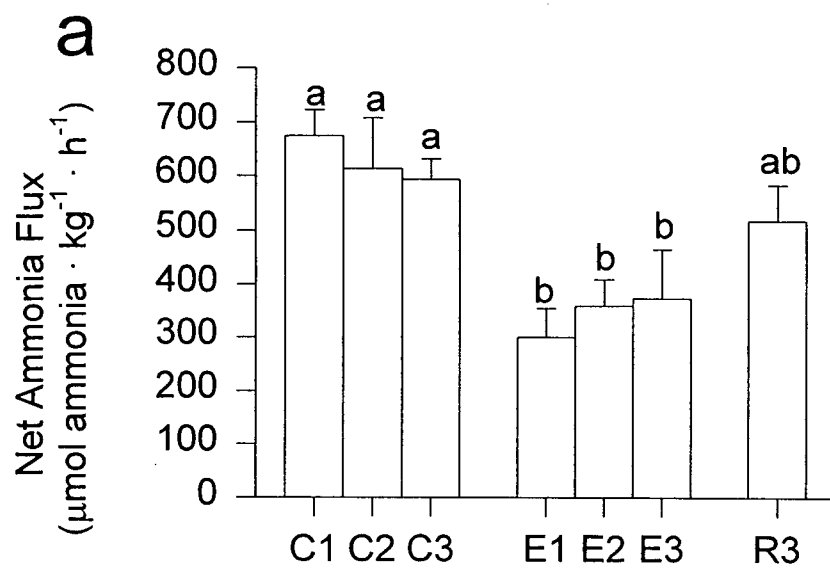
FIGURE 5.1.2 The effects of the carbonic anhydase inhibitor acetazolamide (0.1 mM) on **(a)** net ammonia (J_{AMM}; $\mu mol \cdot kg^{-1} \cdot h^{-1}$) and **(b)** net acid fluxes ($J_{ACID} = J_{TA} + J_{AMM}$; $\mu Eq \cdot kg^{-1} \cdot h^{-1}$) in mudskippers in 50% SW. The flux series **(a)** consists of an initial 3h-control flux (C1-3) followed by 3h exposure (E1-3) and recovery flux (R3) periods. The J_{AMM} is calculated for each hour during the control and exposure periods and only over the 3h period during the recovery. In **(b)** J_{ACID} is calculated from the 3h TA and J_{AMM} values. Values marked with like characters in **(a)** are not significantly different and the asterisks in **(b)** indicate a significant difference from the corresponding initial 3 h control value. Note the significant reduction in J_{AMM} following addition of acetazolamide and the recovery of J_{AMM} with time and the absence of changes in J_{ACID}. n = 6. $P \leq 0.05$

a

Ammonia Flux (μmol ammonia $\cdot$ kg^{-1} $\cdot$ h^{-1})

b

μEq $\cdot$ kg^{-1} $\cdot$ h^{-1}

Control   0.1 mM Acetazolamide

Titratable acidity (TA)
Net Ammonia Flux (J_{Amm})
Net Acid Flux (=TA + J_{Amm})

134
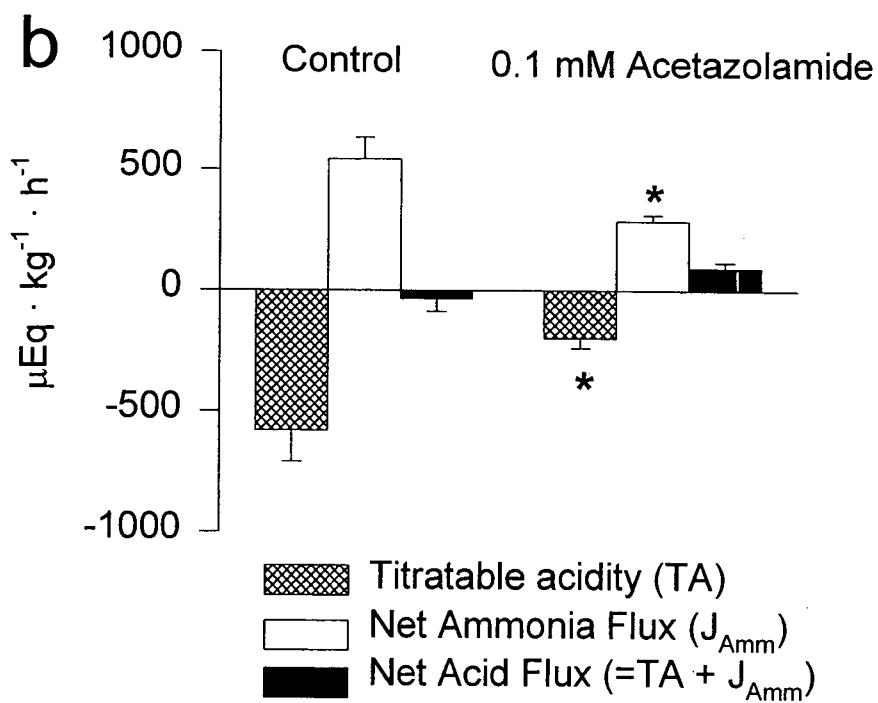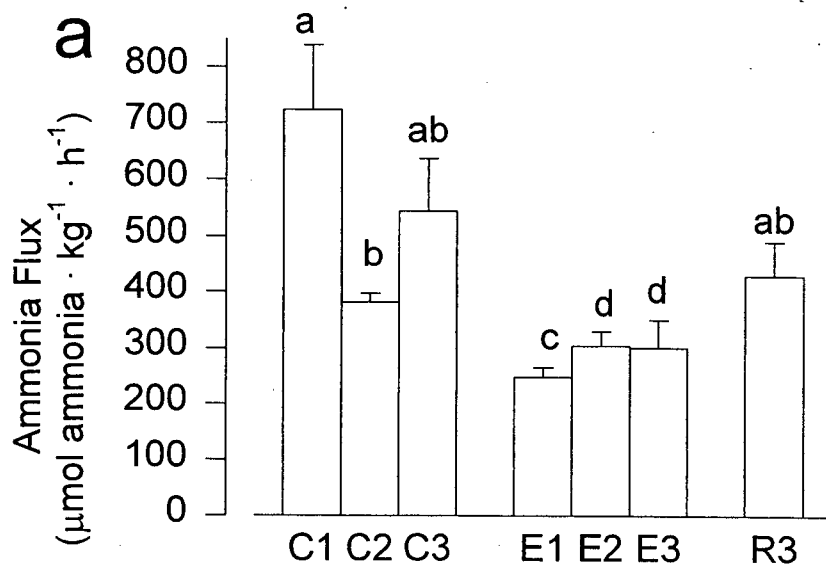
FIGURE 5.1.3 The effects of changes in boundary layer pH by 5mM HEPES pH 7.0 and pH 8.0 on net ammonia (J_{AMM}; $\mu mol \cdot kg^{-1} \cdot h^{-1}$) (**a, c** respectively) and net acid fluxes ($J_{ACID} = J_{TA} + J_{AMM}$; $\mu Eq \cdot kg^{-1} \cdot h^{-1}$) (**b, d** respectively) in mudskippers in 50% SW. The flux series (**a, c**) consists of an initial 3 h control flux (C1-3) followed by 3h exposure (E1-3) and recovery flux (R3) periods. The J_{AMM} is calculated for each hour during the control and exposure periods and only over the 3h period during the recovery. In (**c, d**) J_{ACID} is calculated from the 3h TA and J_{AMM} values. Water pH values during the initial 3h control flux and the following 3h HEPES flux period at 0 ,1 and 3 h are shown in (**e**). The asterisks in (**d**) indicate a significant difference from the corresponding initial 3 h control value. n = 6. P≤ 0.05
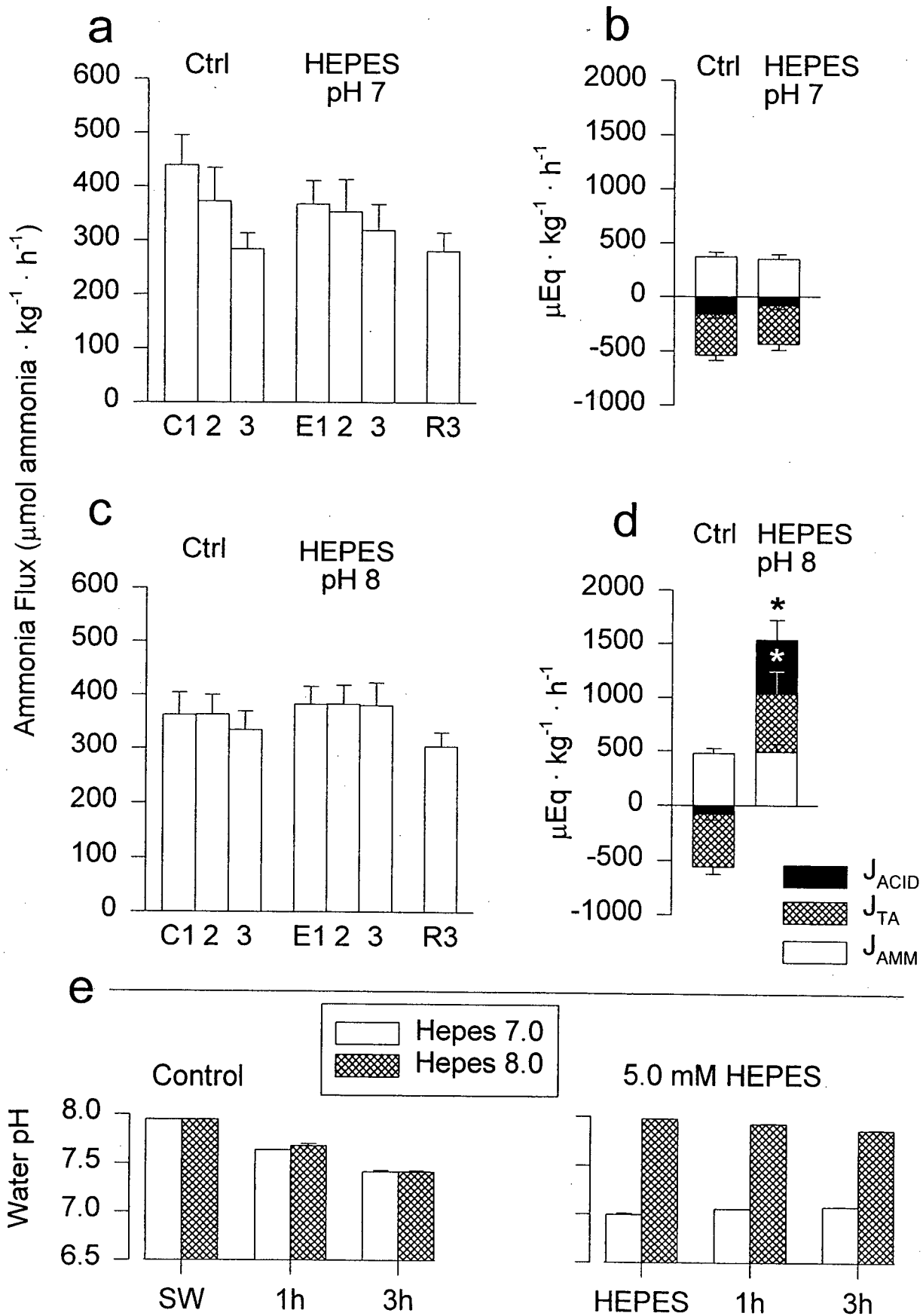
FIGURE 5.1.4 The effects of the vH^+-ATPase inhibitor 100 mM KNO_3 and 100 mM KCl (control) on net ammonia (**a,c** respectively) (J_{AMM}; $\mu mol \cdot kg^{-1} \cdot h^{-1}$) and net acid fluxes (**b,d** respectively) ($J_{ACID} = J_{TA} + J_{AMM}$; $\mu Eq \cdot kg^{-1} \cdot h^{-1}$) in mudskippers in 50% SW over a 3 h period. The flux series consists of an initial 3 h control flux (C1-3) followed by 3h exposure (E1-3) and recovery flux (R3) periods. The J_{AMM} is calculated for each hour during the control and exposure periods and only over the 3h period during the recovery. In (**b, d**), J_{ACID} is calculated from the 3h TA and J_{AMM} values. Values marked with like characters are not significantly different in (**a,c**) and the asterisks indicate a significant difference from the corresponding initial 3 h control value in (**b, d**). Note that the effect of 100 mM KNO_3 on J_{AMM} is not apparent until the 3rd h of exposure and no recovery is seen. n = 6. $P \leq 0.05$
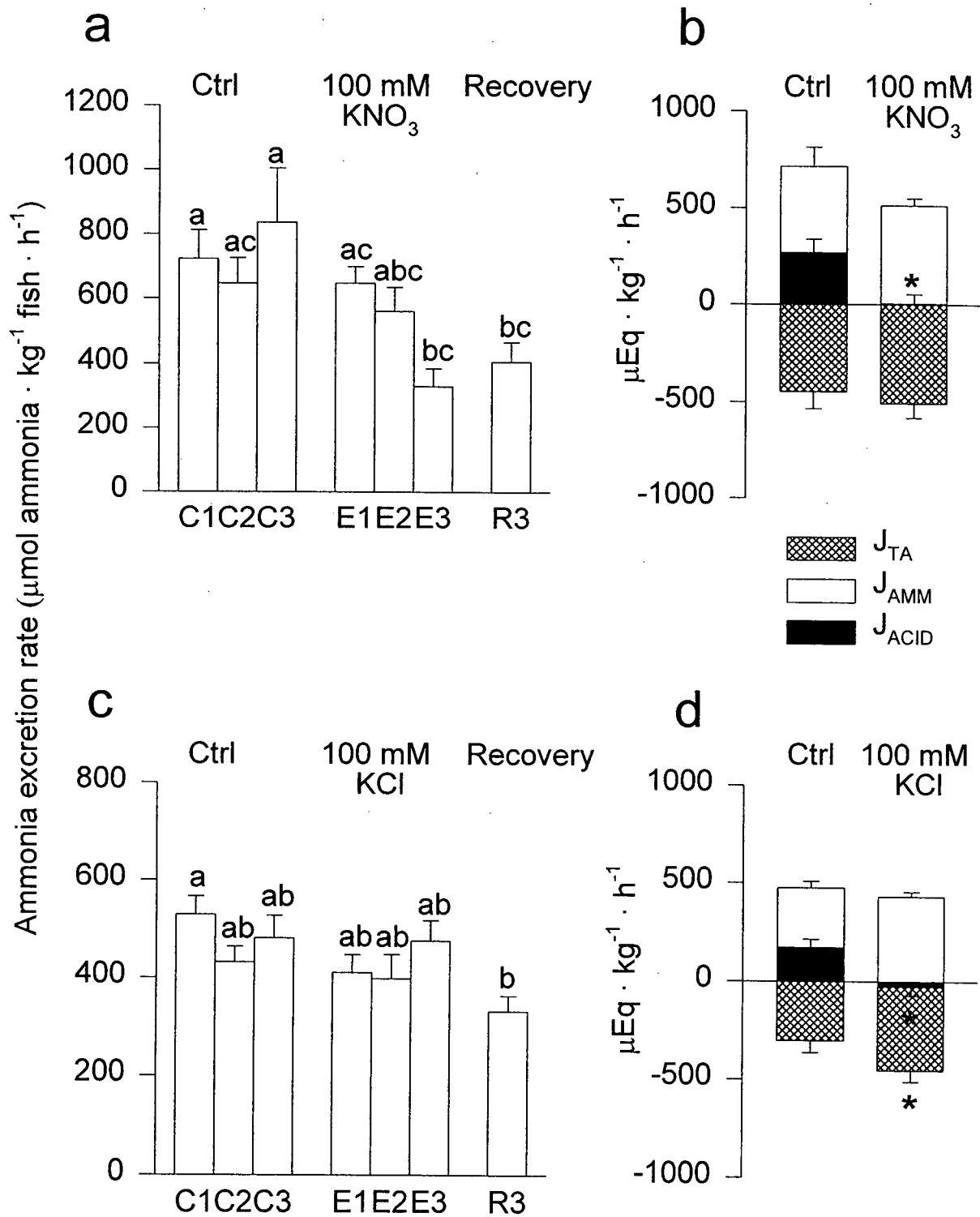
FIGURE 5.1.5 The effect of the specific Na^+,K^+-ATPase inhibitor ouabain (0.1 mM and 0.01 mM) on net ammonia fluxes in *P.schlosseri* in 2mM NH_4Cl in 50%SW. n= 6 and 5 for 0.1 mM and 0.01 mM ouabain treatment groups, respectively. Note that the ammonia excretion rate is significantly reduced in animals exposed to 0.1 mM ouabain while 0.01 mM is without effect. $P \leq$ 0.05
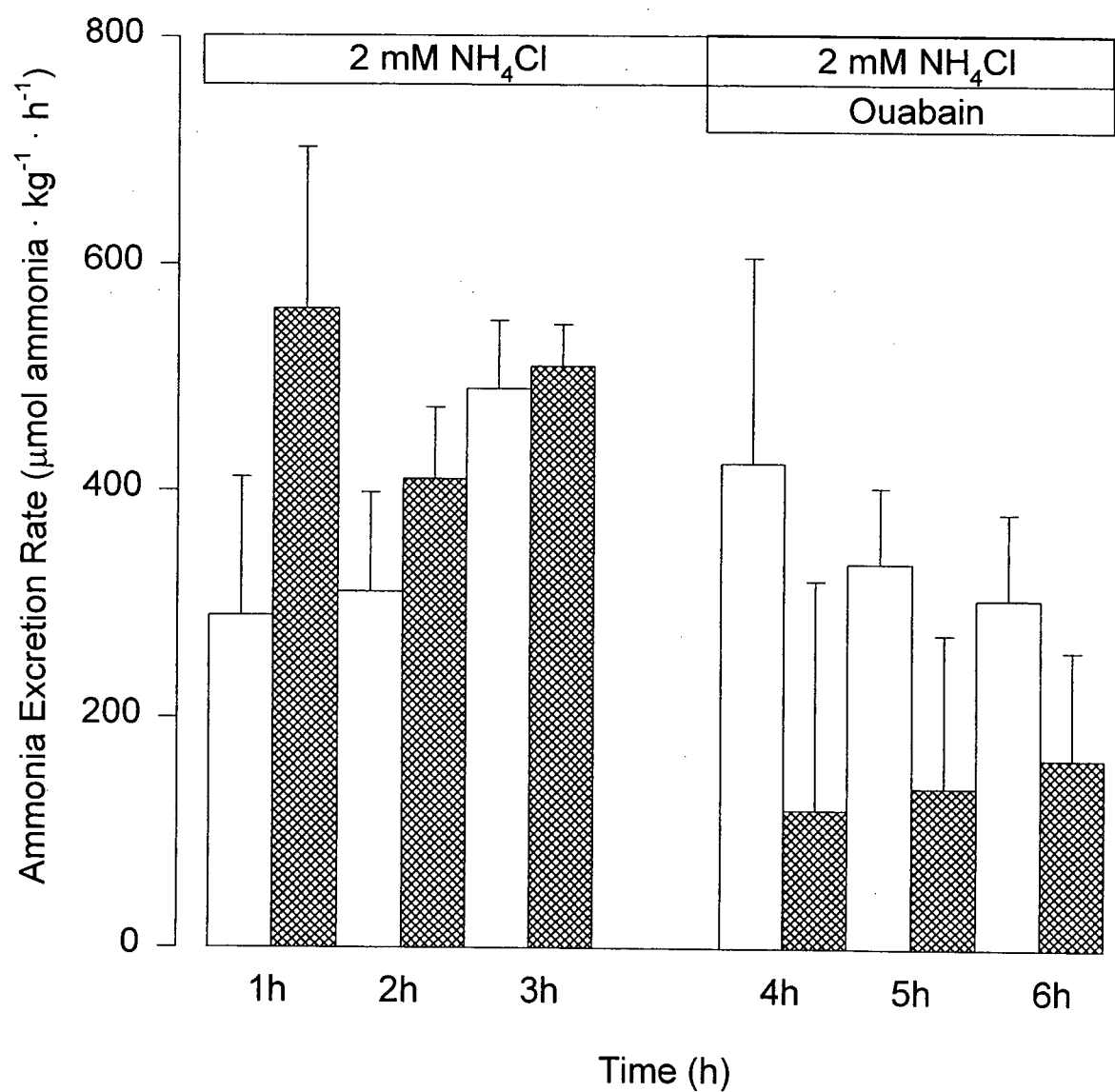
FIGURE 5.2.1 A low magnification light micrograph of a cross section through a gill filament (**a**). Superimposed black boxes indicate the general area of the higher magnification micrographs (**b-e**). Note (**a**) the large afferent (AV) and efferent (EV) arteries and the oblong cross sectional appearance of the filament. An asterisk indicates a cartilaginous support rod. The lamellae, which are arranged in parallel rows perpendicular to the long axis of the filament, are seen in sagital section along the top and bottom sides of the filament (**a**, superimposed white boxes). In higher magnification light micrographs intraepithelial capillaries (**b**, arrows) can be seen at the efferent edge while being absent at the afferent edge (**c**). However, skeletal muscle is observed close to the afferent edge (**c**). The numerous mitochondria of the mitochondria-rich cells found in the lamellae are also visible (**d**). Also note the distance from the marginal channel to the apex of the lamellae (~15μm) (**a, d**). The central venous sinus (CVS), a nerve fascicle (arrow) and an arteriole (asterisk) are located just beneath the base of the lamellae (**e**). Scale bar (**a**) 200μm, (**b-e**) 50μm.

142
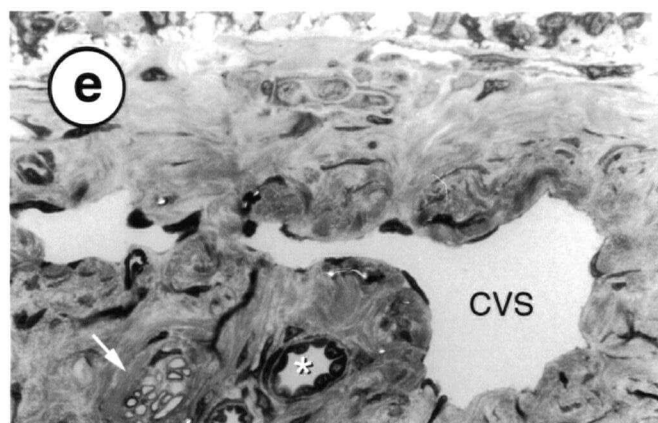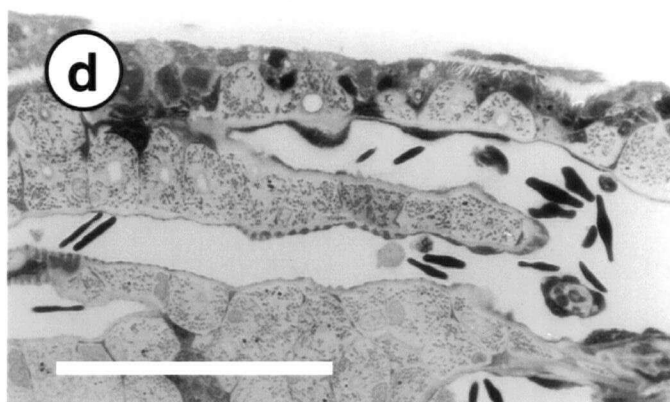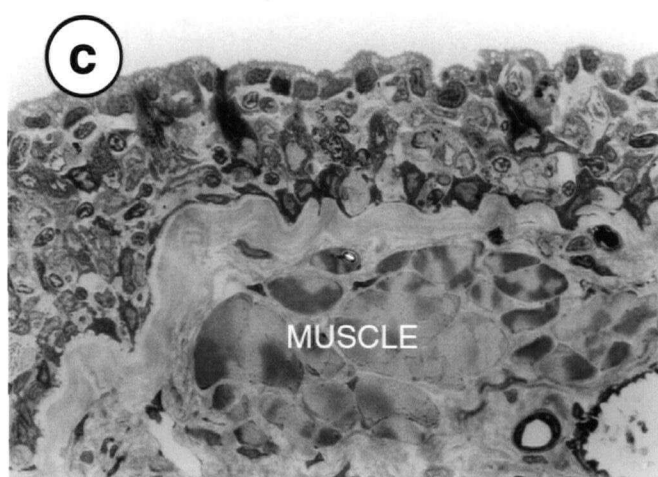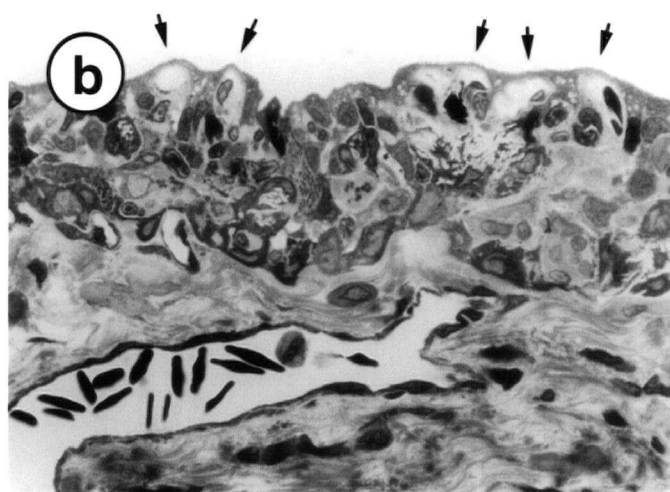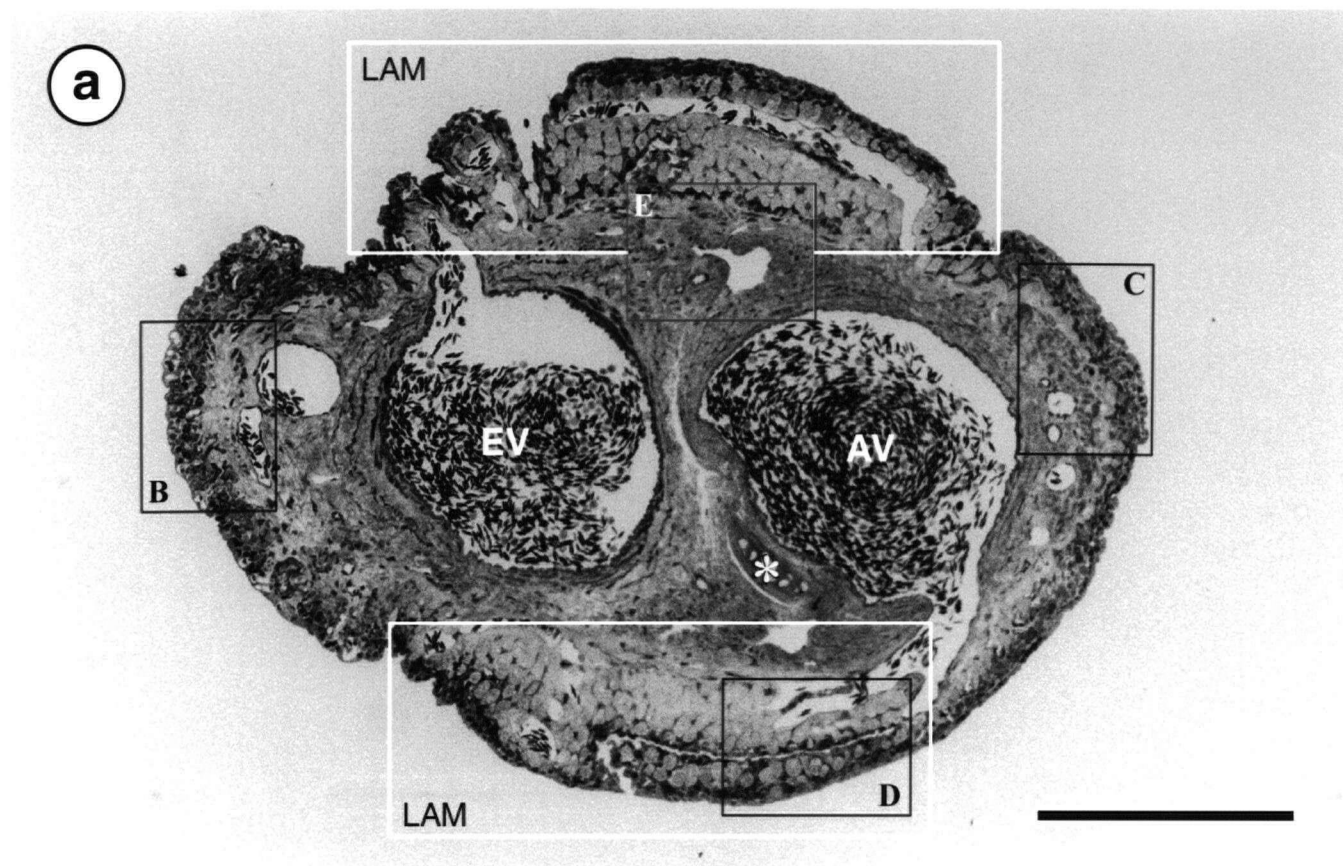
FIGURE 5.2.2 An electron micrograph **(a)** shows a lamellar mitochondria-rich (MR) cell anchored to the basal lamina (arrow) opposite the blood spaces defined by a pillar cell (PiC). The outer epithelium is composed of dense pavement cells (PVC). Note the PVC's numerous vesicles and vacuous mitochondria. The MR cell is flanked by two filament rich cells (asterisk) and connected to the surface by a deep apical crypt (AC) with numerous microvilli. A light micrograph of a sagital section through a gill filament **(b)**. The secondary lamellae appearing in cross section are tightly packed together restricting the water space (arrows) between adjacent lamellae (=interlamellar space). Some pillar cell defined blood spaces are indicated by arrowheads. The efferent or afferent artery occupies the lower part of the figure. Scale Bars **(a)** 5μm **(b)** 50μm.
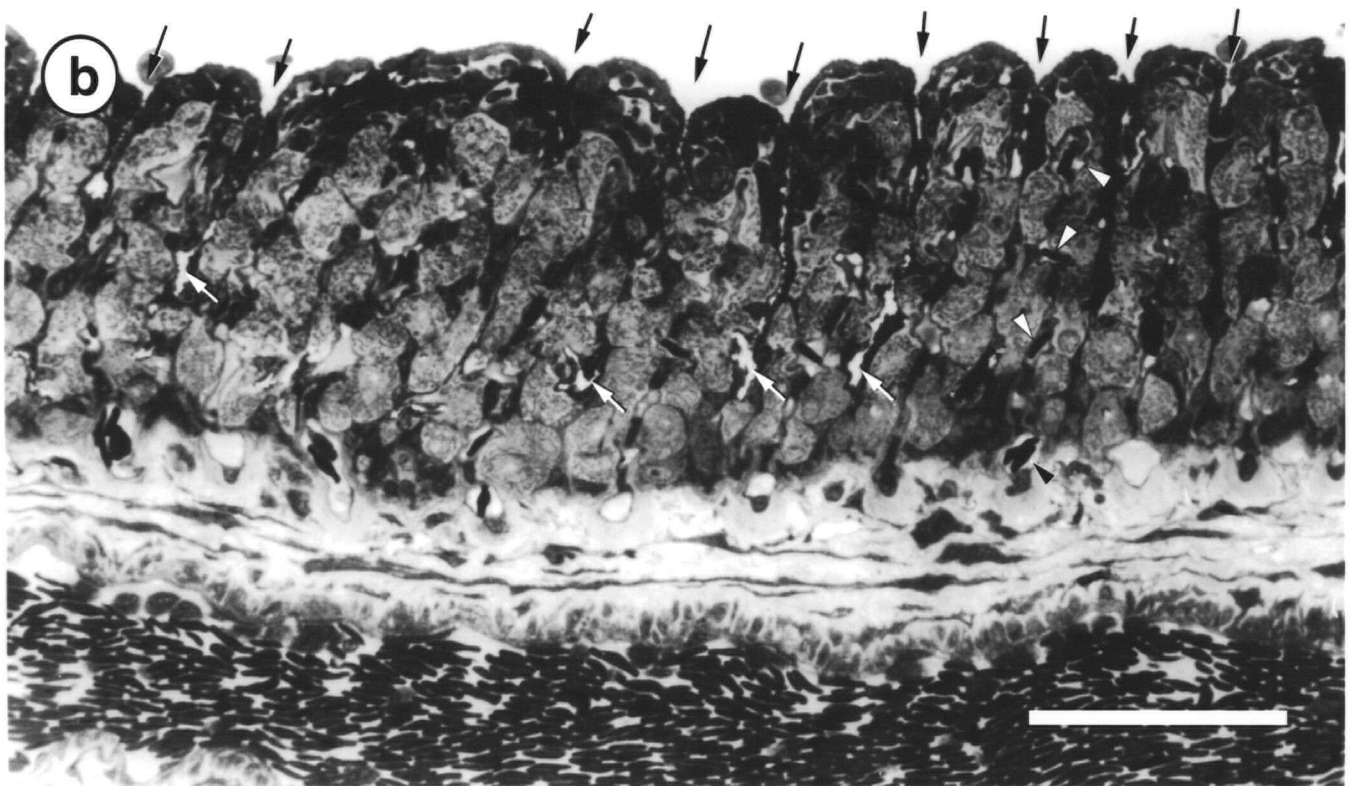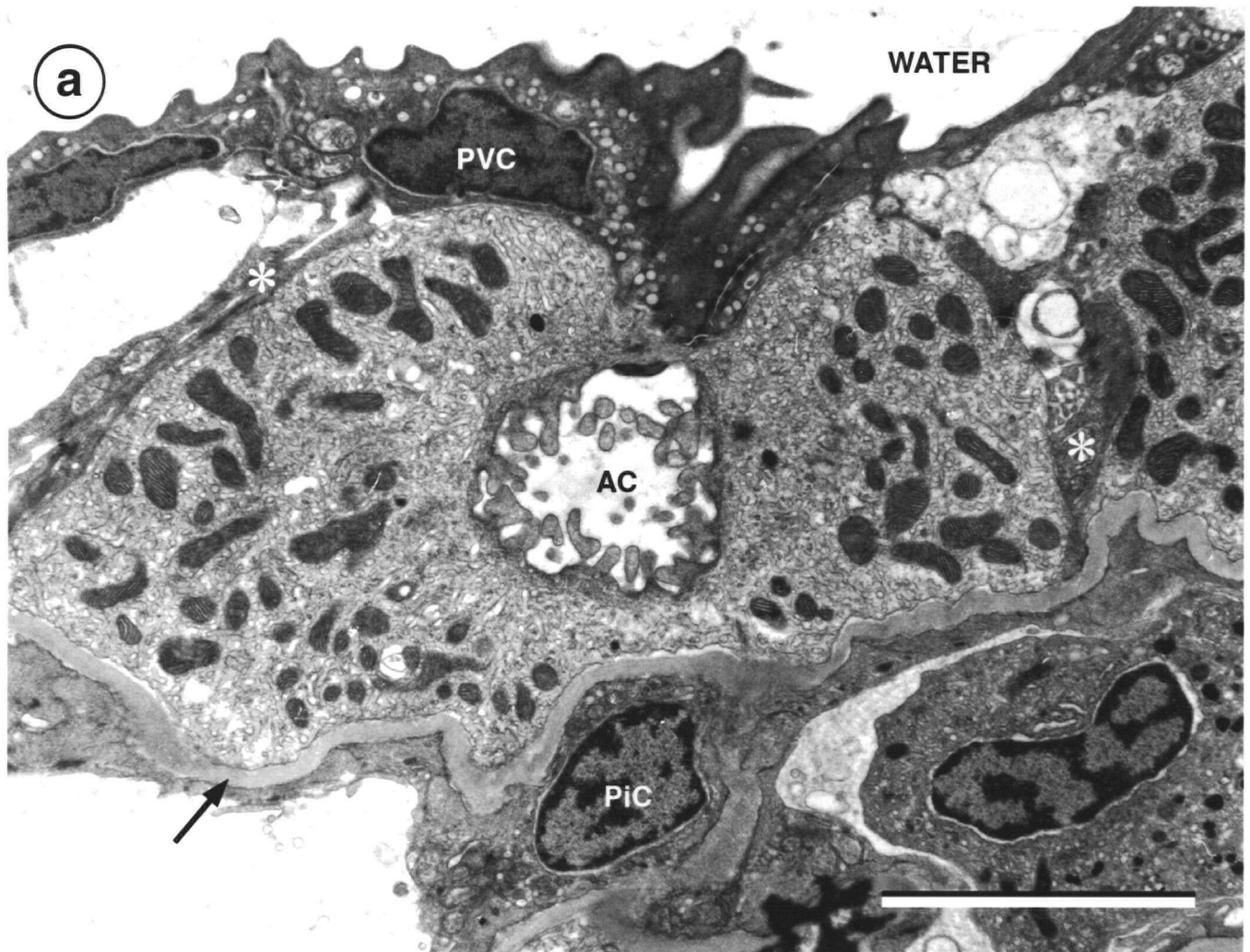
FIGURE 5.2.3a,b Electron micrographs of the apical plasma membrane domain of two lamellar MR cells with accessory cell (**AC**) processes. Arrows indicate leaky or thin tight junctions formed between MR cells and accessory cells. The tight junctions between pavement (**PVC**) and MR cells are much thicker (arrowhead).**FR**: filament rich cell; **M**: mitochondria. Scale bar = 1μm.
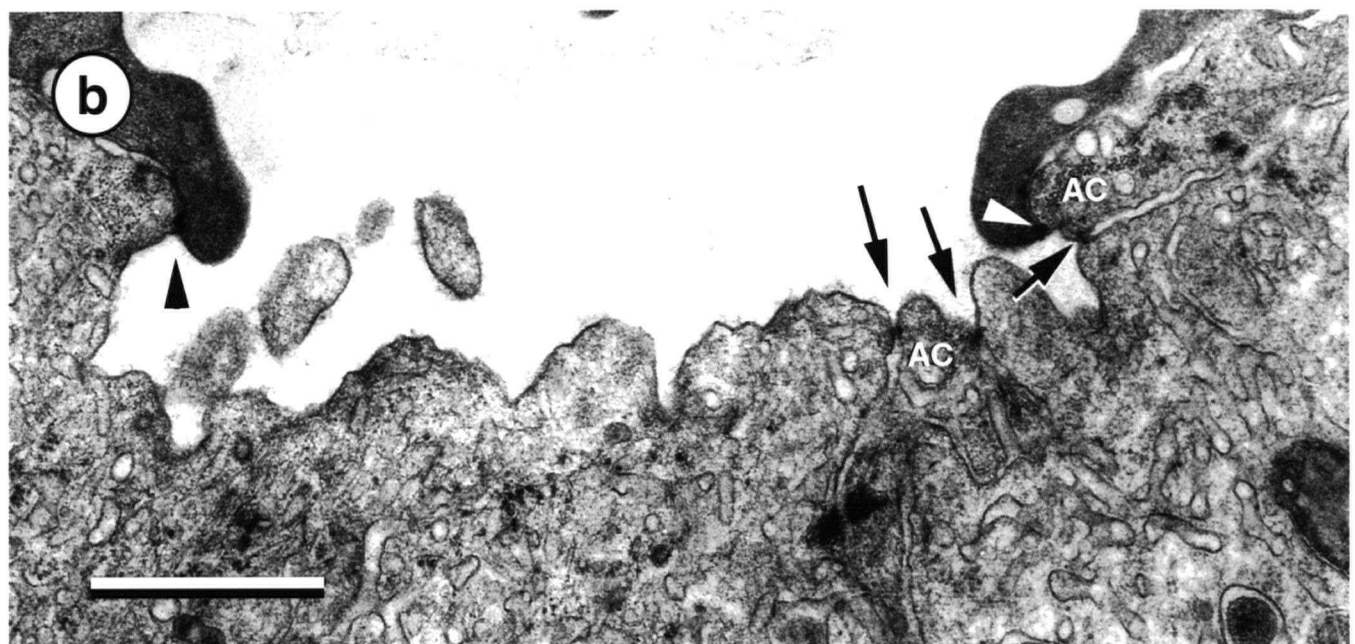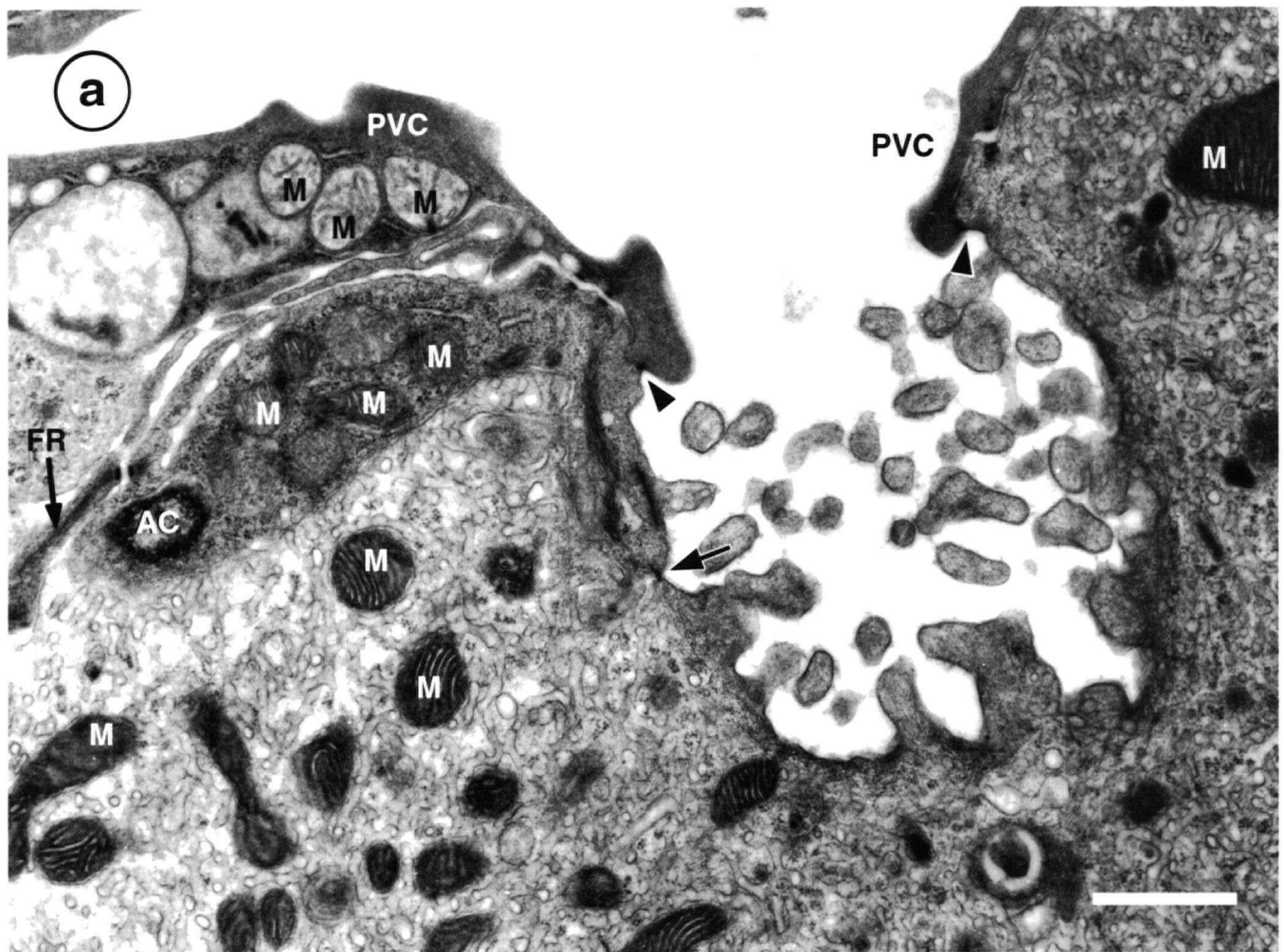
FIGURE 5.2.4 Electron micrographs of filament rich (FR) cells. These epithelial cells are found attached to the basal lamina, and compressed between mitochondria-rich cells extend to contact apical pavement cells. They do not themselves make contact with the external mileux. The FR cells are characterized by thick bundles of intermediate filaments (**a, d**: arrowheads) associated with desmosomes (**d**, arrows). Another noticeable feature is the enfolding and elaborate invaginations of the plasmalemma forming pockets or canaliculi like structures (**a, b, c**: arrows). Scale bar = 1μm.
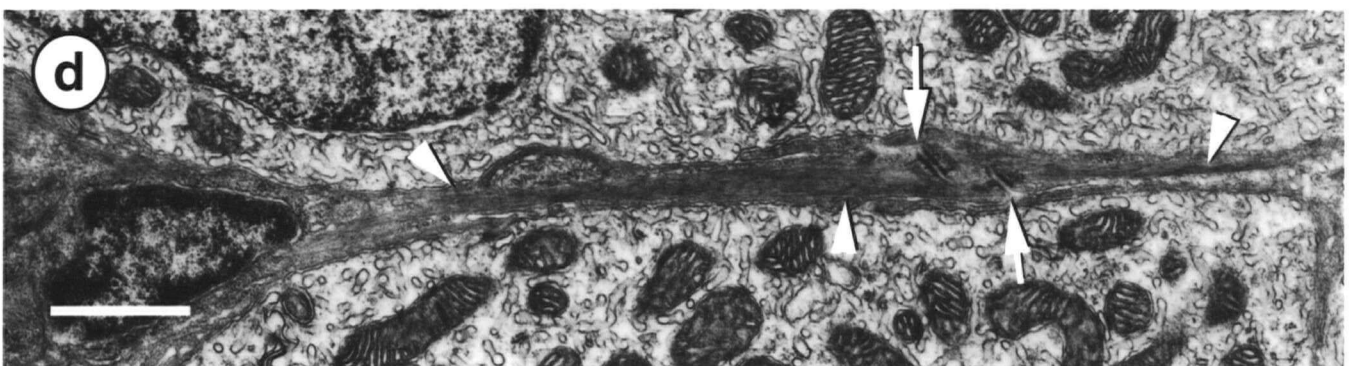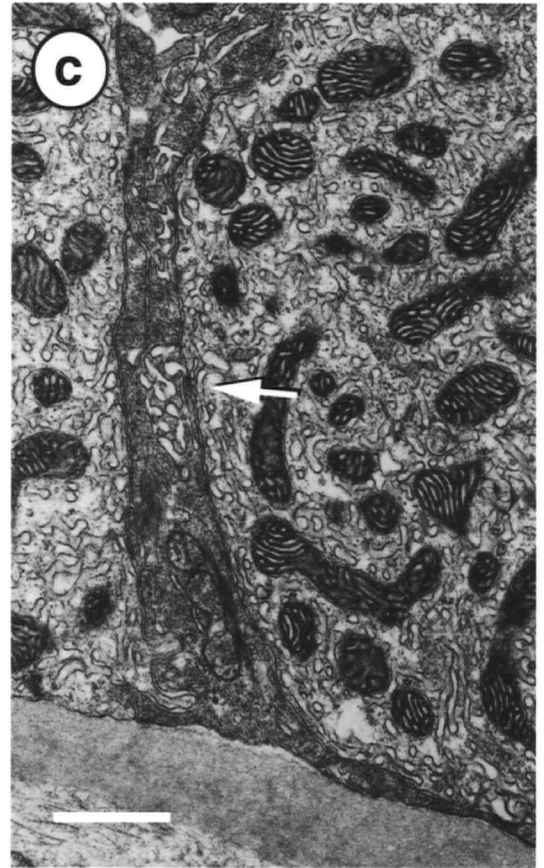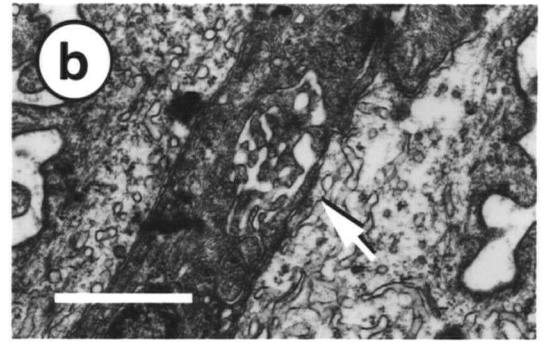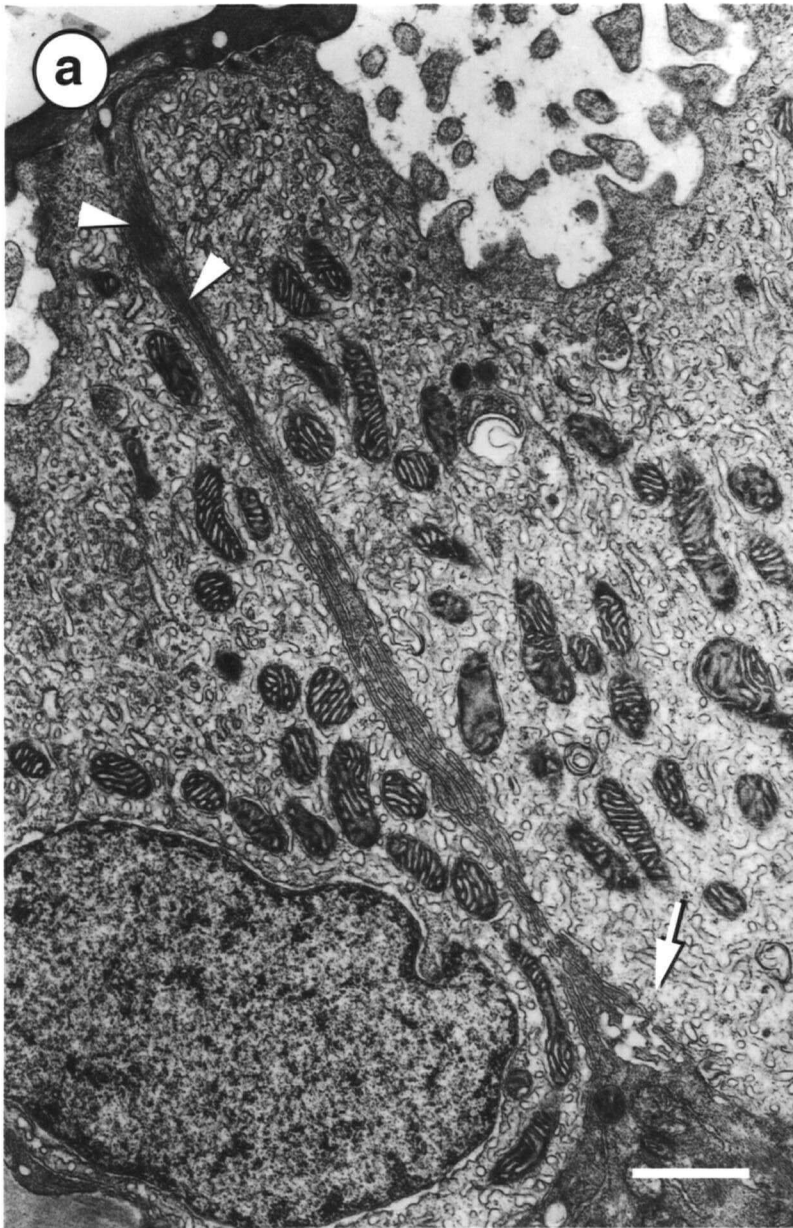
FIGURE 5.2.5 Light (**a**) and electron (**b,c**) micrographs of cross sections through the opercular epithelium with its intraepithelial capillaries (**a**; arrows). Note the similarities in appearance with the gill filament efferent edge epithelium (Figure 1b). The capillaries pass though the basal lamina (**BL**) of the stratified epithelium (**a**), remaining separated from epithelial cells by their retained sheath of basal lamina (**b**). Red blood cells (**RBC**) can be seen inside the capillary lumens (**CAP**) defined by endothelial cells (**ENDO**). The blood-water/air diffusion barrier consists of the endothelial cell, the basal lamina, a capillary associated epithelial cell and an epithelial pavement cell (**c**; < 1μm). Microridges cover the surface cells suggesting mucous adherence may be important in preventing desiccation. Scale Bar = (**a**) 50μm (**b**) 5μm (**c**) 1 μm

a

b

c

EXTERNAL MELIEU

PVC
CAEpith.
BL
Endo.

CAP LUMEN

BL

PVC

CAP

Ac.Epith.

BL

ENDO

RBC

150
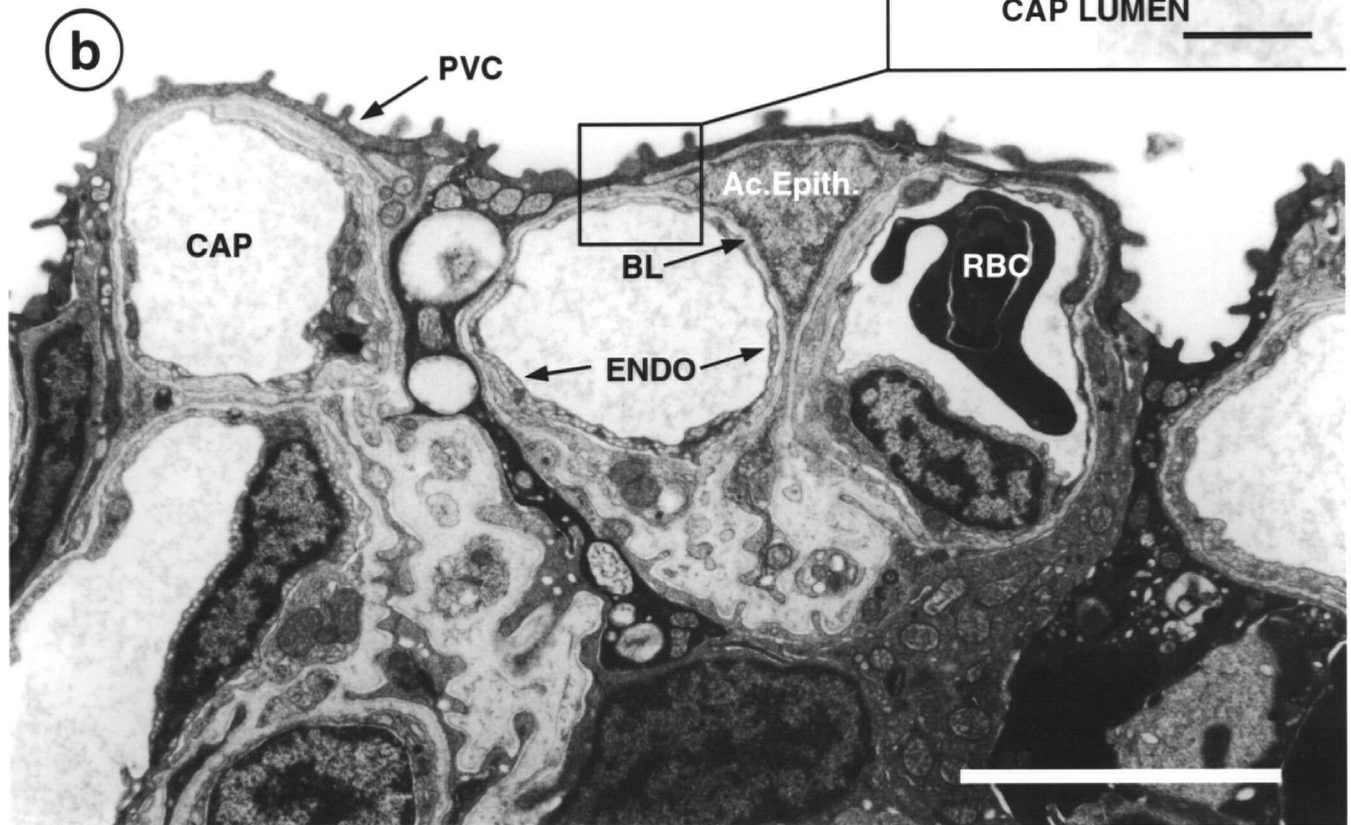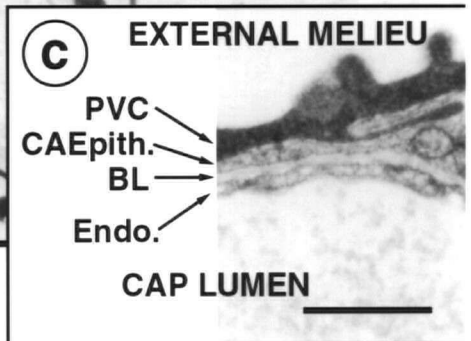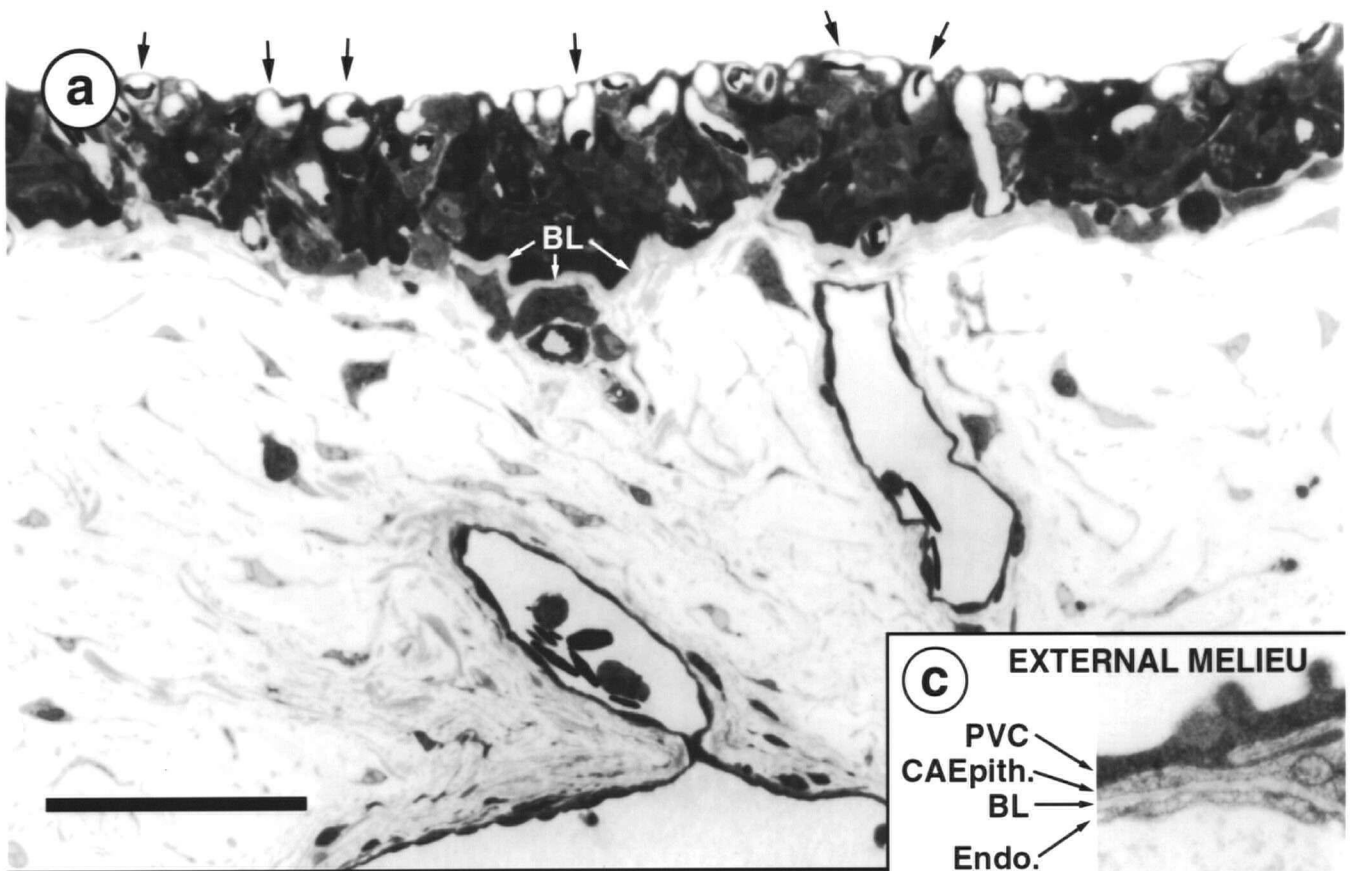
FIGURE 5.3.1 Indirect immunofluorescence (**a**) and phase-contrast (**c**) microscopy showing the distribution of Na^+,K^+-ATPase in the gills of the mudskipper. The mouse monoclonal antibody $\alpha5$ was used to immunolabel a $5\mu m$ fixed-frozen section of 3%PFA/PBS fixed gill tissue. In the two gill filaments in cross section, staining is most intense in the cells of the gill lamellar epithelium. A section in which $\alpha5$ was substituted with normal mouse serum in the immunolocalization procedure serves as a control for comparison (**b,d**). Scale bar = $100\mu m$
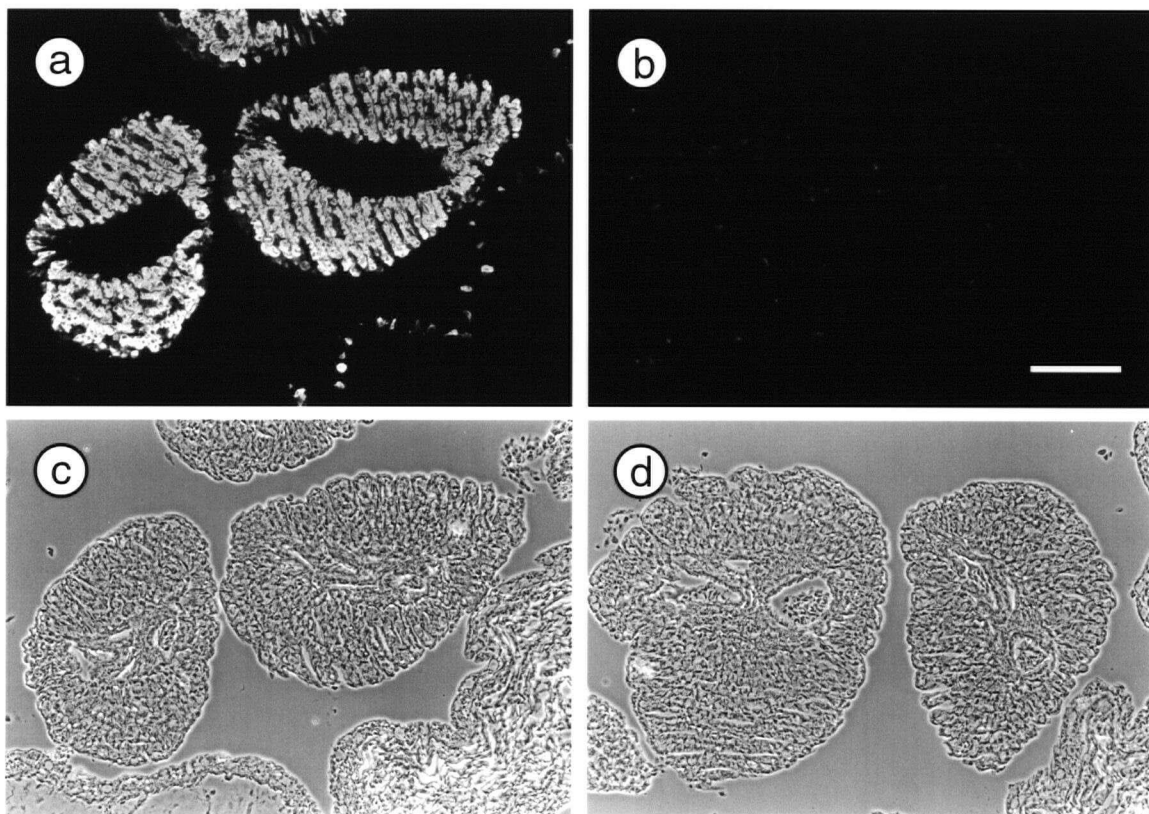
FIGURE 5.3.2 Immunogold localization of Na^+,K^+-ATPase in the mudskipper gill lamellar MR cell using the $\alpha 5$ antibody and a secondary antibody conjugated to 20nm colloidal gold particle. Labeling is greatest in the lower two-thirds of the MR cell (**a**) and is associated with the tubular system (**ts**) (**b**; arrows). No labeling is associated with the MR cell apical crypt (**ac**), pavement cells (**PVC**), pillar cells (**PiC**) or red blood cells (**rbc**). Scale bar = (A) 2 μm and (B) 0.5μm
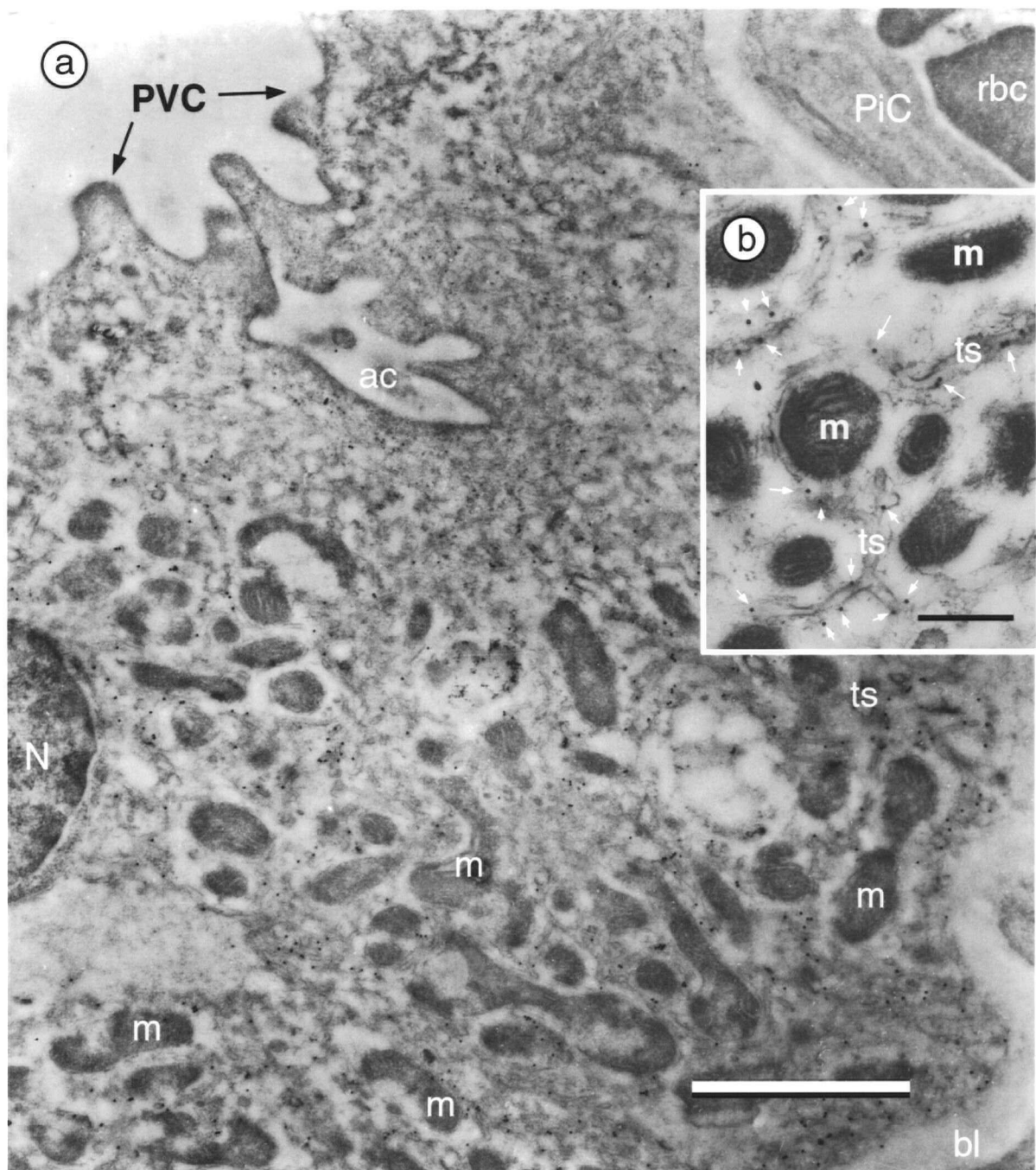
FIGURE 5.3.3 Indirect immunofluorescence and phase-contrast microscopy showing the distributions of Na^+,K^+-ATPase **(a,b)**, CFTR **(c,d)**, and NKCC **(e,f)** in cells of the lamellar epithelium. Micrographs are taken from the bases of lamellae and the asterisks indicate the alternating lamellar blood spaces. Arrows indicate the location of MR cell apical crypts. Na^+,K^+-ATPase and NKCC essential have an identical diffuse cytoplasmic distribution confined to lamellar MR cells. CFTR staining is restricted to MR cell apical crypts region. Scale bar = 25μm
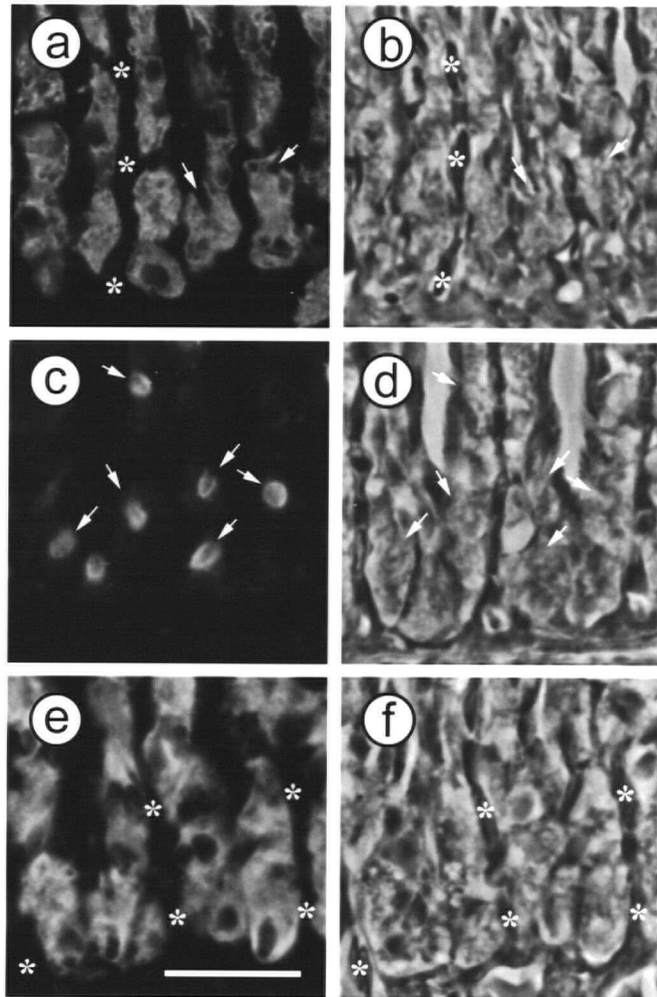
FIGURE 5.3.4 Indirect immunoperoxidase staining of fixed-frozen sections of mudskipper gill tissue. Sections were either labeled with the carbonic anhydrase (**a,b**) or vH^+-ATPase (**c**) antisera. Intense labeling is associated with the apical crypt region of lamellar MR cells. Negligible reactivity was observed in control section incubated with normal rabbit serum (not shown). Scale bar = 20 µm
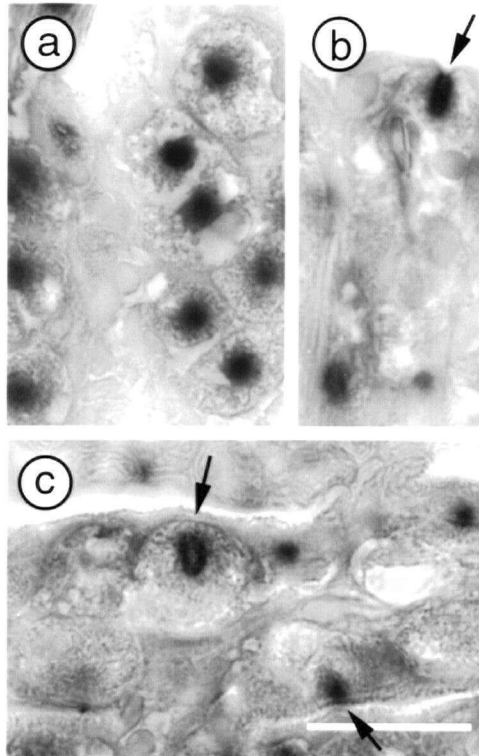
FIGURE 5.3.5 Na$^+$/H$^+$ exchanger 3 (NHE3) distribution in the gills of fixed-frozen sections of mudskipper gill using indirect immunofluorescence and phase-contrast microscopy. The rabbit polyclonal antibody 1380 was used to immunolabel a 5μm fixed-frozen section of 3%PFA/PBS fixed gill tissue. In low magnification micrographs, a punctate labeling pattern is associated with the lamellar epithelial cells (**a,b**). Higher magnification of the boxed area reveals that this staining is specific for MR cell apical crypts (**c,d**; arrows). The asterisks indicate non-specific fluorescence of material associated with the afferent and efferent vessels as is also evident in the final control fluorescence and phase micrograph pair incubated with normal rabbit serum (**e,f**). Scale bars = (**a,b,e,f**) 100μm and (**c,d**) 10μm.
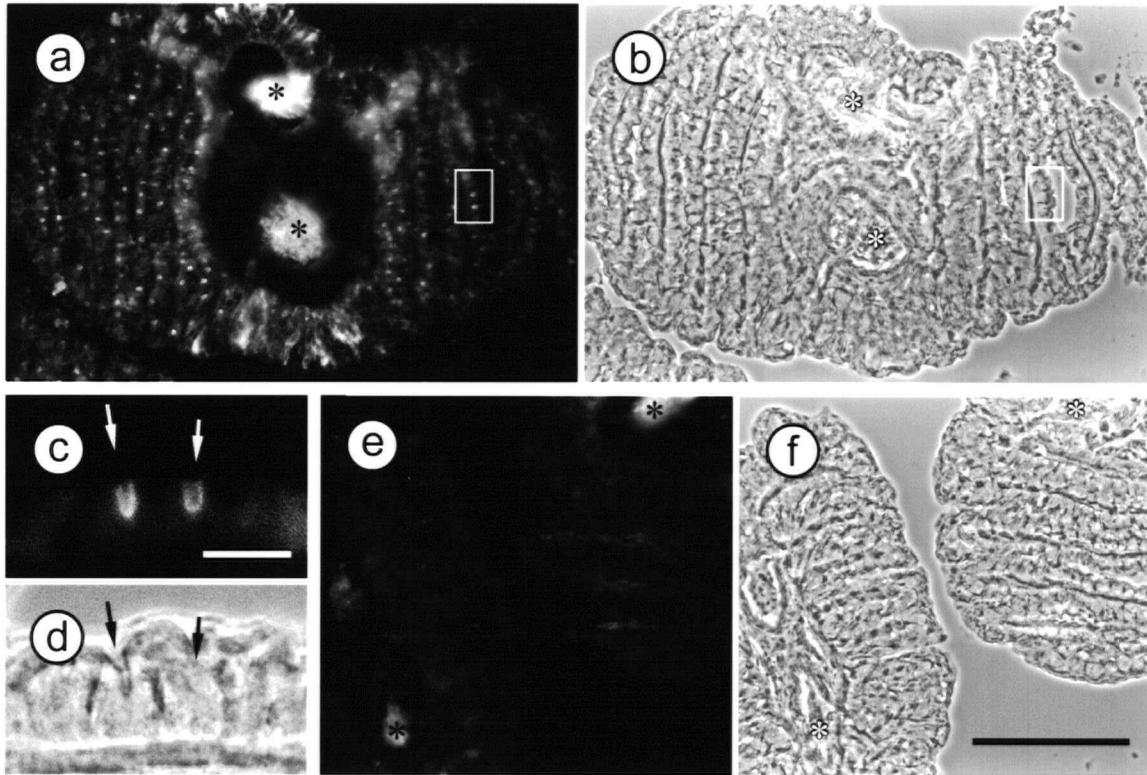
FIGURE 5.3.6 Projection from a z-stack of 50 confocal images (0.2μm z-steps) showing the NHE2 distribution in the mudskipper gill lamellae using indirect immunolabeling with the rabbit polyclonal antibody 597. Staining is associated with the apical crypts of lamellar MR cells and is visible as rings or U shapes of fluorescence in sections. (**b**) is a high magnification of the outlined area in (**a**). The distribution of NHE2 is essential identical to NHE3 using Ab1380 (Figure 5.3.5). Scale bar = (**a**) 25 μm and (**b**) 10 μm.
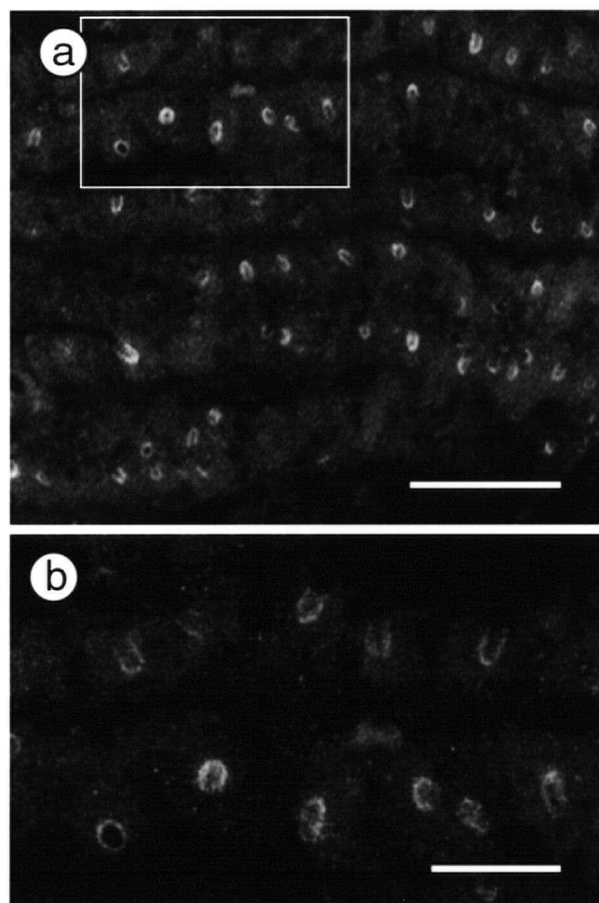
FIGURE 5.3.7 Western blots of mudskipper gill tissue crude homogenate (10µg per lane) separated on 10% polyacrilamide gels probed for (**a**) α subunit of Na^+,K^+-ATPase, (**b**) CFTR protein, (**c**) A-subunit of vH^+-ATPase, (**d**) NHE-2 (Ab 597), and (**e**) NHE-3 (Ab 1380). MW markers: 205, 112, 87, 69, 56, 38.5 and 33.5 kDa. Large arrowheads indicate bands of interest while smaller arrowheads indicate other bands.
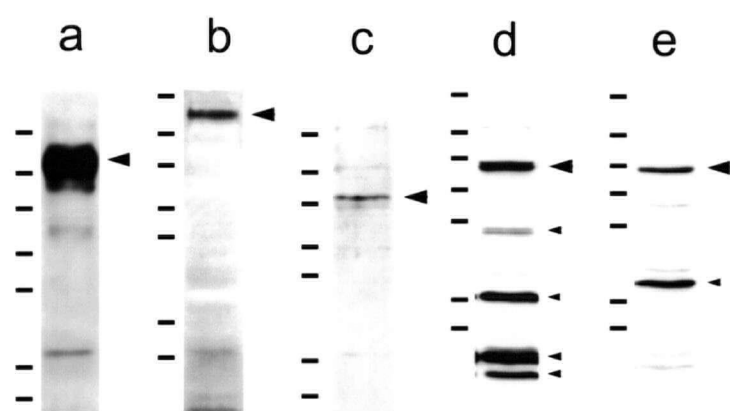
5.4 DISCUSSION

In the amphibious air-breathing mudskipper fish *Periophthalmodon schlosseri*, ion transport proteins in gill MR cells contribute to active ammonia (NH_4^+) excretion. *In vivo* pharmacological studies show that a significant proportion of the total ammonia efflux (J_{Amm}) is sensitive to inhibition of the Na^+ / H^+ (NH_4^+) exchanger (NHE) by amiloride, and carbonic anhydrase (CA) by acetazolamide. The elimination of boundary layer acidification by the addition of 5mM HEPES buffer pH 8.0 to the 50% SW was without effect on J_{Amm} indicating that NH_3 trapping is not an important component of total ammonia excretion. These animals are also capable of excreting ammonia against inward NH_4^+ and NH_3 gradients (2mM NH_4Cl), however, a portion of J_{Amm} is then sensitive to Na^+,K^+ (NH_4^+)-ATPase inhibition by ouabain. Figure 5.4 summarizes the data collected and the proposed pathway of transbranchial NH_4^+ movement.

The branchial epithelium contains an abundance of mitochondria-rich cells with deep apical crypts and an extensive tubular system continuous with the basolateral membrane. Immunological localization studies show the presence of NHE 2 and 3 -like isoforms, CFTR, and CA associated with the apical crypt and Na^+,K^+-ATPase and $Na^+:K^+:2Cl^-$ cotransporter (NKCC) with the tubular system of these MR cells. The fact that we are able to demonstrate the presence of these transporters within the branchial MR cells strongly indicates that these gill MR cells are involved in active ammonia elimination.

Ammonia elimination during air exposure is significantly greater in *P. schlosseri* than in other species of mudskipper (50% vs <10% aquatic rate; Morii *et al.* 1978; Iwata *et al.* 1981). Initially it was thought that mudskippers might use ammonia volatilization as a means of excreting waste nitrogen during land excursions. It has been shown that some terrestrial

crustaceans and isopods use this mechanism (eg Greenaway and Nakamura 1991; Weiser 1972). However, this study indicates that volatilization of ammonia is a minor component of total ammonia excretion, accounting for less than 3% of the total. Alkalinization of the body surface is necessary to enhance volatilization of ammonia by favouring the formation of gaseous NH_3. Our measurements of surface pH indicate that there is no special alkaline area of the mudskipper body. In fact, the gill surface pH was acidic relative to seawater and other parts of the body surface. It is probable, based on these pH measurements, that ammonia volatilization is from the general body surface rather than from the gills. The amount of volatilization is either not sufficient to acidify the body surface or the animal is able to absorb any acid formed on the general body surface, maintaining pH at about seawater levels. Other evidence indicates that the gills are probably involved in the active elimination of ammonium ions involving $Na^+,K^+(NH_4^+)$-ATPase and $Na^+ / H^+ (NH_4^+)$ antiporter. Consistent with the finding of NH_4^+ elimination during air exposure is the observed blood alkalosis during air exposure (Kok *et al*. 1998; Ishimatsu *et al*. 1999).

Boundary layer acidification

In *P. schlosseri* ammonia excretion is not dependent on boundary layer pH. This would indicate that P_{NH3} gradients are not as important a mechanism of total ammonia elimination as in freshwater fishes. Also the contribution of the vH^+-ATPase to ammonia elimination is only significant after 2 h. The facilitation of NH_3 diffusion by trapping of NH_3 ($NH_3 + H^+ \rightarrow NH_4^+$) through the acidification of the boundary layer by hydration of respiratory CO_2 or direct H^+ excretion (NHE or vH^+-ATPase) is important in freshwater fishes (Wright et at. 1989; Wilson *et al*. 1994; Salama *et al*. 1999) and likely important in seawater fishes as well. The mudskippers kept in 50% SW (pH 8), were able to acidify their bath water through the addition of respiratory

CO_2 to a final pH that was around pH 7.4. The net acid excretion tended to hover around zero. The acidification of the gill boundary layer is dependent on the water buffer capacity. Seawater tends to be poorly buffered and thus the gill boundary layer will be acidified. Experimentally, the boundary layer acidification can be eliminated by the addition of buffer to the water. In the mudskipper, the elimination of boundary layer acidification by buffering with 5mM HEPES pH 8.0 results in no change in J_{Amm}. The HEPES pH 8.0 did, however, stimulate a large J_{ACID} flux presumably by providing a large sink for protons. This effect on J_{ACID} has also been observed in freshwater trout (Salama *et al.* 1999). The addition of HEPES buffer at pH 7.0 also had no effect on net ammonia flux rates suggesting NH_3 trapping is not a necessary component of J_{AMM}.

Substitution of NH_4^+ on some ion transport proteins

Na^+,K^+-ATPase

The gill MR cells are associated with high levels of Na^+,K^+-ATPase immunoreactivity and *in vitro* assays of (ouabain-sensitive) enzyme activity are also very high. The levels of Na^+,K^+-ATPase activity are 3-4 times higher than another mudskipper species (*Boleophthalmus boddaeti*; Randall *et al.* 1999) and double the values obtained for seawater adapted coho salmon (using the same assay conditions; Figure 4.5). The levels of immunoreactivity in the other gill cell types (PVC, erythrocytes, pillar cells, FR cells) are below the level of detection although the absence of immunoreactivity is not a good criteria for concluding its absence. There are limits to the sensitivity of the technique in addition to the possibility that other isoforms of the α subunit are present in these cell types. Indeed, Na^+,K^+-ATPase is likely present in all cell types performing cellular housekeeping roles.

In the Gulf toadfish (*Opsanus beta*) Claiborne *et al.* (1982) and Evans *et al.* (1989), were able to demonstrate that inhibition of Na^+,K^+-ATPase by ouabain significantly reduced J_{Amm} in

this marine fish. However, it has been argued that under *in vivo* conditions (plasma $[K^+]$ ~5mM and $[NH_4^+]$ ~0.1mM) K^+ will out compete NH_4^+ for transport binding sites on the Na^+,K^+-ATPase thus making the physiological significance of NH_4^+ substitution questionable (Wall 1996). However, it should be noted that plasma $[K^+]$ may over estimate $[K^+]$ within the tubular system of the gill MR cell which is associated with high Na^+,K^+-ATPase activities, and likely have lower $[K^+]$. Yet, in *P.schlosseri* kept under conditions of low external ammonia ouabain is without effect on J_{Amm} (T. Kok, personal communication). Presumably under these conditions, NH_3 and NH_4^+ diffusion are capable of maintaining ammonia excretion (across the basolateral membrane of the epithelium at least). However, during exposure to high environmental ammonia when NH_4^+ and NH_3 gradients are directed inward (2mM) J_{Amm} is sensitive to ouabain (Figure 5.1.5). This inhibition of J_{Amm} is associated with a significant increase in plasma NH_4^+ levels (Table 5.1). Thus in the absence of favourable diffusion gradients NH_4^+ substitution becomes physiologically significant. Mallery (1983) was also able to show that the sodium pump has a potentially higher affinity for NH_4^+ than K^+.

Although J_{Amm} was inhibited by apically applied ouabain, the effect was likely basolateral. Ouabain is a specific inhibitor of Na^+,K^+-ATPase activity and even though apical Na^+,K^+-ATPase has been described in some cell types (salivary gland; Just and Walz 1994), our immunogold observations indicate a distribution restricted to the basolateral tubular system (Figure 5.3.2). The basolateral effect of apically applied ouabain is believed to be due to entry of ouabain via the shallow tight junction found between MR chloride and accessory cells (Phillpot 1980).

Alternatively, the effect of inhibition of Na^+,K^+-ATPase by ouabain may not be a direct reflection of basolateral NH_4^+ movement but an indirect effect of build up of intracellular Na^+ on an apical Na^+/NH_4^+ exchanger.

Apical Na^+ / H^+ (NH_4^+) exchange

The inhibition of the NHE by amiloride reduces J_{AMM} by 50% yet the elimination of boundary layer acidification is without effect on J_{AMM}. It therefore seems likely that an important component of ammonia elimination is achieved by direct NH_4^+ transport by the NHE rather than a boundary layer pH effect by Na^+ / H^+ exchange. In renal microvillus membrane preparations NH_4^+ has been shown to interact with NHE by Kinsella and Aronson (1981). The concentration of amiloride used in this study does not distinguish which NHE isoform is contributing to J_{AMM}. There are at least five NHE isoforms (NHE1-4, β) although only the NHE2 and NHE3 are found apically. Immunoreactivity of both these isoforms is present in the apical crypt of gill MR cells. However, in the mammalian kidney medulla thick ascending limb (MTAL), although both isoforms are also present, it is the NHE-3 isoform that plays a greater role in the ammonium efflux of this segment (Paillard 1998). Recently, Claiborne *et al.* (1999) reported the presence of βNHE-like and NHE2-like isoforms in gill of the sculpin using RT-PCR. In the marine fish *Opsanus beta*, Evans *et al.* (1989) found no evidence for apical Na^+/NH_4^+ exchange. Instead, they found that total ammonia excretion could be accounted for by non-ionic NH_3 (57%), paracellular ionic NH_4^+ (21%) diffusion and basolateral Na^+,K^+-ATPase (22%). However, their data could be interpreted as indicating that the Na^+,K^+-ATPase and NHE mechanisms are operating in series. In the same study they could not find evidence to support a role for NKCC in transbranchial ammonia transport. Goldstein *et al.* (1980, 1982) found that NH_4^+ diffusion and Na^+/NH_4^+ exchange are important components of ammonia excretion in marine teleost fishes

noting the importance of paracellular leak and the inward Na^+ gradient to drive NHE exchange in marine species. In seawater adapted rainbow trout challenged with 1mM NH_4^+ a base load results, consistent with Na^+ / NH_4^+ exchange (Wilson and Taylor 1992). Randall *et al.* (1999) found increased $[Na^+]_{pl}$ in *P.schlosseri* challenged with high external ammonia consistent with the proposed mechanism of Na^+ / NH_4^+ exchange.

Carbonic anhydrase

Carbonic anhydrase immunoreactivity has been observed in the apical region of gill MR cells and the sensitivity of J_{Amm} to CA inhibition indicates that intracellular CO_2 hydration may be important in providing H^+ for NH_3 protonation to maintain P_{NH3} gradients across the basolateral membrane and providing NH_4^+ for apical Na^+/ NH_4^+ exchange. From the lack of ouabain-sensitive J_{AMM} under conditions of low external ammonia it would appear that the facilitated movement of NH_4^+ across the basolateral membrane is not important. The distribution of CA in the branchial MR cells is similar to that reported by Lacy (1983) in MR cells from the opercular epithelium of seawater adapted killifish.

vH^+-ATPase

The role of the vH^+-ATPase in ammonia excretion is not clearly defined in light of the absence of a pH dependent boundary layer effect and the *in vivo* experiments using KNO_3 which had a delayed effect on J_{AMM}. Also, although KNO_3 reduced J_{ACID} the effect was not different from the KCl control. However, immunoreactivity of the vH^+-ATPase could be demonstrated in apical crypts of MR cells and NO_3^- and bafilomycin sensitive ATPase could be demonstrated in gill homogenates using an *in vitro* assay.

CFTR

It was initially thought that the CFTR could be used as a marker for MR cells involved in Cl$^-$ secretion; a function normally ascribed to this cell type in sea water teleost fishes (chloride cells; Singer *et al.* 1998). In the initial investigation of the fine stucture of the branchial epithelium few chloride cell-accessory cell complexes were found so it was thought that few of the MR cells were actually involved in Cl$^-$ elimination. However, CFTR-like immunoreactivity was associated with the apical crypts in practically every branchial MR cell. So contrary to our morphological observations of few accessory cells, it maybe that all MR cells are involved in Cl$^-$ elimination. This would be the conclusion if the function of the CFTR-like protein were limited to Cl$^-$ conductance; however, the CFTR-like protein is also involved in the regulation of other apical channels as well as the conductance of other anions, notably HCO$_3^-$ (Poulsen *et al.* 1994). It is this latter function that becomes quite intriguing. Assuming that CO$_2$ hydration catalyzed by intracellular CA provides H$^+$ ions for NH$_3$ protonation to produce NH$_4^+$ for NHE then an HCO$_3^-$ is left behind. HCO$_3^-$ must exit the cell either across the basolateral or apical membrane however, basolateral exit would result in a base load during ammonia excretion. Apical exit facilitated by the CFTR, would be acid-base neutral and account for the lack of boundary layer pH effects. It also explains why J$_{ACID}$ is around zero and is not affected by the inhibition of J$_{AMM}$ with acetazolamide or amiloride.

Salinity experiment

In teleost fishes in general, there is a positive correlation between environmental salinity and NH$_4^+$ permeability (Evans and Cameron 1986). This increased permeability is related to the formation of leaky tight junctions between chloride and accessory cells (CC-AC) that provides a route for the paracellular efflux of Na$^+$. CC-AC numbers show a positive correlation with salinity

because they are needed for NaCl elimination (see Laurent 1984). The euryhaline sculpin has been shown to reduce J_{AMM} and a compensatory increase in J_{urea} upon acute and chronic exposure to low salinity (Wright *et al.* 1995). In the mudskipper there is a trend in the data that follows this relationship but it is not significant. Curiously, plasma [NH$_4^+$] and P_{NH3} show a positive relationship with salinity. It is unclear why the fish at higher salinity would have higher plasma ammonia levels. In some other mudskipper species there is the opposite correlation with salinity: higher J_{AMM} at lower salinity while J_{UREA} is lower (Iwata *et al.* 1981; Gordon *et al.* 1965). It also is unclear why this relationship exists.

None of the other plasma variables measured or gill ATPase levels were affected by environmental salinity. Unfortunately, I could not look at morphological changes in the gill (ie increased ACs or leaky tight junction formation) because of the poor quality of the tissue fixation.

From my results it would appear that the paracellular route for NH$_4^+$ is not as important in the mudskipper as it is in other marine fishes (Evans *et al.* 1989). Randall *et al.* (1999) found that branchial TEP is unresponsive to increases in environmental ammonia indicating a very low NH$_4^+$ permeability. The fact that this mudskipper lives in an estuarine environment and faces daily changes in salinity with the changing tides may explain why no differences were seen at the different salinity regimes. Also relatively few CC-AC type complexes were seen in the gill suggesting the paracellular path may not be important for J_{AMM}. In addition, if the burrow in which this animal lives in is filled with 2mM NH$_4^+$ seawater then a high NH$_4^+$ (paracellular) permeability would be disadvantageous. However, Na$^+$ efflux via a paracellular route is still likely as the equilibrium potential of Na$^+$ is close to the measured TEP consistent with other

euryhaline marine fishes (+10 mV; see Chapter 4, and Potts 1984). It is possible that the barrier function of the shallow tight junctions shows selectivity for cations.

Gill Morphology

The abundance of MR cells within the lamellar epithelium is highly unusual for a marine fish. MR cells are generally restricted to the filament epithelium (reviews by Laurent 1984; Pisam and Rambourg 1991). This is also generally true for freshwater fish; however, under ion-poor conditions, numerous MR cells can be found covering their lamellae (Avella *et al.* 1987; Laurent and Perry 1991). In the freshwater aquatic air-breathing fish *Arapiama gigas*, the gills have reduced lamellae and numerous MR cells in the filament epithelium (Hulbert *et al.* 1978). This fish is a bimodal breather and the gill is the site of CO_2 excretion into water while the lung-like accessory respiratory organ (ARO) operates for O_2 uptake (Randall *et al.* 1978). In this case, the gill presumably is still functioning in ion and acid-base regulation and ammonia excretion through the filament and reduced lamellar epithelium.

The gills of the more aquatic mudskipper *Boleophthalmus boddarti* do not have the features of *P. schlosseri* and do not differ so greatly from other teleost fishes in both gross and fine structure (Hughes and Munshi 1979; Al-Kadhomiy and Hughes, 1988; Low *et al.* 1990). Squamous epithelial cells cover the lamellae and MR cells are generally restricted to the filament epithelium. They do not have the abundance of lamellar MR cells or filament rich cells of *P. schlosseri*. From the illustrations of the gills of mudskippers *Periophthalmus vulgaris* and *Periophthamus chrysospilos* it appears as though the lamellae of these species have MR cells, although not in the same densities as *P. schlosseri,* and they also lack interlamellar fusions (Schöttle 1931; Low *et al.* 1990).

The study of Yadav *et al.* (1990) deserves special mention as their observations are possibly on the same species (*P. schlosseri*). Although they also noticed interlamellar fusions, they are reported only at the tip of the filaments while I and Low and co-workers (1990) observed interlamellar fusions along the length of the filament. Yadav *et al.* (1990) also make no mention of MR cells in the lamellae. From their observations of lamellar vascular papillae and blood sinuses they suggest that the gill is still an important site for gas exchange while from my observation I cannot agree. It seems likely that they are looking at another species (*Periophthalmodon septemradiatus* or *Periophthalmus minutus*) as suggested by Clayton (1993).

In *P. schlosseri*, despite the abundance of lamellar MR cells, accessory cells and shared apical crypts were seldom observed. Laurent (1984) observed that NaCl elimination in marine teleosts depends on the intimate relationship between the chloride (mitochondria-rich) cell (CC) and accessory cell (AC). The AC sends cytoplasmic projections into the neighbouring chloride cell which surface within the apical crypt of the CC. The tight junctions between CC and AC are short, consisting of 1-2 strands. In the classical NaCl elimination model (Silva *et al.* 1977; Sardet *et al.* 1979), Cl^- moves through the CC and Na^+ through the leaky paracellular channels (review by Karnaky 1998 and Chapter 4 Introduction). Cl^- moves into the CC across the basolateral membrane via a NKCC and out of the cell across the apical membrane via a CFTR-like Cl^- channel. A number of other changes in MR cell fine structure are associated with seawater adaptation, but it seems that the CC-AC relationship is the most diagnostic (Laurent 1984). For instance, apical crypts have been reported in *Pimephales promelas*, a freshwater species, following chronic exposure to acidic condition (pH 5; Leino and McCormick 1984). In these fish AC were reported to be absent and the crypts were explained to be involved in acid-base regulation at low pH. Also in the freshwater tilapia, apical crypts are a common feature

associated with MR cells (Perry *et al.* 1992; van der Heijden *et al.* 1997). On the basis of fine structure it seems, therefore, that only a minority of MR cells are involved in NaCl elimination in the gills of the mudskipper *P. schlosseri,* while the majority of MR cells, which lack AC, may be specialized for something other than NaCl elimination. However, the immunolocalization of CFTR-like channel to the apical crypt of most would indicate that these cells are also capable of Cl⁻ secretion.

In *P. schlosseri,* MR cells are isolated from one another by neighbouring cells rich in filaments. To my knowledge, such an arrangement has not been observed in the branchial epithelium of any other fish, although a similar cell type has been observed in the opercular membrane of the killifish (*Fundulus heteroclitus*; Lacy 1983). It is possible that the MR cells with their complex tubular system require some form of external reinforcement that may be provided by these cells. It appears that these filament-rich cells are not contractile in nature since the predominant filament type is intermediate and not microfilament. The unusual canaliculi-like structures that are found within these cells may provide a route for the movement of interstitial fluid.

Gas exchange organ

The gill lamellae of *P. schlosseri* are clearly not structurally designed for gas exchange. The interlamellar fusions while allowing the prevention of desiccation of the epithelium during air exposure also effectively extend the diffusion distance from the blood space to the apex of the lamellae. The movement of water through the interlamellar spaces is difficult to imagine. Thus, with the exception of the marginal channel, much of the blood is effectively shunted through the lamellae. Also, the high densities of MR cells within the tissue suggest that it is an oxygen-demanding organ rather than a site for oxygen uptake into the blood.

The inner-opercular lining with its increased surface area and intraepithelial capillaries makes a better gas exchange site than the lamellae. There is also a similar system of intraepithelial capillaries in areas of the leading edge of gill filaments and on the gill arch. The oxygenated blood from both these areas returns to the heart via the venous circulation (Schöttle 1931; review by Laurent 1984) and contributes oxygenated blood to the returning systemic de-oxygenated blood resulting in a higher P_{O2} of blood perfusing the gills. The gills probably consume oxygen from the blood and perhaps the air, the end result is an arterial P_{O2} that has been observed to be quite low, between 25-40 torr (Kok et al. 1998; Ishimatsu et al. 1999).

Summary

In summary, the elimination of ammonia by *P. schlosseri* involves a NHE and CA and is not dependent on boundary layer pH effects. Na^+, K^+-ATPase plays a role in ammonia elimination only against a gradient. Although a vH^+-ATPase is present its role in ammonia elimination is not certain. These animals are able to eliminate significant quantities of ammonia when out of water. The gills of *P. schlosseri* express all of the above proteins and show some unique features that can be used to explain the animal's ability to actively eliminate ammonia. It also is clear that gas exchange across the gill lamellae would be severely handicapped by the long diffusion distances present. The observation of intra-epithelial capillaries in the inner operculum and to a lesser extent in the gill filament would present more practical sites for gas exchange.

FIGURE 5.4 Illustration of the mudskipper gill MR cell and its proposed role in active NH_4^+ elimination. Ammonia enters the MR cells from the blood either by NH_3 diffusion or active transport by $Na^+,K^+(NH_4^+)$-ATPase and/or $Na^+: K^+(NH_4^+): 2Cl^-$ cotransporter. Intracellular carbonic anhydrase (CA) provides H^+ for NH_3 protonation by catalyzing CO_2 hydration. The NH_4^+ formed is moved across the apical membrane in exchange for Na^+ by a NHE-like carrier. The accumulated HCO_3^- exits the cell apically via an CFTR-like anion channel.

Mudskipper Model
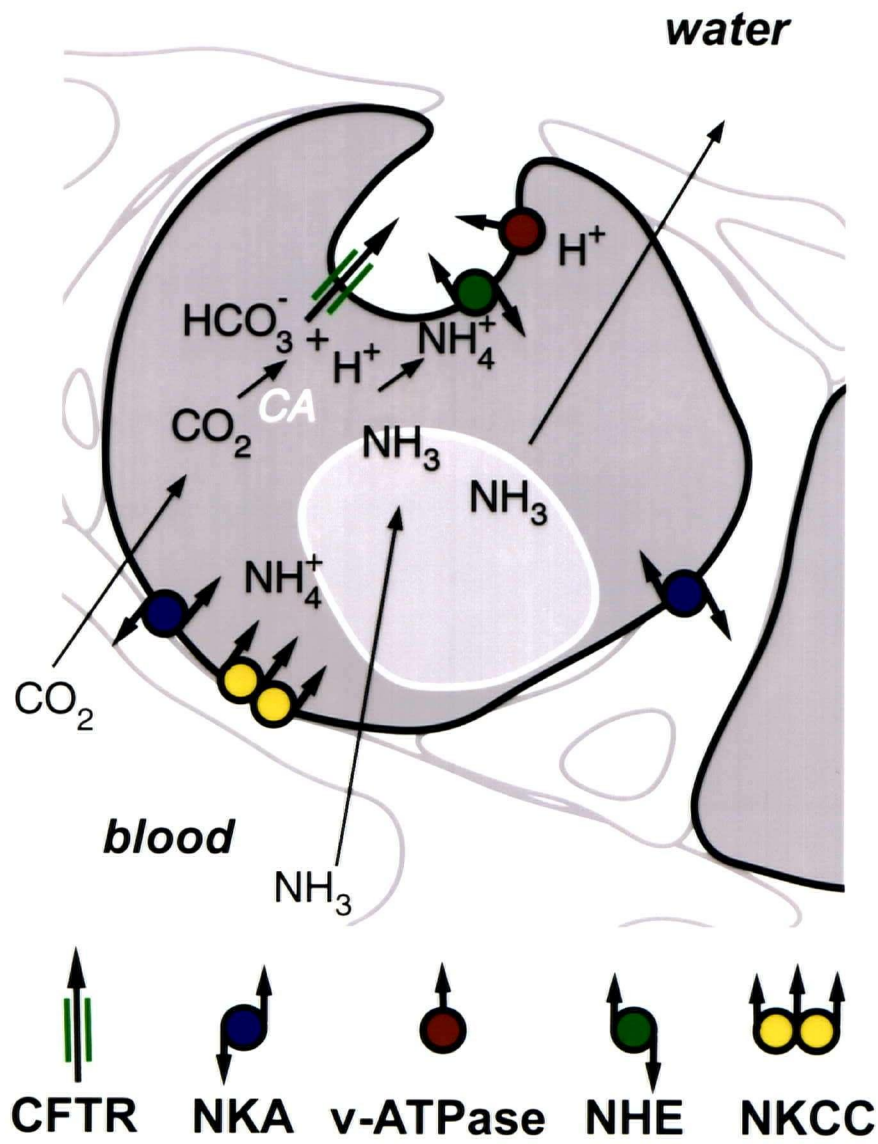
6. GENERAL DISCUSSION

The cellular and subcellular distributions of ion transport proteins can be determined using electrophysiological, biochemical, and immunological techniques. While the first two techniques have the advantage of providing evidence for the functional presence of a protein, the techniques have their limits in application (a point that is well illustrated with the fish gill). The gill epithelium is heterocellular, thin (1-15μm), and arranged in three dimensions on filaments and lamellae. Direct study of the gill using these techniques has proven technically challenging. To date there is but one published report of whole cell recordings from fish gill cells estimating membrane potential differences (Clarke and Potts 1998) and a large number of transepithelial potential measurements (reviewed by Potts 1984). Biochemical studies have made use of differential cell isolation techniques (MR cells from other cells, PVCs) for characterizing cell types (e.g. Wong and Chan 1999) but have not had the benefit of having protocols for isolating the apical plasma membrane fraction from gill epithelial tissue. There have not been any apical membrane markers identified in fish gill to make such an isolation possible and it also is unclear if the techniques for isolating basolateral membrane also do not include apical membrane (Flik and Verbost 1994; Henry *et al.* 1997; Crockett 1999). Thus much of our understanding of the gill's contribution to ion regulation is constructed from data obtained from whole animal experiments, *in vitro* whole gill preparations, isolated epithelial cells, and surrogate models (e.g. Li *et al.* 1998; Marshall and Bryson 1998; Evans *et al.* 1999; Wong and Chan 1999). Immunological detection introduces a level of resolution that has helped in defining the function of branchial cell types.

In this thesis, I have been able to demonstrate the usefulness of the immunological approach to ion transport protein localization. From my observation of freshwater fish species,

179

the vH^+-ATPase and epithelial Na^+ channel have been shown to be co-localized. This lends credence to the vH^+-ATPase driven Na^+ uptake model (Avella and Bornancin 1989; Lin and Randall 1995; Fenwick *et al.* 1999). There is not a clear distinction between the contributions of the MR cell versus the PVC that would allow me to generalize among teleost fishes. The involvement of the MR cell in Na^+ uptake shows species specificity. The freshwater MR cell does however seem to have a clear role in Cl^- uptake as an apical AE is localized to this cell in both the tilapia and coho salmon. Thus initial reference to this cell type as a *chloride* cell seems apt. The MR cell apical AE is lost in sea water adapted coho salmon but present in the stenohaline turbot. The role of the NHE in freshwater Na^+ uptake is not clear, but the antibody I used in this study may prove useful as a marker for MR accessory cells that are found in marine and euryhaline fishes. In marine fishes, it is possible to localize the various ion transport proteins involved in active Cl^- excretion (Na^+,K^+-ATPase, NKCC and CFTR; Marshall and Bryson 1998). I was not able to find evidence to support the proposed role of branchial PVCs in active Cl^- excretion as suggested by the results of Avella, Ehrenfeld and co-workers (1997, 1999; Duranton *et al.* 1997) studying seabass PVC primary cultures.

Immunological localization techniques, of course, have limitations and I would not argue solely on the immunological evidence that these ion transport processes are taking place. So while the technique can demonstrate the presence of a protein, it cannot demonstrate if it is functional. However, there is generally *a priori* evidence for the presence of many of these transporters in the gill of freshwater and seawater fishes (Lin and Randall 1995; Goss *et al.* 1995; Evans *et al.* 1999). Thus the immunodetection data corroborates the physiological studies and provides additional evidence about ion transport protein cellular and subcellular distributions. In

the case of the mudskipper, basic morphological and physiological data was generated to support the immunolocalization data and construct a model for ion exchange in this species.

In the mudskipper a convincing argument can be made that the unusual branchial MR cells are involved in the active NH_4^+ excretion observed when the animal is out of water or in its water filled burrow which has ammonia concentrations around 2mM (Y-K Ip, personal communication). Assembled within the branchial MR cells are ion transport proteins that contribute to net ammonia flux. Lining the MR cell apical crypt are two immunoreactive NHE-like isoforms (NHE-2 and NHE-3). NHE has been found *in vitro* to transport NH_4^+ ions (Kinsella and Aronson 1981), which in the case of the mudskipper makes use of inward Na^+ gradients to drive NH_4^+ efflux (Randall *et al.* 1999). An apical CFTR-like anion channel may account for acid-base neutrality by facilitating the efflux of HCO_3^-. Intracellular carbonic anhydrase (CA) catalyzes the CO_2 hydration reaction to supply H^+ ions for NH_3 protonation to provide NH_4^+ for the NHE. Basolateral Na^+,K^+-ATPase contributes to ammonia excretion when the animal is faced with inward gradients of ammonia. The role of basolateral NKCC has yet to be established. The vH^+-ATPase, although present in the MR cell, makes an uncertain contribution to ammonia excretion.

Western analysis and control tissue staining using sera or IgG from the host animals (rabbit or mouse) were used to assess antibody specificity. In general, staining patterns seen also with the rabbit or mouse control were considered non-specific and not used; however, there are some difficulties with the Western blots. There are cases where antibodies useful for immunohistochemistry have failed to work on immunoblots; recognizing no bands (NKCC) or too many bands (NHE-2, NHE-3). Because of this, the data does have to be interpreted with at least some caution. However, crossreactivity may not have been observed for technical reasons

181

and the additional bands may represent breakdown products (lower MW) or aggregates (higher MW) of the protein of interest. The presentation of proteins for immunodetection on tissue sections and immobilized on membrane supports is different. In tissue sections the protein is in its near native state, however proteins separated by SDS-PAGE and transferred to a support membrane have lost their native conformation and thus in the process may have lost epitopes previously recognized. The other antibodies used generally immunoreacted with bands in the correct molecular weight range (α-subunit Na^+,K^+-ATPase, CFTR, β-subunit ENaC, A-subunit vH$^+$-ATPase).

Another point that needs to be addressed is negative results. Generally, the absence of immunoreactivity with tissue sections can be explained either by the absence of that protein with possibly a different isoform present within the tissue (i.e. the antibody is not specific for the protein) or again by technical problems (i.e. the antibody is unable to recognize the protein (epitope) in its present conformation). Without any sequence information on the protein in question, it not possible to distinguish the cause of this common outcome. The trout gill apical AE illustrates this point well because immunoreactivity within the branchial epithelium was not observed, however, there is much indirect evidence that the trout gill epithelium has an apical Cl$^-$/HCO$_3^-$ exchanger (correlation of Cl$^-$ fluxes with MR cell morphometric changes, Goss et $al.$ 1995; intracellular ion changes, Morgan et $al.$ 1994, Morgan and Potts 1995). Apical immunoreactivity was observed in the freshwater tilapia and coho salmon. A non band 3-like AE isoform may be present in the trout MR cell similar to the mammalian collecting duct β-cell which expresses an apical AE2 (Alper et $al.$ 1997). There are again a number of technical reasons why crossreactivity was not observed ranging from masking of the epitope, poor antibody-antigen avidity (complex stability) or insufficient antigen. The absence of

immunodelectability of the basolateral Na^+,K^+-ATPase in PVCs also illustrates this latter point. Na^+,K^+-ATPase has a cellular housekeeping role contributing to the maintenance of the membrane potential and intracellular Na^+ and K^+ concentrations and thus is expressed in all vertebrate cells. Immunolocalization techniques used in this thesis and by others (Witters et al. 1996, Ura et al. 1996; Deng et al. 1999) have failed to detect the PVC basolateral Na^+,K^+-ATPase. Hootman and Phillpot (1979) were also unable to demonstrate the presence of Na^+,K^+-ATPase in branchial cells other than the MR cells using ^{3}H-ouabain autoradiography. In the freshwater fish PVCs involved in Na^+ uptake, the basolateral Na^+,K^+-ATPase, would be expected to participate in the entry step of Na^+ into the blood (Richards and Fromm 1970; Payan et al. 1975). It is possible that a different α-subunit isoform exists in the PVC that is not recognized by the monoclonal antibody $\alpha5$. Isoform variability and different $\alpha\beta$ dimer combinations impart different pump characteristics for specialized cell or tissue functions (Blanco and Mercer 1998).

The usefulness of using non-homologous antibodies to proteins in such distantly related animals as mammals and teleost fishes is a legitimate concern. In addition, many of these ion transport proteins belong to large multigene families whose members may have divergent functions. It must be remembered however, that some of these proteins are also highly conserved and have functions essential for basic cellular homeostasis. One such example is the vH^+-ATPase, that is found in all living creatures and has a highly conserved A-subunit (archaebacteria to humans; e.g. Finbow and Harrison1997). A peptide antibody was used to immunolocalize the A-subunit and a *Blastp* search (www.cbr.nrc.ca) of the peptide amino acid sequence (Südhof et al. 1989) reveals high identity with other vertebrate and non-vertebrate A-subunit sequences (humans to *Drosophilla melanogaster* 100-73% identity, 16 hits). No non- vH^+-ATPase A-subunit sequences were found in the search. Thus it would seem that this sequence is also present

183

in the fish vH^+-ATPase A-subunit. The peptide from β-subunit of the ENaC used to generate polyclonal antibodies produced similar results with the *Blastp* search. The β-subunit of the ENaC is the most highly conserved of the three ENaC subunits (α,β,γ; Garty and Palmer 1997). The Na^+,K^+-ATPase α-subunit antibody is considered pan-specific recognizing the α-subunit in animals ranging from crayfish to humans (eg Barradas *et al.* 1999; Sabolic *et al*. 1998).

Future directions

While there is a general dearth of information provided by whole cell recordings, patch clamp techniques and the use of ionophores stand to provide valuable information on transporter properties and intracellular ion concentrations. Li *et al.* (1998) have measured intracellular ion concentrations and pH in isolated cells and I know of at least three groups which are preparing to attempt some electrophysiology using patch clamping techniques (CM. Wood, Hamilton Can.; R. Handy, Plymouth UK; S. Thomas CNRS Fr.).

The development of protocols for the isolation of apical membranes would allow for the purification of fish ion transporters for the development of homologous antibodies. I had attempted to do so by using a sucrose gradient and my antibodies as probes for membrane fractions but my method lacked resolution and I lacked the resolve.

The use of surrogate models (primary culture and skin preparations) while currently uncertain, may yet provide results consistent with *in vivo* observations (Burgess *et al.* 1998; Wood *et al.* 1998; Gilmour *et al.* 1998). It is now possible to have MR cells in primary gill culture using a double seeding technique (Kelly *et al.* 1999). With this advance it may be possible to demonstrate NaCl uptake as seen *in vivo*.

Molecular techniques stand to contribute greatly to our understanding of ion regulation in fishes. The use of differential display has already lead to the identification of an upregulated

inwardly rectifying K$^+$ channel (Kir) in MR cells following seawater transfer (Suzuki *et al.* 1998). Cloning of the fish genes will in turn lead to the generation of homologous fish antibodies. However, with 25 000 known species of teleost fishes there are years of work ahead. The recent work on the vH$^+$-ATPase B-subunit illustrates this point as two isoforms were found in the eel (Pelster *et al.* 1999) while only a single isoform in the rainbow trout (Perry *et al.* 1999). Also teleost fishes generally have more functional members of multigene families (paralogues) lacking mammalian counterparts (orthologue) (Wittbrodt *et al.* 1998). Wittbrodt *et al.* (1998) suggested that the complex genomic architechture of fishes has allowed them to speciate quickly in response to changing selective regimes.

The mudskipper represents an interesting creature to study. The story of its ability to tolerate high environmental ammonia levels is far from over. The possible role of the CFTR in HCO$_3^-$ efflux is worth following up. In the duodenum and airways of mammals the CFTR anion channel has been found to have a direct role in HCO$_3^-$ efflux for alkalization of the lumen (Hogan *et al.* 1998; Lee *et al.* 1998). The inability of high environmental ammonia levels to elevate plasma ammonia levels in the mudskipper suggests that the apical membrane permeability to NH$_3$ is likely very low. During terrestrial excursions when ammonia accumulates in the surface film of water an impermeable membrane is also required to prevent a NH$_3$ back flux of the excreted NH$_4^+$. There are examples of membranes impermeable to NH$_3$ such as the kidney medullary thick ascending limb of Henle (Kikeri *et al.* 1989). Interestingly, Kikeri *et al.* (1989) were also able to demonstrate that an apical NHE facilitates NH$_4^+$ efflux but not influx across the apical membrane. Membrane permeability can be decreased by decreasing the fluidity of the membrane by altering the lipid composition either decreasing the amount of unsaturated

hydrocarbon chains, or increasing the amount of cholesterol (see Zeidel 1996). Future studies

focusing on the properties of the apical membrane should provide most interesting results.

Summary Conclusions

1.) In freshwater teleost fishes, I have been able to show that there is a clear link between the

vH^+-ATPase and ENaC, offering strong support to the vH^+-ATPase driven model of Na^+

uptake via an ENaC. I have also been able to demonstrate the presence of an apical band 3-

like AE in MR *chloride* cells in tilapia and coho salmon supporting the idea of this cell type's

role in active Cl^- uptake.

2.) In marine teleost fishes, I have been able to demonstrate the presence of ion transport

proteins involved in active Cl^- elimination in branchial MR *chloride* cells (CFTR-like,

NKCC, Na^+,K^+-ATPase). However, I was unable to support the idea that PVCs are also

involved in active Cl^- elimination. Branchial MR cells may also be involved in acid-base

regulation by means of NHE and AE proteins. Incidentally, the antibody 597 against NHE-2

also appears to be good marker for the accessory cell type.

3.) The mudskipper represents an unusual fish that spends much of its time out of water and is

able to actively eliminate ammonia. In a series of studies I have been able to show that the

branchial epithelium MR cells are likely the sites of active NH_4^+ elimination. NH_4^+

elimination being mediate by an apical NHE-like protein.

REFERENCES

Al-Kadhomiy, N.K. and G.M. Hughes 1988 Histological study of different regions of the skin and gills in the mudskipper, *Boleophthalmus boddarti* with respect to their respiratory function. J.mar.biol.Ass.U.K., *68*:413-422.

Alper, S.L., J. Natale, S. Gluck, H.F. Lodish, and D. Brown 1989 Subtypes of intercalated cells in rat kidney collecting duct defined by antibodies against erythroid band 3 and renal vacuolar H^+-ATPase. Proc.Natl.Acad.Sci.USA, *86*:5429-5433.

Alper, S.L. 1991 The band 3-related anion exchanger (AE) gene family. Ann.Rev.Physiol., *53*:549-564.

Alper, S.L., A. Stuart-Tilley, D. Biemesderfer, B.E. Shmukler, and D. Brown 1997 Immunolocalization of AE2 anion exchanger in rat kidney. Am.J.Physiol., *273*:F601-F614

Altendorf, K., K.U. Bindseil, E.J. Bowman, A. Siebers, and A. Zeeck 1993 Inhibitory effect of modified bafilomycins and concanamycins on P- and V-type adenosinetriphosphatases. Biochemistry, *32*:3902-3906.

Anderson, M.P., R.J. Gregory, S. Thompson, D.W. Souza, S. Paul, R.C. Mulligan, A.E. Smith, and M.J. Welsh 1991 Demonstration that CFTR is a chloride channel by alteration of its anion selectivity. Science, *253*:202-205.

Appel, C., S. Gloor, G. Schmalzing, M. Schachner, and R.P. Bernhardt 1996 Expression of a Na,K-ATPase β_3 subunit during development of the zebrafish central nervous system. J.Neurosci.Res., *46*:551-564.

Appell, K.C. and P.S. Low 1981 Partial structural characterization of the cytoplasmic domain of the erythrocyte membrane protein, Band 3. J.Biol.Chem., *256*:11104-11111.

Avella, M., A. Masoni, M. Bornancin, and N. Mayer-Gostan 1987 Gill morphology and sodium influx in the rainbow trout (*Salmo gairdneri*) acclimated to artificial freshwater environments. J.exp.Zool., *241*:159-169.

Avella, M. and M. Bornancin 1989 A new analysis of ammonia and sodium transport through the gills of the freshwater rainbow trout (*Salmo gairdneri*). J.exp.Biol., *142*:155-175.

Avella, M. and M. Bornancin 1990 Ion fluxes in the gills of freshwater and seawater salmonid fish. In: Animal Nutrition and Transport Processes. 2. Transport, Respiration and Excretion: Comparative and Environmental Aspects. J.P. Truchot and B. Lahlou, eds. Comp Physiol., Basel,Karger, pp. 1-13.

Avella, M. and J. Ehrenfeld 1997 Fish gill respiratory cells in culture: A new model for Cl secreting epithelia. J.Membrane Biol., *156*:87-97.

Avella, M., P. Pärt, and J. Ehrenfeld 1999 Regulation of Cl⁻ secretion in seawater fish (*Dicentrarchus labrax*) gill respiratory cells in primary culture. J.Physiol., *516*:353-363.

Barradas, C., S. Dunel-Erb, and J. Lignon 1997 Transepithelial potential difference of a single gill filament isolated from the crayfish *Astacus leptodactylus* Esch.: A new method. Arch.Physiol.Biochem., *105*:38-44.

Barradas, C., J.M. Wilson, and S. Dunel-Erb 1999 Na⁺/K⁺-ATPase activity and immunocytochemical labeling in podobranchial filament and lamina of freshwater crayfish *Astacus leptodactylus* Eschscholtz: evidence for the existence of a sodium transport in the filaments. Tissue and Cell, (In Press)

Bear, C.E., C. Li, N. Kartner, R.J. Bridges, T.J. Jensen, M. Ramjeesingh, and J.R. Riordan 1992 Purification and functional reconstitution of the cystic fibrosis transmembrane conductance regulator (CFTR). Cell, *68*:809-818.

Benos, D.J. 1982 Amiloride: a molecular probe of sodium transport in tissues and cells. Am.J.Physiol., *242*:C131-C145

Benos, D.J., M.S. Awayda, I.I. Ismailov, and J.P. Johnson 1995 Structure and function of amiloride-sensitive Na⁺ channels. J.Membrane Biol., *143*:1-18.

Bianchini, L. and J. Pouyssegur 1994 Molecular structure and regulation of vertebrate Na⁺/H⁺ exchangers. J.exp.Biol., *196*:337-345.

Biemesderfer, D., P.A. Rutherford, T. Nagy, J.H. Pizzonia, A.K. Abu-Alfa, and P.S. Aronson 1997 Monoclonal antibodies for high-resolution localization of NHE3 in adult and neonatal rat kidney. Am.J.Physiol., *273*:F289-F299

Bijman, J., A.M. Hoogeveen, B.J. Scholte, M. Kansen, A.W.M. van der Kamp, and H.R. de Jonge 1990 Ion transport regulation in cystic fibrosis epithelia. In: Epithelial secretion of water and electrolytes. J.A. Young and P.Y. Wong, eds. Springer-Verlag, Berlin, Heidelberg, pp. 361-369.

Bindon, S.D., K.M. Gilmour, J.C. Fenwick, and S.F. Perry 1994 The effects of branchial chloride cell proliferation on respiratory function in the rainbow trout *Oncorhynchus mykiss*. J.exp.Biol., *197*:47-63.

Blackston, C.R., W. Hollimon, and J.B. Claiborne 1997 Isoforms of the Na⁺/H⁺ antiporter (NHE) in gill mRNA of the marine long-horned sculpin (*Myoxocephalus octodecimspinosus*). Bull.Mt.Desert Isl.Biol.Lab., 22

Blanchard, A., D. Eladari, F. Leviel, M. Tsimaratos, M. Paillard, and R.-A. Podevin 1998 NH₄⁺ as a substrate for apical and basolateral Na⁺-H⁺ exchangers of thick ascending limbs of rat kidney: evidence from isolated membranes. J.Physiol., *506.3*:689-698.

Blanco, G. and R.W. Mercer 1998 Isozymes of the Na-K-ATPase: heterogeneity in structure, diversity in function. Am.J.Physiol., *275*:F633-F650

Blattler, D.P., F. Garner, K. van Slyke, and A. Bradley 1972 Quantitative electrophoresis in polyacrilamide gels of 2-40%. J.Chromatography, *64*:147-155.

Bookstein, C., Y. Xie, K. Rabenau, M.W. Musch, R.L. McSwine, M.C. Rao, and E.B. Chang 1997 Tissue distribution of Na^+/H^+ exchanger isoforms NHE2 and NHE4 in rat intestine and kidney. Am.J.Physiol., *273*:C1496-C1505

Borgese, F., C. Sardet, M. Cappadoro, J. Pouyssegur, and R. Motais 1992 Cloning and expression a cAMP-activated Na^+/H^+ exchanger; evidence that th cytoplasmic domain mediates hormonal regulation. Proc.Natl.Acad.Sci.USA, *89*:6768-6769.

Bornancin, M., G. de Renzis, and R. Naon 1980 $Cl^--HCO_3^--$ ATPase in gills of the rainbow trout: evidence for its microsomal localization. Am.J.Physiol., *238*:R251-R259

Bowman, E.J., A. Siebers, and K. Altendorf 1988 Bafilomycins: A class of inhibitors of membrane ATPases from microorganisms, animal cells, and plant cells. Proc.Natl.Acad.Sci.USA, *85*:7972-7976.

Bradbury, N.A. 1999 Intracellular CFTR: Localization and function. Physiol.Rev., *79*:S175-S191

Bradford, M.M. 1976 A rapid and sensitive method for the quantitation of microgram quantities of protein utilizing the principle of protein-dye binding. Anal.Biochem., *72*:248-254.

Breton, S., P.J.S. Smith, B. Lui, and D. Brown 1996 Acidification of the male reproductive tract by a proton pumping (H^+)-ATPase. Nature Medicine, *2*:470-472.

Brosius III, F.C., S.L. Alper, A.M. Garcia, and H.F. Lodish 1989 The major kidney band 3 gene transcript predicts an amino-terminal truncated band 3 polypeptide. J.Biol.Chem., *264*:7784-7787.

Brosius III, F.C., R.L. Pisoni, X. Cao, G. Deshmukh, D. Yannoukakos, A. Stuart-Tilley, C. Haller, and S.L. Alper 1997 AE anion exchanger mRNA and protein expression n vascular smooth muscle cells, aorta, and renal microvessels. Am.J.Physiol., *273*:F1039-F1047

Brown, D., S. Gluck, and HartwigJ 1987a Structure of the novel membrane-coating material in proton-secreting epithelial cells and identifcation as an H^+-ATPase. J.Cell Biol., *105*:1637-1648.

Brown, D., P. Weyer, and L. Orci 1987b Nonclathrin-coated vesicles are involved in endocytosis in kidney collecting duct intercalated cells. Anat.Rec., *218*:237-242.

Brown, D., S. Hirsch, and S. Gluck 1988 Localization of a proton-pumping ATPase in rat kidney. J.Clin.Invest., *82*:2114-2126.

Brown, D., E.J. Sorscher, D.A. Ausiello, and D.J. Benos 1989 Immunocytochemical localization of Na^+ channels in rat kidney medulla. Am.J.Physiol., *256*:F366-F369

Brown, D., I. Sabolic, and S. Gluck 1992 Polarized targeting of V-ATPase in kidney epithelial cells. J.exp.Biol., *172*:231-243.

Brown, D., J. Lydon, M. McLaughlin, A. Stuart-Tilley, R. Tyszkowski, and S.L. Alper 1996 Antigen retrieval in cryostat tissue sections and cultured cells treatment with sodium dodecyl sulfate (SDS). Histochem.Cell Biol., *105*:261-267.

Burgess, D.W., W.S. Marshall, and C.M. Wood 1998 Ionic transport by the opercular epithelium of freshwater acclimated tilapia (*Oreochromis niloticus*) and killifish (*Fundulus heteroclitus*). Comp.Biochem.Physiol., *121A*:155-164.

Cabantchik, Z.I. and A. Rothstein 1972 The nature of the membrane sites controlling anion permeability of human red blood cells as determined by studies with disulfonic stilbene derivatives. J.Membrane Biol., *10*:311-330.

Cameron, B.A., S.F. Perry, C. Wu, K. Ko, and B.L. Tufts 1996 Bicarbonate permeability and immunological evidence for an anion exchanger-like protein in the red blood cells of the sea lamprey, *Petromyzon marinus*. J.Comp.Physiol., *166*:197-204.

Cameron, J.N. and N. Heisler 1983 Studies of ammonia in the rainbow trout: Physico-chemcal parameters, acid-base behaviour and respiratory clearance. J.exp.Biol., *105*:107-125.

Cameron, J.N. 1986 Responses to reversed NH_3 and NH_4^+ gradients in a teleost (*Ictalurus punctatus*), and elasmobranch (*Raja erinacea*) and a crustacean (*Callinectes sapidus*): evidence for NH_4^+/H^+ exchange in the teleost and elasmobranch. J.exp.Zool., *239*:183

Canessa, C.M., L. Schild, G. Buell, B. Thorens, I. Gautschi, J.-D. Horisberger, and B.C. Rossier 1994 Amiloride-sensitive epithelial Na^+ channel is made of three homologous subunits. Nature, *367*:463-467.

Chambrey, R., J.-M. Achard, P.L. St.John, D.R. Abrahamson, and D.G. Warnock 1997 Evidence for an amiloride-insensitive Na^+/H^+ exchanger in rat renal cortical tubules. Am.J.Physiol., *273*:C1064-C1074

Chew, S.F. and Y.K. Ip 1987 Ammoniagenesis in mudkippers *Boleophthalmus boddaerti* and *Periophthamodon schlosseri*. Comp.Biochem.Physiol., *87B*:941-948.

Chretien, M. and M. Pisam 1986 Cell renewal and differentiation in the gill epithelium of fresh- or salt-water-adapted euryhaline fish as revealed by [^{3}H]-thymidine radioautography. Biol.Cell, *56*:137-150.

Claiborne, J.B., D.H. Evans, and L. Goldstein 1982 Fish branchial Na^+/NH_4^+ exchange is via basolateral Na^+-K^+ activated ATPase. J.exp.Biol., *96*:431-434.

Claiborne, J.B. and D.H. Evans 1988 Ammonia and acid-base balance during high ammonia exposure in a marine teleost (*Myoxocephalus octodecimspinosus*). J.exp.Biol., *140*:89-105.

Claiborne, J.B., E. Perry, S. Bellows, and J. Campbell 1997 Mechanisms of acid-base excretion across the gills of a marine fish. J.exp.Zool., *279*:509-520.

Claiborne, J.B. 1998 Acid-base regulation. In: The physiology of fishes. D.H. Evans, ed. CRC Press, Boca Raton, pp. 177-198.

Claiborne, J.B., C.R. Blackston, K.P. Choe, D.C. Dawson, S.P. Harris, L.A. MacKenzie, and A.I. Morrison-Shetlar 1999 A mechanism for branchial acid excretion in marine fish: Identification of multiple Na^+/H^+ antiporter (NHE) isoforms in gills of two seawater teleosts. J.exp.Biol., *202*:315-324.

Clarke, A.P. and W.T.W. Potts 1998a Isolated filament potentials and branchial ion fluxes in the European flounder (*Platichthys flesus* L.). Evidence for proton pump mediated sodium uptake. J.Zool., *246*:433-442.

Clarke, A.P. and W.T.W. Potts 1998b Sodium, net acid, and ammonia fluxes in freshwater-adapted European flounder (*Platichthys flesus* L.). Pharacological inhibition and effects on gill ventilation volume. J.Zool., *246*:427-432.

Clarke, L.L. and M.C. Harline 1998 Dual role of CFTR in cAMP-stimulated HCO_3^- secretion across murine duodenum. Am.J.Physiol., *274*:G718-G726

Clayton, D.A. 1993 Mudskippers. Oceanogr.Mar.Biol.Annu.Rev., *31*:507-577.

Cohen, L.H., A. Mueller, and P.R. Steinmetz 1978 Inhibition of bicarbonate exit step in urinary acidifcation by a disulfonic stilbene. J.Clin.Invest., *61*:981-986.

Cohn, J.A. 1994 CFTR localization: Implications for Cell and Tissue Pathphysiology. In: Cystic fibrosis: current topics. J.A. Dodge, D.J.H. Brock and J.H. Widdicombe, eds. Wiley, Chichester, UK, pp. 173-191.

Conley, D.M. and J. Mallatt 1987 Histochamical localization of Na^+-K^+ ATPase and carbonic anhydrase activity in gills of 17 fish species. Can.J.Zool., *66*:2398-2405.

Curran, R.C. and J. Gregory 1977 The unmasking of antigens in paraffin sections of tissue by trypsin. Experientia, *33*:1400-1401.

Cutler, C.P., I.L. Sanders, N. Hazon, and G. Cramb 1995a Primary sequence, tissue specificity and mRNA expression of the Na^+,K^+-ATPase β_1 subunit in the European eel (*Anguilla anguilla*). Fish Physiol.Biochem., *14*:423-429.

Cutler, C.P., I.L. Sanders, N. Hazon, and G. Cramb 1995b Primary sequence, tissue specificity and mRNA expression of the Na^+,K^+-ATPase α_1 subunit in the European eel (*Anguilla anguilla*). Comp.Biochem.Physiol., *111B*:567-573.

Cutler, C.P., I.L. Sanders, and G. Cramb 1997 Expression of Na^+,K^+-ATPase beta suubunit isoforms in the European eel (*Anguilla anguilla*). Fish Physiol.Biochem., *17*:371-376.

D'Souza, S., A. Garcia-Cabado, F. Yu, K. Teter, G. Lukacs, K. Skorecki, H.-P. Moore, J. Orlowski, and S. Grinstein 1998 The epithelial sodium-hydrogen antiporter Na^+/H^+ exchanger 3 accumulates and is functional in recycling endosomes. J.Biol.Chem., *273*:2035-2043.

Dang, Z.-C., R.A. Lock, G. Flik, and S.E. Wendelaar Bonga 1999 Responses of Na^+/K^+-ATPase, metallothioneins and cortisol receptor in the gill epithelial cells of copper exposed fish. Comp.Biochem.Physiol., *124A*:S11(Abstract)

de Renzis, G. and J. Maetz 1973 Studies on the mechanism of chloride absorption by the goldfish gill. Relation with acid-base regulation. J.exp.Biol., *59*:339-358.

Degnan, K.J., K.J. Karnaky, and J.A. Zadunaisky 1977 Active chloride transport in the *in vitro* opercular skin of a teleost (*Fundulus heteroclitus*), a gill-like epithelium rich in chloride cells. J.Physiol., *271*:155-191.

Degnan, K.J. and J.A. Zadunaisky 1980 Passive sodium movements across the opercular epithelium: The paracellular shunt pathway and ionic conductance. J.Membrane Biol., *55*:175-185.

Doyle, W.L. and D. Gorecki 1961 The so-called chloride cell of the fish gill. Physiol.Zool., *34*:81-85.

Drenckhahn, D., M. Oelmann, P. Schaaf, M. Wagner, and S. Wagner 1987 Band 3 is the basolateral anion exchanger of dark epithelial cells of turtle urinary bladder. Am.J.Physiol., *252*:C570-C574

Dröse, S. and K. Altendorf 1997 Bafilomycins and concanamycins as inhibitors of V-ATPases and P-ATPase. J.exp.Biol., *200* :1-8.

Dschida, W.J.A. and B.J. Bowman 1995 The vacuolar ATPase: sulfite stabilization and the mechanism of nitrate inactivation. J.Biol.Chem., *270*:1557-1563.

Dubinsky, W.P. and L.B. Monti 1986 Resolution of apical from basolateral membrane of shark rectal gland. Am.J.Physiol., *251* :C721-C726

Dunel-Erb, S. and P. Laurent 1980 Ultrastructure of the marine teleost gill epithelium: SEM and TEM study of the chloride cell apical membrane. J.Morph., *165*:175-186.

Duranton, C., M. Tauc, M. Avella, and P. Poujeol 1997 Chloride channels in primary cultures of seawater fish (*Dicentrarchus labrax*). Am.J.Physiol., C874-C882

Ehrenfeld, J., I. Laccoste, F. Garcia-Romeu, and B. Harvey 1990 Interdependence of Na^+ and H^+ transport in frog skin. In: Animal Nutrition and Transport Processes. 2. Transport, Respiration and Excretion: Comparative and Environmental Aspects. J.P. Truchot and B. Lahlou, eds. Comparative Physiology, Basel,Karger, pp. 152-170.

Ehrenfeld, J. and U. Klein 1996 A primary cation transport by a V-type ATPase of low specificity. J.exp.Biol., *199*:1327-1334.

Epstein, F.H., P. Silva, and G. Kormanik 1980 Role of Na-K-ATPase in chloride cell function. Am.J.Physiol., *238*:R246-R250

Eriksson, O., N. Mayer-Gostan, and P.J. Wistrand 1985 The use of isolated fish opercular epithelium as a model tissue for studying intrinsic activities of loop diuretics. Acta Physiol.Scand., *125*:55-66.

Evans, D.H. 1979 Fish. In: Comparative physiology of osmoregulation in animals. G.M.O. Maloiy, ed. Academic Press, Orlando, pp. 305-390.

Evans, D.H. and J.N. Cameron 1986 Gill ammonia transport. J.exp.Zool., *239*:17-23.

Evans, D.H., K.J. More, and S.L. Robbins 1989 Modes of ammonia transport across the gill epithelium of the marine teleost fish *Opsanus beta*. J.exp.Biol., *144*:339-356.

Evans, D.H. 1993 Osmotic and ionic regulation. In: The Physiology of Fishes. D.H. Evans, ed. CRC Press, Inc, Boca Raton, pp. 315-341.

Evans, D.H., P.M. Piermarini, and W.T.W. Potts 1999 Ionic transport in the fish gill epithelium. J.exp.Zool., *283*:641-652.

Feng, Y. and M. Forgac 1994 Inhibition of vacuolar H^+-ATPase by disulfide bond formation between cystein 254 and cysteine 532 in subunit A. J.Biol.Chem., *269*:13224-13230.

Fenwick, J.C., S.E. Wendelaar Bonga, and G. Flik (1999) In vivo bafilomycin-sensitive Na^+ uptake in young freshwater fish. J. exp. Biol., *202*: 3659-3666.

Finbow, M. and M.A. Harrison 1997 The vaculoar H^+-ATPase: a universal proton pump of eukaryotes. Biochem.J., *324*:697-712.

Flik, G. and P.M. Verbost 1994 Ca^{2+} transport across plasma membranes. In: Biochemistry and molecular biology of fishes. P.W. Hochachka and T.P. Mommsen, eds. Elsevier Science, Amsterdam, pp. 625-637.

Flik, G., P.M. Verbost, and B. Wendelaar 1995 Calcium transport processes in fishes. In: Fish Physiology. C.M. Wood and T.W. Shuttleworth, eds. Academic Press, Boca Raton, pp. 317-342.

Forgac, M. 1989 Structure and function of vacuolar class of ATP-driven proton pumps. Physiol.Rev., *69*:765-796.

Forgac, M. 1999 The vacuolar H^+-ATPase of clathrin-coated vesicles is reversibly inhibited by S-nitrosoglutathione. J.Biol.Chem., *274*:1301-1305.

Foskett, J.K. and C. Scheffey 1982 The chloride cell: definitive identification as the salt-secretory cell in teleosts. Science, *215*:164-166.

Fuller, C.M., M.S. Awayda, M.P. Arrate, A.L. Bradford, R.G. Morris, C.M. Canessa, B.C. Rossier, and D.J. Benos 1995 Cloning of a bovine renal epithelial Na^+ channel subunit. Am.J.Physiol., *269*:C641-C654

Garty, H. and L.G. Palmer 1997 Epithelial sodium channels: function, structure, and regulation. Physiol.Rev., *77*:359-396.

Garvin, J.L., M.B. Burg, and M.A. Knepper 1985 Ammonium replaces potassium in supporting sodium transport by the Na-K-ATPase of renal proximal straight tubules. Am.J.Physiol., *249*:F785-F788

George, A.A., R.W. Lehrich, S.G. Aller, and J.N. Forrest 1998 Partial cloning and apical membrane localization of an anion exchanger (AE-2) in shark (*Squalus acanthias*) rectal gland tubules: preliminary studies. Bull.Mt.Desert Isl.Biol.Lab., *37*:32

Gilmour, K.M., P. Prunet, M. Pisam, D.G. McDonald, and C.M. Wood 1998 Permeability and morphology of a cultured branchial epithelium form the rainbow trout during prolonged apical exposure to fresh water. J.exp.Zool., *281*:531-545.

Gluck, S. 1992 V-ATPases of the plasma membrane. J.exp.Biol., *172*:29-37.

Gluck, S. and R. Nelson 1992 The role of the V-ATPase in renal epithelial H^+ transport. J.exp.Biol., *172*:205-218.

Gluck, S.L., R.D. Nelson, B.S. Lee, Z.Q. Wang, X.L. Guo, J.Y. Fu, and K. Zhang 1992 Biochemistry of the renal V-ATPase. J.exp.Biol., *172*:219-229.

Goldstein, L., J.B. Claiborne, and D.E. Evans 1982 Ammonia excretion by the gills of two marine teleost fish: The importance of NH_4^+ permeance. J.exp.Zool., *219*:395-397.

Goldstein, L., J.B. Claiborne, and D.E. Evans 1982 Ammonia excretion by the gills of two marine teleost fish: The importance of NH_4^+ permeance. J.exp.Zool., *219*:395-397.

Goss, G., S. Perry, and P. Laurent 1995 Ultrastructural and morphometric studies on ion and acid-base transport processes in freshwater fish. In: Cellular and Molecular Approaches to Fish Ionic Regulation. AnonymousAcademic Press, San Diego, pp. 257-284.

Goss, G.G. and C.M. Wood 1990 Na^+ and Cl^- uptake kinetics, diffusive effluxes and scidic equivalent fluxes across the gills of rainbow trout I. Response to environmental hyperoxia. J.exp.Biol., *152*:521-547.

Goss, G.G., P. Laurent, and S.F. Perry 1992 Evidence for a morphological component in acid-base regulation during environmental hypercapnia in the brown bullhead (*Ictalurus nebulosus*). Cell Tissue Res., *268*:539-552.

Goss, G.G., P. Laurent, and S.F. Perry 1994 Gill morphology during hypercapnia in brown bullhead (*Ictalurus nebulosus*): role of chloride cells and pavement cells in acid-base regulation. J.Fish Biol., *45*:705-718.

Goss, G.G., S.F. Perry, J.N. Fryer, and P. Laurent 1998 Gill morphology and acid-base regulation in freshwater fishes. Comp.Biochem.Physiol., *119A*:107-115.

Graham, J.B. 1976 Respiratory adaptations of marine air-breathing fishes. In: Respiration of amphibious vertebrates. G.M. Hughes, ed. Academic Press, London, pp. 165-187.

Graham, J.B. 1997 Air-breathing fishes. Academic Press, San Diego, pp. -299

Greenaway, P. and T. Nakamura 1991 Nitrogenous excretion in two terrestrial crabs (*Gecarcoidea natalis* and *Geograpsus grayi*). Physiol.Zool., *64*:767-786.

Gregory, R.B. 1977 Synthesis and total ecretion of waste nitrogen by fish of the *Periophthalmusi* (mudskipper) and *Scartelaos* families. Comp.Biochem.Physiol., *57A*:33-36.

Handy, R.D. 1989 The ionic composition of rainbow trout body mucus. Comp.Biochem.Physiol., *93A*:571-575.

Harvey, B.J. 1992 Energization of sodium absorption by the H^+-ATPAse pump in mitochondria-rich cells of frog skin. J.exp.Biol., *172*:289-309.

Harvey, W.R. 1992 Physiology of V-ATPases. J.exp.Biol., *172*:1-17.

Harvey, W.R. and H. Weiczorek 1997 Animal plasma membrane energization by chemiosmotic H^+ V-ATPases. J.exp.Biol., *200*:203-216.

He, X., C.M. Tse, M. Donowitz, S.L. Alper, S.E. Gabriel, and B.J. Baum 1997 Polarized distribution of key membrane transport proteins in the rat submandibular gland. Pflugers Arch., *433*:260-268.

Heisler, N. 1993 Acid-Base Regulation. In: The Physiology of Fishes. D.H. Evans, ed. CRC Press Inc, Boca Raton, pp. 343-378.

Hemken, P., X.L. Guo, Z.Q. Wang, K. Zhang, and S. Gluck 1992 Immunological evidence that vaculoar H^+ ATPases with heterogeneous forms of $Mr = 31,000$ subunit have different membrane distributions in mammalian kidney. J.Biol.Chem., *267*:9948-9957.

Hirsch, S., A. Strauss, K. Masood, S. Lee, V. Sukhatme, and S. Gluck 1988 Isolation and sequence of a cDNA alone encoding the 31-kDa subunit of bovine kidney vacuolar H^+-ATPase. Proc.Natl.Acad.Sci.USA, *85*:3004-3008.

Hong, L. N. A comparative study of the effects of environmental pH on two mudskippers. 1-94. 1997. School of Biological Sciences, National Univerisity of Singapore. (GENERIC) Ref Type: Thesis/Dissertation

Hoogerwerf, W.A., S.C. Tsao, O. Devuyst, S.A. Levine, C.H. Yun, J.W. Yip, M.E. Cohen, P.D. Wilson, A.J. Lazenby, C.M. Tse, and M. Donowitz 1996 NHE2 and NHE3 are human and rabbit intestinal brush-border proteins. Am.J.Physiol., *270*:G29-G41

Hootman, S.R. and C.W. Philpott 1979 Ultracytochemical localization of Na^+,K^+-activated ATPase in chloride cells from the gills of a euryhaline teleost. Anat.Rec., *193*:99-130.

Hootman, S.R. and C.W. Philpott 1980 Accessory cells in the teleost branchial epithelium. Am.J.Physiol., *238*:R199-R206

Hughes, G.M. and E.R. Weibel 1972 Similarity of supporting tissue in fish gills and the mammalian reticuloendothelium. Journal of Ultrastrucure Research, *39*:106-114.

Hughes, G.M. and J.S.D. Munshi 1979 Fine structure of the gills of some Indian air-breathing fishes. J.Morph., *160*:169-194.

Hughes, G.M. 1984 General anatomy of the gills. In: Fish Physiology. W.S. Hoar and D.J. Randall, eds. Academic Press, New York, pp. 1-72.

Hulbert, W.C., T.W. Moon, and P.W. Hochochka 1978 The erythrinid gill: correlations of structure, function, and metabolism. Can.J Physiol.Pharmacol., *56*:814-819.

Ip, Y.K., C.Y. Lee, S.F. Chew, W.P. Low, and K.W. Peng 1993 Differences in the responses of two mudskippers to terrestrial exposure. Zool.Sci., *10*:512-519.

Ishimatsu, A., N.M. Aguilar, K. Ogawa, Y. Hishida, S. Oikawa, T. Kanda, and K.K. Huat 1999 Blood gas levels and cardiovascular functions during varying environmental conditions in a mudskipper fish *Periophthalmodon schlosseri*. J.exp.Biol., *202*:1753-1762.

Ismailov, I.I., B.K. Berdiev, A.L. Bradford, M.S. Awayda, C.M. Fuller, and D.J. Benos 1996 Associated proteins and renal epithelial Na^+ channel function. J.Membrane Biol., *149*:123-132.

Iwata, K., I. Kakuta, M. Ikeda, S. Kimoto, and N. Wada 1981 Nitrogn metabolism in the mudskipper, *Periophthalmus cantonensis* : a role of free amino acids in detoxification of ammonia produced during its terrestrial life. Comp.Biochem.Physiol., *68A*:589-596.

Iwata, K. 1988 Nitrogen metabolism in the mudskipper, *Periophthalmus cantonesis*: Changes in free amino acids and related compounds in various tissues under conditions of ammonia loading, with special reference to its high ammonia tolerance. Comp.Biochem.Physiol., *91A*:499-508.

Just, F. and B. Walz 1994 Immunocytochemical localization of Na^+/K^+-ATPase and $V-H^+$-ATPase in the salivary glands of the cockroach, *Periplaneta americana*. Cell Tissue Res., *278*:161-170.

Justensen, N.P.B., T. Dall-Larsen, and L. Klungsoyr 1993 Proton transport and chloride cells in the gill of rainbow trout (*Oncorhynchus mykiss*). Can.J.Fish.Aquat.Sci., *50*:988-995.

Jürss, K. and R. Bastrop 1995 The function of mitochondria-rich cells (chloride cells) in teleost gills. Rev.Fish Biol.Fish., *5*:235-255.

Karnaky, K.J., L.B. Kinter, W.B. Kinter, and C.E. Sterling 1976 Teleost chloride cell II: Autoradiographic localization of gill Na,K-ATPase in killifish *Fundulus heteroclitus* adapted to low and high salinity environments. J.Cell Biol., *70*:157-177.

Karnaky, K.J. 1986 Structure and function of the chloride cell of *Fundulus heteroclitus* and other teleosts. Amer.Zool., *26*:209-224.

Karnaky, K.J. 1998 Osmotic and ionic regulation. In: The physiology of fishes. D.H. Evans, ed. CRC Press, Boca Raton, pp. 157-176.

Kawakami, K., S. Noguchi, M. Noda, H. Takahashi, T. Ohta, M. Kawamura, H. Nojima, K. Nagano, T. Hirose, S. Inayama, H. Hayashida, T. Miyata, and S. Numa 1985 Primary structure of the α-subunit of *Torpedo californica* $(Na^+ + K^+)$ ATPase deduced from cDNA sequence. Nature, *316*:733-736.

Kerstetter, T.H. and L.B. Kirschner 1972 Active chloride transport by the gills of rainbow trout (*Salmo gairdneri*). J.exp.Biol., *56*:263-272.

Kerstetter, T.H. and L.B. Kirschner 1974 HCO_3^--dependent ATPase activity in the gills of rainbow trout (*Salmo gairdneri*). Comp.Biochem.Physiol., *48B*:581-589.

Keys, A. 1931 Chloride and water secretion and absoption by the gills of the eel. Z.vgl.Physiol., *15*:364-388.

Keys, A. and E.N. Willmer 1932 'Chloride secreting cells" in the gills of fishes, with special reference to the common eel. J.Physiol., *76*:368-378.

Kikeri, D., A. SUN, M.L. Zeidel, and S.C. Hebert 1989 Cell membranes impermeable to NH_3. Nature, *339*:478-480.

Kim, J., W.J. Welch, J.K. Cannon, C.C. Tisher, and K.M. Madsen 1992 Immunocytochemical response of type A and type B intercalated cells to increased sodium chloride delivery. Am.J.Physiol., *262*:F288-F302

Kinne, R., E. Kinne-Saffran, H. Schutz, and B. Scholermann 1986 Ammonium transport in medullary thick ascending limb of rabbit kidney: Involvement of the Na^+,K^+,Cl^--cotransporter. J.Membrane Biol., *94*:279-284.

Kinsella, J.L. and P.S. Aronson 1981 Interaction of NH_4^+ and Li^+ with the renal microvillus membrane Na^+-H^+ exchanger. Am.J.Physiol., *241*:C220-C226

Kisen, G., C. Gallais, B. Auperin, H. Klungland, O. Sandra, P. Prunet, and O. Andersen 1994 Northern blot analysis of the Na^+,K^+-ATPase α-subunit in salmonids. Comp.Biochem.Physiol., *107B*:225-259.

Klanke, C.A., Y.R. Su, D.F. Callen, Z. Wang, P. Meneton, N. Baird, R. Kandasamy, J. Orlowski, B.E. Otterud, M. Leppert, G.E. Shull, and A.G. Menon 1995 Molecular cloning and physical and genetic mapping of a novel human Na^+/H^+ exchanger (NHE5/SLC9A5) to chromosome 16q22.1. Genomics, *25*:615-622.

Klein, U., M. Timme, W. Zeiske, and J. Ehrenfeld 1997 The H^+ pump in frog skin (*Rana esculenta*): Identification and localization of a V-ATPase. J.Membrane Biol., *157*:117-126.

Kleyman, T.R. and E.J. Cragoe Jr. 1988 Amiloride and its analogues as tools in the study of ion transport. J.Membrane Biol., *105*:1-21.

Kleyman, T.R., P.R. Smith, and D.J. Benos 1994 Characterization and localization of epithelial Na^+ channels in toad urinary bladder. Am.J.Physiol., *266*:C1105-C1111

Klungsoyr, L. 1987 Magnesium ion activated ATPase and proton transport in vesicles from the gill of rainbow trout (*Salmo gairdnerii*). Comp.Biochem.Physiol., *88B*:1125-1134.

Kohn, O.F., P.P. Mitchell, and P.R. Steinmetz 1990 Characteristics of apical $Cl^-HCO_3^-$ exchanger of bicarbonate-secreting cells in turtle bladder. Am.J.Physiol., *258*:F9-F14

Kok, W.K., C.B. Lim, T.J. Lam, and Y.K. Ip 1998 The mudskipper *Periophthalmodon schlosseri* respires more efficiently on land than in water and vice versa from *Boleophthalmus boddaerti*. J.exp.Zool., *280*:86-90.

Krogh, A. 1937 Osmotic regulation in fresh water fishes by active absorption of chloride ions. Z.vgl.Physiol., *24*:656-666.

Krogh, A. 1939 Osmotic regulation in aquatic animals. Cambridge University Press, London, pp. 1

Kudrycki, K.E. and G.E. Shull 1989 Primary structure of the rat kidney band 3 anion exchange protein deduced from a cDNA. J.Biol.Chem., *264*:8185-8192.

Kurtz, I. and R.S. Balaban 1986 Ammonium as a substrate for Na^+-K^+-ATPase in rabbit proximal tubules. Am.J.Physiol., *250*:F497-F502

Lacy, E.R. 1983 Histochemical and biochemical studies of carbonic anhydrase activity in the opercular epithelium of the eurhaline teleost, *Fundulus heteroclitus*. Am.J.Anat., *166*:19-39.

Laemmli, U.K. 1970 Cleavage of structural proteins during the assembly of the head bacteriophage T4. Nature, *227*:680-685.

Larsen, E.H. 1991 Chloride transport by high-resistance heterocellular epithelia. Physiol.Rev., *71*:235-283.

Larsen, E.H., N.J. Willumsen, and B.C. Christoffersen 1992 Role of proton pump of mitochondria-rich cells for active transport of chloride ions in toad skin epithelium. J.Physiol., *450*:203-216.

Laurent, P. 1984 Gill internal morphology. In: Fish Physiology. W. Hoar and D.J. Randall, eds. Academic Press, New York, pp. 73-183.

Laurent, P., H. Hobe, and S. Dunel-Erb 1985 The role of environmental sodium chloride relative to calcium in gill morphology if freshwater salmonid fish. Cell Tissue Res., *240*:675-692.

Laurent, P. and S.F. Perry 1990 Effects of cortisol on gill chloride cell morphology and ionic uptake in the freshwater trout, *Salmo gairdneri*. Cell Tissue Res., *259*:429-442.

Laurent, P. and S.F. Perry 1991 Environmental effects on fish gill morphology. Physiol.Zool., *64*:4-25.

Laurent, P., G.G. Goss, and S.F. Perry 1994 Proton pumps in fish gill pavement cells? Arch.Int.Physiol.Biochim.Biophys., *102*:77-79.

Lee, M.C., C.M. Penland, J.H. Widdicombe, and J.J. Wine 1998 Evidence that Calu-3 human airway cells secret bicarbonate. Am.J.Physiol., *274*:L450-L453

Lee, T.H., J.C. Tsai, M.J. Fang, M.J. Yu, and P.P. Hwang 1998 Isoform expression of Na^+-K^+-ATPase α-subunit in gills of the teleost *Oreochromis mossambicus*. Am.J.Physiol., *275*:R926-R932

Lehrich, R.W., C. Marino, H. Henschel, C. Kelmenson, M. Ratner, and J.N. Forrest 1995 Immunolocalization of DFTR with the rodent CFTR antibody R3195 in the rectal gland of the dogfish shark, *Squalus acanthias*. Bull.Mt.Desert Isl.Biol.Lab., *34*:28-31.

Leino, R.L. and J.H. McCormick 1984 Morphological and morphometrical changes in chloride cells of the gills of *Pimephales promelas* after chronic exposure to acid water. Cell Tissue Res., *236*:121-128.

Levine, S.A., M.H. Montrose, C.M. Tse, and M. Donowitz 1993 Kinetics and regulation of three cloned mammalian Na^+/H^+ exchangers stably expressed in a fibroblast cell line. J.Biol.Chem., *268*:25527-25535.

Li, J., J. Eygensteyn, R.A. Lock, S.E. Wendelaar Bonga, and G. Flik 1997 Na^+ and Ca^{2+} homeostatic mechanisms in isolated chloride cells of the teleost *Oreochromis mossambicus* analyzed by confocal laser scanning microscopy. J.exp.Biol., *200*:1499-1508.

Lignot, J.H., M. Charmantier-Daures, and G. Charmantier 1999 Immunolocalization of Na^+,K^+-ATPase in the orgnas of the branchial cavity of the European lobster *Homarus gammarus* (Crustacea, Decapoda). Cell Tissue Res., *296*:417-426.(Abstract)

Lin, H. and D.J. Randall 1990 The effect of varying water pH on the acidification of expired water in rainbow trout. J.exp.Biol., *148*:149-160.

Lin, H. and D. Randall 1991 Evidence for the presence of an electrogenic proton pump on the trout gill epithelium. J.exp.Biol., *161*:119-134.

Lin, H. and D.J. Randall 1993 H^+-ATPase activity in crude homogenates of fish gill tissue: inhibitor sensitivity and environmental and hormonal regulation. J.exp.Biol., *180*:163-174.

Lin, H., D.C. Pfeiffer, A.W. Vogl, J. Pan, and D.J. Randall 1994 Immunolocalization of proton-ATPase in the gill epithelia of rainbow trout. J.exp.Biol., *195*:169-183.

Lin, H. and D. Randall 1995 Proton Pumps in Fish Gills. In: Cellular and Molecular Approaches to Fish Ionic Regulation. AnonymousAcademic Press, San Diego, pp. 229-255.

Low, W.P., D.J.W. Lane, and Y.K. Ip 1988 A comparative study of terrestial adaptations of the gills in three mudskippers- *Periophthalmus chrysospilos, Boleophthalmus boddaerti,* and *Periophthalmodon schlosseri.* Biol.Bull., *175*:434-438.

Low, W.P., Y.K. Ip, and D.J.W. Lane 1990 A comparative study of th gill morphometry in the mudskippers- *Periophthalmus chrysospilos, Boleophthalmus boddaerti* and *Periophthalmodon schlosseri.* Zool.Sci., *7*:29-38.

Lowry, O.H., N.J. Rosebrough, A.L. Farr, and R.J. Randall 1951 Protein measurement with the Folin phenol reagent. J.Biol.Chem., *193*:265-275.

Lönnerholm, G. and P.J. Wistrand 1984 Carbonic anhydrase in the human kidney: A histochemical and immunocytochemical study. Kidney Int., *25*:886-898.

Lytle, C., J.C. Xu, D. Biemesderfer, M. Haas, and B. Forbush III 1992 The Na-K-Cl cotransport protien of shark rectal gland. I Development of monoclonal antibodies, immunoaffinity purification and partial biochemical characterization. J.Biol.Chem., *267*:25438-25443.

Lytle, C., J.C. Xu, D. Biemesderfer, and B. Forbush III 1995 Distribution and diversity of Na-K-Cl cotransporter proteins: a study with monoclonal antibodies. Am.J.Physiol., *269*:C1496-C1505

Madsen, K.M. and C.C. Tisher 1985 Structure-function relationships in H^+-sectreting epithelia. Federation Proc., *44*:2704-2709.

Madsen, K.M., J.W. Verlander, J. Kim, and C.C. Tisher 1991 Morphological adaptation of the collecting duct to acid-base disturbances. Kidney Int., *40 Suppl. 33*:S57-S63

Maetz, J. and R. Garica 1964 The mechanism of sodium and chloride uptake by the gills of a fresh-water fish, *Carassius auratus.* II Evidence for NH_4^+ / Na^+ and HCO_3^- / Cl^- exchanges. J.Gen.Physiol., *47*:1209-1227.

Mallery, C.H. 1983 A carrier enzyme basis for ammnium excretion in teleost gill. NH_4^+-stimulated Na-dependent ATPase activity in *Opsanus beta*. Comp.Biochem.Physiol., *74A*:889-897.

Marshall, T. and K.M. Williams 1984 Artifacts associated with 2-mercaptoethanol upon high resolution two-dimensional electrophoresis. Analytical Biochemistry, *139*:502-505.

Marshall, W.S., S.E. Bryson, A. Midelfart, and W.F. Hamilton 1995 Low conductance anion channel activated by cAMP in teleost Cl^- secreting cells. Am.J.Physiol., *268*:R963-R969

Marshall, W.S., S.E. Bryson, P. Darling, C. Whitten, M. Patrick, M.P. Wilkie, C.M. Wood, and J. Buckland-Nicks 1997 NaCl transport and ultrastructure of opecular epithelium from a freshwater-adapted euryhaline teleost, *Fundulus heteroclitus*. J.exp.Zool., *277*:23-37.

Marshall, W.S. and S.E. Bryson 1998 Transport mechanisms of seawater teleost chloride cells: An inclusive model of a multifunctional cell. Comp.Biochem.Physiol., *119A*:97-106.

Marshall, W.S., T.R. Emberley, T.D. Singer, S.E. Bryson, and S.D. McCormick 1999 Time course of salinity adaptation in a strongly euryhaline estuarine teleost, *Fundulus heteroclitus*: a multivariable approach. J.exp.Biol., *202*:1535-1544.

Martínez-Ansó, E., J.E. Castillo, J. Díez, J.F. Medina, and J. Prieto 1994 Immunochemical detection of chloride/bicarbonate anion exchangers in human liver. Hepatology, *19*:1400-1406.

McCormick, S.D. 1990 Fluorescent labelling of Na^+,K^+-ATPase in intact cells by use of a fluorescent derivative of ouabain: Salinity and chloride cells. Cell Tissue Res., *260*:529-533.

McCormick, S.D. 1993 Methods for nonlethal gill biopsy and measurement of Na^+,K^+-ATPase activity. Can.J.Fish.Aquat.Sci., *50*:656-658.

McCormick, S.D. 1995 Hormonal control of gill Na^+,K^+-ATPase and chloride cell function. In: Fish Physiology. C.M. Wood and T.W. Shuttleworth, eds. Academic Press, Boca Raton, pp. 285-315.

McDonald, D.G. and C.M. Wood 1981 Branchial and renal acid and ion fluxes in the rainbow trout, *Salmo gairdneri*, at low environmental pH. J.exp.Biol., *93*:101-118.

McDonald, D.G., Y. Tang, and R.G. Boutilier 1989 Acid and ion transfer across the gills of fish: mechanisms and regulation. Can.J.Zool., *67*:3046-3054.

McDonald, D.G., V. Cavdek, and R. Ellis 1991 Gill design in freshwater fishes: Interrelationships among gas exchange, ion regulation, and acid-base regulation. Physiol.Zool., *64*:103-123.

McDonald, F.J., P.M. Snyder, P.B. McCray Jr, and M.J. Welsh 1994 Cloning, expression, and tissue distribution of a human amiloride-sensitive Na^+ channel. Am.J.Physiol., *266*:L728-L734

McDonald, F.J., M.P. Price, P.M. Snyder, and M.J. Welsh 1995 Cloning and expression of the β–and γ–subunits of the human epithelial sodium channel. Am.J.Physiol., *268*:C1163

McLean, I.W. and P.K. Nakane 1974 Periodate-lysine-paraformaldehyde fixative. A new fixative for immunoelectron mircoscopy. J.Histochem.Cytochem., *22*:1077-1083.

Medina, J.F., A. Acin, and J. Prieto 1997 Molecular cloning and characterization of the human AE2 anion exchanger (SLC4A2) gene. Genomics, *39*:74-85.

Morgan, I.P., W.T.W. Potts, and K. Oates 1994 Intracellular ion concetrations in branchial epithelial cells of brown trout (*Salmo trutta* L.) determined by x-ray microanalysis. J.exp.Biol., *194*:139-151.

Morgan, I.P. and W.T.W. Potts 1995 The effects of thiocynate on the intracellular ion concentrations of branchial epithelial cells of brown trout. J.exp.Biol., *198*:1229-1232.

Morgan, J.D. and G.K. Iwama 1999 Energy cost of NaCl transport in isolated gills of cutthroat trout. Am.J.Physiol., *277*:R631-R639

Morii, H., K. Nishikata, and O. Tamura 1978 Nitrogen excretion of mudskipper fish *Periophthalmus cantonensis* and *Boleophthalmus pectinirostris* in water and on land. Comp.Biochem.Physiol., *60A*:189-193.

Moriyama, Y. and N. Nelson 1987 The purified ATPase from chromaffin granule membrane is an anion-dependent proton pump. J.Biol.Chem., *262*:9175-9180.

Mount, D.B., E. Delpire, G. Gamba, A.E. Hall, E. Poch, R.S. Hoover Jr., and S.C. Hebert 1998 The electroneutral cation-chloride cotransporters. J.exp.Biol., *201*:2091-2102.

Nagami, G.T. 1988 Luminal secretion of ammonia in the mouse proximal tubule perfused *in vitro*. J.Clin.Invest., *81*:159-164.

Nelson, I.D., W.T.W. Potts, and H. Huddart 1997 The use of amiloride to uncouple branchial sodium and proton fluxes in the brown trout, *Salmo trutta*. J.Comp.Physiol., *167*:123-128.

Nelson, N. and W.R. Harvey 1999 Vacuolar and plasma membrane proton-adenosinetriphosphatases. Physiol.Rev., *79*:361-385.

Newstead, J.D. 1967 Fine structure of the respiratory lamellae of teleostean gills. Z.Zellforsch, *79*:396-428.

Nielsen, S., A.B. Maunsbach, C.A. Ecelbarger, and M.A. Knepper 1998 Ultrastructural localization of Na-K-2Cl cotransporter in thick ascending limb and macula densa of rat kidney. Am.J.Physiol., *275*:F885-F893

O'Grady, S.M., H.C. Palfrey, and M. Field 1987 Characteristics and functions of Na-K-Cl cotransport in epithelial tissues. Am.J.Physiol., *253*:C177-C192

Oluwatosin, Y.E. and P.M. Kane 1997 Mutations in the *CYS4* gene provided evidence for regulation of the yeast vacuolar H^+-ATPase by oxidation and reduction *in vivo*. J.Biol.Chem., *272*:28149-28157.

Onken, H., K. Graszynski, and W. Zeiske 1991 Na^+-independent, electrogenic Cl^- uptake across the posterior gills of the Chinese crab (*Eriocheir sinensis*): Voltage-clamp and microelectrode studies. J.Comp.Physiol., *161*:293-301.

Onken, H. and M. Putzenlechner 1995 A V-ATPase drives active, electrogenic and Na^+-independent Cl^- absorption across the gills of *Eriocheir sinensis*. J.exp.Biol., *198*:767-774.

Paillard, M. 1998 H^+ and HCO_3^- transporters in the medullary thick ascending limb of the kidney: molecular mechanisms, function and regulation. Kidney Int., *53*:S-36-S-41

Pan, J., D.C. Pfeiffer, C.L. Reimer, B.J. Crawford, A.W. Vogl, and N. Auersperg 1993 Lack of inter-species reactivity etween antigens and antibodies is overcome by protease treatment of Western blots. Electrophoresis, *14*:892-898.

Payan, P. and A.J. Matty 1975 The characteristics of ammonia excretion by a perfused head of trout (*Salmo gairdneri*): Effect of temperature and CO_2-free ringer. J.Comp.Physiol., *96*:167-184.

Pärt, P. and C.M. Wood 1996 Na/H exchange in cultured epithelial cells from fish gills. J.Comp.Physiol.B, *166*:37-45.

Pelster, B. and H. Niederstätter 1999 Acid release in cultured gas gland cells. Comp.Biochem.Physiol., *124A*:S37(Abstract)

Peng, K.W., S.F. Chew, C.B. Lim, S.S.L. Kuah, W.K. Kok, and Y.K. Ip 1998 The mudskipper *Periophthalmodon schlosseri* and *Boleophthalmus boddaerti* can tolerate environmental NH_3 concentrations of 446 and 36 µM, respectiviely. Fish Physiol.Biochem., *19*:59-69.

Peränen, J., M. Rikkonen, and L. Kääriäinen 1993 A method for exposing hidden antigenic sites in paraformaldehyde-fixed cultured cells, applied to initially unreactive antibodies. J.Histochem.Cytochem., *41*:447-454.

Pereira, C.M., J.M. Wilson, and A. Oliva-Teles 1999 Utilization of dietary carbonhydrate and fat by juvenile turbot (*Scophthalmus maximus*): The effect of rearing temperature. Comp.Biochem.Physiol., *124A*:S140(Abstract)

Perry, S.F., M.S. Haswell, D.J. Randall, and A.P. Farrell 1981 Branchial ionic uptake and acid-base regulation in the rainbow trout, *Salmo gairdneri*. J.exp.Biol., *92*:289-303.

Perry, S.F. and D.J. Randall 1981 Effects of amiloride and SITS on branchial ion fluxes in rainbow trout, *Salmo gairdneri*. J.exp.Biol., *215*:225-228.

Perry, S.F., G.G. Goss, and P. Laurent 1992 The interrelationships between gill chloride cell morphology and ionic uptake in four freshwater teleosts. Can.J.Zool., *70*:1775-1786.

Perry, S.F. and J.N. Fryer 1997 Proton pumps in the fish gill and kidney. Fish Physiol.Biochem., *17*:363-369.

Perry, S.F. 1997 The Chloride Cell: Structure and function in the gills of freshwater fishes. Ann.Rev.Physiol., *59*:325-347.

Perry, S.F., M.L. Beyers, and D.A. Johnson 1999 Cloning and molecular characterization of the trout (*Oncorhynchus mykiss*) vacuolar H^+-ATPase B subunit. J.exp.Biol., (In Press)

Philpott, C.W. 1980 Tubular system membranes of teleost chloride cells: osmotic response and transport sites. Am.J.Physiol., *238*:R171-R184

Piermarini, P.M. and D.H. Evans 1999 Expression of sodlium, potassium-ATPase in the gills and rectal gland of a euryhaline elasmobranch (*Dasyatis sabina*). The Society for Experimental Biology Annual Meeting, *Animal and Cell Biology*:30(Abstract)

Piiper, J. and P. Scheid 1984 Model analysis of gas transfer in fish gills. In: Fish Physiology. W.S. Hoar and D.J. Randall, eds. Academic Press, New York, pp. 229-262.

Pisam, M., C. Sardet, and J. Maetz 1980 Polysaccharidic material in chloride cell of teleostean gill: modifications according to salinity. Am.J.Physiol., *238*:R213-R218

Pisam, M. 1981 Membranous systems in the "chloride cell" of teleostean fish gill; their modifications in response to the salinity of the environment. Anat.Rec., *200*:401-414.

Pisam, M., A. Caroff, and A. Rambourg 1987 Two types of chloride cells in the gill epithelium of a freshwater-adapted euryhaline fish: *Lebistes reticulatus*; their modifications during adaptation to seawater. Am.J.Anat., *179*:40-50.

Pisam, M., P. Prunet, G. Boeuf, and A. Rambourg 1988 Ultrastructural features of chloride cells in the gill epithelium of the Atlantic salmon. *Salmo salar*, and their modifications during smoltification. Am.J.Anat., *183*:235-244.

Pisam, M., P. Prunet, and A. Rambourg 1989 Accessory cells in the gill epithelium of freshwater rainbow trout *Salmo gairdneri*. Am.J.Anat., *184*:311-320.

Pisam, M., G. Boeuf, P. Prunet, and A. Rambourg 1990 Ultrastructural features of mitochondria-rich cells in stenohaline freshwater and seawater fishes. Am.J.Anat., *187*:21-31.

Pisam, M. and A. Rambourg 1991 Mitochondria-rich cells in the gill epithelium of teleost fishes: An ultrastructural approach. Inter.Rev.Cytol., *130*:191-232.

Potts, W.T.W. 1994 Kinetics of sodium uptake in freshwater animals: a comparison of ion-exchange and proton pump hypotheses. Am.J.Physiol., *266*:R315-R320

Potts, W.T.W. 1984 Transepithelial potentials in fish gills. In: Fish Physiology. W.S. Hoar and D.J. Randall, eds. Academic Press, SanDiego, pp. 105-128.

Poulsen, J.H., H. Fischer, B. Illek, and T.E. Machen 1994 Bicarbonate conductance and pH regulation capability of cystic fibrosis transmembrane conductance regulator. Proc.Natl.Acad.Sci.USA, *91*:5340-5344.

Powell, M.D., D.J. Speare, and G.M. Wright 1994 Comparative ultrastructural morphology of lamellar epithelial, chloride, and mucous cell glycocalyx of the rainbow trout (*Oncorhynchus mykiss*). J.Fish Biol., *44*:725-730.

Pressley, T.A. 1992 Phylogenetic conservation of isoform-specific regions within α-subunit of Na,K-ATPase. Am.J.Physiol., *262*:C743-C751

Puopolo, K., C. Kumamoto, I. Adachi, R. Magner, and M. Forgac 1992 Differential expression of the "B" subunit of the vacuolar H^+-ATPase in bovine tissues. J.Biol.Chem., *267*:3696-3706.

Rahim, S.M., J.P. Delaunoy, and P. Laurent 1988 Identification and immunocytochemical localization of two different carbonic anhydrase isoenzymes in teleostean fish erythrocytes and gill epithelia. Histochem., *89*:451-459.

Randall, D., H. Lin, and P.A. Wright 1991 Gill water flow and the chemistry of the boundary layer. Physiol.Zool., *64*:26-38.

Randall, D.J., A.P. Farrell, and T. Heming 1978 Carbon dioxide excretion in the pirarucu (*Arapaima gigas*), an obligate air-breathing fish. Can.J.Zool., *56*:970-973.

Randall, D.J. and P.A. Wright 1987 Ammonia distribution and excretion in fish. Fish Physiol.Biochem., *3*:107-120.

Randall, D.J., C.M. Wood, T.P. Mommsen, S.F. Perry, H. Bergman, G.M.O. Maloiy, and P.A. Wright 1989 Urea excretion as a strategy for survival in a fish living in a very alkaline environment. Nature, *337*:165-166.

Randall, D.J., J.M. Wilson, K.W. Peng, W.K. Kok, S.S.L. Kuah, S.F. Chew, T.J. Lam, and Y.K. Ip 1999 The mudskipper, *Periophthalmodon schloesseri*, actively transports NH_4^+ against a concentration gradient. Am.J.Physiol., (In Press)

Reynolds, E. 1963 The use of lead citrate at high pH as an electron-opaque stain in electron microscopy. J.Cell Biol., *17*:208-212.

Richards, B.D. and P.O. Fromm 1970 Sodium uptake by isolated-perfused gills of rainbow trout (*Salmo gairdneri*). Comp.Biochem.Physiol., *33*:303-310.

Riestenpatt, S., G. Petrausch, and D. Siebers 1995 Cl⁻ influx across posterior gills of the chinese crab (*Eriocheir sinensis*): potential energization by a V-type H^+-ATPase. Comp.Biochem.Physiol., *110A*:235-241.

Riordan, J.R., B. Forbush III, and J.W. Hanrahan 1994 The molecular basis of chloride transport in shark rectal gland. J.exp.Biol., *196*:45-418.

Sabolic, I., C.M. Herak-Kramberger, S. Breton, and D. Brown 1999 Na/K-ATPase in intercalated cells along the rat nephron revealed by antigen retrieval. Journal of the American Society of Nephrology, *10*:913-922.(Abstract)

Saha, N. and B.K. Ratha 1990 Alterations in excretion pattern of ammonia and urea in freshwater air-breathing teleost, *Heteropneustes fossilis* (Boch) during hyperammonia stress. Ind.J.Exp.Biol., *28*:597-599.

Salama, A., I.J. Morgan, and C.M. Wood 1999 The linkage between Na^+ uptake and ammonia excretion in rainbow trout: Kinetic analysis, the effects of $(NH_4)_2SO_4$ and NH_4HCO_3 infusion and the influence of gill boundary layer pH. J.exp.Biol., *202*:697-709.

Sandbacka, M., H. Lilius, M.O.K. Enkvist, and B. Isomaa 1998 Rainbow trout gill epithelial cells in primary culture communicate through gap junctions as demonstrated by dye-coupling. Fish Physiol.Biochem., *19*:287-292.

Sardet, C., M. Pisam, and J. Maetz 1977 The surface epithelium of teleostean fish gills. Cellular and junctional adaptations of the chloride cell in relation to salt adaptation. J.Cell Biol., *80*:96-117.

Scala, C., G. Cenacchi, C. Ferrari, G. Pasquinelli, P. Preda, and G.C. Manara 1992 A new acrylic resin formulation: A useful tool for histological, ultrastructural, and immunocytochemical investigations. J.Histochem.Cytochem., *40*:1799-1804.

Scharschmidt, B.F., E.B. Keefe, N.M. Blankenship, and R.K. Ockner 1979 Validation of a recording spectrophotometeric method for measurement of membrane associated Mg- and NaK-ATPase activity. J.Lab.Clin.Med., *93*:790-799.

Schönrock, C., S.D. Morley, Y. Okawara, K. Lederis, and D. Richter 1991 Sodium and potassium ATPase of the teleost fish *Catostomus commersoni*- sequence, protein structure and evolutionary conservation of the alpha subunit. Biol.Chem.Hoppe-Seyler., *372*:279-286.

Schöttle, E. 1931 Morphologie und physiologie der atmung bei wasser-, schlamm-, und landlebenden Gobiiformes. Z.Wiss.Zool., *140*:1-114.

Schuster, V.L., S.M. Bonsib, and M.L. Jennings 1986 Two types of collecting duct mitochondria-rich (intercalated) cells: lectin and band 3 cytochemistry. Am.J.Physiol., *251*:C347-C355

Schwiebert, E.M., D.J. Benos, M.E. Egan, M.J. Stutts, and W.B. Guggino 1999 CFTR is a conductance regulator as well as a chloride channel. Physiol.Rev., *79*:S145-S166

Scoazec, J.-Y., A.-F. Bringuier, J.F. Medina, E. Martinez-Anzó, D. Veissiere, G. Feldmann, and C. Housset 1997 The plasma membrane polarity of human biliary epithelial cells: *in situ* immunohistochemical analysis and functional implications. Journal of Hepatology, *26*:543-553.

Shephard, K.L. 1992 Studies of the fish-gill microclimate: interactions between gill tissue, mucus and water-quality. Env.Biol.Fish., *34*:409-420.

Silva, P., R. Solomon, K. Spokes, and F.H. Epstein 1977 Ouabain inhibition of gill Na-K-ATPase: Relationship to active chloride transport. J.exp.Zool., *199*:419-426.

Simpson, I.A. and O. Sonne 1982 A simple, rapid, and sensitive method for measuring protein concentration in subcellular membrane fractions prepared by sucrose density ultracentrifugation. Analytical Biochemistry, *119*:424-427.

Singer, T.D., S.J. Tucker, W.S. Marshall, and C.F. Higgins 1998 A divergent CFTR homologue: highly regulated salt transport in the euryhaline teleost *F. herteroclitus*. Am.J.Physiol., *274*:C715-C723

Skou, J.C. and M. Esmann 1992 The Na,K-ATPase. J.Bioenerg.Biomembr., *24*:249-261.

Smith, H.W. 1929 The excretion of ammonia and urea by the gills of fish. J.Biol.Chem., *81*:727-742.

Smith, J.J. and M.J. Welsh 1992 cAMP stimulates bicarbonate secretion across normal, but not cystic fibrosis airway epithelia. J.Clin.Invest., *89*:1148-1153.

Smith, P.R. and D.J. Benos 1991 Epithelial Na$^+$ channels. Ann.Rev.Physiol., *53*:509-530.

Smith, P.R., A.L. Bradford, V. Dantzer, D.J. Benos, and E. Skadhauge 1993 Immunocytochemical localization of amiloride-sensitive sodium channels in the lower intestine of the hen. Cell Tissue Res., *272*:129-136.

Sorscher, E.J., M.A. Accavitti, D. Keeton, E. Steadman, R.A. Frizzell, and D.J. Benos 1988 Antibodies against purified epithelial sodium channel protein from bovine renal papilla. Am.J.Physiol., *255*:C835-C843

Speeg, K.V. and J.W. Campbell 1968 Formation and volatilization of ammonia gasby terrestial snails. Am.J.Physiol., *214*:1392-1402.

Stetson, D.L. and P.R. Steinmetz 1985 α and β types of carbonic anhydrase-rich cells in turtle bladder. Am.J.Physiol., *249*:F553-F565

Stuart-Tilley, A., C. Sardet, J. Pouyssegur, M.A. Schwartz, D. Brown, and S.L. Alper 1994 Immunolocalization of anion exchanger AE2 and cation exchanger NHE-1 in distinct adjacent cells of gastric mucosa. Am.J.Physiol., *266*:C559-C568

Sullivan, G.V., J.N. Fryer, and S.F. Perry 1995 Immunolocalization of proton pumps (H^+-ATPase) in pavement cells of rainbow trout gill. J.exp.Biol., *198*:2619-2629.

Sullivan, G.V., J.N. Fryer, and S.F. Perry 1996 Localization of mRNA for the proton pump (H^+-ATPase) and Cl^-/HCO_3^- exchanger in the rainbow trout gill. Can.J.Zool., *74*:2095-2103.

Sun, A.M., Y. Liu, L.D. Dworkin, C.M. Tse, M. Donowitz, and K.P. Yip 1997 Na^+/H^+ exchanger isoform 2 (NHE2) is expressed in the apical membrane of the medullary thick ascending limb. Journal of Membrane Biology, *160*:85-90.

Suzuki, Y., M. Itakura, M. Kashwagi, N. Nakamura, T. Matsuki, H. Sakuta, N. Naito, K. Takano, T. Fujita, and S. Hirose 1999 Identification by differential display of a hypertonicity-inducible inward rectifier potassium channel highly expressed in chloride cells. J.Biol.Chem., *274*:11376-11382.

Südhof, T.C., V.A. Fried, D.K. Stone, and P.A. Johnston 1989 Human endomembrane H^+ pump strongly resembles the ATP-synthetase of Archaebacteria. Proc.Natl.Acad.Sci.USA, *86*:6067-6071.

Tago, K., V.L. Schuster, and J.B. Stokes 1986 Stimulation of chloride transport by $HCO_3^-CO_2$ in rabbit cortical collecting tubule. Am.J.Physiol., *251*:F49-F56

Takeyasu, K., M.M. Tamkun, K.J. Renaud, and D.M. Fambrough 1988 Ouabain-sensitive ($Na^+ + K^+$)-ATPase activity expressed in mouse L cells by transfection with DNA encoding the α-subunit of an avian sodium pump. J.Biol.Chem., *263*:4347-4354.

Tamura, S.O., H. Morii, and M. Yuzuriha 1976 Respiration of the amphibious fishes *Periophthalmus cantonensis* and *Boleophthalmus chinensis* in water and on land. J.exp.Biol., *65*:97-107.

Taylor, C.R., S.-R. Shi, and R.J. Cote 1996 Antigen retrieval for immunohistochemistry. Status and need for greater standardization. Applied Immunohistochemistry, *4*:144-166.

Teixeira da Silva Jr., J.C., R.D. Perrone, C.A. Johns, and N.E. Madias 1991 Rat kidney band 3 mRNA modulation in chronic respiratory acidosis. Am.J.Physiol., *260*:F204-F209

Thurston, R.V., R.C. Russo, and G.R. Phillips 1983 Acute toxicity of ammonia to fathead minnow. Trans.Am.Fish.Soc., *112*:705-711.

Tokuyasu, K.T. and S.J. Singer 1976 Improved procedures for immunoferritin labeling of ultrathin frozen sections. J.Cell Biol., *71*:894-906.

Towbin, H., T. Staehelin, and J. Gordon 1979 Electrophoretic transfer of proteins from polyacrylamide gels to nitrocellulose sheets: procedure and some applications. Proc.Natl.Acad.Sci.USA, *76*:4350-4354.

Towle, D.W. and T. Hølleland 1987 Ammonium ion substitutes for K^+ in ATP-dependent Na^+ transport by basolateral membrane vesicles. Am.J.Physiol., *252*:R479-R489

Tse, C.M., S.A. Levine, C.H. Yun, S.R. Brant, J. Pouyssegur, M.H. Montrose, and M. Donowitz 1993 Functional characteristics of a cloned epithelial Na^+/H^+ exchanger (NHE3): resistance to amiloride and inhibition by protein kinase C. Proc.Natl.Acad.Sci.USA, *90*:9110-9114.

Ura, K., K. Soyano, N. Omoto, S. Adachi, and K. Yamauchi 1996 Localization of Na-K-ATPase in tissues of rabbit and teleosts using an antiserum directed against a partial sequence of the α-subunit. Zool.Sci., *13*:219-227.

Van Der Heijden, A.J.H., P.M. Verbost, J. Eygensteyn, J. Li, S.E. Wendelaar Bonga, and G. Flik 1997 Mitochondria-rich cells in gills of tilapia (*Oreochromis mossambicus*) adapted to fresh water or sea water: Quantification by confocal laser scanning microscopy. J.exp.Biol., *200*:55-64.

van Hille, B., H. Richener, D.B. Evans, J.R. Green, and G. Bilbe 1993 Identification of two subunit A isoforms of the vacuolar H^+-ATPase in human osteoclastoma. J.Biol.Chem., *268*:7075-7080.

van Hille, B., H. Richener, P. Schmid, I. Puettner, J.R. Green, and G. Bilbe 1994 Heterogeneity of vacuolar H^+-ATPase: differential expression of wo human subunit B isoforms. Biochem.J., *303*:191-198.

Verdouw, H., C.J.A. van Echeld, and E.M.J. Dekkers 1978 Ammonia determination based on indophenol formation with sodium salicylate. Water Res., *12*:399-402.

Verlander, J.W., K.M. Madsen, P.S. Low, D.P. Allen, and C.C. Tisher 1988 Immunocytochemical localization of band 3 protein in the rat collecting duct. Am.J.Physiol., *255*:F115-F125

Vonnegut Jr., K. (1969). Slaughter house five or; The children's crusade, a duty dance with death. (New York: Delacorte Press).

Wagner, S., R. Vogel, R. Lietzke, R. Koob, and D. Drenckhahn 1987 Immunochemical characterization of a band 3-like anion exchanger in collecting duct of human kidney. Am.J.Physiol., *253*:F213-F221

Wall, S.M. and L.M. Koger 1994 NH_4^+ transport mediated by Na^+-K^+-ATPase in rat inner medullary collecting duct. Am.J.Physiol., *267*:F660-F670

Wall, S.M. 1996 Ammonium transport and the role of the Na,K-ATPase. Mineral and Electrolyte Metabolism, *22*:311-317.

Walsh, P.J. 1998 Nitrogen excretion and metabolism. In: Physiology of fishes. D.H. Evans, ed. CRC Press, Boca Raton, pp. 199-214.

Wang, Z.-Q. and S. Gluck 1990 Isolation and properties of bovine kidney brush border vacuolar H^+-ATPase. J.Biol.Chem., *265*:21957-21965.

Wendelaar Bonga, S.E. and C.J.M. van der Meij 1989 Degeneration and death, by apoptosis and necrosis, of the pavement and chloride cells in the gills of the teleost *Oreochromis mossambicus*. Cell Tissue Res., *255*:235-243.

Werner, G. and H. Hagenmaier 1984 Bafilomycins, a new group of macrolide antibiotics. Production, isolation, chemical structure and biological activity. Journal of Antibiotics, *37*:110-117.

Werner, M., R. von Wasielewski, and P. Komminoth 1996 Antigen retrieval, signal amplification and intensification in immunohistochemistry. Histochem.Cell Biol., *105*:253-260.

Wieser, W. 1972 Oxygen consumption and ammonia excretion in *Ligia beaudiana* M.-E. Comp.Biochem.Physiol., *43A*:869-876.

Wilson, J.M., D.J. Randall, A.W. Vogl, and G.K. Iwama 1997 Immunolocalization of proton-ATPase in the gills of the elasmobranch, *Squalus acanthias*. J.exp.Zool., *278*:78-86.

Wilson, R.W. and E.W. Taylor 1992 Transbranchial ammonia gradients and acid-base responses to high external ammonia concentration in rainbow trout (*Oncorhynchus mykiss*) acclimated to different salinities. J.exp.Biol., *166*:95-112.

Wilson, R.W., P.M. Wright, S. Munger, and C.M. Wood 1994 Ammonia excretion in freshwater rainbow trout (*Oncorhynchus mykiss*) and the importance of gill boundary layer acidification: lack of evidence for Na^+/NH_4^+ exchange. J.exp.Biol., *191*:37-58.

Wilson, R.W., K.M. Gilmour, R.P. Henry, and C.M. Wood 1996 Intestinal base excretion in the seawater-adapted rainbow trout: A role in acid-base regulation? J.exp.Biol., *199*:2331-2343.

Wittbrodt, J., A. Meyer, and M. Schartl 1998 More genes in fish? BioEssays, *20*:511-515.

Witters, H., P. Berckmans, and C. Vangenechten 1996 Immunolocalization of Na^+,K^+-ATPase in the gill epithelium of rainbow trout, *Oncorhynchus mykiss*. Cell Tissue Res., *283*:461-468.

Wong, C.K.C. and D.K.O. Chan 1999 Isolation of viable cell types from the gill epithelium of Japanese eel *Anguilla japonica* . Am.J.Physiol., *276*:R363-R372

Wood, C.M. and G.G. Goss 1990 Kinetic analysis of relationships between ion exchange and acid-base regulation at the gills of freshwater fish. In: Animal Nutrition and Transport

Processes. 2. Transport, Respiration and Excretion: Comparative and Environmental Aspects. J.P. Truchot and B. Lahlou, eds. Comp Physiol., Basel,Karger, pp. 119-136.

Wood, C.M. 1991 Branchial ion and acid-base transfer in freshwater teleost fish: Environmental hyperoxia as a probe. Physiol.Zool., *64*:68-102.

Wood, C.M., K.M. Gilmour, and P. Part 1998 Passive and active transport properties of a gill model, the cultured branchial epithelium of the freshwater rainbow trout (*Oncorhynchus mykiss*). Comp.Biochem.Physiol., *119A*:87-96.

Wright, P.A. and C.M. Wood 1985 An analysis of branchial ammonia excretion in the freshwater rainbow trout: Effects of environmental pH change and sodium uptake blockage. J.exp.Biol., *114*:329-353.

Wright, P.A., D.J. Randall, and S.F. Perry II 1989 Fish gill water boundary layer: a site of linkage between carbon dioxide and ammonia excretion. J.Comp.Physiol., *158*:627-635.

Wright, P.A., P. Pärt, and C.M. Wood 1995 Ammonia and urea excretion in the tidepool sculpin (*Oligocottus maculosus*):sites of excretion, effects of reduced salinity and mechanisms of urea transport. Fish Physiol.Biochem., *14*:111-123.

Wright, S.H. 1991 The inferface of animal and aqueous environment: strategies and constraints on the maintenance of solute balance. In: Biochemistry and molecular biology of fishes. P.W. Hochachka and T.P. Mommsen, eds. Elsevier Science, pp. 165-180.

Xu, J.C., C. Lytle, T.T. Zhu, J.A. Payne, J. Benz, and I.I.I. Forbush 1994 Molecular cloning and functional expression of the bumetanide-sensitive Na-K-Cl cotransporter. Proc.Natl.Acad.Sci.USA, *91*:2201-2205.

Yadav, A.N., M.S. Prasad, and B.R. Singh 1990 Gross structure of the respiratory organs and dimensions of the gill in the mud-skipper, *Periophthalmus schlosseri* (Bleeker). J.Fish Biol., *37*:383-392.

Zadunaisky, J.A., S. Cardona, L. Au, D.M. Roberts, E. Fisher, B. Lowenstein, E.J. Cragoe Jr., and K.R. Spring 1995 Chloride transport activation by plasma osmolarity during rapid adaptation to high salinity of *Fundulus heteroclitus*. J.Membrane Biol., *143*:207-217.

Zadunaisky, J.A. 1996 Chloride cells and osmoregulation. Kidney Int., *49*:1563-1567.

Zaugg, W.S. 1982 A simplified preparation for adenosine triphospate determination in gill tissue. Can.J.Fish.Aquat.Sci., *39*:215-217.

Zeidel, M.L. 1996 Low permeabilities of apical membranes of barrier epithelia: what makes watertight membranes watertight? Am.J.Physiol., *271*:F243-F245

Ziegler, A. 1997 Immunocytochemical localization of Na^+,K^+-ATPase in the calcium-transporting seternal epithelium of the terrestial isopod *Porcellio scaber* L. (Crustacea). J. Histochem. Cytochem., *45*:437-446.

APPENDIX 1. List of antibodies tested. Note that not all of the results are included in the thesis.

Antibody	Antigen	Host	Source	Reference	Comments
α5	α subunit Na⁺,K⁺-ATPase	mouse	DSHB[1]	Takano et al. 88	pan specific
vH⁺-ATPase	peptide 70 kDa subunit	rabbit	UBC[2]	Sudhof et al. 89	fish Okay
vH⁺-ATPase	peptide 31 kDa subunit	rabbit	S.F. Perry[3]	Sullivan et al. 95	negative
bαENaC	bovine αsubunit ENaC fusion protein	rabbit	D. Benos[4]	Ismailov et al. 96	Western only
hβENaC	peptide human β subunit ENaC	rabbit	D. Benos[4]	unpublished	fish Okay
ENaC	bovine renal papillae ENaC	rabbit	D. Benos[4]	Sorscher et al. 88	Western only
NHE-2	fusion protein (597)	rabbit	M. Donowitz[5]	Tse et al. 1994	fish Okay
NHE-3	fusion protein (1380)	rabbit	M. Donowitz[5]	Hoogerwerf et al. 96	fish Okay
NHE-3	fusion protein (1381)	rabbit	M. Donowitz[5]	Hoogerwerf et al. 96	negative
NHE-3	fusion protein C-term peptide (2B9)	mouse	Chemicon Int.[6]	Biemesderfer et al. 97	rat kidney only
NHE-3	fusion protein C-term peptide (4F5)	mouse	Chemicon Int.[6]	Biemesderfer et al.97	rat kidney only
NHE-3	fusion protein C-term peptide (2B9)	mouse	Chemicon Int.[6]	Biemesderfer et al.97	rat kidney only
AE1t	trout erythroid band 3	rabbit	B. Tufts[7]	Cameron et al. 93	fish Okay
AE1m	cytoplasmic domain peptide (mouse)	rabbit	R. Kopito[8]	Cameron et al. 93	rat kidney only
cdb3 (AE1)	cytoplasmic domain fragment (human)	rabbit	P. Low[9]	Verlander et al. 88	rat kidney only
AE2	peptide AE2	rabbit	J. Prieto[10]	M.-Anzo et al. 96	negative
CAII	chick retinal CAII	rabbit	P. Linser[11]	Linser 83	fish Okay
CAII	bovine erythrocyte	rabbit	Biogenesis[12]	na	negative
CFTR	clone TAM16	mouse	NeoMarker[13]	na	fish Okay
Ca⁺⁺ATPase	clone 5F10	mouse	Sigma[14]	Borke et al. 89	negative
NKCC	human NKCC (T4)	mouse	DSHB[1]	Lytle et al. 95	fish Okay
NKCC	shark NKCC (J3)	mouse	DSHB[1]	Lytle et al. 92	fish Okay

[1]DSHB, Developmental Studies Hybridoma Bank, Univeristy of Iowa; [2]UBC, Univeristy of British Columbia, Peptide Synthesis Service; [3] Dept. Biology, University of Ottawa; [4]Dept. Biophysics and Physiology, University of Alabama at Birmingham; [5] School of Medicine and Physiology, Johns Hopkins University, MD; [6] Chemicon International, CA; [7] Dept. Biology, Queens University, ON; [8] Dept. Biological Sciences, Stanford University, CA; [9] Dept. Chemistry, Perdue University IN; [10] Dept. Medicine, University of Navarra, Pamplona ES; [11] Whitney Laboratory, University of Florida, FL; [12] Biogenesis UK; [13] NeoMarker, CA; [14] Sigma Chemical Co., MO.

APPENDIX 2.

Summary of immunohistochemistry. (+) positive; (–) negative immunoreaction; (blank) not tried; (?) non specific. Note, not all species listed below appear in the thesis.

Antibodies against:	Marine				Euryhaline sw/fw			Freshwater				
	Mud-skipper	Turbot	Dogfish	Hagfish	Coho	Tilapia	Trout	Guppy	Neon Tetra	Eel	Catfish	Killifish
vH$^+$-ATPase	+	+	+	-	+/+	+/+	+	+	?	+	?	+
Na$^+$,K$^+$-ATPase	+	+	+	+	+/+	+/+	+	+	+	+	+	+
CA	+		+		+/+	+/+	+		+	+	+	
AE1t	-	+	-	-	+/-	+	-			-	-	-
ENaC	-					+	+					
NKCC (J3,T4)	+	+	+	-	+/+	+/+	+		-			
CFTR	+	-	-	-		-	-					
NHE-2 (597)	+	+		-	+/+	+/	-		-		-	
NHE-3 (1380-81)	+	-		-	-	+/+			-		-	-

Mudskipper, *Periophthalmodon schlosseri*; Turbot, *Scophthalmus maximus*; Dogfish, *squalus acanthias*; Hagfish, *Eptatretus stouti*; Coho salmon, *Oncorhynchus kisutch*; Tilapia, *Oreochromis mossambicus*; Trout, *Oncorhynchus mykiss*; Guppy *Lebistes reticulatus*; Neon Tetra, *Paracheirodon innesi*; Eel, *Anguilla rostrata*; Catfish, *Ictalurus nebulosus*; Killifish, *Fundulus heteroclitus*